



## **Simultaneous Cutting of Two Separate Sheets Using Plasma and Parameters Optimisation**

**Engineering Doctorate**

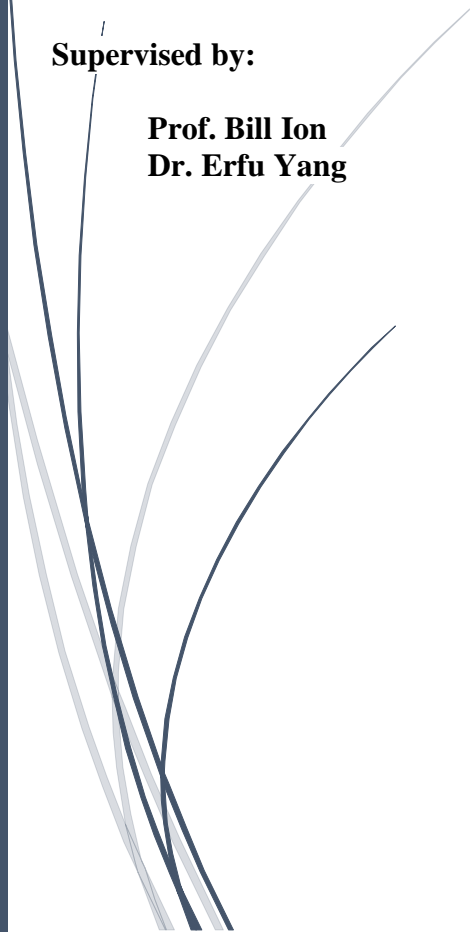
**Advanced Manufacturing: Forging and Forming**

**2021**

**Adel Gani**  
(201771954)

**Supervised by:**

**Prof. Bill Ion**  
**Dr. Erfu Yang**



## **Abstract**

This thesis investigates on the ability of using plasma technique for cutting simultaneously two parallel thin layers at different gap distances. Previous research emphasised that plasma cutting can be optimised to improve the quality and reduce phenomena. The investigation performed previously was made primarily in two-dimensional cutting plan. However, there is a lack of publication and research regarding optimisation of a three-dimensional structure cutting. This current work would help engineers to understand the practicability of thermal cutting such as plasma to process zones in the vehicle chassis similar to box sections or double layered areas. This research is aimed at wheelchair accessible vehicle converters that performs modifications in the chassis floor. This work is part of the engineering doctorate program.

The research questions raised of this study lie primarily on assessing the possibility of simultaneous cutting of a double sheet (separated with an air distance) using plasma, expressly examining the possibility to reuse the energy heat exiting the first sheet's kerf to perform a cut on the second layer. In addition, optimising the double sheets cutting, analysing the effect of the heat on thin material and reduce the resulting phenomena to their lower level (mainly surface deformation and heat affected zones). Lastly, assess the relationship strength between the parameters and the quality.

Experiments were performed in four progressive phases. The first step was made to test the suitability of the plasma to process single thin sheets of 0.6 mm thick. This step was required to analyse the impact of the heat on the surface deformation and then optimise the cutting to improve the quality. The second phase of the tests were performed to verify the plasma ability to process a 3D-Structure such as double layered zones. The third phase of test was made to assess the cutting parameters suitable to process two layers simultaneously at a fixed gap 20 mm. These parameters were used as a reference for the following stage. The fourth phase was performed to optimise the double sheets structure cutting process (separated with an air distance) and minimise the impact of the heat generated during the plasma cutting on the top sheet.

The Hypothesis of re-using the heat was tested and proven true, it is possible to re-employ the heat energy exiting the kerf to perform another cut. The tests showed that there was a considerable heat impact on the surface. However, this can be controlled and reduced. Cutting two sheets simultaneously may result to an offset between the top and bottom edge of the cut. Optimisation using the DOE based Taguchi approach resulted to an improvement in quality and the regression analysis showed a good fit of the models constructed, none of the values measured were outside the interval of prediction. Final tests were performed on a vehicle chassis and the results showed that a

good automation can reduce the cutting process by approximately 40min compared to manual cutting.

## **Statement of Academic Honesty**

*I declare that this submission is entirely my own original work.*

*I declare that, except where fully referenced direct quotations have been included, no aspect of this submission has been copied from any other source.*

*I declare that all other works cited in this submission have been appropriately referenced.*

*I understand that any act of Academic Dishonesty such as plagiarism or collusion may result in the non-award of my degree.*

*Signed*    **Adel Gani**

*Dated*    **14/07/2021.**

## **Acknowledgements**

First, I thank the almighty god for giving me the strength and the knowledge to complete this thesis. Then, I am heartily thankful to all my family, including my wife, my little son, parents, brothers and sisters, gran and all my friends without exception who were there when needed and supported me even with nice words and smile. I would like to thank also all my academic supervisors including the engineering doctorate coordinator, a big thank you also goes to Allied Vehicles and the company's supervisor for giving me the chance to widen my skills, I am grateful for all their support provided. I also thank Glasgow college who helped me and made all the tests required possible. Thanks to the Advanced Forming Research Centre for all their support. This acknowledgment would not be complete without thanking the authors of the Automotive body V1 book, Springer Netherlands, ESAB, TWI, AFRC and Struers Ltd for granting me permission to reuse their Figures in my thesis.

May God Bless Everyone.

## Table of contents

ABSTRACT	- 2 -
STATEMENT OF ACADEMIC HONESTY	- 4 -
ACKNOWLEDGEMENTS	- 5 -
TABLE OF CONTENTS	- 6 -
LIST OF FIGURES	- 9 -
LIST OF TABLES	- 11 -
NOMENCLATURE	- 12 -
LIST OF PUBLICATION	- 13 -
<b>CHAPTER 1 INTRODUCTION</b>	<b>- 1 -</b>
1.1 OVERVIEW	- 1 -
1.2 RESEARCH AIM AND OBJECTIVE	- 3 -
1.3 STRUCTURE OF THE THESIS	- 5 -
<b>CHAPTER 2 WHEELCHAIR ACCESSIBLE VEHICLES INDUSTRIAL CONTEXT</b>	<b>- 7 -</b>
2.1 INTRODUCTION	- 7 -
2.2 ALLIED VEHICLES CONVERSION PROCESS	- 7 -
2.3 CUTTING STAGE ISSUES	- 7 -
2.4 CHASSIS MATERIAL	- 11 -
2.5 ADHESIVE AND SEALING	- 15 -
2.6 REQUIREMENTS AND TOLERANCES	- 15 -
2.7 RELATED WORK	- 18 -
2.8 SUMMARY	- 26 -
<b>CHAPTER 3 PLASMA CUTTING LITERATURE REVIEW</b>	<b>- 27 -</b>
3.1 INTRODUCTION	- 27 -
3.2 PLASMA ARC CUTTING	- 27 -
3.3 LASER CUTTING	- 29 -
3.4 ABRASIVE WATER JET	- 30 -
3.5 CUTTING TECHNIQUES COMPARISON	- 32 -
3.6 PLASMA CUTTING RELATED RESEARCH	- 33 -
3.7 CONCLUSION AND KNOWLEDGE GAP	- 41 -
<b>CHAPTER 4 RESEARCH METHODOLOGY</b>	<b>- 43 -</b>
4.1 INTRODUCTION	- 43 -
4.2 RESEARCH APPROACH	- 45 -
4.3 DESIGN OF EXPERIMENT	- 45 -
4.4 FACTORS AND LEVELS	- 46 -
4.4.1 Parameters	- 47 -
4.4.2 Levels	- 47 -
4.4.3 Response	- 49 -
4.5 DOE BASED TAGUCHI PARAMETERS DESIGN APPROACH PROCESS	- 50 -
4.6 EXPERIMENTAL PROCEDURES	- 52 -
4.6.1 Phase One (Thin material cutting)	- 53 -
4.6.2 Phase Two (3D-Structure Cutting Capability)	- 53 -
4.6.3 Phase Three (Cutting Parameters Identification)	- 54 -
4.6.4 Phase Four (Parameters Optimisation of a Double Sheets)	- 54 -
4.7 SAMPLES PREPARATION	- 54 -
4.8 MEASURING METHODS	- 55 -
4.8.1 Deformation, Kerf, Dross and Edge Offset	- 55 -
4.8.2 Heat Affected Zones (HAZ)	- 56 -
4.8.3 Microhardness	- 59 -
4.8.4 Measurement Handling	- 60 -
4.9 SUMMARY	- 61 -
<b>CHAPTER 5 DATA COLLECTION AND ANALYSIS</b>	<b>- 63 -</b>

5.1 INTRODUCTION	- 63 -
5.2 EXPERIMENTAL PROCESS	- 63 -
5.2.1 Phase One - Single Sheet Cutting	- 65 -
5.2.1.1 Deformation Measured	- 66 -
5.2.1.2 Heat Affected Zones measured	- 67 -
5.2.1.3 Parameters Optimisation and Analysis	- 69 -
5.2.1.4 Signal to Noise Ratio	- 69 -
5.2.1.5 Analysis of Variance (ANOVA)	- 72 -
5.2.1.6 Interaction	- 74 -
5.2.1.7 Three-Dimensional Surface Plot	- 75 -
5.2.1.8 Single Sheet Modelling	- 76 -
I. Assumptions	- 76 -
II. Mathematical Modelling	- 78 -
5.2.2 Phase Two – plasma Capability to cut through two layers.	- 87 -
5.2.3 Phase Three – Starting Reference	- 88 -
5.2.4 Phase Four – Optimising the Double sheets cutting	- 90 -
5.2.4.1 Surface Deformation	- 92 -
5.2.4.2 Dross	- 93 -
5.2.4.3 Kerf	- 93 -
5.2.4.4 Cut Edge Offset Between the Top and Bottom Sheet	- 94 -
5.2.4.5 Heat Affected Zones	- 95 -
5.2.4.6 Hardness	- 96 -
5.2.4.7 Variables Optimisation and Analysis	- 97 -
i. Signal to Noise Ratio	- 97 -
ii. Analysis of variance (ANOVA)	- 101 -
iii. Interaction	- 101 -
iv. Three-Dimensional Surface Plot	- 103 -
v. Double Sheet Modelling	- 104 -
5.3 CONFIRMATION TESTS	- 116 -
5.3.1 Single Sheet	- 116 -
5.3.2 Double Sheets	- 117 -
5.4 SUMMARY	- 117 -
<b>CHAPTER 6</b>	<b>PRACTICAL IMPLEMENTATION</b>
	<b>- 119 -</b>
6.1 INTRODUCTION	- 119 -
6.2 REAR FLOOR CHASSIS CUTTING	- 119 -
6.3 PLASMA CUTTING PROCESS AUTOMATION	- 122 -
6.4 CUTTING PROCEDURES:	- 124 -
6.5 SUMMARY	- 126 -
<b>CHAPTER 7</b>	<b>DISCUSSION AND CONCLUSION</b>
	<b>- 127 -</b>
7.1 CONCLUSION	- 133 -
7.2 LIMITATION AND FUTURE WORK	- 135 -
7.2.1 Limitation	- 135 -
7.2.2 Future Work	- 136 -
<b>REFERENCES</b>	<b>- 137 -</b>
<b>APPENDIX</b>	<b>- 148 -</b>
APPENDIX-A STAGES AND LINE LAYOUT	- 148 -
Table A1 Vehicle Conversion Process	- 148 -
APPENDIX-B DOUBLE LAYERED CUTTING AND TRIALS RESULTS	- 149 -
Table B1 Settings Used to cut two layers simultaneously.	- 149 -
Table B2 Settings Recorded for the Trials Performed Cut Two Layers Simultaneously at a Fixed Gap	- 149 -
APPENDIX-C SINGLE SHEETS PARTS SCANNED AND MATERIAL MICROSTRUCTURE	- 151 -
Figure C1 Parts Scanned for Deformation Single Sheets 0.6 mm, respectively (a) to (i) Represent Trial one to Trial Nine	- 153 -
Figures C2 Material Microstructure of the Specimens, Heat Affected Zones Width, (a) to (i) Represent Trial One to Nine	- 158 -
APPENDIX-D SIMULTANEOUS CUTTING OF TWO PARALLEL SHEETS USING TAGUCHI METHOD	- 159 -
Figure D1 Tests Result for the Experiments for differen models top and bottom view	- 159 -
Figures D2 Samples collected from the experiment, maximum deformation measured	- 164 -
Figures D3 Microstructure of the material and heat affected zones width	- 167 -

APPENDIX-E VALIDATION TESTS

- 168 -

Figures E2 Validation tests for the prediction model deformation sheet 0.6 mm and Heat Affected Zones - 171 -

Figures E3 Optimal parameters validation for double sheets cutting. Maximum deformation of the material and the heat affected zones. - 172 -

Figures E4 Validation tests for the deformation and heat affected zones respectively from trial one to six. Two sheets cutting simultaneously. - 175 -

## List of Figures

Figure 1 Schematic of the Floor Pan Fit	- 8 -
Figure 2: Gap between the chassis and the floor pan, (top view of the underbody floor)	- 9 -
Figure 2: Cutting profile.	- 9 -
Figure 3: underbody floor alteration, (a) seat rail sheet alteration, (b) chassis alteration during horizontal cutting	- 10 -
Figure 4: Edge deformation	- 11 -
Figure 5 Allied Vehicles (Van Chassis)	- 12 -
Figure 6: Overall design of the underbody frame chassis[23]	- 12 -
Figure 7:Underbody floor parts assembly[23]	- 13 -
Figure 8 Allied Vehicles cut out structure, (a) Ford model rear cut out, (b) Partner rear cut, (c) Partner front cut.	- 14 -
Figure 9: Cut dimensions (Allied Vehicles, Engineering Design Department, Partner Chassis Design, Solidworks). The figure was taken from Peugeot Partner floor vehicle chassis, dimensions are in millimeters	- 16 -
Figure 10: Plasma Arc Cutting, "Courtesy of TWI Ltd" [14]	- 28 -
Figure 11 CO <sub>2</sub> Laser technology [91]	- 29 -
Figure 12: Abrasive water jet head Injector [94]	- 31 -
Figure 13 Research Methodology and Process of the Thesis.	- 44 -
Figure 14 Ishikawa Diagram for Parameters Identification	- 47 -
Figure 15: CNC Plasma cutter	- 53 -
Figure 16: Samples Preparation Machines (AFRC). (a) Abrasive Sectioning Machine [165], (b) Mounting Press, (c) Grinding and Polishing Machine, (d) Samples Obtained	- 55 -
Figure 17 Atos 3D TripleScan (AFRC)	- 56 -
Figure 18 Leica DM12000 Microscope (AFRC)	- 57 -
Figure 19 Heat Affected Zones Size	- 59 -
Figure 21 Struers Durascan 70 Microhardness[175]	- 60 -
Figure 22 Measuring Equipment	- 61 -
Figure 23 Experimental Model, Separation into Three Zones	- 65 -
Figure 21 scanned part (Trial number one)	- 66 -
Figure 22 Trial 4 Heat Affected Zones Width for Single Sheet	- 68 -
Figure 23 Optimal Parameters for Sheet Deformation	- 70 -
Figure 24 Optimal Parameters for HAZ	- 71 -
Figure 25 Parameters Effect for Sheet Deformation	- 71 -
Figure 26 Parameters Effect for HAZ	- 72 -
Figure 27 Variable Interactions (Deformation)	- 74 -
Figure 28 Variables Interaction (HAZ)	- 75 -
Figure 30 3D Surface Plot HAZ	- 75 -
Figure 31 3D Surface Plot Surface Deformation	- 76 -
Figure 31 Residuals and fits graph for HAZ	- 77 -
Figure 32 Residuals and fits graph for surface deformation	- 77 -
Figure 33 Response prediction Surface Deformation	- 78 -
Figure 34 Response prediction for HAZ	- 78 -
Figure 35: First Experiment. (a) part Assembly, (b) Top Cut view of the test model, (c) Bottom Side View	- 88 -
Figure 36 Second Set of the Tests for Parameters Identification (Top View of the Model)	- 89 -
Figure 37 Second Set of the Tests for Parameters Identification (Bottom View of the Model)	- 89 -

Figure 38 Part Scanned for a double layered cutting. Trial Number one Lower Sheet Specimen	- 92 -
Figure 39 Offset Between the Top Sheet Cut Edge and the Bottom	- 94 -
Figure 40 HAZ Width Trial Seven Upper Side	- 96 -
Figure 41 Main Effect Plot S/N Ratio for the Top Sheet Deformation	- 99 -
Figure 42: Main Effect Plot S/N Ratio for the Top Sheet HAZ.	- 99 -
Figure 43 Main Effect Plot for Means Surface Deformation	- 100 -
Figure 44: Main Effect Plot for Means HAZ.	- 100 -
Figure 45: Gap Interaction for Top Sheet Deformation	- 102 -
Figure 46 Gap Interaction for Top Sheet HAZ	- 103 -
Figure 47 Surface Plot for Top Sheets Surface Deformation	- 104 -
Figure 48 Surface Plot for Top Sheets HAZ	- 104 -
Figure 49 Fits graph Surface Deformation	- 105 -
Figure 50 Fits graph HAZ	- 106 -
Figure 51 Residuals graph for top sheet Deformation	- 106 -
Figure 52 Residuals graph for top sheet HAZ	- 107 -
Figure 53 Probability Plot top sheets Deformation	- 107 -
Figure 54 Probability Plot top sheets HAZ	- 108 -
Figure 50 Peugeot Partner Chassis Cutting (a) Torch Position Before Percing (b) Plasma Torch During the Cutting Process	- 120 -
Figure 51 Different Cuts with or without Sealant Underneath the Sheet	- 121 -
Figure 52 Cut Edge Quality (Sealant underneath the material)	- 121 -
Figure 53 Quality Obtained after Sealant Removed using Sand Belt.	- 122 -
Figure 54 Vehicle Chassis (Allied Vehicles)	- 124 -
Figure 55 Cutting Profile.	- 124 -
Figure 56 Underneath the Vehicle Cut Profile	- 125 -

## List of Tables

Table 1 High steels grades[26].....	- 14 -
Table 2 Tool Requirements.....	- 18 -
Table 3 Cutting Techniques Comparison .....	- 32 -
Table 4 Quality requirements (Allied Vehicles) .....	- 50 -
Table 5 Mechanical Properties[178].....	- 63 -
Table 6 Parameters and their levels.....	- 65 -
Table 7 Experimental Layout.....	- 66 -
Table 8 Deformation results (mm) .....	- 67 -
Table 9 Heat Affected Zones Measured .....	- 68 -
Table 10 Data Collected from the tests.....	- 69 -
Table 11 S/N Ratio for Sheet Deformation.....	- 70 -
Table 12 S/N Ratio for HAZ.....	- 70 -
Table 13 Contribution Effect .....	- 73 -
Table 14 Data Parameters and Observations .....	- 83 -
Table 15 CNC Plasma Tests 1 results .....	- 88 -
Table 16 CNC Cut Test 2 results .....	- 90 -
Table 17 Number of Parameters and levels .....	- 90 -
Table 18 Experimental Layout.....	- 91 -
Table 19 Surface Deformation .....	- 92 -
Table 20 Dross Size.....	- 93 -
Table 21 Kerf Width.....	- 94 -
Table 22 Cut Edge Offset Deviation .....	- 95 -
Table 23 HAZ Width.....	- 96 -
Table 24 Hardness test values and percentage of change .....	- 97 -
Table 25 S/N Ratio for the Top Sheet Deformation .....	- 98 -
Table 26 S/N Ratio for the HAZ .....	- 98 -
Table 27 Effects Contribution.....	- 101 -
Table 28 Data Parameters and Observations .....	- 110 -
Table 29: Estimation values.....	- 115 -
Table 30 Optimal parameters tests .....	- 116 -
Table 31 Predicted Tests Analysis .....	- 116 -
Table 32 Optimal parameters tests .....	- 117 -
Table 33 Predicted Tests Analysis .....	- 117 -
Table 34 Feed Rate and Trajectory of the Robotic Arm.....	- 126 -

## **Nomenclature**

AV: Allied Vehicles  
AHSS: Advanced High Strength Steels  
AWJ: Abrasive Water Jet  
ANOVA: Analysis of Variance  
ASSY: Assembly  
AFRC: Advanced Forming Research Centre  
BIW: Body in White  
CO<sub>2</sub>: Carbon-dioxide  
CNC: Computer Numerical Control  
DOE: Design of Experiment  
Det: Determinant  
EDM: Electro-Discharge Machining  
ε: Error Term  
GPS: Giga Pascal Steel  
HSS: High Strength Steels  
HD: High Density  
HAZ: Heat Affected Zones  
L: Left Side  
Ltd: Limited Liability  
MPV: Multi-Purpose Vehicle  
MRR: Material Rate Removal  
MLR: Multi-Linear Regression  
Min: Minimum  
Max: Maximum  
OEM: Original Equipment Manufacturer  
OA: Orthogonal Array  
PCMM: Portable Coordinate Measuring Machines  
R: Right side  
SUV: Sport Utility Vehicles  
S/N: Signal to Noise Ratio  
SSE: Sum Squared Error  
SST: Sum Squared Total Error  
T: Transpose  
TWI: The Welding Institute  
USLAB: Ultralight Steel Auto Body  
UHSS: Ultra High Strength Steels  
UV: Ultra-violet  
UK: United Kingdom  
WAV: Wheelchair Accessible Vehicles  
YS: Yield-Strength  
3D: Three-Dimensional  
2D: Two-Dimensional

## List of Publication

- An abbreviated version of the research part of this thesis was published in a peer reviewed journal.

1. Name of the journal: **Journal of Manufacturing Processes (Elsevier).**

Title of the article : “**Experimental investigation of plasma cutting two separate thin steel sheets simultaneously and parameters optimisation using Taguchi approach**”.

Date Published: 27/01/2021

The article can be found online in : <https://doi.org/10.1016/j.jmapro.2021.01.055>

2. Name of the Journal: **Advances in Mechanical Engineering (Sage).**

Title of the Article: " **Optimisation of cutting parameters and surface deformation during thin steel sheets plasma processing using Taguchi approach**".

Date Published: 16/06/2021

The article can be found online in : <https://doi.org/10.1177/16878140211030401>

# Chapter 1

# Introduction

## 1.1 Overview

Wheelchair Accessible Vehicles can be defined as the cars or vans that have been modified by engineers to allow a disabled person to travel in their wheelchair safely. This can be achieved by lowering the floor and assembling a new customized (manual or automated) ramp for an easy access at the rear or side of the vehicle. The business of converting vehicles started at the end of the 2<sup>nd</sup> world war just after the appearance of the National Health Service when help was needed for the handicap and injured patients [1]. The market has kept growing as the demand for these vehicles among wheelchair users was increasing. The market in the UK is expected to increase at rate of 5.7% for the coming year up to 2025 [2].

Allied Vehicles Ltd is one of the UK leading manufacturers of wheelchair accessible vehicles, founded in 1993, since then the business was growing consistently. The annual turnover of Allied Vehicles is just over £150 million. The company converts around 100 vehicles each week [3]. Due to the increase of the demand, the company needs to enhance their production lines and look for new possibilities to improve the conversion process.

The major issue encountered during the conversion process arises from the cutting stage due to the complexity of the task and time consuming. The tools used to process the chassis were found to have limitations. To perform a cut out on the underbody rear floor usually a circular saw is used. However, some areas in the chassis are composed of a three-dimensional structure e.g., double-layered zones, rails and box sections, these structures are very challenging and cannot be cut easily using manual tools and often leads to deformation at the edge of the material, profiling issues and lack of accuracy.

Three-dimensional structures such as hydroformed or stamped sheets used in the vehicle chassis are necessary. The evolution of the vehicles during time has resulted in an increase in mass due to technology progress and parts added to the car [4]. Therefore, these structures play a big role in reducing the weight of the vehicle and the environmental impact of carbon dioxide (CO<sub>2</sub>) emission. These structures can also offer a higher stiffness. Hence, they are extensively used in the automotive industry [5].

Sectioning the underbody chassis vehicle can be a complex task as it requires first a good knowledge and specialized equipment [6]. Therefore, finding an adequate method for cutting or trimming in a fast and efficient manner is highly desirable in the production line, especially when profiling is involved or when material deformation at the edge of the cut needs to be avoided [7]. These problems are also common in similar industries where traditional tools are used. Therefore, there is a need to develop a new and efficient cutting methods [8]. When the process involves contour cutting, usually a second process to clean the edge from burrs, constant sharpening or changing the blades is required [9]. Cutting with thermal methods can also result to a deformation of the material, but the tests showed that the level of deformation is smaller compared to mechanical cutting [10].

The proposal of this thesis was to identify an alternative solution that can be used to overcome the issues encountered during the cutting stage, as traditional methods were found to be limited and time consuming [11]. These problems are encountered due to the complexity of the chassis structure, for instance 3D-structures, hydroformed sheets and multi-layered zones. To select the suitable cutting tool, a comparative study between methods (e.g., plasma and laser technology) were made. However, this highlighted also a lack of knowledge using these techniques when complex structures are processed [12]. Therefore, tests are necessary to widen our understanding regarding processing these structures.

The motivation of this study was primarily to investigate the plasma cutting as an alternative cutting tool to a traditional method for the WAV industry. Plasma is known as a fast process and widely used in the industry for metal cutting. However, there is a lack of knowledge and scientific publications about how this technology performs when cutting multiple layers is required. The common technique used in the market nowadays for thin sheet metals cutting is a laser [13], this technique is widely used in the automotive industry for trimming, profiling and drilling the hydroformed sheet structures with an excellent quality [14]. Laser technology can result to less heat impact on the material compared to plasma or oxyfuel cutting [15]. However, this technique is not a cost effective for all businesses [16].

Plasma technology was found to be productive [8] but similarly to laser they are only known for linear cutting in one plan (X, Z axis). There are no documentations available about plasma cutting in two plans, in this case usually mechanical methods (AWJ or Saws) are well known to cut these structures [17]. Some publications emphasized that plasma processing three-dimensional structures is an area of research in the automotive industry which is not documented [12]. Therefore, investigating on this technology to expand the boundary of its application was required. Furthermore,

it is necessary to find the best way to optimise the plasma cutting process and minimize the resulted defects and ensure process accuracy. Research made by A. Klimpel et al [15] on cutting materials highlighted that there is a lack of knowledge on how to optimise the machine for a specific material or thickness as the manufacturers do not provide this information. Therefore, it is necessary to conduct an experimental research analysis to achieve acceptable quality. Research questions of this study can be summarized as follows:

- Would that be possible to cut simultaneously two separate sheets with an air gap using plasma technique? In other words, examining the possibility to re-use the energy heat exiting the kerf of the first sheet to perform a cut on the second layer.
- What would be the effect of the heat generated during the plasma processing on thin material? primarily in the range of 0.6 or 0.7 mm, this material thickness can be altered easily if a high quantity of energy is transferred instantly to the surface of the material, phenomenon such as surface deformation can occur.
- What would be the size of the heat affected zones generated during the cut? this can identify if a second processing is required to remove the altered area that undergo a microstructure change.
- Is there a possibility to optimise the cutting process in two plans and reduce the resulted phenomena to a minimum level?
- Does plasma simultaneous cutting of two sheets cause a deviation (edge offset) between the top sheet layer edge of the cut and the bottom and what would be the material loss level?
- What would be the relationship strength between plasma parameters and the quality?

## **1.2 Research Aim and Objective**

The aim of this thesis was to investigate on the possibility of plasma to cut two separate thin sheets with an air gap distance simultaneously and assess the impact of the heat on thin materials. In addition, optimising the process of cutting to reduce the phenomena such as surface deformation and HAZ to a minimum degree possible and analyse the quality resulted. Assess the relationship strength between the input variables and the output response. To fill this knowledge gap, an experimental investigation was performed to evaluate the possibility to re-use the plasma heat energy exiting the first layer to cut through a second sheet and achieve an acceptable quality. The main objectives of the thesis can be summarised as follows:

- Analyse the suitability of plasma technique to process thin materials under one millimetre.
- Use Design of Experiment based on Taguchi parameters design method to perform tests and extract data on the level of deformation and HAZ size.

- Identify The most influential parameters affecting the phenomena and assess the possibility to minimise the defects.
- Create a 3D structure experimental models to assess the possibility of plasma to perform a cut in two sides with one pass.
- Assess the possibility to optimise the cutting process of a three-dimensional structure using DOE based Taguchi technique and identify the parameters that have the most effect on surface deformation and HAZ.
- Assess the relationship between the plasma parameters and the phenomena resulted from the cutting process.
- Evaluate the feasibility of the technique and findings on real chassis.

The research was made in progressive four stages, the first step of the experiment was necessary to identify the suitability of plasma to cut a thin single sheet 0.6 mm without altering the material (this was the minimum sheet thickness value measured in the floor chassis). This required to assess the effect of the heat generated during the cut on the surface material deformation, followed by optimising the settings, as previous research [18] raised that sheet deformation issue might result if unsuitable parameters are used. Furthermore, HAZ was measured to evaluate the edge alteration, this would give an indication if a second processing is required. The second stage was to problem solve the unknown cutting process (double layered cutting) and identify if plasma capability. A model was assembled for this experiment using two identical sheets to create a 3D-structure, trial and error technique was adopted in this stage until obtention of the desired results (cut in two sides). The gap was incremented to find the maximum gap that can be cut. The third tests were made to identify the suitable parameters necessary to cut two layers for a fixed gap (20mm), this would be used as a starting reference for the optimisation of a double sheets cutting. The last stage of experiments was made to optimise the double sheet cutting and identify the key parameters influencing the process.

Three different models were built for the optimisation stage using three different gaps (three levels). Taguchi parameters design approach was selected to perform nine trials. ANOVA was used as method for the analysis and to identify the effect significance. The quality obtained was assessed mainly dross size, kerf width, cut edge offset between the two layers, material hardness, sheet deformation and heat affected zone width. The cut edge offset analysis between the top and bottom sheet was carried out in this study to assess if the two edges were aligned properly as this could

cause an engineering problem. Regression models were constructed using the least square method to assess the strength relationship between the input and output variables.

Additional tests were carried out to confirm the results and verify the level of improvement of the optimal parameters obtained, and also to test the accuracy of the mathematical models constructed. Finally, trials were performed on a rear floor chassis to assess the practicality of the findings

### **1.3 Structure of the Thesis**

The concept of this thesis was organised as follows:

- Overview of the work
- Industrial context
  - Conversion process and production line issues.
  - Problem Identification (cutting process).
  - Identify potential alternative tools to overcome the issues encountered before.
  - Techniques used in other companies to process the vehicle chassis.
- Literature review and knowledge gap identification
  - Identifications of the most used techniques in the automotive industry.
  - Cutting techniques evaluation and identification of the most suitable technology that can be used at Allied Vehicles Ltd.
  - Plasma cutting related research and identification of the gap knowledge
- Establish the adequate research methodology
  - Hypothesis identification
  - Choice of the research method and Design of Experiment selection for data collection.
  - Identification of the input parameters and the output result.
  - Establish of the necessary tests required.
  - Selection of DOE based on Taguchi method parameters optimisation
  - Assess the most influential parameters on the output result using Analysis of Variance.
  - Analysis of the relationship between the parameters and the quality cut obtained using multi-linear regression.
- Experimental set up and construct the necessary experimental models.

- Perform the tests.
  - Extract the necessary data.
  - Evaluate the quality and optimise the plasma process
  - Construct the mathematical models.
  - Assess the level of the improvement using optimal parameters.
  - Test the regression models
- Testing plasma on real chassis for practical implementation.
  - Interpret the results and identify the limitation of this research and potential future work.

## **Chapter 2 Wheelchair Accessible Vehicles Industrial Context**

### **2.1 Introduction**

The aim of this chapter is to overview the production process adopted at Allied Vehicles to convert their cars into wheelchair accessible vehicles. This section of work intended also to illustrate the issues encountered during the cutting stage. The line analysis at Allied Vehicles showed that the dominant problem lay in the cutting stage due to the complexity of the task. This can result to an increase of the vehicle cycle time, in addition to queuing problems generated after this stage. Overall, the vehicles experience three different main phases, including parts removal, structure modification and then assembly stages. The study looked to similar industries in the UK and also to the main leading converters in the world, as this would help to evaluate and contrast the conversion process.

### **2.2 Allied Vehicles conversion process**

The conversion process at AV can be classified into four categories; the first phase is vehicle preparation, this includes the removal of carpets, rear seats and bumpers, fuel tank, trims, exhausts and brakes pipes, underbody shields removal and bracing fit, and then followed by a second phase of chassis alteration, the third phase includes mechanical ASSY and then electrical ASSY. Full detail is illustrated in the [APPENDIX-A TABLE A1](#). This table shows different stages and time spent to perform the tasks, including queuing time involved after each stage, parts removed or added for each station.

### **2.3 Cutting Stage Issues**

A schematic of the floor pan that is fitted on the vehicle chassis is illustrated in the Figure 1 below, Area close to the cut edge required to have a small deformation. A good flatness of the floor chassis around the edge area of the cut out would provide an effective fitment and sealing between the chassis and the new customized floor pan. In case of using plasma cutting, the HAZ around this edge also required to be very small (as specified above in section 2.6). Failure to achieve the tolerance would lead to further issues when fixing the pan using rivets between (sealing issues and vibrations). In addition, Dross needed to be small to avoid a second processing to clean the edge. The main issues

identified at Allied Vehicle's conversion line mainly at the cutting stage can be summarized as follows:

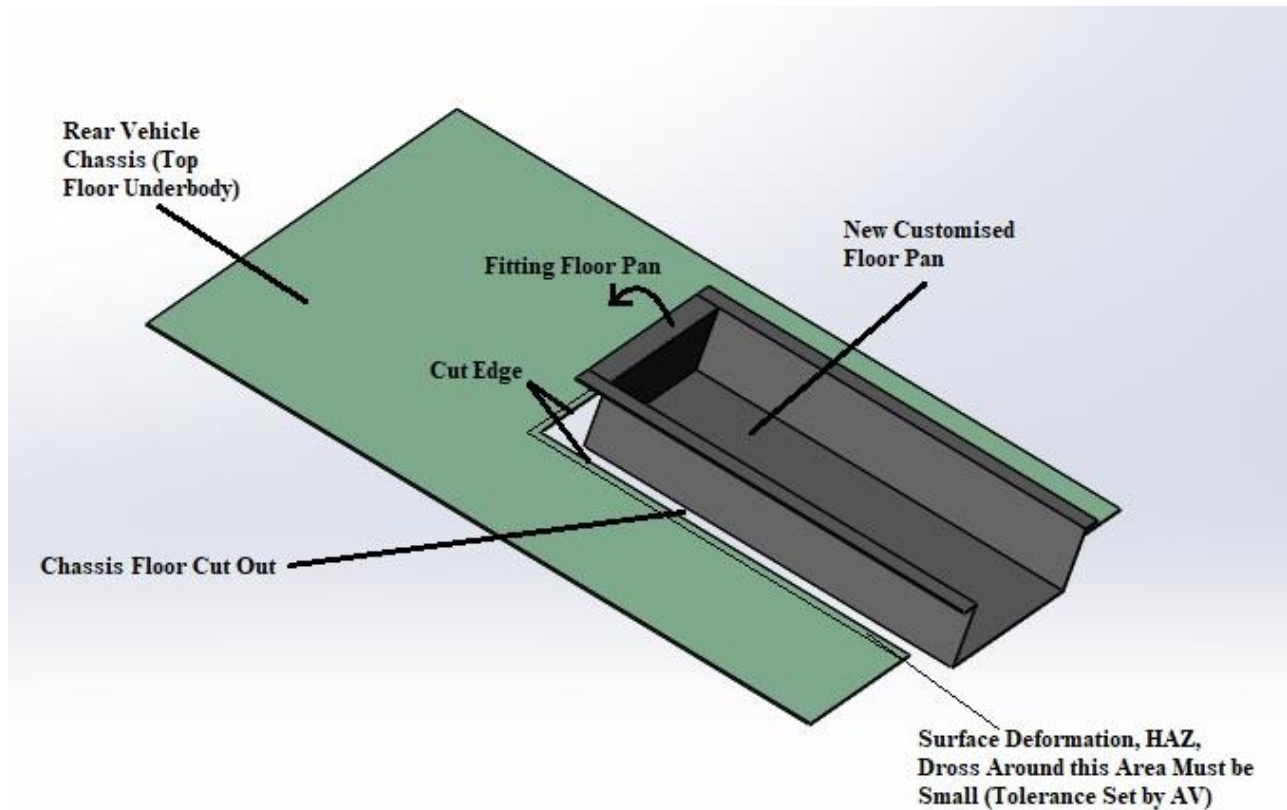


**Figure 1** Schematic of the Floor Pan Fit (Solidworks)

- Slow cutting process and unpredictable, average 45 min for a full cut (this was measured multiple times using stopwatch at the shopfloor). This requires additional stages sometimes to cover the daily target (Eight vehicles a day for Partner).
- Tolerances ([described below in Section 2.6](#)) were practically difficult to achieve using current cutting tool (traditional cutting method e.g., circular saw, grinder, jigsaw) [19].
- Difficult to maintain a straight cut and follow the cutting path [20].
- Gap between the cut line edge of the vehicle and the ramp assembled can sometimes be wide up to 5 mm in each side. See Figure.1 below.



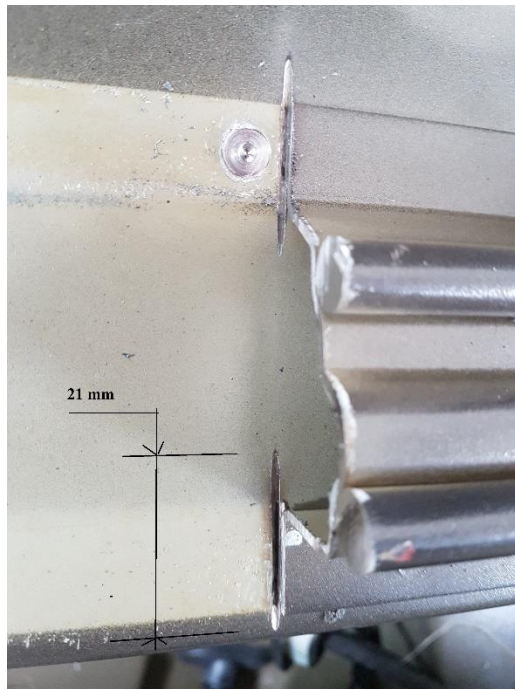
**Figure 2:** Gap between the chassis and the floor pan, (top view of the underbody floor)

- Profiling accurately using circular saw is practically not possible. Corners showed an alteration as shown in the Figure 2 below.

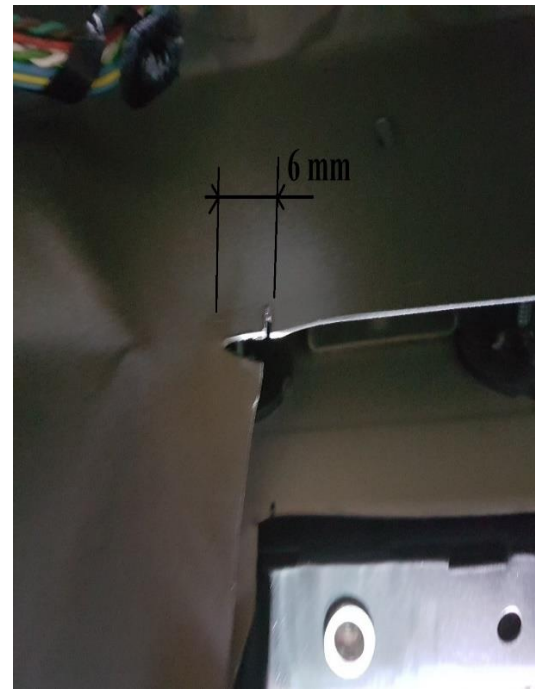


**Figure 3:** Cutting profile.

- The vehicle chassis can be altered when using circular saw. Figure 3 (a) illustrates the seat rail after the cutting process, the blade of the tool can scratch the material of the second sheet. Figure 3 (b) shows the final cut out obtained, the blade is altering the chassis, this cannot be avoided when using circular saw, this can happen when processing corners, angles or cutting horizontally.



(a)



(b)

**Figure 4:** underbody floor alteration, (a) seat rail sheet alteration, (b) chassis alteration during horizontal cutting

- Deformation of the chassis at the edge of the cut (Figure. 4), this is a common problem using mechanical tools. This problem was extensively emphasised by other researchers when cutting thin sheets [7]. The tool when used for a long period can be excessively exhausting.



**Figure 5:** Edge deformation

- Human labour limitation, this includes exhaustion, time consuming, potential injuries, uncontrolled breaks and operators' shortage.
- To perform a full cut out, the engineer must cut in both sides of the underbody from the top floor and from the underneath due to double layered zones. The vehicle is required to be lifted multiple times up and down. These tasks can put the engineer at risk of injury especially when processing restricted zones.
- Tool size and weight which prevent the engineers performing the task efficiently. This tool can go out of control sometimes during the cutting.

## **2.4 Chassis material**

The Monocoque (French word that means Single Shell), Unibody or integrated structures is the most used chassis in the automotive industry nowadays [21]. It consists of an assembly of the frame which is mainly made of hydroformed parts such as box section, rails, gussets and stamped steel panels. All parts are joint together to form a single body using spot welding techniques mainly as this process is found to be suitable for the steel metal sheets assembly [2]. This type of chassis has the advantage of reducing the vehicle weight. The top sheet parts of the chassis body and the side parts contribute to the torsional stiffness and vehicle bending [3]. The vehicle structure was also known for their ability to give a better protection against collision [22]. Figure 5 below illustrates the type of chassis processed at Allied Vehicles.



**Figure 6** Allied Vehicles (Van Chassis)

The structure of the chassis can be different from vehicle to another, depending on the category, size and the loads required. The underbody frame is made of multiple parts called sub frames as shown in the Figure 6 below where 1 and 2 are the cross member and 3 L/R are the side members (Left and Right side), cross members are joined to the side frame by an intermediate plates called Gussets [23].

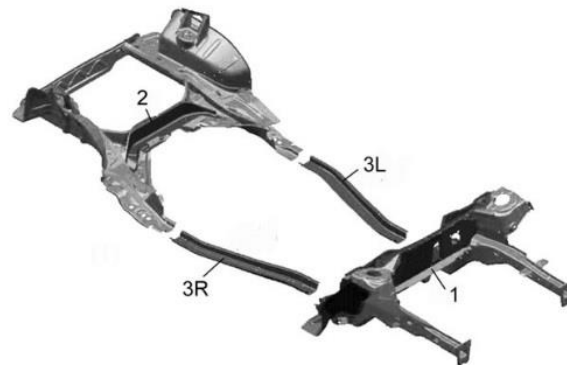


**Figure 7:** Overall design of the underbody frame chassis[23]

To form the underbody, several sheets and parts are welded to the frame as shown in the Figure 7 below. For a typical car, the underbody is formed in overall with part 1 which is the underbody frame, 2 is the front floor, 3 is the rear seat cross member, 4 and 5 are the rear floor front and back side, 6 is the dash top panel (water box), 7 L/R are the Rocker panels, 8 L/R are the front inner body sides, 9 L/R are the strut towers reinforcement, 10 L/R are the upper rails boxing.

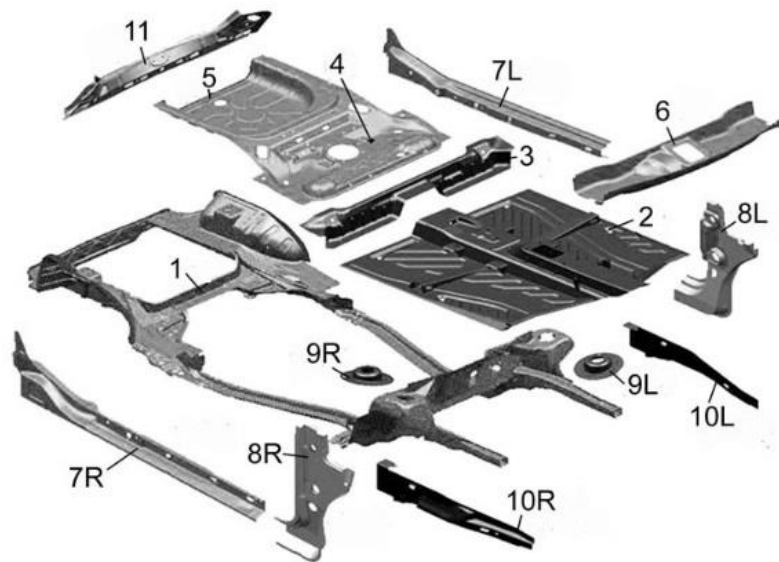


**Figure 8:** Underbody floor parts assembly[23]

Allied Vehicles underbody chassis structure is composed of a larger frame, rails and has a flat rear floor. This would provide an increased space and accommodate more seats, known as people carrier vehicles. The structure of the vehicle is depending on the size, load and brand. The chassis frame for these models needs to be designed differently (at the rear side) compared to the conventional structure, as this would help to reduce the vehicle's weight and also to give them the stiffness required to make the entire body an ideal lightness and strength [4]. Rear frame and cross member parts have different shapes and larger cross section [4] depends on the size and load as shown in Figure 8.



*(a)*



*(b)*



(c)

**Figure 9** Allied Vehicles cut out structure, (a) Ford model rear cut out, (b) Partner rear cut, (c) Partner front cut.

There are 35 worldwide steel sheet manufacturers (from 18 countries in North America, Europe, and Asia). They have collaborated to reduce the body structure mass while at the same time preserve the safety of the vehicle, performance and comfort at no cost. ULSAB consortium (program) was working for years to find solution to the challenges, reduce weight, cost effectiveness, material selection, optimise the body design, a better strength and structure performance are the main concerns. After 15 months of work in 1995, the research mainly lead by Porsche Engineers, ULSAB consortium have managed to decrease by 25% the weight of the vehicle's body structure considerably compared to the conventional design [5]. The material used for the chassis is named High Strength Steels (HSS), the main grades [24] are shown in the Table 1 below. Any steel less than 210 MPa YS is considered as Mild Steels [24].

**Table 1** High steels grades[24]

High Steel Grades	Yield Strength (MPa)
HSS	210 <YS< 550
AHSS	YS>550
UHSS	YS>780
GPS	YS>1000

These optimised steels (Soft mild steel, reduced in carbon) are mainly designed to offer a high strength with a minimum weight ratio. The more advanced and optimised UHSS grades are competing with the Aluminium structure chassis (considering all the aspects such as cost, weight and strength). BMW i8 all aluminium chassis incorporated in their structure around 40% of the new grades of UHSS [6]. Approximately 90% of the body structure were made from ULSAB designed steels grade, this can reduce the weight body by a quatre [24].

## **2.5 Adhesive and sealing**

It is important to understand the type of coating applied to the underbody as this could affect the cutting process. These layers added to the material surface can serve as a protection against corrosion and stones impact. To prevent the body in white from corrosion, chipping or water penetration, the assembled chassis vehicle undergoes several steps, pre-treated at the beginning (BIW stage), cleaned from any oil and welding residues. The first action the engineers take after the pre-treatment stage is the protection of the BIW against corrosion, this operation is called sinking stage, the chassis is submerged in three different baths, degreasing, conditioning and phosphating. The following step is the electrodeposition bath stage to give the structure an additional strength against the corrosion. Poly Vinyl chloride sealing is applied after to close the gaps between sheets welded and prevent them from water penetration, this sealing is beneficial also to protect against chipping and reduce vibration noise in addition protection against corrosion. Primer is added to the surface to give them a smoother finish and strengthen the first layers, this also helps the structure to fight against chipping, flying stones in addition to fighting corrosion. Coating is applied afterwards on the surface, including basecoat (for the colour appearance) and clear coat to prevent the chassis from UV lights and environmental effects [25]. Special treatment is given to the underbody to fight corrosion as this is subjected to water, humidity, road salt, and stone impacts from the underneath, usually an additional protection such as asphalt based materials, polyvinyl chloride, polyurethane and wax are used [2] [9].

## **2.6 Requirements and Tolerances**

Figure 9 below illustrates all the main dimensions of the cut out required for fitting a new customized floor pan. Cutting tolerance (cut out) set by the engineering designers at the Allied Vehicles company is  $X^{+/- 1.5 mm}$  mm, this means in this experiment that for a part size of 40 mm width, it is acceptable to achieve 41.5 mm as the maximum value and also it is acceptable to achieve 38.5 mm as the minimum value, for the length of 150 mm size, anything between 148.5 to 151.5 mm is acceptable.

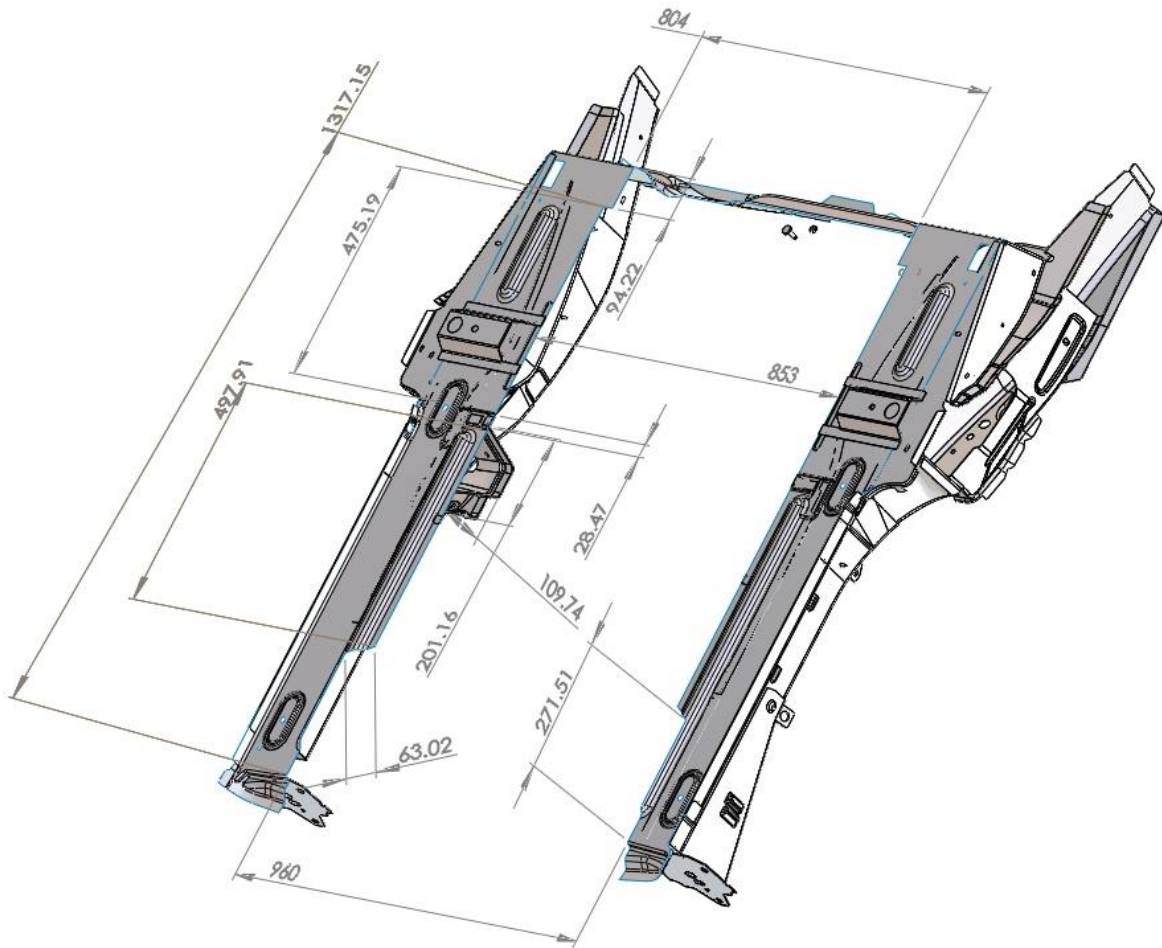


**Figure 10:** Cut dimensions (Allied Vehicles, Engineering Design Department, Partner Chassis Design, Solidworks).  
The figure was taken from Peugeot Partner floor vehicle chassis, dimensions are in millimeters

To identify the alternative cutting tool to traditional method, it was necessary first to understand the nature of the cut performed and the requirements. A summary of the cut-out characteristics are given as follows:

- The tool needs to move in 3D plan to perform the cutting (multiple sheets) (See.Figure.9 above).
- Profiling required (including cutting in angles).
- Curved surface.
- Non-homogeneous thickness, 9 mm in some zones where 3 sheets are welded together (measured using calliper).
- The material is thin, thickness of the sheets vary between 0.6 mm to 3 mm [26].
- The largest sheets on the underbody top floor were measured 0.7 mm [26].
- The materials are coated and painted.
- Presence of the sealant material in some areas underneath the sheets.

The requirement (See Table 2 below) of the alternative tool needs to have the ability to deal with the main points highlighted above in addition to work and respect the tolerances set by the company for the cut, the criteria of the tool can be summarized as follows:

- Ability to cut thin thicknesses from 0.6 mm to 9 mm.
- Ability to cut through coated and painted sheets.
- Ability to cut through sandwich material.
- Profiling ability.
- No second processing is required or minimal.
- Minimal deformation (in current method 5mm of deformation can be seen in some areas, mainly at the angles of the cutting profile)
- Process in dry conditions.
- Automation possibility.
- Three-dimensional structures cutting capability.
- Ability to access restricted areas underneath the vehicle.
- Process all vehicle models.
- Fast cutting (Circular saw requires an average time of 45min)
- Safe Process
- Environmentally friendly
- Cost effective (cost of operation / implementation)
- Reduce the processing time.
- Able to cut non-homogenous sheet thicknesses and surfaces.

**Table 2** Tool Requirements

Criterion	Tool Requirements
Multiple Sheets	2 Sheets Simultaneously
Thickness	0.6 mm minimum
Cutting Plan	3 Dimensional (X,Y,Z)
Sandwich Material	Yes, Including Sealant and Paint
Deformation	0.2 mm for Single Sheet/ 0.5 mm Double Sheets Cutting.
Condition of Cutting	Dry
Drive	Automatic
Feed Rate	High
Homogenous thicknesses	Varying up to 9 mm
Target of Time Reduction	At least ½ Time
Profiling	90° Angles

The quality and Tolerances set by the quality are summarised below:

- Part size accuracy  $X^{+/- 1.5 mm}$  mm for both single sheets cutting or double sheets cutting (top layer only).
- Maximum deformation in single sheet cutting is 0.2 mm and heat affected zones width 0.2 mm.
- The deviation between the top sheet cut edge and bottom (offset) 2 mm maximum.
- Maximum deformation for double sheet cutting is 0.5 mm (top sheet) and heat affected zones width is 0.2 mm (top sheets).
- Dross size maximum of 1 mm.

## 2.7 Related work

A comparative study was performed in this section to understand how similar businesses are converting their vehicles. In the UK there are around 20 manufacturers approved and involved in motability program scheme to convert vehicles [27]. These companies can be slightly different

depending on their expertise which is necessary to cover customer's requirements and needs. The converters manufacture different vehicle brands, wheelchair accessibility (whether rear, side, or dual entry), ramp or lifting equipment, type of adaptation required and whether travel upfront, rear or drive. Below are the list of the main manufacturers in the UK and also lead converters worldwide [28].

Gowings Manufacturer started their business in the field of conversion in 1960, the company was the first to join the mobility scheme in UK, based in Berkshire England, their main brands are Peugeot, Fiat, Renault, Vauxhall and Ford [29]. The process of conversion adapted at Gowings is similar to Allied Vehicles rear side entry models, it begins (after purchasing a base vehicle from one of their suppliers) by stripping the interiors and covering the sensitive parts, then the vehicle is lifted to proceed for the underside removal, this includes also fuel tank, exhausts, brake pipes. To cut out the floor, both circular saw and jigsaw were used for sectioning the original manufactured underbody chassis. The engineers proceed then for rebuilding process, the vehicle undergo changes through the production line and a new reconfigured lowered floor is implemented. Some parts are modified to adapt the new reconfiguration, this would give the wheelchair users an extra room and a better visibility inside the car. The final stage is quality control and test drive then stored in the yard [30].

Brotherwood is one of the largest manufacturers in the UK based in Dorset, with 35 years' experience in the field. To convert their vehicle the car moves through 10 different stages. Research and development team take approximately 18 months for a new vehicle to be completely designed, then the vehicle is prototyped and tested for 190 kg wheelchair. The conversion starts in the shop floor by stripping the inside and underneath car. The company removes also the front seats, then using a saw [31] the rear floor chassis car is sectioned at the rear side and replaced with new reconfigured floor, then the process of the re-build begin. Similar to allied vehicles, some original parts are kept, and the rest are redesigned to fit the new lowered floor model e.g., fuel tank and exhaust. Once the rebuild is achieved the car is sent to the quality control department followed by a test drive [32]. Brotherwood converter has the experience also to convert and lower the rear chassis floor of an electric vehicle in the UK, Nissan eNV-200 Combi, this gives them an edge of expertise over Allied Vehicles.

Sirus Automotive is one of the leaders in wheelchair accessible vehicles in the UK. Headquartered in Wednesbury, established in 2004, known for their converted vehicle best seller Renault Kangoo. The company received the queen's award in 2009 for their product innovation. The company has the experience to manufacture side or rear entry with the possibility of the wheelchair to move up front [33]. The process of conversion starts by stripping the car from the inside, taking front seats out, then

the car is lifted from the ground to remove the underneath parts including fuel tank, exhaust and other parts which requires reconfiguration [34]. The cutting tool used for sectioning is a circular saw, engineers proceed for a cut out at the rear followed by a cleaning, parts assembly, vehicle rebuild, quality check and test drive [35].

Bristol Street Versa have been in the business for more than 25 years, headquartered in West Yorkshire England. The company is the 6<sup>th</sup> largest retailer in the UK, specialised in rear and side entry, their main brands are Ford Connect, VW Caddy, Transporter and Caravelle, Renault Master and Traffic. After stripping the floor and the undersides, the engineers use jigsaw and a circular saw to cut out the floor, sectioning is also performed on the structure wall of the car, an opening is performed using jigsaw in the rear sides wall of the vehicle to add a new windows to offer a better visibility for the wheelchair users [36]. New reconfigured and OME parts (original manufacturers equipment) are then assembled. Lastly, the vehicle undergo a quality check and test drive then shipped to customer [37].

Lewis Reed process also their models in the same method as other converters, stripping the inside and underside of the vehicle, cutting out the floor with a circular saw [38]. The floor pan is replaced with a customised ramp and module. The rebuild process includes putting back the original and non-original parts. To check if the vehicle is converted adequately an in-depth quality check is performed and then sent to a test drive. Lewis Reed Group is also one of the leading companies that manufacture Wheelchair Accessible Vehicles, based in Bromborough, with 20 years' experience in the field, specialised in both side and rear entry, the vehicle can be manufactured with a choice of ramp or lifting device, also with the choice of rear, upfront or drive option. The main vehicle brand used are Mercedes, SEAT or Volkswagen [39]

TBC Mobility Conversion is a large converter of WAV in the UK, founded in 2006, they possess two main factories based in Bromborough in England and Co-Tyrone in Northern Ireland. TBC are well-known for their best seller Volkswagen Caddy Maxi Life, Citroën Berlingo. Awarded in 2012 from Motability as the national supplier. The company can convert with a choice of rear passenger, front passenger or drive from wheelchair, with the option of automated or manual wheelchair vehicle access device at the rear or side Door [40]. The conversion process is also similar to other manufacturers, sectioning the floor is performed using a manual tools, then followed by a rebuild stages and quality control [41].

Braun Ability is one of the world leaders in the field of wheelchair accessible vehicles [42], providing products to more than 70 country, founded by Ralph Braun in USA, started their business in 1972, known for the state of the art manufacturing. The company was the first to build a Tri-Wheeler battery motorised scooter. Their main vehicle brands used on the shop floor are Chevrolet, Toyota, Dodge, Honda and Chrysler with the possibility of manufacture a side or rear wheelchair access, also with the choice of manual or powered ramps [43]. The company does not only converts vans, mini-vans or buses but also for disabled customers who prefers other type of vehicles such as SUV models giving the Braunability an edge in the conversion field [44]. The components needed for the conversion are mainly customised in-house to insure the best quality [45]. Contrary to manufacturers mentioned before where only part of the rear floor is sectioned, Braun process their floor differently, the entire floor is removed, giving the vehicle an extra room inside after fitting the reconfigured parts [46]. The company can produce the most spacious vehicles in the market [47]. The overall conversion process remain the same in overall [48], begun by stripping the entire interiors and undersides, then bracing from the inside to keep the shape of the structure stable, then using mechanical tools a few cuts are made at a specific areas, spots weld drilled then the entire floor is removed. A new reconfigured 8" lowered floor is then replaced and fitted, welded to the vehicle chassis, followed by a build-up component through different stages. The vehicle is then quality checked and drive tested [49].

VMI Mobility is one of the largest manufacturer in the world based in Arizona, USA, they have more than 25 years' experience converting vehicles [50]. The company can manufacture rear or side entry accessibility using a manual or motorised lifting device. The factory uses state of the art technology to convert the cars, building their own vehicle floor inside the factory using robotic arms for joining and spot welding the sheets. The conversion begins by removing all the insides, trims, carpet, wires and original front and rear seats exposing the structure of the car, and then the undercarriage parts. Some sensitive areas of the car are covered, then a bracing system is used to prevent the structure chassis from deformation after the cut out. The vehicle is moved then to the cutting station, the process of the cut adopted in this company is different than all the other companies. The entire floor is removed by using state of the art technology welding technique to separate the floor from the frame [51], this required to application of the heat to remove the welding material from the sheets and then dismantle the floor completely from the chassis [52]. A new reconfigured (homemade) floor is welded carefully to the chassis to give more room to wheelchair users. The benefit from reconfiguring the whole floor is the flexibility to redesign their own components required for the assembly, this would give the vehicle an original look at the end of the process. After the cutting stage, vehicles are rebuilt throughout the assembly line adding progressively their home-made components, each part

added is controlled and measured using a Portable Coordinate Measuring Machines (PCMMs) to insure a best fit. The cars finish their pathway with quality check and test drive [53].

Rollx Vans, is one of the American converters based mainly in Minnesota with the experience of converting over than 45 years. The main vehicle brands used are Chrysler, Dodge, Toyota, Honda for minivans, and Ford, GMC, Chevy and Dodge for full size van vehicles. The products can be manufactured with rear or side entry, manual ramp or powered lift, with the choice of rear, front passenger fit or drive from wheelchair [54]. The conversion of the minivan undergoes 23 stages in overall using the state-of-the-art conversion techniques. The steps followed are similar to VMI. The interiors are first stripped including front and rear seats, all the underside parts are also removed. Bracing is assembled to preserve and keep the shape of the vehicle in place after the floor cutting. Sensitive parts are then covered to protect them from any damage that might be caused during the conversion process. The engineers cut the entire floor using mechanical tools, mainly reciprocating saw [55]. The reconfigured home-made floor is then assembled and welded to the chassis using the latest technology [56]. Parts used for the assembly are mixed original equipment manufactured and Rollx customised components. Paint is applied at the end to give the vehicle an original look and then quality check and test drive [57].

One of successful American wheelchair accessible vehicles builder in the market is the Mobility Ventures known as MV-1, previously owned by Vehicle Production Group, designed purposely for handicap users [58]. The company started business in 2011 in Indiana USA, the vehicles were criticised at the beginning for the basic look. However, these offered a longer body structure life if compared to other converters and longer warranty for customers. The brand can design an up-front passenger with side entry access, manual or powered ramp with an option to shorten or widen the ramp's length. The vehicle is powered by Ford engine. The feature that made the brand unique was their home-made chassis which was built from ground [59]. There is no alteration made to the structure of the vehicle, contrary to other builders, this gives the wheelchair users a better safety, reliability, durability in addition to their wider door access compared to the rest of the manufacturers.[60]

Savaria Vehicles Group is another large manufacturer based in north America, Montreal Canada, founded in 1979 and became a public company in 2002. The business was involved not only in wheelchair accessible vehicles but also with other fields related to finding solutions to disability problems e.g., house solution, wheelchair lifting device for stairs. Due to the increase demand these last years, the company expanded their business and opened a large new factory in Huizhou China in

2007. Savaria distributed their product worldwide [61]. The main brands converted are Chrysler, Dodge and Toyota, offering a choice of rear, side and dual entry [62]. The conversion process begun by stripping all the interior including front seats and bumpers, then removing the underside, fuel tank, wheels, exhausts, brake pipes, suspension, leaving the vehicle underbody exposed, then the vehicle is moved to the cutting station where a reciprocating saw is used to cut a large section of the chassis floor at the rear of the vehicle. The engineers weld the customised lowered floor to the chassis, providing 40 cm head room to the wheelchair users. The vehicle then is rebuilt through stages adding progressively some reconfigured parts and original components. The company's name sticker is added at the end of the process, then the vehicle is sent to the quality check and test drive.[63]

All-Terrain Conversions (ATC) is one of the large successful well-known wheelchair accessible vehicles builders in market, based in the North Carolina USA. The company managed to create their own unique features in 2009 by taking a step ahead introducing the converted Pick-up trucks [64] in addition to SUV and Vans models. The new design can give the wheelchair users more flexibility to use their cars, reducing the load and unload time, better durability and cost less than a minivan [65]. The dealer can convert any pick-up truck as long it is a GMC Sierra or Chevrolet Silverado but no older than the 2014 year. SUV conversions used Cadillac Escalade and GMC Acadia and Yukon. For Van conversions Dodge Caravane, Chrysler and Toyota Sienna are the main brands. ATC are known for their lateral access door and the inside automated ramp design (side access) with an option of either passenger or driver fit [66]. The conversion process begins by stripping the inside and underside, but prior to cutting the floor, the entire side vehicle wall is removed including front, rear door and B-post replaced by a customised home-made large lateral door. A circular saw is used to cut a large section of the chassis floor at the side, then replaced by a customised lowered floor welded to the chassis. Lifting device is fitted to load and unload the wheelchair, followed by the door assembly step which is mounted to an automated device for opening and closing. Parts and component are painted to match the original colour. The company offers the choice to keep the original manufactured or home-made upgraded seats. Lastly the car is quality checked and then tested for a driving.[67]

In the other hand, businesses which convert vehicles outside the disability domain such as the world well-known luxury vehicles converter "Limousine", was in the field since 1928, specialised in stretching vehicles. The steps of cutting taken to transform their models did not either show a big different in methods, apart a slight variation to adapt their needs. The vehicle conversion process begins from the stripping stage, covering most parts with fire resistant paper, then the vehicle is assembled on a jig and sliced into half using a circular saw to cut the roof and reciprocating saw for

the floor cut [68]. Some Limousine shopfloor use a laser guided device to ensure the cut path line is respected as it is difficult to perform a precise straight cuts using saws [20] (this issue was highlighted in the previous section 2.3). Extension rails are then added at the mid-chassis inside the box sections frame to extend the length of the vehicle, clamped and fixed using braces to ensure the structure of the car stays in shape. New galvanised steel floor pan is added and welded to the chassis, then pillar post frame is welded to the structure followed by a roof panel fit. An outer body panels is integrated with hardened crash bars and welded to the structure. Parts implemented are checked for position accuracy. Paint is applied to much the vehicle's colour, then followed by a glass fit and the rebuild of customised parts, this included new seats, screen, phone and inside lights.[69]

K. Mehok [6] in his book sectioning unibody vehicle emphasised that in order to perform sections on the vehicle chassis, it is necessary to understand first the type of material being processed and the composition of the component to avoid damage to the car. To perform sectioning on a unibody chassis efficiently and safely, it requires a specialised tooling and knowledge, each vehicle and car maker is different, we must always refer to the manufacturer's guidelines and recommendations to find out what are the zones that can be cut and the ones to be avoid. It is possible sometimes to process two similar vehicles in completely different ways. Therefore, we can never assume that two comparable vehicles can be cut in the same way. The author highlighted those procedures and methods employed to section the chassis including the materials and tools are commonly used in every shopfloor, for instance to remove the front rail, the original equipment manufacturers suggest drilling the spot welds, detach the rail and replace it with a new part welded at the same location of the previous spot weld. However, if it is required to remove only a small segment of the component, then the manufacturers recommendations for the cut would be to disconnect first the negative battery and the airbag system, mark the cut profile, in some cases it is necessary to perform a cut in two sides of the component in order to remove the part, front and rear side, then using a grinder carefully and safely cut out the unwanted section, then replace it with a new component welded in place making sure that the part is perfectly positioned. Measuring and inspection are necessary before and after welding. The author emphasised also that the process requires a slow cutting to achieve a good accuracy using these tools and it is the engineer's responsibility to research what is the best for their business and welcome anything that has the potential to improve the work process.

James E. Daffy [70] noted in his book "the automotive body repair technology" that for a vehicle chassis sectioning, the proper procedures of cut must be respected and the engineer needs to be precise when cutting. The author highlighted the importance of being aware prior to cutting of all the reinforcements present under the chassis floor e.g., brackets, brake pipes, as these parts could be

damaged during the process therefore it might require removal before the process. Recommendations and instructions about sectioning including how and where to cut is usually provided by the manufacturers. To section a floor, two main tools are required usually, a circular and reciprocating saw. However, the author assumed that for body repairs, also a plasma torch can be used as a cutting tool. One of the problems faced after cutting sections is the exposure of the material to corrosion, this issue can be seen using any cutting method. Therefore, restoring all the coating necessary to prevent the metal from damage is very important. Even though the author suggested an alternative cutting tool to the saws, but it is still not clear from his book if this technique can achieve a better quality of cut, the effect of the heat on thin sheets of the chassis remains unknown.

Andrew Livesey and Alan Robinson [71] listed the tools required in every repair shopfloor in order to perform a cutting tasks on a unibody vehicle chassis. The author stressed that the work on car structure is complicated and required skills and special tools which in general are made of high carbon and heat treated. Tools required for cutting are different depending on the area of the vehicle where the work is needed, mainly manual and power (pneumatic or electric) hand tools. These can include all sort of hammers such as Bumper, dinging, pick and finish, straight and curved pein hammer, hand Dollies, body spoons, body files, hand snips, panel beating tools, clamps, punches, jogglers to prevent distortion while welding, edge setters, Rivet set, in addition to cutting tools which include saws, jig saws, sanding machines, drills and metal shears, Etc. The author referred also to other techniques such as thermal processing which can be used in the automotive e.g., oxy-fuel or plasma. These techniques can be easily mechanised to obtain a better accuracy but required a constant vigilance as toxic fumes are generated, and also there is a risk of fire involved due to inflammable materials. Therefore, an extinguisher must be close to the workstation during the process.

Eastwood is another company specialised in providing solutions to auto-restorations and customisation. The company was in the automotive refurbishing market business since 1978, known worldwide today for their expertise including training and quality of their products in the field [72]. In their article made on a best way to cut and replace a floor (Chevy Camaro model), they stressed at the cutting stage that saws are used for the task but also he assumed that plasma cutter can be an option to cut an old floor, the choice according to the author is depending on the shop budget and type of car [73].

I-CAR is an international not profit organisation devoted to giving companies a recognised cutting-edge training solutions, information, skills and knowledge required in order to achieve a high-quality automotive repair in a safe manner. The organisation was founded in 1979 in USA, all repair

industries who adopt the I-CAR methodology of vehicle cutting process and procedures are assured to perform alteration to the vehicles without changing the OEM's quality or safety [74]. I-CAR experts stressed that it was crucial when sectioning parts of the vehicle chassis to respect the manufacturers procedures and recommendations, failure to comply could result in serious injury in case of collision. Therefore, industries must avoid a non-approved cutting [75], especially when performing cuts on vehicle chassis around reinforcement zones in the chassis [76]. I-CAR concluded that instructions and methods provided by the Original Equipment Manufacturers (OEM's) for cutting and sectioning chassis were built, verified and tested in 80's before the introduction of the high strength steels, therefore a new tests and study must be performed with these new steels to provide companies with an up-to-date sectioning guideline. They emphasised that sectioning and cutting must be stopped and should not be performed under any circumstance until further study [76]. I-CAR warned the automotive manufacturers to discontinue the training for cutting and sectioning vehicle chassis (circular saw is used to cut through the chassis) until new tests are done [77]. This might be the reason why almost all vehicle converters and repairers are using a similar old methods and tools to perform a cut. Furthermore, the organisation in charge of training engineers is also using the same old methods of cutting and manual tools.

## **2.8 Summary**

The wheelchair accessible vehicle manufacturers can be categorised into three different categories. The first group, sections the chassis using a mechanical tool. The second group which removes the entire floor chassis using mechanical tools or a combination of welding technology and mechanical tools. The third category builds their underbody floor in-home. The main method used for the cut out and converting vehicles are traditional tools such as circular saws or reciprocating saws, excluding Vantage Mobility International, none of these companies showed any novelty or better way to cut the floor. This confirmed the claim of some articles about the methodology used for sectioning the chassis which are old fashioned needing revision and practically the same in every company [6].

There are few industries specialised in body repair who assumed that the vehicle chassis might be processed using a thermal technique such as Oxy-fuel or Plasma [71]. The claim was made without showing any evidence of a real case or mentioning the level of the quality that can be achieved. These non-traditional cutting methods could be imported to the vehicle conversion businesses but a prior investigation on the technique is required.

## Chapter 3

## Plasma Cutting Literature Review

### 3.1 Introduction

The most used techniques in the market for sheet metal cutting are illustrated in this chapter. The main unconventional cutting methods used in the automotive industry for trimming metal sheets were found to be plasma arc cutting, laser machining and abrasive waterjet cutting [78]. A comparison was carried out between these technologies in order to select the most adequate method needed. These techniques are assumed to be versatile, effective, precise and can process materials at a good speed of cut [79].

### 3.2 Plasma arc cutting

Plasma arc cutting is a thermal process that uses a high speed ionised gas which can reach temperatures of 30000°C [80] at the velocity of sound or higher [81]. The technique in general can cut any electric conductive materials. This process is widely used in the industry for cutting and profiling, it provides a good cutting speed, low investment and operating cost compared to water jet or laser [82]. The range of metal plate thickness used for this technology is usually between 5 to 40 mm for standard machines [83], the more advanced technologies can process beyond that range up to 150mm thick [16][84].

Plasma is the fourth state of matter, it is formed when energy is added to a gas and heated at high temperature between 5000 to 7000°C [3]. The atoms are then excited at this stage leading the electrons to move and leave their orbits, creating a powerful source of energy called plasma. Engineers managed to manipulate this energy and use it as a tool to cut material, the process is called plasma arc cutting (Figure 10). The functionality of the plasma lies also in the design of the torch, after the ionized gas is injected under pressure and forced to exit through a small nozzle bore at high velocity, the critical zone at the orifice transforms the ionized gas into plasma due to excessive amount of energy added, creating a channel of conductive plasma focused in a cross section causing the base material to melt and partly evaporate [71]. The gas used for plasma is depends on the material to be cut, in general air, oxygen, argon or nitrogen are used, the purity of the gas is very important for the process as this can affect the electrode life and the quality of the cut. [85].

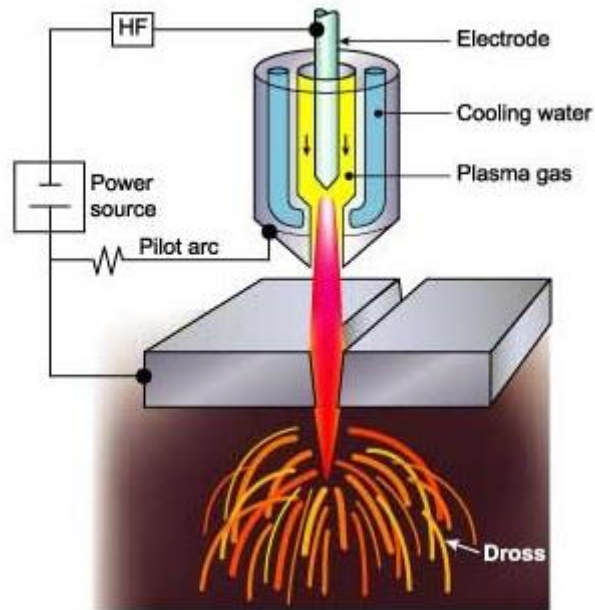


**Figure 11:** Plasma Arc Cutting, "Courtesy of TWI Ltd" [14]

The advantages and disadvantages of the plasma cutting can be summarised as follows [19]:

- Fast cutting process
- Able to process more materials compared to Oxy fuel.
- Can process any conductive materials.
- Plasma is the adequate process for cutting steel materials thickness range small and medium from 5 mm to 40 mm.
- Smaller heat affected zones compared to oxy fuel.
- Low consumable costs.
- Good quality cut.
- The process is safe.

Disadvantages:

- Level of noise is high when cutting thick thicknesses.
- Fumes can be harmful.
- The light generated by the plasma can damage the operator's eyes.
- Process only conductive materials (unless a special torch design is used).

### 3.3 Laser cutting

Laser beam cutting started in 1960's, this process is the common method used to cut thin sheets for various materials e.g., nonferrous or ferrous metals, plastics, stones, wood, ceramics, and rubbers. Etc.[86] The laser generates a high intensity non-visible single wavelength light which can be reflected. The beam then is directed using benders or mirrors and focused on a small area (see Figure 11). The high energy is then absorbed and converted into heat and caused the material to evaporate or melt. A compressed gas is used in the process, the common gases are Nitrogen or Oxygen, depends on the material to be cut [17]. Laser cutting is usually a fast process and the first choice for cutting sheet metal thickness under 6 mm. Some industrial machines showed the ability to process thicknesses up to 100 mm [87]. There are different types of lasers used for cutting materials in addition to the commonly used CO<sub>2</sub> lasers, these are mainly employed for cutting, engraving and boring. The laser beam is generated as a result of an electric discharge passing through a CO<sub>2</sub> gas chamber. The second type is the fibre laser (solid state category) which is expensive compared to CO<sub>2</sub>, but their life cycle is higher, also they require less maintenance and less energy compared to CO<sub>2</sub> to process the same thin material thickness. The beam is generated using diodes, transferred through a fibre optic, amplified, and then focused on the material using mirror. These kinds of machines are very good for engraving, marking and cutting thin materials [88]. These machines are better at processing reflective materials. Nd:YAG and disk lasers are ranked in the same category than the fibre. there is also the latest model known as direct diode laser (solid state lasers category) which gained ground these days in the industry for cutting materials.[88]

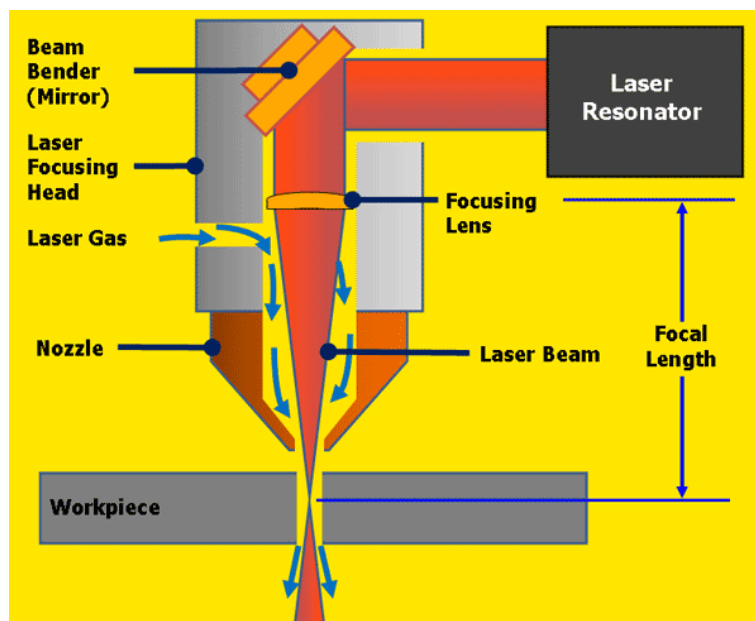


Figure 12 CO<sub>2</sub> Laser technology (ESAB) [89]

There are some advantages and drawbacks of cutting with laser [23]; these are summarised below:

- Faster process compared to plasma in thin materials.
- Fast Cutting speed, excellent at profiling complex shapes.
- Can achieve a better accuracy than plasma or oxy fuel.
- Can cut simultaneously sandwich material at varied thicknesses.
- Small kerf.
- Less heat input to the material (small heat affected zones) compared to other thermal methods.
- Can process metallic or non-metallic materials.

Disadvantage:

- Cost of initial investment is high compared to other technologies.
- Operating cost is higher than plasma.
- Consumption of power is high.
- Setting the machine requires high accuracy and expertise.
- Not suitable for reflective materials.

### **3.4 Abrasive Water Jet**

Abrasive waterjet cutting technique concept consist of forcing a quantity of water under high pressure to exit through a small nozzle diameter at velocity higher than speed of sound (see Figure 12). Abrasive particles are used for this process e.g., silicon carbide or aluminium oxide in order to increase the material removal rate by mean of erosion. In overall any material metallic or non-metallic can be cut using AWJ. This process is known to cut thick materials. However, it is a slow process when cutting steel, for instance it require an average of 700 mm/min feed rate to cut through a 3 mm thick steel material [90]. A narrowed cutting stream and a controlled movement can allow the method to produce an efficient cut and obtain a very precise part. This process is particularly suitable for heat sensitive materials which are practically difficult to cut using other methods. Therefore, Heat affected zones are avoided using this process. Abrasive water jet cutting is extensively used in the aerospace, automotive and electronic industries. In the automotive sector, parts such as interior trims, head liners, trunk liners, door panels and fibre glass body components and bumpers are made using this process [91].

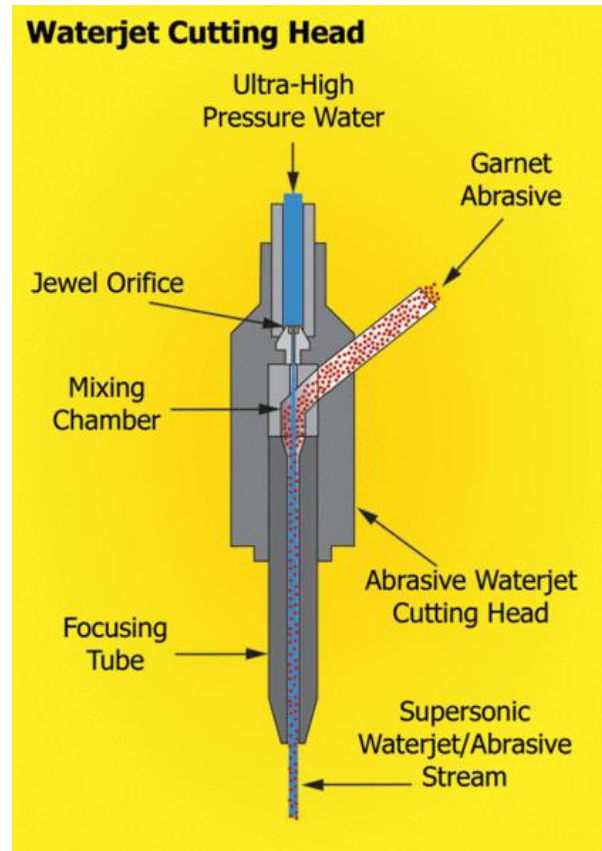


**Figure 13:** Abrasive water jet head Injector (ESAB) [92]

The main components of the machine are in overall Compressor, Air filter cum drier, Relief valve, Pressure gauge, opening valve, mixing chamber nozzle holder, nozzle, work piece [93]. After the abrasive water leaves the kerf, the jet can remain still under high pressure. Therefore, a system for water collection is required to absorb this excess energy, a catcher is used usually under the material.

Advantages and disadvantages can be summarised as follows [23]:

- Can process practically any material.
- There is no heat generated during the cutting and heat affected zones practically non-existent.
- There are no hazard wastes has been reported using this technique.
- Disposal costs are minimal.
- Excellent accuracy
- Can process thick materials.

Disadvantage:

- Machine parts can be affected during time by the abrasive dust generated during the cut.
- The speed of cut is slow.

- The process of cutting is noisy.
- The cost of the abrasive is high.

### 3.5 Cutting Techniques Comparison

In the following Table 3 below illustrates the comparison between the non-traditional common techniques.

**Table 3** Cutting Techniques Comparison

Cutting Techniques Vs Capabilities	Plasma	Laser	Abrasive Waterjet
<b>Thickness Range</b>	Used mainly for 5mm to 40mm plates[83], can cut up to 150 mm[16][84].	Good Quality up to 50mm mild steel[94] but used mainly to cut sheets of 6 mm or less[95] as it provides a fast speed.	25mm Thick steel material[96]
<b>Operating Cost</b>	Low operating cost[95][97]	High Operating Cost[95][97]	High operating cost, higher than laser (due to maintenance routine) [95][97]
<b>Material</b>	Good for mild steel and conductive materials[84]	Homogeneous and nonreflective materials[84]	Any materials in general, but limited when cutting very hard materials[79]
<b>Accuracy</b>	Average accuracy around +/- 0.5mm[95][97] ( $\approx$ 12.5mm mild steel)	Can Achieve around +/- 0.25mm[95] ( $\approx$ 12.5mm mild steel)	+/-0.127mm[95] ( $\approx$ 12.5mm mild steel)
<b>Kerf</b>	3.81mm ( $\approx$ 12.5mm mild steel)[98]	0.64mm ( $\approx$ 12.5mm mild steel)[98]	0.89mm ( $\approx$ 12.5mm mild steel) [98]
<b>Distortion</b>	Higher than Laser[84]	Low distortion, better than plasma[84]	No detorsion practically[79] [84]
<b>Speed of Cut</b>	Fast in plates $\geq$ 6mm[84][95][15]	Fast in sheet steel below 6mm[84] [95] [15]	Very slow when processing steel compared to plasma or laser[84] [95]
<b>Metallurgy and Mechanical Properties Change</b>	Higher than laser[95][84][79]	Narrow HAZ compared to plasma[[95][84][79]	HAZ are neglected usually when using this process, properties of the material are very close to the base material [95][84][79]
<b>Cut Edge Quality</b>	Less than laser, dross and bevel can be seen[97][95]	Better than plasma and close to AWJ, small bevel angle and very small dross[97] [95]	Better than laser, square edge no dross practically [97] [95]
<b>Hazard</b>	Gas, Fumes, Noise, sparks, hot metals, hot slugs, electrocution, Ultraviolet radiation[99]	Gas, Fumes, Noise, sparks, hot metals, hot slugs, laser beam (damage eye and skin/ Ultraviolet radiation)[100]	High level of noise, potential flying abrasive particles, pumps under high pressure sometime even if not working, risk of hand injury, electrocution[101]
<b>Capital Investment</b>	Cost Effective, low investment compared to other technologies[95][97]	Very high investment, higher than AWJ[95][97]	Higher than plasma and lower than Laser[95][97]
<b>Speed of cut</b>	Fast Process (A Level), 2450mm/min (10mm steel). [102]	1000mm/min (10mm thick steel). [102]	Slow process 380mm/min (10mm steel)[102]
<b>Productivity</b>	Very Good Productivity, best on thicknesses between 6 to 50mm the lowest cost in this range[103][95][97]	Excellent for thin sheets in general very good production rate up to 6mm, the best[103][95][97]	Slow process for steel materials but can process a variety of material at tight tolerances and high accuracy without HAZ[103][95][97]

Laser is most productive on materials thinner than 6mm, tolerances are excellent on most materials, the operating cost and initial investment are considerable. The technique was found to have some limitation when processing uneven thicknesses [104], to overcome this issue, additional costs are required to adapt the laser to the type of process e.g. Adaptive lens and sensors for instant feedback. Plasma in other hand is a universal process, good at processing conductive material primarily mild steel, it is the most productive process on carbon steel for medium thicknesses, medium capital for initial investment, low operating cost, fast process, and good accuracy. AWJ can be considered as a universal cutting technique for all materials including non-metallic materials, it is the choice number

one where heat affected zones are not tolerated, medium to high capital cost is required but in general lower compared to laser technology, but the operating cost is higher if compared to laser and plasma due to the maintenance routine. AWJ is a slow process for steel materials compared to other techniques, also a catcher is required to collect the abrasive material after leaving the kerf. Processing vehicle chassis with this technique and under moisture environment can lead to problems, in our case dry cutting is required to prevent corrosion generation. Oxy-Fuel is a cost-effective process also and could be included as a cheap option for cutting the vehicle chassis. However, this technology is not adequate when dealing with very thin materials, mainly used for medium and thick plates. Quality issues starts to appear when using this process for thicknesses under 9 mm [105]. Cutting under 3mm would result to deformation issues and buckling [106], unless the quality and deformation are not a requirement for the manufacturer and a second processing is at no cost. A special nozzle to process thin materials might be used but a more advanced automation system is needed [71].

After evaluating the techniques, the suitable technology to perform the task and replace the traditional cutting in this case would be the plasma cutter due to their cost effective compared to other technologies. The process is fast, accurate, easy to automate, and the operating cost and initial investment was lower than the other techniques (falls within Allied Vehicles Budget). In addition, some automotive body repair engineers [71][72] assumed that plasma cutter might be used to section an old vehicle chassis as an alternative. Therefore, an investigation on plasma cutting is necessary to qualify this technique.

### **3.6 Plasma Cutting Related Research**

Plasma arc is widely used in the industry nowadays to process conductive materials. The technique was found to have a good ability to reduce the cost two to three times and whilst increasing the productivity to almost three times compared to other non-conventional methods[8]. There is a lot of research carried out on plasma cutting materials, below is the summary of the main research conducted. This literature review would help to identify the gaps in the field and identify the research questions.

A. Iosub, Gh. Nagit, F. Negoescu [107], have conducted a research to show the ability of the plasma arc to cut a sandwich material. The research consisted of using two outer laminated aluminium sheets of 0.3mm thick and a thin layer of polyethylene core in the middle the process was made to assess the quality cut, surface integrity and heat affected zones, varying the input parameters (current, gas size, intensity, speed) then analyse the quality outcome. The results showed that it was possible for a

plasma to cut a sandwich material. However, the two outer layers and the mid-sheet had different material composition and the melting points for aluminium was higher than the polyethylene. Therefore, it was not possible to obtain a good quality cut due to the middle layer excessively exposed to the heat. The research showed that the main parameter that influenced the process was cutting speed. The research concluded that a machine with a good feed rate can make difference, by increasing the cutting speed the middle layer would be less exposed to the heat and can potentially result to a better quality. The research emphasised that the use of waterjet technique would be the suitable process to overcome this issue. The study never attempted to optimise the plasma parameters to reduce the phenomenon before making the final claim about the quality result.

A study made by Dr. A. Lazarevich [108] where a Hypertherm plasma CNC machine was used to cut a different stainless steel material thicknesses of 4, 6, 8, 12 and 15mm. The author assessed the relation between the input parameters (Current, material thickness and cutting speed) and the output cut result e.g., kerf width, surface roughness and angle bevel. The input plasma setting was varied, results were collected and analysed using MATLAB software. Ninety-nine recline cuts were made for four different work pieces. The experiments results showed that the kerf width was influenced by the cutting speed and current, the size was smaller when the cutting speed increased, and when the current decreased the size narrowed. The surface roughness increased with the increase of the speed and current. Bevel angle also increased with the increase of cutting speed and current. All tests showed that the thickness of the material interacted with the cutting speed and current, when the thickness increased then the speed required to slow down and current to increase. The author emphasised the need of further study considering other input parameters.

A research was undertaken by Y. H. Celik [109] on the Effects of Cutting Parameters on S235JR steel Materials using a CNC Plasma. The quality cut of the material for various thicknesses range of 4, 6 and 8mm was assessed using cutting speed from 1000mm/min to 1500mm/min, arc voltage 115v to 125v, amperage from 80A to 130A. Heat affected zone width, surface roughness, hardness, and the temperature of the material during the cut were assessed. The results showed that increasing amperage the temperature during the cutting would increase, also the paper highlighted that thickness, amperage and cutting speed have a significant effect on the heat affected zones, whereas temperature measured on the top surface and the arc voltage are linked to the cutting power, this could reflect on the shape of the kerf. The author emphasised that temperature and HAZ were affected by the feed rate, this would decrease by the increase of the speed. Cutting thin sheets required the voltage and

the current to be at lower level and the speed of cut needs to be high for a best quality result. The paper highlighted that cutting thick materials required the current to be high and the arc voltage at lower level.

J. Aldazabal, A. M. Meizoso, S. Cicero et Al [110] performed another study investigating on plasma parameters effect on the quality cut edge and heat affected zones. The experiments used 15mm S460M steel grade to perform multiple straight cuts using a Hypertherm CNC plasma machine starting from the manufacturing recommended settings. Wire EDM technology was then used to slice layers of 300µm thick on the cut side to assess the HAZ width. Residual stress distribution was assessed using x-ray and micro-hardening. The purpose of this work was to evaluate if a second processing was required to remove the unwanted area. The study showed after measuring and analysing the specimens that the affected zones were small and uniform along the surface and disappear after 700 µm. The paper highlighted that using plasma gave less heat affected zones compared to oxyfuel but higher than laser. However, the depth of the heat affected zones in the cut edge was uniform with plasma contrary to laser or oxyfuel.

K. Rana, Dr. P. Kaushik, S. Chaudhary [111] have optimised the plasma cut in both term consumables and quality of cut. The purpose of the work was to vary the input parameters e.g., cutting speed, current, air pressure and standoff of the nozzle, and then assess and minimise the heat affected zones. The test was performed on KALI- Plasma cutter air/air, the thickness of the material was a thin mild steel plate of 10mm. Qualitek-4 and Taguchi method were used to optimise the parameters and their settings using L9 orthogonal arrays. The results showed that the current had maximum effect on the heat affected zones with more than 65% then the cutting speed at 34% then stand off and finally the gas pressure.

S.M.Ilii and M,Coteata [112] conducted a study on Plasma Arc Cutting Costs. The paper highlighted that knowledge of the costs (technical and operating side) were important when working towards investments. Mathematical formulas were built to illustrate different costing including maintenance and tools. The author concluded that it is very important to prove that the selected tool can provide an economical advantage over traditional cutting. They have mentioned also that the tool's consumables life, quality cut and productivity were the main cost advantage compared to other techniques mainly for materials such as mild steel, aluminium, and stainless steel for a wide range of thickness. The author highlighted that plasma is very convenient in matter of quality, operating cost

and productivity compared to other processes. The author illustrated different formulas to evaluate the cost but there was no real data to support his claim nor compared other techniques to plasma.

S. S. Pawar and K. H. Inamdar [113] have assessed the Heat Affected Zones for 4mm and 12mm Stainless Steel material, known for their ability to resist against corrosion. CNC plasma Hypertherm Powermax 1650 air/air was used for this study, the input parameters voltage, cutting speed and gas pressure were varied, the current and gas pressure were kept constant. Settings were chosen according to manufacturer's thickness recommendation of cut. The output variables were analysed, nine cuts of 200 mm straight lines were performed for both plates, then specimens were taken from each cut, polished using sandpaper 400, 800 and 1200, and chemically etched using Aqua Regia liquid to expose the material for the HAZ analysis. Design of experiment was used (Taguchi parameters design approach) to optimise the input parameters and ANOVA to determine which parameters were most influential on the quality. The result showed that the Heat Affected Zones increased with the increase of the Voltage and Gas pressure and decreased with the increase of cutting speed.

L. Schleuss, R. Ossenbrink, T. Richter et al [12] investigated plasma cutting a honeycomb structure thin material using a robotic KUKA arm. The author emphasised the lack of knowledge concerning processing three-dimensional structures thin materials using plasma technology in the automotive sector. The purpose was to qualify this process instead of a laser due to high costs involved, this work can be beneficial to railways industry and also to the automotive industry. Roughness, straightness, and burrs were assessed then compared to the laser quality. The research concluded that the quality obtained from the tests using plasma on structured material were acceptable in general and highlighted the importance of the distance control between the torch and workpiece to obtain a better quality. However, an advanced level of automation was required due to complex profile of the cut.

K. Rakhimyanov, M. Heifetz and A. Rakhimyanov [114] have conducted research to investigate the latest plasma technology known as high density plasma to cut two stacked different metals. Two materials were used, the first sheet was made from steel material ST3 and the second was Aluminium A5M, the two sheets were joint together using explosive welding technique to create a new bimetallic sheet of 6 mm thick used as structure materials. The paper emphasised that high precision plasma was chosen due to their ability to obtain quality of cut closer to laser or waterjet technique. The objective of the work was to optimise the cut and define the best plasma parameters required for the

process, using two different HD machines and gases for each side. The study concluded that in order to cut a bimetallic material effectively, it was necessary to cut on the side of the metal which possessed a higher melting point.

An experiment was made by Bahram Asiabanpour, Jesus Jimenez, Clara Novoa et al [18] on stainless steel material of 6mm thick plate. Plasma parameters were optimised using the response surface approach to improve multiple output variable at the same time, the response analysed included flatness of the surface. The experiment used the plasma parameters primarily current, cutting speed, pressure, stand-off torch, slower speed of cut on the curves and tool type, all at three levels and the cut direction at two levels. The output parameters measured were flatness, roughness, straightness of cut, bevel angle, dross, the sample size change after the cut, tool life, start point cut quality and the depth of the cut. 89 trials were performed on the material. Manual tools were used to assess the output, then a design of experiment (design expert software) was implemented to identify the relation between the plasma variables input and the quality results. Regression models were constructed to predict the output responses. The results showed that the quality of cut overall was affected by the torch height, tool type and the direction of the cut. However, the optimal settings obtained did not show any improvement during the validation tests, leaving a room to an additional test in the future to confirm. The response measured and the predicted values were close.

Evan L. Floyd, Jun Wang, James L. Regens et al [115] have investigated plasma cutting technique and the effect of the input parameters (current and processing time) on the output (volume of the fume and particles characteristics were measured). The research aim was to understand the nature of the fume as it was found that this might release toxicants such as chromium. Therefore, these gases could be harmful and reflect on human health if overexposed. The experiment used a stainless steel ER308L 4.8mm thick as a material for tests, plasma current was varied from 20 to 50A, multiple cutting was performed manually at different processing time 5, 10 or 30 second. Fume chamber and pump were used to collect the fume, the volume size generated during each trial was determined using a Gravimetric approach, a fibre glass filter was used to catch particles on the top of the chamber then assessed with a scan mobility technique and then weighed. The results showed after tests that the rate increased by increasing the current, the values registered were in overall 16.5 mg/min when 20A was used and 119 mg/min when 50A was used, this last value registered 480 µg/min of harmful chromium gas. The author claimed that cutting with plasma released more toxic gas than during the

welding process. The author did not clarify the reason of comparing plasma cutting to welding process as these two methods are two completely different processes.

P Mariya Felix, K Ramesh and S Roseline [116] have assessed the quality cut of a CNC plasma on SS410 Stainless steel. Design of experiment was used for the tests, Taguchi method and Analysis of Variance were employed to optimise and analyse the effect of the input variables e.g., Cutting speed, arc voltage and piercing delay at three levels on the output variables e.g., flatness, perpendicular, parallelism and roughness. Optimum plasma settings were defined for each response. The findings showed that piercing delay was the most influential for perpendicular and flatness whereas roughness and parallelism were respectively cutting speed and arc voltage. Even though the authors have mentioned that the process was improved using Taguchi method. However, there were no additional tests shown performed in their paper to confirm the claim.

R. Miroslav, M. Jankovic, B. Nedic et al [16] have investigated on the plasma cutting quality as part of the research for the latest non-conventional technologies for manufacturing applications. S235 steel plate 15mm thick was used for the experiment as a material, then 17 samples were cut using CNC Plasma cutter varying two input parameters, cutting speed and current at 60, 80, 100, 120A, and also using different cutting speed varied from 425 to 1585 mm/min. The quality was assessed based on ISO 9013 EN criteria, the responses included dross formation, angularity, squareness, melting of the top edge, average pick to valley (roughness) and drag line. The findings showed that cutting with plasma always resulted to two different sides of quality usually the left side is better than the right side, also a better quality of roughness and bevel angle of 1 to 3 degrees deviation from the good side and 3 to 8 degrees in the right side. The authors mentioned that an equal repartition of quality could be obtained if a swirl gas is used. Lastly, a good quality was obtained when the cutting speed was increased. The author did not attempt to optimise the process to minimise the phenomenon.

D. B. Ghane, L. B. Abhang, P. A. Makasare et al [117] have conducted research on the effect of different plasma nozzles on the quality cut. The study also included the analysis of the effect of the settings variation on the quality. Four identical mild steel plates of 200 × 200 mm × 20 mm thick were used for the tests and four cuts were performed using a CNC plasma in each plate with different nozzles. The input variables were plasma torch type, this included 4 different nozzles Kalpak industry, ESAB, Mass cutting system Machine and company's own nozzle provider, in addition to plasma

parameters which included cutting speed, gas pressure and stand-off distance between workpiece and torch. Variables measured were dimension accuracy, roughness and material removal size. The authors emphasised that the requirements to perform a cut using plasma for a specific work usually do not match the factory's settings recommendation. Therefore, it was necessary to perform tests to identify the adequate settings suitable for the company's needs. The results showed that the best quality obtained using the company's own nozzle, the author have also highlighted that material removal size correlated with the length of the processing time and roughness.

S. Tossen, T. Kavka, A. Maslani et al [118] have investigated on plasma flame energy flow exiting the nozzle. The main parameter assessed was mainly gas pressure varying from 4.5, 5.5 and 6.5 bar using water steam-ethanol base mixture. Current of 60 ampers, 30 cm/min cutting speed and 2mm stand-off distance between the workpiece and nozzle were fixed during the experiment, a 15 mm thick mild steel S235JR slightly rusted was used for the tests. The research used a theoretical approach to estimate the quantity the energy of the plasma jet in different zones. The size of the material removed was calculated based on the kerf width. The temperature of the heat exiting the material was measured using a thermocouple and water vessel device underneath the workpiece, also a pyrometer infrared was fixed to constantly register the temperature at the cut edge for 150 mm long. The findings showed the possibility to estimate the quantity of energy required for the cut by knowing the material removal size and the temperature. The plasma energy decreased with the decrease of plasma flow, furthermore the energy after the kerf showed a decrease but it was not possible to effectively estimate the quantity. The research estimated that only 20% of the plasma jet energy was used for the cutting and the rest was dissipated in the material and exited the kerf.

The effect of the nature of different plasma gases on material was assessed by T. Kavka, A Maslani, M Harbovski et al [119]. 15mm thick mild steel was used for the experiment using different gases air, nitrogen, oxygen, and steam based on mixture of pressurised water and ethyl alcohol (the liquid was heated and evaporated in the torch). The current used was 60A, cutting speed 30 cm/min, stand-off 2mm were kept constant during the experiment. The gas volume was varied from 8 to 16 g/min. A thermocouple was positioned underneath the working piece to register the temperature and a pyrometer monochromatic was employed for measure the cutting temperature, then a spectroscopy was used to evaluate different temperature zones. The research showed that air and nitrogen resulted to a similar kerf feature, the kerf was wider at the top of the workpiece and smaller at the bottom. Oxygen and steam shape were wider, and both showed a similar feature of a bell-shaped kerf structure,

meaning that the heat distribution was not uniform for these two gases, the best quality was obtained using nitrogen. The research showed that cutting using oxygen would not result to an oxidation. Finally, the authors claimed that improving the gas flow would result to a better quality of cut for all gases.

J. Kechagias et al [120] optimised the CNC plasma parameters to reduce the right side bevel angle of 15 mm mild steel. Taguchi parameters design method was used to perform Nine (09) trials considering four parameters at three levels L9 ( $3^4$ ). ANOVA was used to analyse the results and identify the most influential parameters.

R. Bhuvanesh and B. Abdalnasser [121] optimised a CNC plasma parameters to minimize the material removal rate and surface roughness of aluminum alloy independently. Taguchi parameters design method was employed with Three parameters at three levels, nine trials were conducted L9 ( $3^3$ ) to cut rectangle 100 mm  $\times$  40 mm. ANOVA was used to analyse the data and identify the most influential parameters at 95% interval of confidence. P-Value was used to identify the significant effects.

S. S. Pawar and K. H. Inamdar [113] used Taguchi parameters design method to optimise plasma parameters, three parameters at three levels and 9 trials were performed L9 ( $3^3$ ) to obtain a cut of 200 mm long in two different plates 4 mm and 12 mm thick stainless steel grade. The response observed was heat affected zones width using a microscope. To identify the most influential parameters ANOVA was used at 95% level of confidence.

R. Bhuvanesh et al [122] investigated on surface roughness and material removal rate independently of a 6 mm thick steel grade material AISI 1017 using a manual plasma. Taguchi parameters design method was used to optimise four parameters (three levels) and nine trials were performed L9 ( $3^4$ ).

Another study was conducted by K. Rana et al [123] to assess the kerf and heat affected zones independently. Four plasma parameters were optimised at three levels to improve the quality result. Taguchi parameters design method was used and L9 ( $3^4$ ) was used to cut a 10 mm mild steel. ANOVA was used as a statistic tool to analyse the results and obtain the percentage of the effects.

Optimisation of holes cutting using plasma machining was performed by J. C. Chen et al [124]. The main responses assessed independently was bevel magnitude and hole deviation. Four parameters

were considered for this study at three levels and Taguchi parameters design method L9 ( $3^4$ ) was used.

H. Ramakrishnan et al [8] used Taguchi method to optimise four CNC plasma machining parameters at three levels of a 3 mm stainless steel grade plate. To reduce the number of the runs L9 ( $3^4$ ) was chosen to perform a random closed profile. The output assessed independently were surface roughness, kerf and heat affected zones width using a microscope. ANOVA was employed to analyse the data at 95% level of confidence for most influential parameters and P-value was used to identify the significant effects. Three-dimensional surface plot was used to assess the effect of the two most influential parameters on the response and finally, a regression model was built for each response to assess the relationship strength between the input and output parameters.

S. Vatousianos and K. Salonitis [125] investigated on CNC plasma cutting of 15 mm mild steel grade. Three responses were analysed, angle bevel, kerf and heat affected zones (using a microscope). Taguchi parameters design method was used to optimise four parameters at three level and 9 trials were performed L9 ( $3^4$ ) to cut a  $150 \times 50$  mm rectangles. ANOVA and regression analysis were performed to find out the most influential parameters and the strength relationship between the input and output parameters.

### **3.7 Conclusion and Knowledge Gap**

Plasma arc cutting acquired a massive ground in the industry these last year's [116]. Tremendous amount of work was carried out on this technology. However, scientific publications on plasma cutting process remain still limited, this can be classified in two categories either metal plate analysis or plasma study [126], the work performed on the material focused mainly on the edge of the cut. Dattu B. Ghane assessed the effect of plasma parameters and the nozzle type on mild steel cutting quality [117]. Yahya H. Celik looked at ways to optimise the plasma settings to reduce heat affected zones and roughness for a different mild steel material thicknesses [127]. Another experimental research made by A. Lazarevic [108] on stainless steel material to assess the influence of the input parameters on the output, also to process materials such as Hardox 400 and assess the quality [128] or titanium [129]. S.M.Illi carried out a research on what drives the cost in plasma [112]. Evan Floyd looked at the characteristic of the fume generated during the plasma cutting [115]. T. Kavka assessed experimentally the effect of different gases on the performance of plasma cutting [119]. A research was performed on dual material aluminum and steel processed using latest plasma technology known as high density model [114], other research on sandwich or structured thin materials also was carried

out previously [12,19]. These articles were primarily assessing plasma cutting quality in two-dimensional plan and linear cutting. However, there is no documentation available which assessed plasma when an additional plan of cut is required for instance how plasma would perform on cutting a three-dimensional part such as double-layered or box section. D. Krajcarz [84] reviewed the three main best cutting methods used to cut metals including abrasive waterjet, laser and plasma, their conclusion suggested only abrasive waterjet can perform a cut in multi-layered sheets. L. Schleuss et al [12] stressed that cutting a three-dimensional structures was not a well-known field. To sum up, considerable work has been done for assessing one single sheet. However, there are no scientific documentations until today investigated on plasma cutting two layers simultaneously and optimised the process. S. Tossen, T. Kavka, A. Maslani et al [118] stressed in their experimental research that only 20% of the plasma energy was used to cut the material and the remaining energy was dissipated in the plate and the largest quantity exited the kerf. Therefore, in my case this leftover heat energy exiting the kerf could be re-used to cut an additional layer. This hypothesis if tested and proved correct would give the plasma technology a step forward on their application and an additional dimension of cutting. This research could be beneficial for businesses where vehicles are converted and a cut-out on the chassis floor is required, as some parts in the underbody chassis are made of two layers, this work could also benefit other industries.

### 4.1 Introduction

The aim of this thesis is to fill a gap knowledge of the feasibility to reuse the heat energy exiting the kerf to perform a cut in a second sheet. This research seeks to identify the optimised way for processing two layers effectively and reduce the phenomena resulted to their lower level, mainly deformation of the surface and heat affected zones. Therefore, it is necessary to analyse the effect of the heat on thin material and assess the quality results. This study will help the industry to understand the plasma ability to process a three-dimensional structure. Research performed previously assumed that plasma technique is not suitable for thin materials under one millimetre due to the high energy input transferred instantly to the material surface [130][83]. In our case, the thinnest sheet part in the underbody floor chassis vehicle measured was 0.6 mm [26]. Therefore, it is important to identify the optimised way to process this range of thickness, as a wrong setting might result to material alteration [15]. The Figure 13 below show the process of the research and the methodology approach adopted in this thesis.

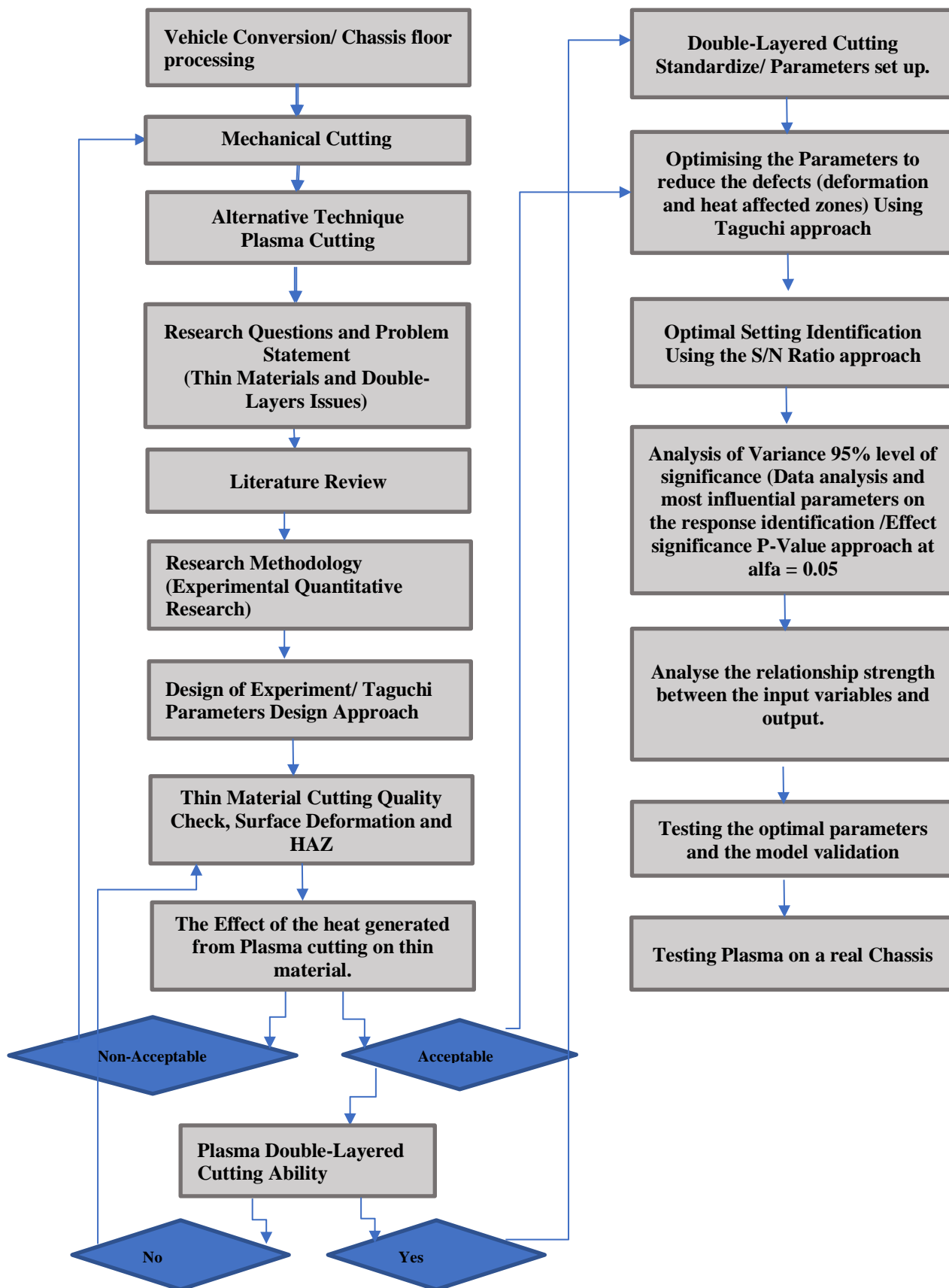


Figure 14 Research Methodology and Process of the Thesis.

## **4.2 Research Approach**

Experimental method is a valid and effective way which is widely used by researchers to collect data in the engineering field. Trial-and error involves repeating tests using different combination until obtention of the results needed [132][133][108]. There are different methods that can be used by engineers and scientists to conduct research. The objective of this thesis is to problem solve and gain a deeper understanding of a unique cutting process in addition to measuring phenomena. The adequate methodology that should be adopted in this case when testing hypothesis and examining the cause and effect is the experimental quantitative approach. This was the standard approach adopted by other researchers (for a similar work) and this was clearly emphasized in the literature review conducted in the previous chapter. For instance, L. Schleuss et al [12] investigated on plasma cutting honeycomb material using experimental approach. A. Iosub et al [107] have conducted an experimental research using trial and error method to show the ability of the plasma to cut a sandwich material effectively. S. Pawar et al [113] investigated on plasma cutting stainless steel material to assess HAZ, this was achieved using experimental approach. Methods such as qualitative, applied, fundamental, analytical, descriptive or conceptional research were not the most suitable approaches due to the nature of this study especially when converting phenomena into numerical data and analysing results using a statistical software are necessary in order to draw a conclusion [131]. .

## **4.3 Design of Experiment**

Design of experiment (DOE) is a statistical method used in different fields as an efficient and alternative technique to the traditional approach which assessed one factor at time [134], this was Introduced in 1920 by R. Fisher [135]. DOE can be divided into three main categories: Screening design which is more adapted to identify among a considerable number of variables the key factors. The second choice is the full factorial design where all combinations of the factors are considered, however this method was criticized due to their high cost and time consume. To overcome these issues the third method was developed by researchers named fractional factorial approach, this method possess the potential to assess the main effect at minimum experimental runs possible whilst remaining accurate, this type of design is the most used technique in the industry [136].

One of the problems found when processing sheets was to identify the optimal cutting conditions for each specific material and thickness required to obtain the best cutting quality possible[137]. There are several statistical tools which could be used as a research technique and optimising method,

however to date none of them were found to be better than the other. The choice is generally driven by the type of problem investigated and the objective of the work [138]. Among the fractional factorial designs, the DOE based on Taguchi method is one of the widely used approach in the engineering field for process optimisation e.g. automotive industry, and this technique is an efficient tool for quality improvement which highlights a reduction in cost and time [139]. This method is extensively used within the research field for improvements and process optimisation especially in manufacturing shop floor and metal cutting [140]. In general if we need to examine four parameters at three levels this normally requires  $3^4 = 81$  trials[8]. Taguchi approach for parameters optimisation process can reduce the tests to a minimum trial whilst preserving the accuracy. This method is suitable in my case where sample are doubled in number due to cutting multiple layers simultaneously. The method was also suggested in the literature review.

Taguchi method is a robust design which uses orthogonal arrays, the main objective of the technique is to build a reliable system that can perform efficiently even if a considerable nuisance (noise) is present. This method focuses on the mean and the quantity of variation (noise) generated when the input variables change, in other words, identify the highest mean corresponding to the least quantity of variation (highest signal to noise ratio) [140].

There are other suitable methods which could be used in this study e.g., Response Surface Methodology (RSM). However, the research showed that Taguchi was better at identifying optimal conditions with less trials. RSM is better suited when more complex designs are studied using several factors to assess two responses or more at the same time [141]. Grey Relation Analysis (GRA)[142][143] and Fuzzy Neural Network (FNN) [144] are another approaches that could be adopted as a research technique for this work but similarly to RSM, these methods are usually used for complex designs, multi-response analysis and for decision making when not enough information is available. For simple designs Taguchi remain the first choice, even though these fractional designs including Taguchi are well-known for efficiency and cost effectiveness. However, full factorial design is the most accurate and effective when time and costs are not an issue for the company [140]. The limitation of the fractional designs including Taguchi is the interactions, sometimes these techniques fail to detect their effect significance especially at order three or more [140][138][135].

#### **4.4 Factors and Levels**

Figure 14 below illustrates the parameters that can influence the quality cut mainly for surface deformation and heat affected zones.

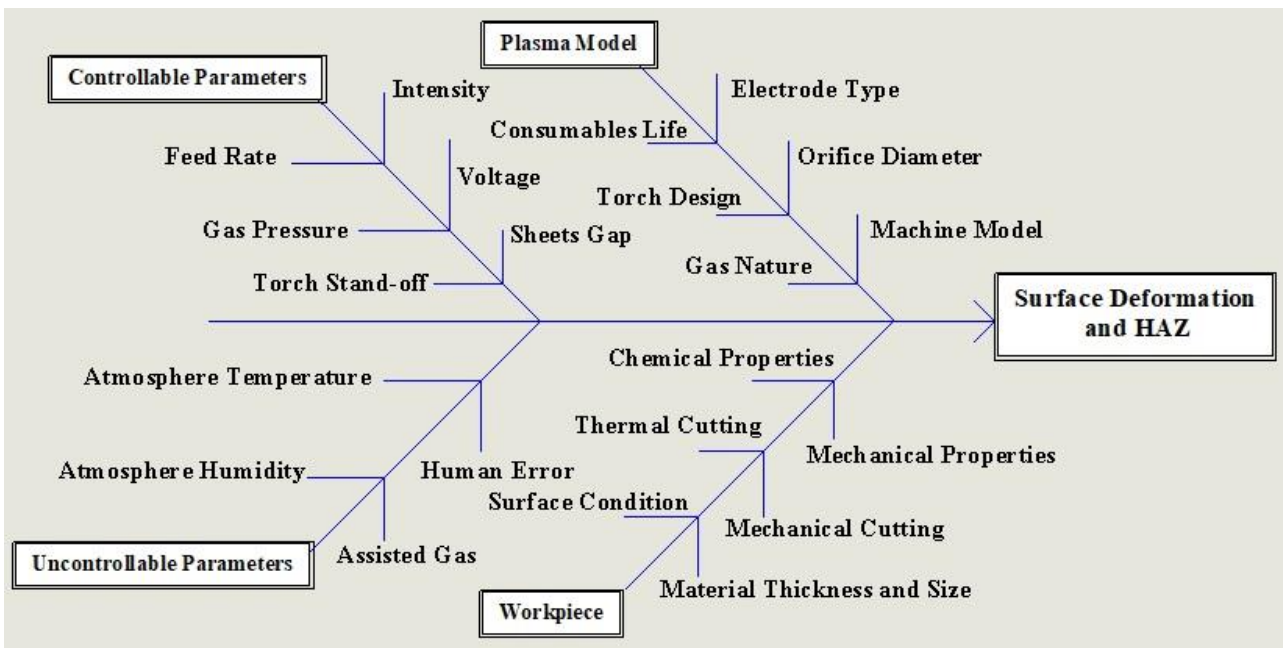


Figure 15 Ishikawa Diagram for Parameters Identification

#### 4.4.1 Parameters

For cutting materials, the convenient way to conduct a design of experiment is to include in the study all the important factors influencing the response. This could help to effectively generate the necessary information and identify the optimum settings [140]. The schematic above Figure 14 was used to help identifying the important parameters that can be selected for this design. According to the literature review, the main parameters used to conduct a research on plasma processing are cutting speed, current and pressure [145]. In this thesis, we have considered all possible input plasma variables, including cutting speed, gas pressure and power (Intensity I) for the single sheets cutting. There is an additional input variable added to the study for cutting double sheets (air gap distance between the two sheets). The plasma torch stand-off was adjusted automatically, and the shield gas was also constant.

#### 4.4.2 Levels

In metal cutting two or three levels are in general chosen to conduct experiments, sometime more levels are used. Some researchers criticized the two levels analysis as this might have some limitation and lack of accuracy to generate all the information needed to improve the quality [139][124]. Therefore, a three levels experiment was selected for this work.

There is a lack of information on scaling levels and how to attribute a new value to the factors. Some researchers have selected the settings randomly as long as the new value has an effect on the response[140]. V.P. Astakhov [139] in his book mentioned that a simple mathematical formula to set

the upper and lower value could be used, these new settings were represented by +1(upper) and -1 (lower) and 0 represented the chosen factor value or the reference.

$$X(+1/Upper): \frac{X(Upper) - X_o}{\Delta X} = +1$$

$$X(-1/Lower): \frac{X(Lower) - X_o}{\Delta X} = -1$$

X (+1) is the new Upper value.

X (-1) is the new lower value.

X<sub>o</sub> is the available value of the factor (reference)

ΔX represent the variance interval of the settings in real (machine settings)

- Cutting a single sheet (Three Parameters at Three Levels):

X<sub>o</sub>: represent the chosen cutting parameters (mid-level or level zero), which in this case was the closest settings values to manufacturing recommendation plasma parameters for a mild steel 0.6 mm thick.

Cutting speed 8500 mm/min, Air Pressure 75 Psi and Intensity 25A

Settings graduations ΔX (Pressure and Intensity are respectively 500 mm/ min, 5 Psi and 5A).

From the formulas above we obtain:

$$X(+1/Upper): \frac{X(Upper) - X_o}{\Delta X} = +1 \rightarrow X(Upper) - X_o = \Delta X \rightarrow X upper = X_o + \Delta X$$

$$X(-1/Lower): \frac{X(Lower) - X_o}{\Delta X} = -1 \rightarrow X lower = X_o - \Delta X$$

Replacing the values in the equations above we obtain:

Cutting speed Upper level 9000 mm/min, Cutting speed lower level 8000 mm/min.

Pressure Upper level 80 Psi and Lower level 70 Psi

Intensity upper level 30A and the lower is 20A.

- Cutting Two separate sheets with air gap distance (Four Parameters at Three Levels):

In this case we have the X upper which represents the maximum level obtained for gap distance at level 20 mm cutting speed 500 mm/min, pressure 80 Psi and current 35A. The settings variation ΔX for Cutting Speed, Pressure and Intensity are respectively 100 mm/ min, 5 Psi and 5A.

$$X_o (mid - level or reference zero) = X upper - \Delta X$$

$$X_{\text{lower}} = X_o - \Delta X = X_{\text{upper}} - \Delta X - \Delta X = X_{\text{upper}} - 2 \Delta X$$

Therefore, we obtain the remaining levels using the two above equations:

Cutting speed at mid-level 400 mm/min and lower is 300 mm/min.

Pressure at mid-level 75 Psi and lower is 70 Psi.

Current mid-level 30A and lower is 25A.

The higher gap was fixed to 20 mm,  $\Delta X$  used was 5 mm, therefore we obtained a mid-level 15 mm and lower gap 10 mm.

#### 4.4.3 Response

EN ISO 9013 defined quality cut when processing materials using thermal methods as bevel angle, material formation possibility on the top or bottom edge (dross or spatter), angularity and squareness, dragline lag, top edge melting, roughness and average pick to valley in addition to the heat affected zones and kerf width [130]. However, there was another issue encountered when processing thin materials, the phenomenon is known as the deformation of the surface of the material. According to literature review this was a common issue in the engineering field [18][146][84]. Furthermore, the response is selected depending on the industry needs. Even though ISO defined the meaning of the quality in thermal cutting but there is no mention on what is the accepted quality level[15], this is usually defined by the company. At Allied Vehicles, all the quality requirements are set and shown in the Table 4 below.

**Table 4** Quality requirements (Allied Vehicles)

Quality (Allied Vehicles)	Quantitative Value (mm)	
	Single Sheet Cutting	Double Sheets Cutting (Requirements only for the Top Layer)
Part Accuracy $X^{+/- 1.5 mm}$ Width 40 mm Length 150 mm	Width: 38.5 (min)/ 41.5 (max) Length 148.5 (min)/ 151.5 (max)	Width: 38.5 (min)/ 41.5 (max) Length 148.5 (min)/ 151.5 (max)
Deformation	0.2 mm (max)	0.5mm (max)
HAZ	0.2 mm (max)	0.2 mm (min)
Edge Offset	N/A	2 mm (max)
Dross	1 mm (max)	1 mm (max)

#### 4.5 DOE Based Taguchi Parameters design approach Process

To conduct an effective design of experiment based on Taguchi parameters design approach, the research should follow the steps below [147][138][124]:

- Problem Statement and the objective of the work.
- Select a measurable outcome (Response).
- Identify the factors affecting the process (response) and their levels.
- Build the adequate orthogonal array for the experiment (Taguchi parameters design method).
- Assign values and perform the experiment.
- Identify the optimal settings using the signal to noise ratio.
- Collect and analyse the data.
- Interpret the results.
- Conduct the confirmation tests.

There is a tremendous amount of research conducted on plasma cutting using DOE using Taguchi approach parameters design. Based on literature review, an experiment can be performed using three

or four parameters mainly at three levels and L9 or L27 can be adopted. In this case, due to time constraints and the cost of the tests, a minimum trial using L9 array was selected.

There are several statistical tools that can be used in the research. One of the most powerful techniques used is Minitab. The software is a reliable and effective, also extensively used as a tool for hypothesis testing, analysing data and make a meaningful interpretation of the findings [148][147]. Minitab is widely used in the industry to increase quality, solve issues and optimise the process [149]. The software is a user friendly and known as the preferred tool for researchers when there is no programming or building complex mathematical formulas compared to MATLAB, Statistica, Design expert, IBM, Maple or other software. In addition, Minitab was chosen as similar articles in this field suggested this software for variables analysis [145]. The version used is Minitab 19.2.

The Literature review for plasma cutting showed that the main method used for data analysis was ANOVA (analysis of variance). This method was developed by R. Fisher as an improved version to overcome the issues encountered using other methods such as T tests or Z tests [138]. ANOVA is a reliable statistical tool which is employed by other researchers to analyse data and the effects of the parameters [150]. General linear model (known previously as two ways ANOVA) was used for this work to identify the variables the most influential on the response. The analysis was made at 95% confidence (level of significance) [151] known also as the level of uncertainty [152].

To justify the choice of ANOVA approach, there are two main branches that can be identified for data analysis for quantitative research. This is depending on what the study is investigating and if a hypothesis testing is required (similar to this study), then the suitable approach in this case would be inferential data analysis method. This technique allows the researcher to predict the variables based on what is being observed, for that ANOVA, T-test or regression for instance can be used. A Descriptive data analysis is another approach that is mainly used to characterise and categorise the samples which is not the case in this thesis, Mean or Midian techniques can be used to analyse the descriptive data.

There are three families of statistical analysis in general Chi Squared family used if a comparison is required or if we seek to find a deference in groups and we possess only categorical data (qualitative data). T-test family is used if a comparison is performed or to find the difference in mean groups and if we have both category and continuous data, this includes T-test for two groups, ANOVA for three or more groups. Z-tests is the same than T-test but used when large data is available. Correlation family is used when we are studying relationship and we only have continuous data (used for

estimation mainly). MANOVA is similar to ANOVA but used when two responses are assessed. T-test can be used in my case, but it can only compare two groups at time which is time consuming when ANOVA is available, and in this case we might fail to detect the effects significance, this can result to an inflated P-value [154].

ANOVA method was selected for this research, as in my case it involves testing hypothesis. Two ways ANOVA can be selected to compare the mean's levels of a groups if two factors or more on a single response are used whereas one way ANOVA compares levels of one factor and one response only [153]. In overall, in any research it is the purpose of the work that dictates the technique required, depending on what we are using if either a comparison or relationship study and the type of data we possess if it is a categorical "qualitative data" or a continuous data "quantitative data".

Furthermore, Regression analysis was used to assess the strength relationship between the input and the output parameters. This is a powerful way to demonstrate if the experimental design is valid and reliable [155]. The oldest and widely used technique in science is the multivariable linear regression [156]. In this thesis, two mathematical models were built (single sheet and double sheet) which are used to analyse the variables for both phenomena deformation and the HAZ.

#### **4.6 Experimental Procedures**

CNC Plasma was used for the experiments, the machine can automatically control the speed and direction of the cut in X and Y axis. Based on literature review, this method is widely used by researchers to control the parameters, profile, and perform cutting tests. The model used for this research is a CNC Plasma Hypertherm Powermax 1250 Torchmate T80M automatic distance adjustment torch-workpiece with capacity of 50% duty cycle [158] (see Figure 15), Voltage 240V, pressure ranging between 40 to 90 Psi and current between 20 to 80A. Plasma with current capacity up to 200A was categorised by fabricators as low current machines [159]. This model was chosen due to their ability to work at harsh conditions, also their consumables life was higher than standard plasma up to 10 times longer due to a new patented electrode Hylife implemented in the torch which prevents nozzle wear. The machine was known for flexibility, quality, reliability and can switch from manual, CNC to robotic arm with ease [160]. Furthermore, the machine employs air for both cutting and shielding, this gas is commonly employed for cutting materials up to one inch thick. The technique was convenient also when a low current is used [162]. Air plasma offers a versatile cutting and a good quality of cut at high speed, thus by using air we eliminated the need to purchase the gas therefore the cost of operation was lower [163]. In this work we consider deformation of the surface

sheet, heat affected zones size, dross size and the offset between the two sheets are the main qualities to be assessed.



**Figure 16:** CNC Plasma cutter

The Research was categorized in four different phases summarised as follows:

#### **4.6.1 Phase One (Thin material cutting)**

This stage was necessary to understand the effect of the heat generated during the plasma cutting process on thin material and how the defects resulted could be minimised. Tests performed would illustrate the suitability of plasma to process thin material under one millimetre. The thinnest sheet part in the underbody vehicle chassis floor measured was 0.6 mm [26]. Therefore, to reduce the phenomenon of deformation in thin materials. DOE based Taguchi parameters design approach was used and three parameters at three levels were considered for the tests. L9 ( $3^3$ ) orthogonal array was used to optimise the single sheet, 9 rectangles of  $40 \times 150$  mm were cut from a large sheet size of  $500 \text{ mm}^2 \times 0.6$  mm thick.

#### **4.6.2 Phase Two (3D-Structure Cutting Capability)**

This stage will determine the capability of plasma to perform a cut in two separate sheets with an air gap distance (3D-Structure) simultaneously. Two identical sheets of  $500 \text{ mm}^2$  and 0.7 mm thick was used to create a three-dimensional structure, this was assembled using bolts, washers and nuts, the two sheet were separated using spacers at a desired distance. The plasma parameters were varied randomly using trial and error method, a series of cuts 150 mm long were performed until the obtention of the cut in two sides (simultaneously). To identify the maximum gap that can be cut, the spacers were changed to increase the distance gap between the two sheets.

#### **4.6.3 Phase Three (Cutting Parameters Identification)**

The third experiment was made to determine the starting parameters required to cut two layers. The gap was fixed at 20 mm distance between the two layers, as the quality cut showed a better level than the higher gap (quality was assessed visually). The settings which resulted to the best quality cut were used as a reference and a starting point for the next set of experiment which meant to optimise the parameters. Two identical 0.7 mm thick sheets were assembled to create a 3D structure similar to previous model and a series of straight lines cut of 50 mm long were performed.

#### **4.6.4 Phase Four (Parameters Optimisation of a Double Sheets)**

Taguchi parameters design method was used to optimise and improve the quality of a double sheets (3D structure). Four parameters at three levels were considered for this tests including the gap distance between the layers. Therefore, three models were built at different distance 10 mm, 15 mm and 20 mm (gap levels), sheets of  $300 \text{ mm}^2 \times 0.7 \text{ mm}$  were used for the assembly of the models, bolts, nuts and washers were used and the sheets were separated using spacers at a desired distance. L9 ( $3^4$ ) OA was chosen for the experiment and nine trials were performed to cut rectangles of  $150 \text{ mm} \times 40 \text{ mm}$ . Three trials for each model were made, the models were kept cooling at room temperature after each trial.

#### **4.7 Samples preparation**

The samples collected from the experiments were scanned, then a small pieces of  $20 \times 10 \text{ mm}$  size were taken from each trial in the same area. The machine used for sectioning was Buehler AbrasiMatic 300 abrasive cutting, the pieces were mounted on a 40mm diameter mould. The mounting press used was SimpliMet3000 Buehler automatic model and the Compound used was ProbeMet, pressed to 290bars at  $150^\circ\text{C}$ . The specimens obtained were grinded and polished using a rotating machine AutoMet300 Buehler model with a sandpapers, P120, P240, P400, P800, P1200 Grit Sic, followed by a mirroring process using  $9\mu\text{m}$  and  $3\mu\text{m}$  Metadi Supreme Diamond then

0.05 $\mu$ m MasterPrep Alumina solution, finally, samples were etched using 5 % Nital acid [164] to expose the gains. See Figure.16.



(a) [165]



(b)



(c)



(d)

**Figure 17:** Samples Preparation Machines (Pictures Taken at AFRC). (a) Abrasive Sectioning Machine [165], (b) Mounting Press, (c) Grinding and Polishing Machine, (d) Samples Obtained

## 4.8 Measuring Methods

### 4.8.1 Deformation, Kerf, Dross and Edge Offset

The instrument used to measure the deformation, kerf and dross was a 3D ATOS TripleScan (Figure 17) this technique is the state-of-the-art technology used for surface analysis. This technique is widely used nowadays in the metrology field and also in the automotive industry. This technology uses a non-contact blue light [166] and just with one single scan it can take up to 16 million points of the surface with an accuracy of 10 Microns (0.01 mm) [167], this can be considered as the error of the equipment, this means the part measured and the actual one can have a 0.01 mm difference. This technique can achieve higher accuracy compared to a digital gauge. Furthermore, this method was suggested by researchers as an efficient way to capture features detail in short time whether small or

large scale [168]. GOM inspect was used as a software to measure the maximum deformation of each specimen, using Gaussian best fit virtual plan method. The values obtained were in millimetres, a simulation of the deformation was illustrated on the surface to contrast different levels of distortion, zones with the red colour are the areas where maximum deformation level compared to the plan constructed. The 3D scanner can reveal all the features with precision making the assessment easier for also measuring other phenomena such as kerf and dross which were difficult to assess using alternative tools such as feeler gauge, dial indicator gauge or calliper.

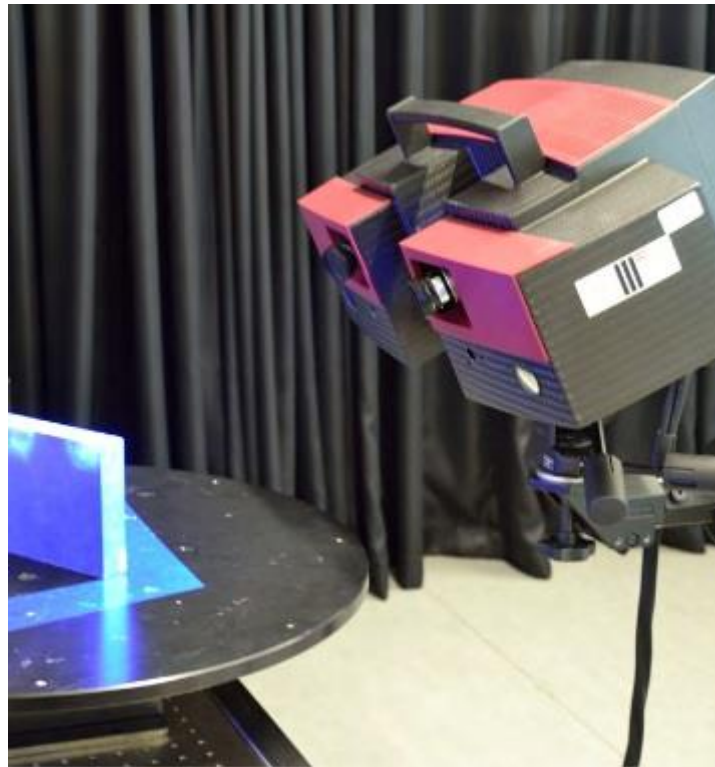


**Figure 18** Atos 3D TripleScan (AFRC) [165]

The offset cut edge is the shift between the top and bottom edges. This phenomenon was a very important to measure, as this can cause issue when fitting the customised floor pan. We noticed after the tests that there is a difference in size between the top and bottom samples. Calliper was used to measure the sizes of each sample and then mathematically we have calculated the offset and the difference between the upper and lower sheets. The tolerance of the offset in each side was set to 2 mm maximum.

#### **4.8.2 Heat Affected Zones (HAZ)**

Microscope LEICA DM12000M (see Figure 18) was used to assess the heat affected zones, the model magnification available was 5, 10, 20, 50 and 100 times. The equipment offers a resolution in both directions (X,Y) of  $0.01\mu\text{m}$  and an accuracy of  $\pm 5\mu\text{m}$  [154]. The size of the affected zones was measured from the cut edge to the base metal, the values obtained were in millimetres.



**Figure 19** Leica DM12000 Microscope (AFRC) [165]

To identify the HAZ under the microscope it was necessary to know first the structure of the material, the difference between steel grains, also how these gains were formed. When metal is heated at high temperature above the transformation degree and below the melting point austinite grains are formed, each grain is composed of millions of atoms arranged in a space lattice cube, at room temperature atoms are arranged in body centred cubic form (BCC). When critical temperature is reached (transformation temperature) the atoms are reorganised and change shape to face centred cubic (FCC) space lattice, this change is called allotropy. Carbon atoms are significantly small, they are scattered around the iron atoms in the interstitial space. When the allotropy transformation begins an additional room is generated in the lattice increasing the capacity for carbon accommodation. Below the transformation temperature and allowing time for cooling, the lattice change back to initial form BCC causing the carbon atoms to migrate away, the process is called diffusion, this process will contribute in the formation of the pearlite grains in later stage [169].

At normal cooling time during solidification small crystals are formed in the austinite and expand to meet with their neighbouring crystals, a new form of light white tinted grains due to iron presence appears called ferrites. These types of grains allow the material to possess the ductility properties, then progressively during the cooling process, the diffusion of carbon begins and starts to form pearlite grains which can be seen as a zebra structure grains, white is the iron and black hashed lines are iron carbide (cementite), these types of grains give the properties of hardness and strength. The proportion number of grains ferrite-pearlite can be different depending on the amount of carbon present in the material (low, medium or high carbon steel), if the material is high in carbon then the

pearlite grains will be dominant and vis versa [170]. The other scenario is when the material is cooled quickly not allowing the diffusion process to happen naturally. Carbon atoms would be trapped in the space lattice and become distorted allowing only a small quantity of carbon to escape, a new form of grains appears known as martensite which can be seen under the microscope as grains with black thin cementite needles shape oriented in any random directions, these grains are hard and brittle, similar grains can be formed when cooling process is fast but not as fast to form martensite, known as bainite grains seen under the microscope with similar appearance to pearlite, thinner black cementite needles shape oriented roughly in the same direction at around 50 to 60°[171]. These grains are excessively present at the cut edge when a thermal cutter is used [109]. Figure.19.

Heat Affected Zone is the volume material between the cut edge and the base material which the mechanical properties were altered due to high heat input and fast cooling. This area is weak compared to the unaffected base and can easily crack and cause problems. Hence, it is undesirable for engineering applications. HAZ can be divided into four areas, the closest to the unaffected base material is called tempered zone, then partly changed area, recrystallised and grain growth area which are close to the cutting edge[172][173]. This different area in the HAZ can be contrasted (heat tint) and visible due to high temperature distribution impact across the material and surface oxidation

during a cut. In overall the HAZ size is depending on the material used, the quantity of heat applied and the length of exposure [173].

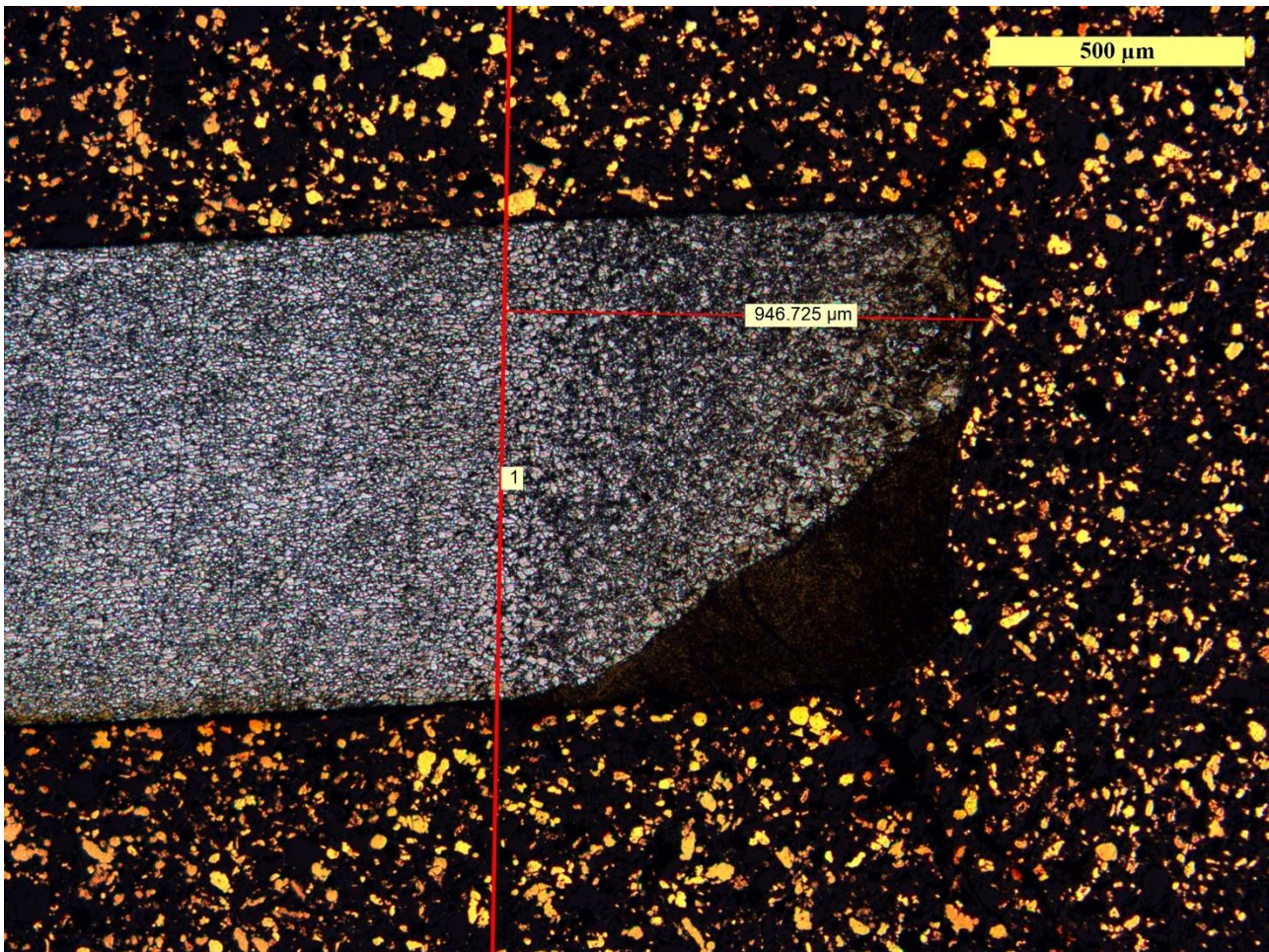


**Figure 20** Heat Affected Zones Size

#### **4.8.3 Microhardness**

To identify the maximum hardness resulted after the cutting, a series of micro hardening tests were performed from 0.1 mm of the edge of the cut up to 5 mm incrementing each 0.3 mm. Struers Durascan 70 model machine Vickers Microhardness HV was used for the tests (Figure. 21), 1kg force load applied for 12 second. The hardness of the unaffected metal base was measured first and an average value of HV 123 was measured.



**Figure 21** Struers Durascan 70 Microhardness[174]

#### **4.8.4 Measurement Handling**

In any experimental research it is important to make sure that the method of measurement used is reliable and valid. This would ensure that other researchers can replicate the tests (in the same conditions) and obtain the same results. The observational or measurement error can be seen as the difference between the true and measured value. To ensure the validity of the results in this study, the measurement was repeated three times. The samples were also inspected using the conventional methods such as calliper, gap filler and micrometre gauge as shown in the Figure 22 below.



**Figure 22** Measuring Equipment

There are two types of error to minimise, random error which naturally happens such as human error and also the systematic errors which can occur when equipment is not properly calibrated [175]. In this research, due to time constraints and the scope of work, the measurement errors were not calculated. However, these were minimised, and the validity of the measurement was ensured by following these steps:

- Repeat the measurement three times and compare the values obtained (test-retest), in addition to conventional inspection method.
- Ensure the following set of measurement are not biased by the previous ones. (Disregard the previous tests to be sure the values obtained are not biased).
- The measurement was double checked for accuracy with other researchers and Laboratory technicians to eliminate the human error.
- Make sure that the technicians in the laboratory are fully trained and have enough experience to perform the measurement (this was applicable only for 3D Atos Triple Scan measurement and sample's surface etching process).
- Check for consistency of the measurement using different means of measuring instruments.
- Ensure the equipment are accurate to eliminate the instruments errors. preliminary tests were performed to verify the reliability and proper calibration of the equipment.

#### **4.9 Summary**

In this chapter, a detail of the experimental process followed in this research was given. This work was performed in four different phases, starting from thin layer analysis tests, two sheets cutting tests, identification of the effective parameters tests and optimization of the two sheets cutting tests. The main points of this chapter are given below:

- Experimental quantitative methodology was selected in this thesis as this research intend to verify a hypothesis of plasma heat re-employment.
- DOE based Taguchi parameters design was selected as the adequate approach to reduce the cost, number of trials and optimize the process.
- Ishikawa diagram was used to identify the main parameters to assess the surface deformation and HAZ phenomena.
- L9 ( $3^3$ ) was selected to process a single sheet 0.6 mm thick.
- CNC plasma was selected for the tests and the input parameters included cutting speed, intensity, and air pressure for single cutting. In addition, gap distance between the two sheets was considered as an input parameter in the double sheets cutting.
- L9 ( $3^4$ ) was used for a simultaneous cutting of two parallel sheets with an air gap distance, the thickness of the sheets used was 0.7 mm.
- To ensure the validity of the data collected, the measurement was repeated three times and the same values were obtained in each process.

# Chapter 5 Data Collection and Analysis

## 5.1 Introduction

The initial stage of the experiment was performed to analyse single layer cutting using Taguchi parameters design method. The second stage of tests were mainly to assess the possibility of re-employment of the heat power exiting the kerf to perform an additional cut (simultaneous cutting of double sheets). The third stage was to identify the adequate settings required to process this structure, the fourth stage was made to optimise the process and reduce the defects to their minimum level possible. ANOVA was used to analyse the results at 95% level of confidence, the most influential parameters were identified. Lastly regression models were constructed to assess the strength relationship between the input and output variables.

## 5.2 Experimental Process

The material used for the experiments was a thin sheets cold rolled deep drawing steel DC01 grade, similar steel used for some underbody vehicle chassis floor parts [176]. The chemical composition of the material is 0.12% Carbon, 0.6% Manganese, 0.045% phosphorus and 0.45% Sulfur [177]. The mechanical properties of the metal are given in the Table 5 below:

**Table 5** Mechanical Properties[177]

Density ( $\rho$ )kg/dm <sup>3</sup>	Young's Modulus E(GPa)	Yield Stress Y(MPa)	Tensile Stress R(MPa)	% Elongation A/80mm gauge	Anisotropy (r)	Poisson's ratio ( $\nu$ )	Strain hardening exponent (n)	Strength Coefficient k
7.83	210	140-280	270-710	Min 28	1.53	0.35	0.21	619

Five models were prepared for the experiment in addition to flat sheet, the first test used a single layer 500 mm square and 0.6 mm thick. The second model was assembled for the double sheet cutting, two identical sheets of 500 mm square and 0.7 mm thick were used, assembled using blots, nuts and washers, spacers were used to keep the gap at a desired distance between the two sheets (16, 25, and 35mm). The third model was assembled to identify the starting points at fixed gap of 20mm between the two sheets. For the last experiment, three identical models at different gaps 10, 15, 20 mm distance between the layers were assembled for optimisation process, 300 mm  $\times$  300 mm  $\times$  0.7 mm were assembled in the same manner.

The CNC plasma machine was checked and calibrated to ensure the validity of the tests and eliminate the errors. There are two categories of errors [178] identified in plasma cutting: errors after cutting which can be compensated by optimising the process and the errors before cutting and these can be controlled by following the steps above before the starting the experiments:

- Assist the operator from start to finish of experiment process.
- Check the level of flatness of the sheets with digital prob gauge
- Ensure the technicians are trained and qualified.
- Perform initial tests to verify the accuracy of the machine and size of the parts obtained using a calliper, this also includes software's programming error and graphic size error.
- Assess the level of phenomena obtained to the manufacturer standards.
- Replace all the consumable, check fluctuation of the voltage and air flow.
- Ensure the accuracy of the torch-workpiece distance using filler gage (arc voltage automatic height control).
- Check the screen for any error.
- Verify the correct setting by two engineers, pressure gauge indicator, proper voltage, amperage and cutting speed.

The gap between the two sheets was maintained using spacers at a desired length (as needed), these were placed around the model, the length of the spacers was checked with a calliper before use. Different spacers were used for different gaps. Two spatulas were used to handle the top samples carefully during and after the cutting, this will prevent the top samples from bending under the effect of their weight and also from colliding with the lower sheets. The small pieces taken from the samples to analyse the HAZ were cut from the same area where the defect meant to be maximal (at the corner see Figure 22). The parameters were identified using initial tests as explained in the 5.2.3 section. Preliminary tests were performed to check the quality of the cut obtained. This would give an indication if the correct settings were used. After each test the model were left to cool at room temperature before proceeding to the next trial. For the experiment in phase four, each model (three models at different gaps) was separated into three zones and fixed properly using bolts, nuts, washers and spacers between the sheets as shown in the Figure 23 below to avoid the deformation to move to the next trial. The levels of the parameters were calculated as explained in the section 4.4.2.

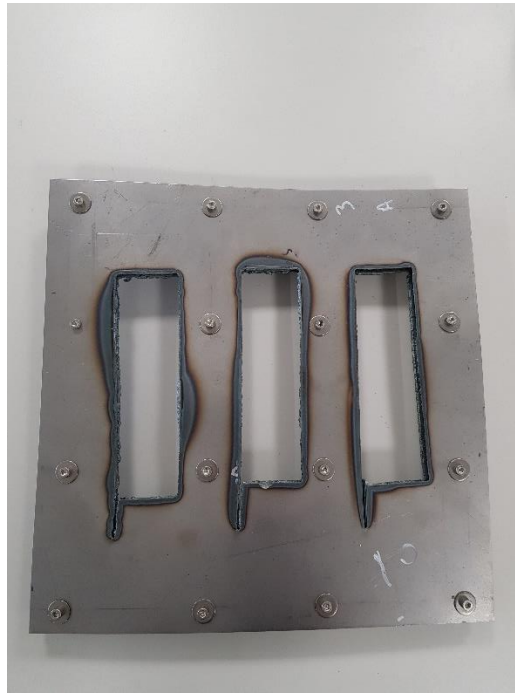


**Figure 23** Experimental Model, Separation into Three Zones

### 5.2.1 Phase One - Single Sheet Cutting

In this stage a flat sheet of  $500 \times 500 \times 0.6$  mm was used to verify if plasma machine can result to an acceptable cut in thin sheets without altering the surface. In other words, assessing the effect of the heat generated by plasma cutting on thin materials.

Taguchi parameters design method was selected, and orthogonal array was constructed for this test to cut and optimise the quality (deformation and heat affected zones mainly). Nine tests were selected (see Table 7) and nine rectangles of  $150 \times 40$  mm. The parameters chosen were three input variables [145], cutting speed, current and gas pressure at three levels ( $3^3$ ) as shown in the Table 6 below.

**Table 6** Parameters and their levels

parameters / Levels	L1	L2	L3
Cutting Speed (mm/min)	8000	8500	9000
Air Pressure (Psi)	70	75	80
Current (A)	20	25	30

**Table 7** Experimental Layout

<b>Trials</b>	<b>Cutting Speed (mm/min)</b>	<b>Pressure (Psi)</b>	<b>Intensity (A)</b>
<b>Test 1</b>	8000	70	20
<b>Test 2</b>	8000	75	25
<b>Test 3</b>	8000	80	30
<b>Test 4</b>	8500	70	25
<b>Test 5</b>	8500	75	30
<b>Test 6</b>	8500	80	20
<b>Test 7</b>	9000	70	30
<b>Test 8</b>	9000	75	20
<b>Test 9</b>	9000	80	25

### 5.2.1.1 Deformation Measured

Nine samples of  $40 \times 150$  mm size collected from the  $500 \text{ mm}^2$  single sheet part 0.6 mm thick and then scanned using 3D Atos TripleScan. The Figure 21 below shows one of the specimens (Trial number one) scanned and assessed using GOM software. The entire scanned specimen's figures can be found in the [APPENDIX-C FIGURES C1](#) at the end of this thesis.

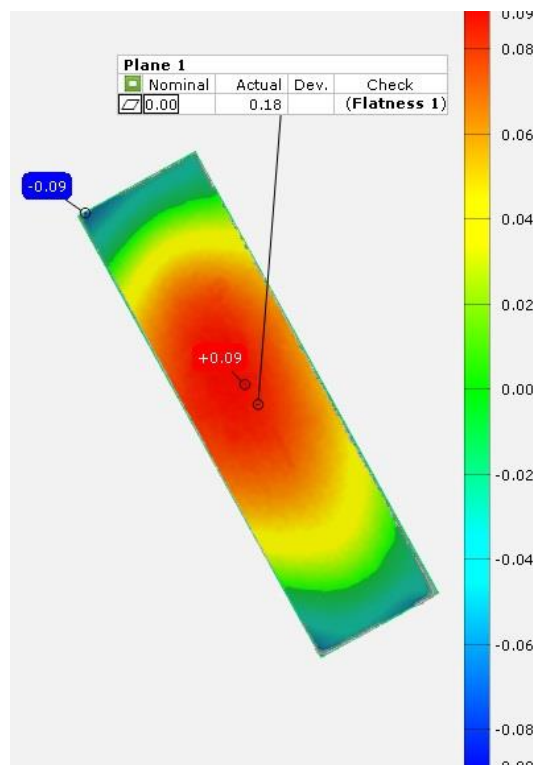


**Figure 24** scanned part (Trial number one)

Nine values measured using GOM Inspect were recorded on Table 8 as shown below:

**Table 8** Deformation results (mm)

<b>Trials</b>	<b>Deformation (mm)</b>
<b>Trial 1</b>	0.18
<b>Trial 2</b>	0.12
<b>Trial 3</b>	0.16
<b>Trial 4</b>	0.18
<b>Trial 5</b>	0.22
<b>Trial 6</b>	0.30
<b>Trial 7</b>	0.20
<b>Trial 8</b>	0.28
<b>Trial 9</b>	0.18

The results showed in Table 8 above that the deformation did not exceed 0.3 mm. The values measured fluctuated between 0.12 mm to 0.3 mm. The minimum value was obtained using parameters of the trial number 2 and the maximum deformation was obtained when parameters of the trial number 6 were used. The tolerance set for the deformation is 0.2 mm maximum, it is noticeable that most of the trials were within the tolerance, only trial 5, 6 and 8 fell outside the tolerance value.

#### **5.2.1.2 Heat Affected Zones measured**

Figure 22 below shows one of the sample's (trial 4) measured for heat affected zones using a microscope. The values obtained were shown in the table 9 below. The remaining figures can be found in the [APPENDIX-C2](#). The boundary between the unaffected zones (base material) and the area that undergo material change can be contrasted due to the amount of carbon released to the surface. This can be also contrasted by the grain size (larger compared to unaffected grains) and the structure of the grains as explained before in section 4.8.2.

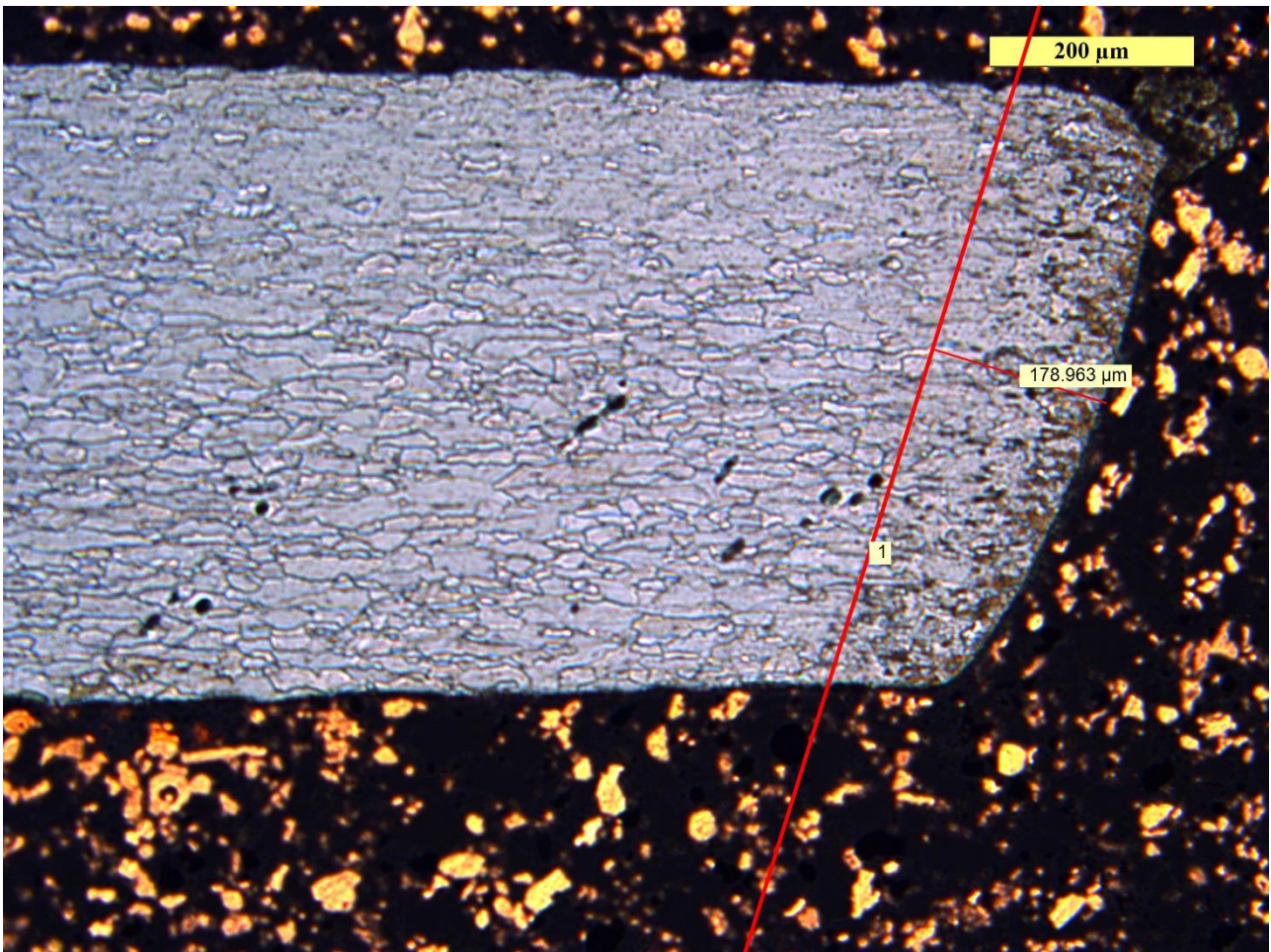


**Figure 25** Trial 4 Heat Affected Zones Width for Single Sheet

**Table 9** Heat Affected Zones Measured

<b>Trials</b>	<b>HAZ(mm)</b>
<b>Trial 1</b>	0.403
<b>Trial 2</b>	0.383
<b>Trial 3</b>	0.221
<b>Trial 4</b>	0.179
<b>Trial 5</b>	0.154
<b>Trial 6</b>	0.167
<b>Trial 7</b>	0.212
<b>Trial 8</b>	0.195
<b>Trial 9</b>	0.161

Based on the Table 9 above, the values of the heat affected zones width varied from 0.154 mm to 0.403 mm. The values are showing that a second processing might not be required due to small size of the defect (less than half millimetre in size). The minimum value was obtained using parameters of the trial 5 whereas the maximum width measured was obtained when parameters of the trial one is used. The tolerance was 0.2 mm maximum for the heat affected zones, trials 1, 2, 3 and 7 were falling above the tolerance value.

### 5.2.1.3 Parameters Optimisation and Analysis

Taguchi parameters design approach was used as an optimisation technique, this would help to achieve the best quality possible. The requirement of the study was to minimise the phenomena of the deformation and HAZ. Therefore, a smaller is the better option was chosen, the equation is given as follow[113]:

$$S/N = -10 \log \frac{1}{n} \sum_{i=1}^n Y^2$$

Y is the observed response and n is the number of trials.

n: is the number of the observed values.

The results obtained from the Taguchi parameters design experiment are shown in the Table 10 below:

**Table 10** Data Collected from the tests

Trials	Sheet Deformation (mm)		HAZ (mm)	
	Response Measured	S/N Ratio	Response Measured	S/N Ratio
<b>Trial 1</b>	0.18	14.8945	0.403	7.8939
<b>Trial 2</b>	0.12	18.4164	0.383	8.3360
<b>Trial 3</b>	0.16	15.9176	0.221	13.1122
<b>Trial 4</b>	0.18	14.8945	0.179	14.9429
<b>Trial 5</b>	0.22	13.1515	0.154	16.2496
<b>Trial 6</b>	0.30	10.4576	0.167	15.5457
<b>Trial 7</b>	0.20	13.9794	0.212	13.4733
<b>Trial 8</b>	0.28	11.0568	0.195	14.1993
<b>Trial 9</b>	0.18	14.8945	0.161	15.8635

### 5.2.1.4 Signal to Noise Ratio

Using S/N ratio we can identify the optimal settings that can be used to reduce the defects to their lower level. The highest value of the S/N ratio represents the optimal setting [179] as shown in the Table 11 and 12 below and S/R Ratio in Figure 23 and 24.

**Table 11** S/N Ratio for Sheet Deformation

Level Sheet Deformation	Cutting Speed (mm/min)	Pressure (Psi)	Intensity (A)
1	16.41	14.59	12.14
2	12.83	14.21	16.07
3	13.31	13.76	14.35
Delta	3.57	0.83	3.93
Rank	2	3	1

**Table 12** S/N Ratio for HAZ

Level HAZ	Cutting Speed (mm/min)	Pressure (Psi)	Intensity (A)
1	9.781	12.103	12.546
2	15.579	12.928	13.047
3	14.512	14.840	14.278
Delta	5.799	2.737	1.732
Rank	1	2	3

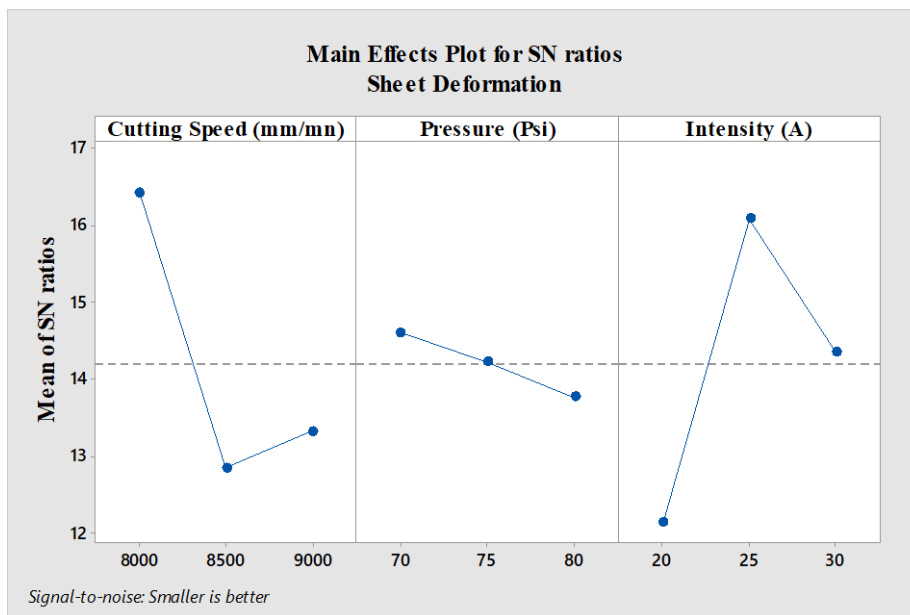


**Figure 26** Optimal Parameters for Sheet Deformation

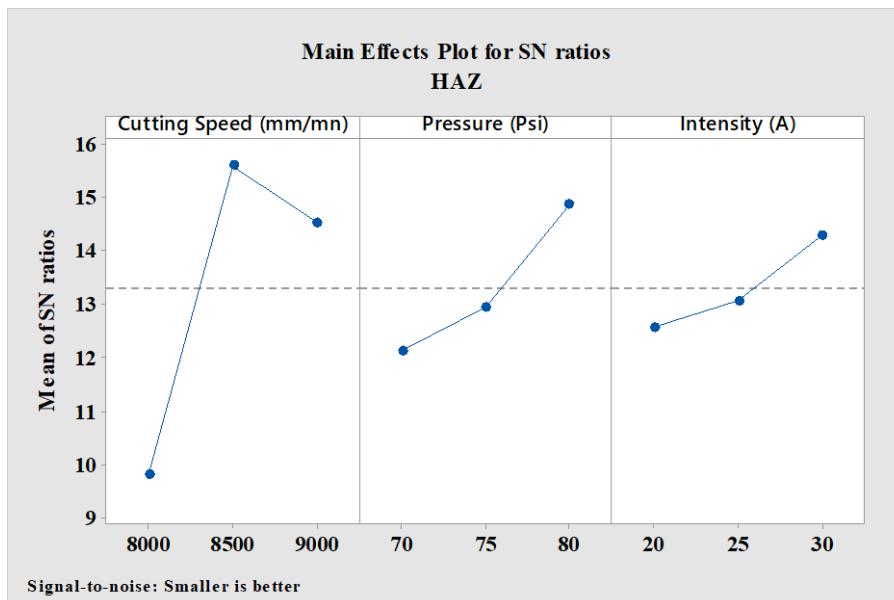


**Figure 27** Optimal Parameters for HAZ

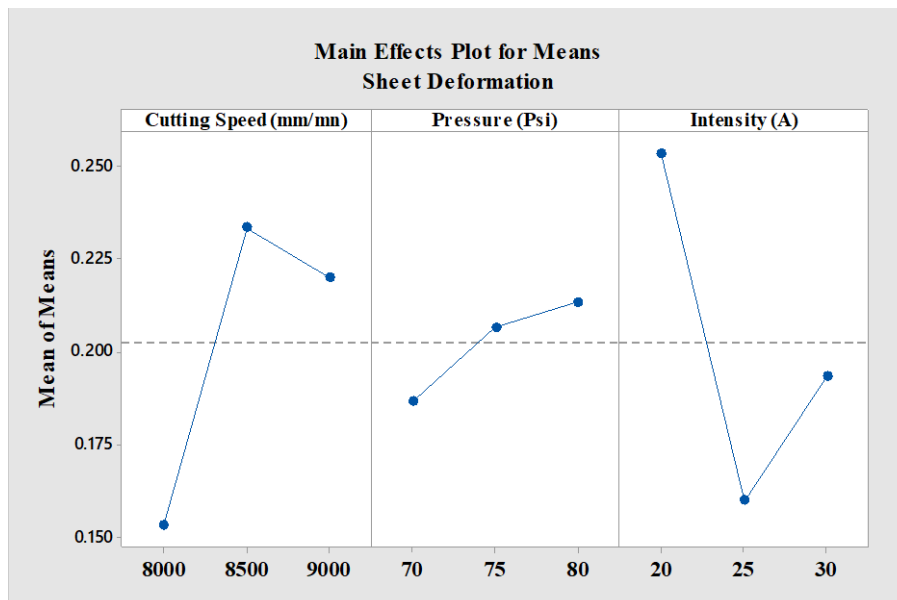


**Figure 28** Parameters Effect for Sheet Deformation

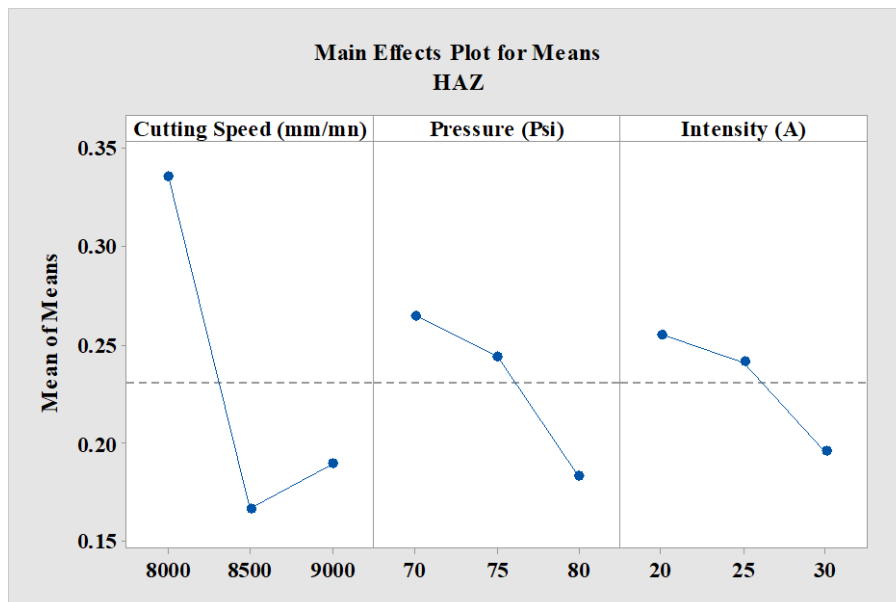


**Figure 29** Parameters Effect for HAZ

From the Figures 24 and 25 above for signal to noise ratio, the highest value of S/N Ratio corresponding to the optimal parameters to minimise the sheet deformation are Cutting speed at 8000mm/min, pressure at 70Psi and Intensity at 25A whereas Heat Affected Zones are Cutting speed at 8500mm/min, pressure at 80Psi and Intensity at 30A.

The main effect plot for means can indicate the parameters influencing the response. The levels possessing the highest inclination line to the horizontal and largest amplitude are the ones that have the most influence [180]. It is clear from the sheet deformation means graphs (Figures 25 and 26) that cutting speed and Intensity have a considerable level of inclination compared to Pressure. However, the highest effect for the heat affected zones was mainly cutting speed and then the other parameters at approximately the same effect level but the pressure is slightly higher.

#### 5.2.1.5 Analysis of Variance (ANOVA)

ANOVA is an effective statistical tool used by researchers to analyse the effect of the parameters and obtain an approximative percentage of the controlled variables which were most influential on the response. The analysis was done at 95% confidence, this represents the level of uncertainty [152]. This means that if the tests are repeated a second time the results obtained will be matching precedent one at 95%. In this study, the purpose of using ANOVA was to identify the most influential parameters, the significance of the effects and assess the interactions. Therefore, repeat measurements were made but without estimating the errors due to time constraints and the scope of the work. The results obtained can be seen in the Table 13 below.

**Table 13** Contribution Effect

Source	Contribution	
	HAZ	Sheet Deformation
Cutting Speed (mm/min)	70.05%	42.47%
Intensity (A)	8.01%	51.71%
Pressure (Psi)	15.01%	4.45%
Error	6.93%	1.37%
<b>Total</b>	100.00%	

Table 13 above shows the most influential parameters on both responses deformation and heat affected zones obtained using ANOVA. We can conclude that cutting speed has high impact on both phenomena, HAZ at 70% and deformation 43%. Intensity has a biggest effect on surface deformation to just below 52% whereas HAZ showed a small effect of just above 8%. Pressure also did not show a big impact on both responses, but it reflected most on the HAZ compared to sheet deformation, respectively 15.01% and 4.45%.

We assume that the effects of the plasma parameters on the response are caused due only to random chance and there is no difference in the process of generating data, this would be considered as the hypothesis testing in this analysis (null hypothesis). P-Value is a statistical approach that can test if the hypothesis is true. The alternative hypothesis would mean that the effects are significant and did not result due to random chance. The interval of confidence selected in this study is 95%, therefore any P-Value that is smaller than 5% (or 0.05) can be considered as evidence that the effects are significant, and the alternative hypothesis is accepted in this case.

Based on the ANOVA results obtained from Minitab, there is, there is a statistical evidence for surface deformation phenomenon that the effects of cutting speed and intensity are significant as the P-Values obtained were less than 0.05 [151], the values obtained were successively 0.031 and 0.026. There was no evidence that pressure had a significant effect as the P-Value was 0.235. In the other hand, the results showed that there was no statistical evidence that the effects were significant for the heat affected zones.

R-Squared known as the coefficient of determination that can give an indication of quality of the model and the level of prediction [181]. The Value can illustrate the percentile of the variation in the response that can be explained by the variation of the input variables. Even though,  $R^2$  can give an indication on how good the model can be predictive. However, it is also known that adding variables

to the model could increase the value of  $R^2$  regardless of whether the value added can benefit the model or not. Adjusted  $R^2$  can be used in this case to eliminate this issue as their values increase only if the variables added contribute to the robustness of the model [182]. R-Squared and Adjusted R-Squared obtained from the analysis result were respectively 98.63% and 94.52% for surface deformation whereas HAZ was 93.07% and 72.28%.

### 5.2.1.6 Interaction

The interaction plot graphs below Figure 27 for deformation and Figure 28 for HAZ were obtained using Minitab. The graphs illustrate that the effect of one parameter is depending on the level of other parameters [183]. The results showed that there is an interaction between the parameters for both deformation and heat affected zones. The variation of the response was affected by the change of both parameters level. However, for both responses there were no statistical evidence that the interactions were significant as the P-value obtained for all interactions were above the P-value of 0.05. The analysis was done at order two and at 95% level of confidence.

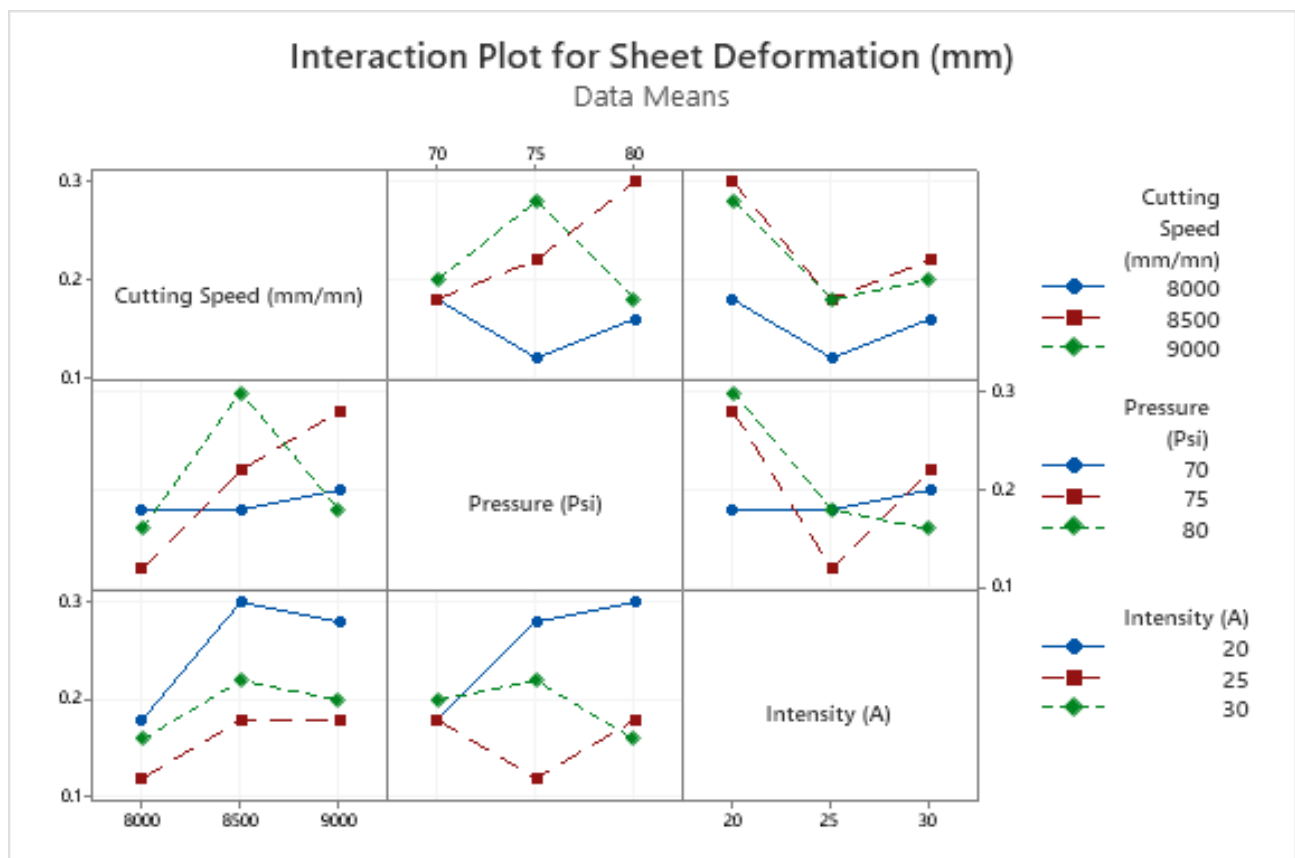
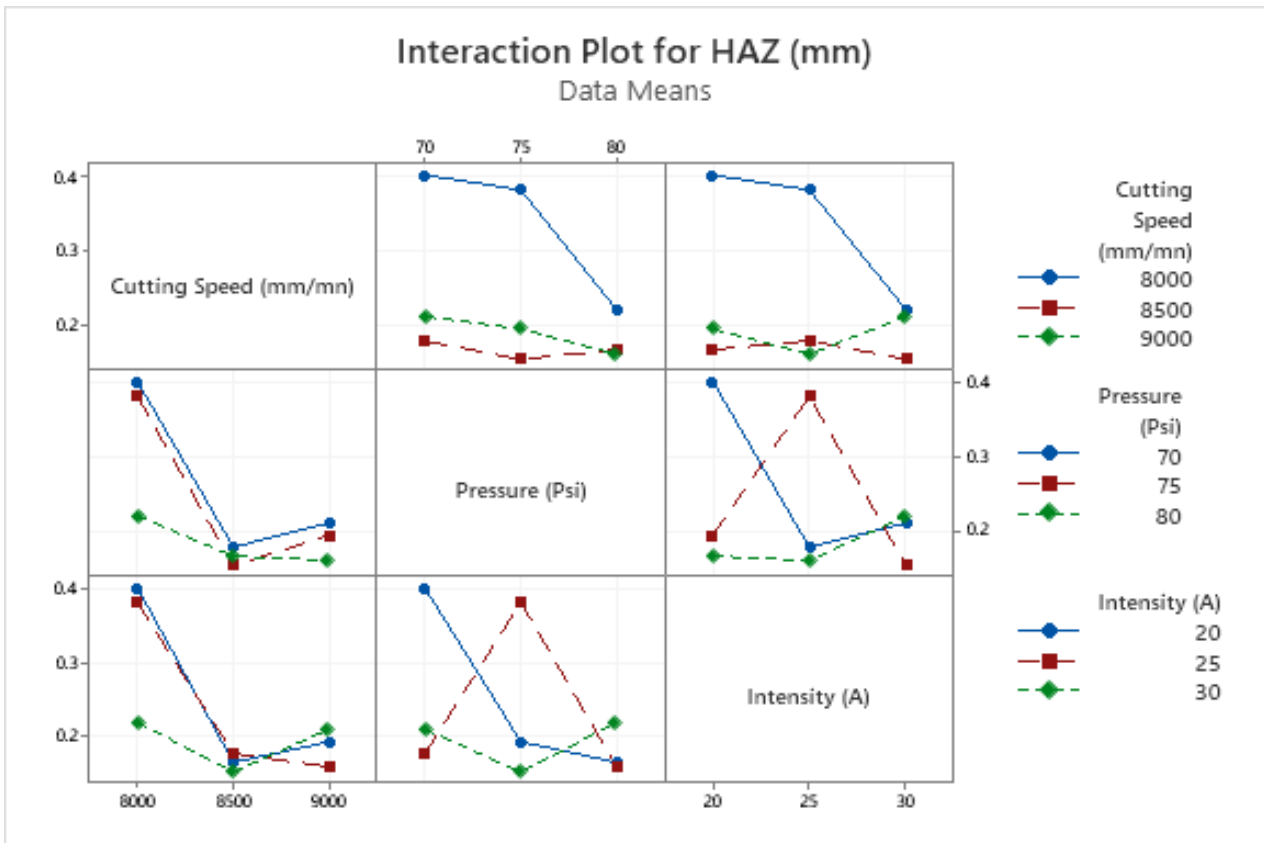


Figure 30 Variable Interactions (Deformation)



**Figure 31** Variables Interaction (HAZ)

### 5.2.1.7 Three-Dimensional Surface Plot

Three-dimensional surface plot was used to assess the effect of the two most influential parameters on the surface deformation and the heat affected zones as shown in the Figures 30 and 31 below. The surface plot for surface deformation showed that using the power at level one and cutting speed at

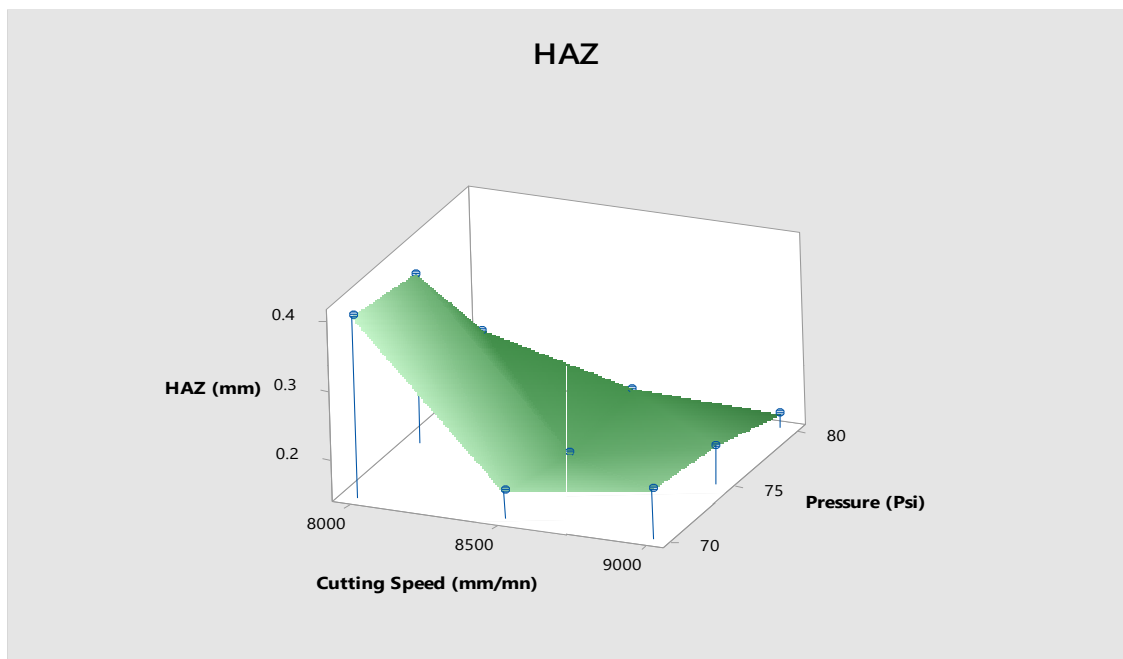


**Figure 32** 3D Surface Plot HAZ

level two can result to a maximum deformation. However, using power at level two associated with cutting speed at level one the deformation can be reduced to their lowest level. Heat affected zones

surface plot showed a maximum defect when both cutting speed and pressure at level one. The minimum value can be obtained if cutting speed used at level two mainly or three using pressure at level three.

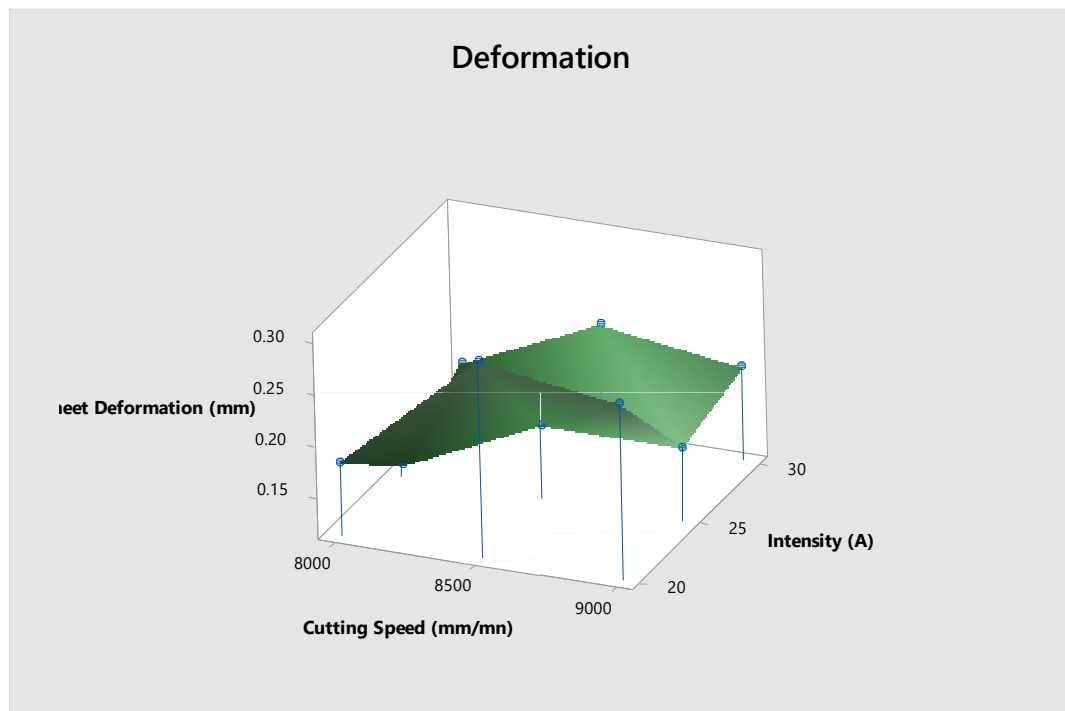


**Figure 33** 3D Surface Plot Surface Deformation

### 5.2.1.8 Single Sheet Modelling

In this section, two equations were constructed, the first was to estimate the deformation of the sheets and the second was for the heat affected zones.

#### *I. Assumptions*

From the Figures below 31 and 32 of the residuals plots for fits which is the difference between the observed and predicted values were spaced and falling randomly to the horizontal line (zero value mid-axis) [184]. Percent graphs showed that the variation and the distribution of residuals was practically similar for each level.

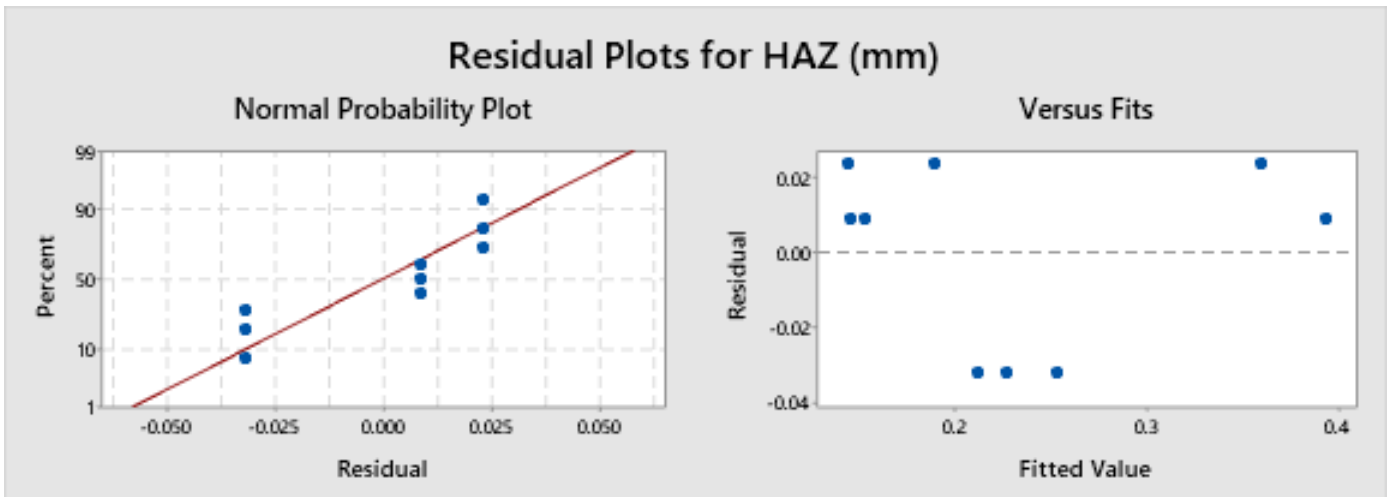


**Figure 34** Residuals and fits graph for HAZ

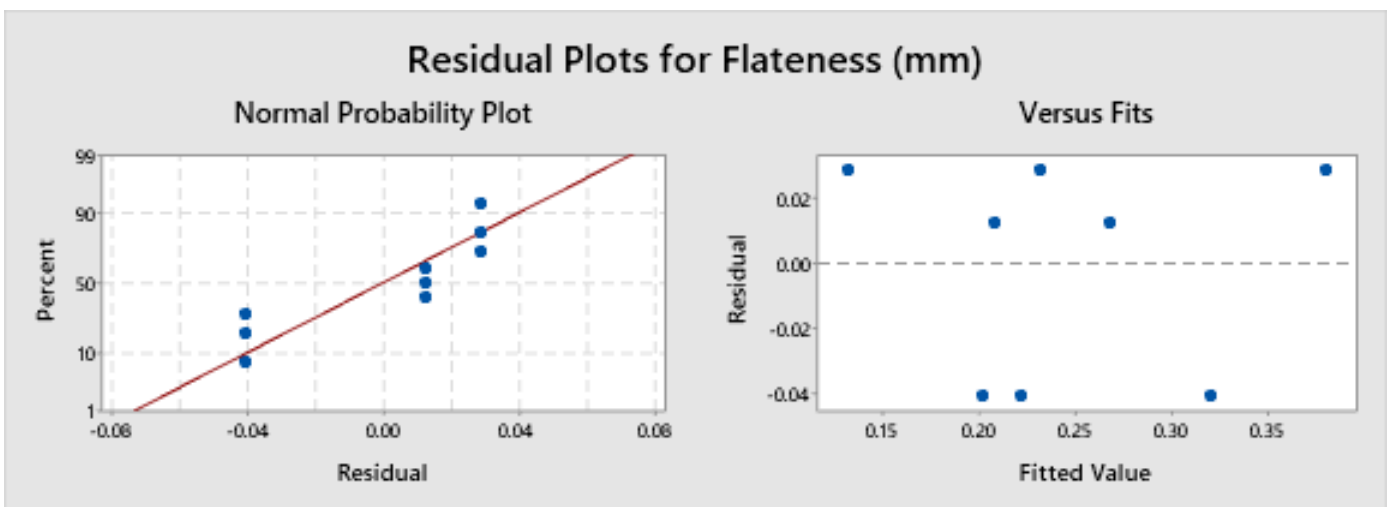


**Figure 35** Residuals and fits graph for surface deformation

These two conditions were necessary to assume that there is a linear relationship between the input parameters and the response. In addition, multicollinearity between the independent variables were analysed using pearson correlation. The coefficient for each independent variable in the regression model can indicate the average change of the response when the independent variable is changed by one unit assuming the other terms remain constant. However, if multicollinearity exists then this would not be the case [185]. From the correlation analysis conducted using Minitab, the coefficients of Pearson r obtained were all equal to zero, this indicates that there was no linear relationship between the independent variables.

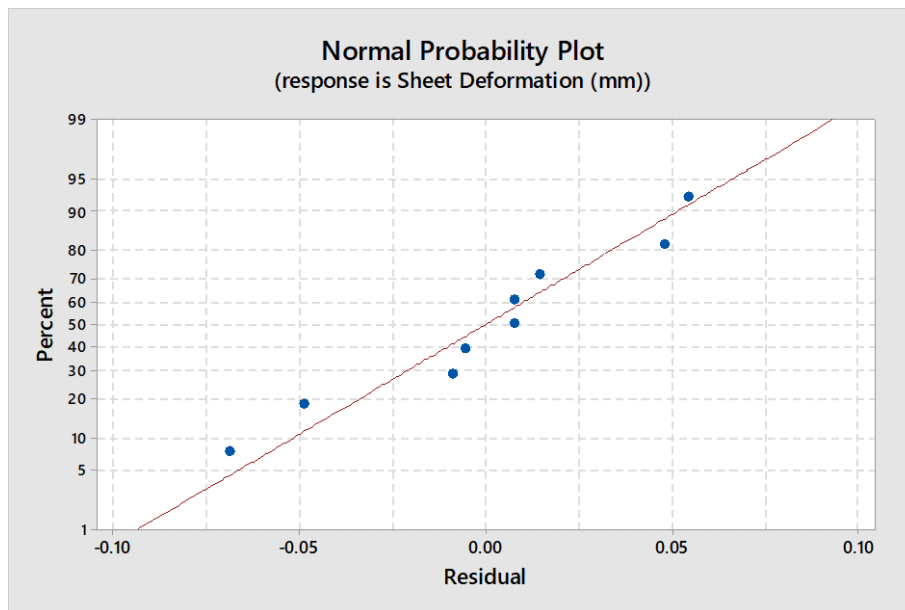


**Figure 36** Response prediction Surface Deformation

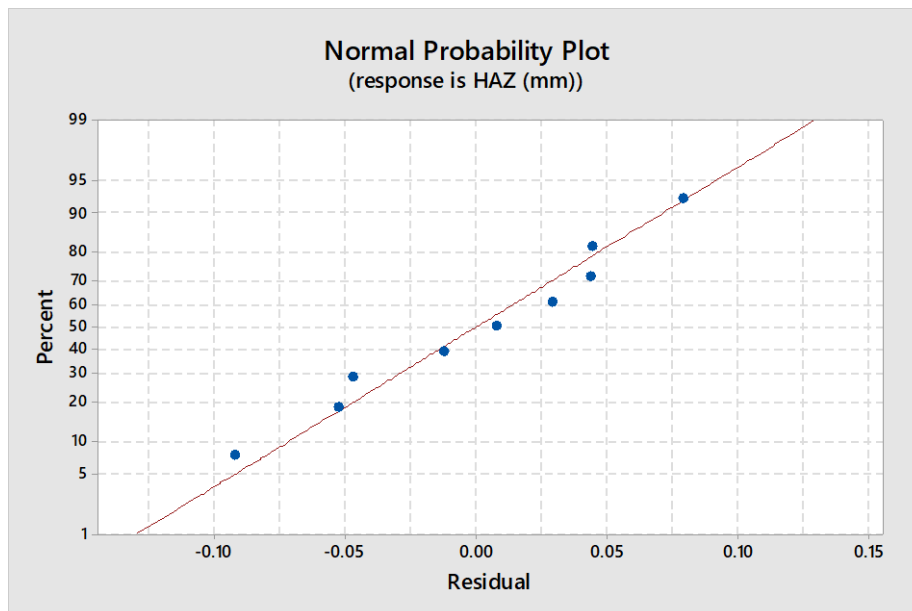


**Figure 37** Response prediction for HAZ

From the Figures 33 and 34 above, it is clear that the residuals are all scattered along and close to the diagonal line which represents the ideal normal distribution. Errors are the vertical distance between the residuals and the diagonal line. Accurate regression requires that the distance of residuals (errors) to be very small. In this case, this condition is satisfactory as the residuals are normally distributed. Therefore, the numerical data follows the assumption and the model used [186].

## ***II. Mathematical Modelling***

The general multi-variable linear regression model can be written as follows [187]:



$$y_i = \hat{y}_i + \epsilon_i \rightarrow \epsilon_i = y_i - \hat{y}_i$$

$y_i$  is the observed value,  $\hat{y}_i$  is the predicted value and  $\epsilon_i$  is the error

The purpose is to minimise the errors between the observed or actual values  $y$  and the predicted values of the model  $\hat{y}$ , this technique is known as least square method[189][190]. Summing the errors would result to zero  $\sum_{i=1}^n e_i = 0$  due to some residuals located under the regression line possess negative signs and the ones above the line are positive and when all values are added we obtain zero, to overcome this issue we need to square each error to eliminate the minus signs and change all the values to positive[191].

Using the equation (4) :  $y_i = b_0 + b_1x_{i1} + b_2x_{i2} + b_3x_{i3} + \epsilon_i$

$$\epsilon_i = y_i - (b_0 + b_1x_{i1} + b_2x_{i2} + b_3x_{i3})$$

$$\epsilon_i = [y_i - \sum_{r=0}^k (b_r \times x_{ir})]$$

The equation obtained above was for one particular observation, for  $n$  observations the equation becomes :

$$\sum_{i=0}^n \epsilon_i = \sum_{i=0}^n [y_i - \sum_{r=0}^k (b_r \times x_{ir})]$$

We square the equation to obtain the Sum Squared Errors (SSE) :

$$\sum_{i=0}^n \epsilon_i^2 = \sum_{i=0}^n \left[ y_i - \sum_{r=0}^k (b_r \times x_{ir}) \right]^2 = SSE \dots (6)$$

(When  $r = 0 \rightarrow x_{i0} = 1$ )

To estimate the coefficient of the multi-linear regression model ( $b_r$ ,  $r = i$  to  $k$ ) in a way that the Equation 6 for SSE is minimal we need to make the derivative of the sum squares with respect to  $b_r$  set to zero [192]

$$\frac{\partial SSE}{\partial b_r} = 0$$

$$\left[ \begin{array}{l} \frac{\partial SSE}{\partial b_0} = 0 \rightarrow \frac{\partial(\sum_{i=0}^n [y_i - \sum_{r=0}^k (b_r \times x_{ir})]^2)}{\partial b_0} = 0 \\ \frac{\partial SSE}{\partial b_1} = 0 \rightarrow \frac{\partial(\sum_{i=0}^n [y_i - \sum_{r=0}^k (b_r \times x_{ir})]^2)}{\partial b_1} = 0 \\ \frac{\partial SSE}{\partial b_2} = 0 \rightarrow \frac{\partial(\sum_{i=0}^n [y_i - \sum_{r=0}^k (b_r \times x_{ir})]^2)}{\partial b_2} = 0 \\ \frac{\partial SSE}{\partial b_3} = 0 \rightarrow \frac{\partial(\sum_{i=0}^n [y_i - \sum_{r=0}^k (b_r \times x_{ir})]^2)}{\partial b_3} = 0 \end{array} \right.$$

Alternatively, there is a easier way to solve this problem, when using a large number of variables, it is convenient to convert these equations above (0) into matrices and vectors, the equations then can be transformed into:

$$\begin{array}{c} \begin{pmatrix} y_1 \\ y_2 \\ \vdots \\ y_i \\ \vdots \\ y_n \end{pmatrix} \\ (n \times 1) \end{array} = \begin{array}{c} \begin{pmatrix} 1 & x_{11} & x_{12} & x_{13} \\ 1 & x_{21} & x_{22} & x_{23} \\ \vdots & \vdots & \vdots & \vdots \\ 1 & x_{i1} & x_{i2} & x_{i3} \\ \vdots & \vdots & \vdots & \vdots \\ 1 & x_{n1} & x_{n2} & x_{n3} \end{pmatrix} \\ (n) \times (k+1) \end{array} \times \begin{array}{c} \begin{pmatrix} b_0 \\ b_1 \\ b_2 \\ b_3 \end{pmatrix} \\ (k+1) \times 1 \end{array} + \begin{array}{c} \begin{pmatrix} \varepsilon_1 \\ \varepsilon_2 \\ \vdots \\ \varepsilon_i \\ \vdots \\ \varepsilon_n \end{pmatrix} \\ (n \times 1) \end{array}$$

Where n is the number of observation (in our case n=9) and k is the number of parameters (k=3)

We consider that:

$$Y = \begin{pmatrix} y_1 \\ y_2 \\ \vdots \\ y_i \\ \vdots \\ y_n \end{pmatrix}; \quad X = \begin{pmatrix} 1 & x_{11} & x_{12} & x_{13} \\ 1 & x_{21} & x_{22} & x_{23} \\ \vdots & \vdots & \vdots & \vdots \\ 1 & x_{i1} & x_{i2} & x_{i3} \\ \vdots & \vdots & \vdots & \vdots \\ 1 & x_{n1} & x_{n2} & x_{n3} \end{pmatrix}; \quad B = \begin{pmatrix} b_0 \\ b_1 \\ b_2 \\ b_3 \end{pmatrix} \quad \text{and} \quad E = \begin{pmatrix} \varepsilon_1 \\ \varepsilon_2 \\ \vdots \\ \varepsilon_i \\ \vdots \\ \varepsilon_n \end{pmatrix} \quad (7)$$

Then:

$$Y = X \times B + E \quad (8)$$

The equation 8 above is the multi-linear regression model (MLR), the objective is to estimate the model parameters of the vector  $B = (b_0, b_1, b_2, b_3)^T$  which minimise the errors to allow the model to be closer to the ideal (theoretical) line [193].

The equation obtained (6) above of the sum squared errors:

$$SSE = \sum_{i=0}^n \epsilon^2_i = E^T \times E$$

where E is the error vector with (n×1) dimension and E<sup>T</sup> is their transpose (T) with (1×n) dimension

$$(\epsilon_1 \ \epsilon_2 \ \dots \ \epsilon_i \ \dots \ \epsilon_n) \times \begin{pmatrix} \epsilon_1 \\ \epsilon_2 \\ \vdots \\ \epsilon_i \\ \vdots \\ \epsilon_n \end{pmatrix}$$

Starting from the equation (8)

$$Y = X \times B + E \rightarrow E = Y - XB$$

We have

$$\begin{aligned} SSE &= \sum_{i=0}^n \epsilon^2_i = E^T E = (Y - XB)^T (Y - XB) \\ &= Y^T Y - Y^T X B - (X B)^T Y + (X B)^T X B \\ &= Y^T Y - Y^T X B - B^T X^T Y + B^T X^T X B \end{aligned}$$

Using matrices, vectors and scalar properties, it is possible to change  $Y^T X B = B^T X^T Y$ , as the product result is a scalar with 1×1 dimension, their transpose remain the same [194] (knowing that  $(X B)^T = B^T X^T$  and  $(Y^T)^T = Y$  [195][196], therefore  $B^T X^T Y$  can be written as  $(X B)^T Y$  which is equal to  $[Y^T (X B)]^T$ , the result of this product is a scalar with a (1×1) dimension. The product of the dimensions of  $(1 \times n) \times [n \times (k+1)] \times [(k+1) \times 1]$  will result to (1×1) dimension scalar, and by definition its transpose remain the same, we obtain the following result:

$$[Y^T (X B)]^T = Y^T (X B)$$

We write

$$SSE = Y^T Y - 2B^T X^T Y + B^T X^T X B$$

To minimise the sum squared errors we need to find the derivative of SSE with respect to B set to zero

$$\frac{\partial SSE}{\partial B} = 0$$

$$\frac{\partial(Y^T Y - 2B^T X^T Y + B^T X^T X B)}{\partial B} = 0$$

$$- 2X^T Y + X^T X B + X X^T B^T = 0$$

$(\frac{\partial(B^T X^T X B)}{\partial B}) = 2X^T X B = 2X^T X B^T$ , as  $\frac{\partial(B^T B)}{\partial B}$  is the derivative of a product transpose vector with the same vector, the result is equal to  $2 \times B$  or  $2 \times B^T$ , taking into account that the product result of  $X^T X$  is  $(k+1) \times (k+1)$  symmetric matrix that is independent of B, see matrix below  $X^T X$  for symmetry) [197][198], then we obtain:

$$-2X^T Y + 2X^T \hat{B} = 0 \rightarrow X^T Y = X^T X \hat{B}$$

Where  $\hat{B}$  represents the vector estimated coefficients that minimise the SSE, the values of the B vector are a the real value of the regression and theoretically can not be calculated, therefore we only estimate their values, for this reason we use the hut sign  $\hat{B}$  [199], if we multiply each side by the inverse matrix  $(X^T X)^{-1}$  ( $A A^{-1} = A^{-1} A = I$  identity matrix [200])  $(X^T X)^{-1} X^T Y = (X^T X)^{-1} X^T X \hat{B}$  we obtain then the final equation:

$$\hat{B} = (X^T X)^{-1} X^T Y \quad (9)$$

Using the data collected from the experiment,  $\hat{B}$  can be estimated using the Equation 9 above, we have:

**Table 14** Data Parameters and Observations

	Cutting Speed (mm/min) $X_1$	Pressure (Psi) $X_2$	Intensity (A) $X_3$	Deformation (mm) $Y_1$	HAZ (mm) $Y_2$
<b>Trial 1</b>	8000	70	20	0.18	0.403
<b>Trial 2</b>	8000	75	25	0.12	0.383
<b>Trial 3</b>	8000	80	30	0.16	0.221
<b>Trial 4</b>	8500	70	25	0.18	0.179
<b>Trial 5</b>	8500	75	30	0.22	0.154
<b>Trial 6</b>	8500	80	20	0.30	0.167
<b>Trial 7</b>	9000	70	30	0.20	0.212
<b>Trial 8</b>	9000	75	20	0.28	0.195
<b>Trial 9</b>	9000	80	25	0.18	0.161

We can use the data obtained previously from the experiments (Table 14 above) for numerical applications and assign values to variables  $X_i$  and  $Y_i$  in the matrix and vector obtained previously (7) and resolve the equation (9), starting first with top sheet deformation  $Y_1$ . We obtain:

$$Y_1 = \begin{pmatrix} 0.18 \\ 0.12 \\ 0.16 \\ 0.18 \\ 0.22 \\ 0.3 \\ 0.2 \\ 0.28 \\ 0.18 \end{pmatrix} \quad X = \begin{pmatrix} 1 & 8000 & 70 & 20 \\ 1 & 8000 & 75 & 25 \\ 1 & 8000 & 80 & 30 \\ 1 & 8500 & 70 & 25 \\ 1 & 8500 & 75 & 30 \\ 1 & 8500 & 80 & 20 \\ 1 & 9000 & 70 & 30 \\ 1 & 9000 & 75 & 20 \\ 1 & 9000 & 80 & 25 \end{pmatrix} \quad B_1 = \begin{pmatrix} b_0 \\ b_1 \\ b_2 \\ b_3 \end{pmatrix} \quad E = \begin{pmatrix} \varepsilon_1 \\ \varepsilon_2 \\ \varepsilon_3 \\ \varepsilon_4 \\ \varepsilon_5 \\ \varepsilon_6 \\ \varepsilon_7 \\ \varepsilon_8 \\ \varepsilon_9 \end{pmatrix}$$

(9×1)                      (9×4)                      (4×1)                      (9×1)

We use the equation (9) to estimate the coefficients of vector  $\hat{B}$ :  $\hat{B}_1 = (X^T X)^{-1} X^T Y_1$

$$\text{Calculate } X^T X = \begin{pmatrix} 1 & 1 & 1 & 1 & 1 & 1 & 1 & 1 & 1 \\ 8000 & 8000 & 8000 & 8500 & 8500 & 8500 & 9000 & 9000 & 9000 \\ 70 & 75 & 80 & 70 & 75 & 80 & 70 & 75 & 80 \\ 20 & 25 & 30 & 25 & 30 & 20 & 30 & 20 & 25 \end{pmatrix} \times \begin{pmatrix} 1 & 8000 & 70 & 20 \\ 1 & 8000 & 75 & 25 \\ 1 & 8000 & 80 & 30 \\ 1 & 8500 & 70 & 25 \\ 1 & 8500 & 75 & 30 \\ 1 & 8500 & 80 & 20 \\ 1 & 9000 & 70 & 30 \\ 1 & 9000 & 75 & 20 \\ 1 & 9000 & 80 & 25 \end{pmatrix}$$

(4×9) × (9×4)

$$X^T X = \begin{pmatrix} \mathbf{9} & \mathbf{76500} & \mathbf{675} & \mathbf{225} \\ \mathbf{76500} & \mathbf{651750000} & \mathbf{5737500} & \mathbf{1912500} \\ \mathbf{675} & \mathbf{5737500} & \mathbf{50775} & \mathbf{16875} \\ \mathbf{225} & \mathbf{1912500} & \mathbf{16875} & \mathbf{5775} \end{pmatrix}$$

(4×4)

The inverse of a square matrix (4×4) can be calculated using the following formula [201]

$$(X^T X)^{-1} = \frac{\text{Adjoint matrix of } (X^T X)}{\text{Determinant matrix of } (X^T X)} = \frac{\text{adj } (X^T X)}{|X^T X|}$$

The matrix inverse exists only if the determinant  $|X^T X| \neq 0$  [201]

$$\det |X^T X| = 303750000000 \neq 0$$

The convenient way to calculate the inverse when we have a large matrix with n columns and n rows, usually larger than (2×2) is to transform  $(X^T X)$  into identity matrix by modifying, adding or subtracting the lines and at the same time we perform the same and identical operations

simultaneously to an identity matrix, once we transform the matrix into identity then the other identity matrix become the matrix inverse [202].

$$[(X^T X) | I] \rightarrow [I | (X^T X)^{-1}]$$

$$[(X^T X) | I] = \left[ \begin{pmatrix} 9 & 76500 & 675 & 225 \\ 76500 & 651750000 & 5737500 & 1912500 \\ 675 & 5737500 & 50775 & 16875 \\ 225 & 1912500 & 16875 & 5775 \end{pmatrix} \middle| \begin{pmatrix} 1 & 0 & 0 & 0 \\ 0 & 1 & 0 & 0 \\ 0 & 0 & 1 & 0 \\ 0 & 0 & 0 & 1 \end{pmatrix} \right]$$

To obtain in the first column and first row a value of 1, then we need to multiply the first line by 76500 and the second line by 9 then we divide the first line by the second  $76500 \times L_1 / 9 \times L_2$ , following this method (multiplying lines, adding, dividing and subtracting) until we obtain the identity matrix in the left side, then the right side matrix become the inverse, the final result is given as follow.

$$\left[ \begin{pmatrix} 1 & 0 & 0 & 0 \\ 0 & 1 & 0 & 0 \\ 0 & 0 & 1 & 0 \\ 0 & 0 & 0 & 1 \end{pmatrix} \middle| \begin{pmatrix} 1619/18 & -17/3000 & -1/2 & -1/6 \\ -17/3000 & 1/1500000 & 0 & 0 \\ -1/2 & 0 & 1/150 & 0 \\ -1/6 & 0 & 0 & 1/150 \end{pmatrix} \right]$$

Therefore, the matrix inverse is:

$$(X^T X)^{-1} = \begin{pmatrix} 1619/18 & -17/3000 & -1/2 & -1/6 \\ -17/3000 & 1/1500000 & 0 & 0 \\ -1/2 & 0 & 1/150 & 0 \\ -1/6 & 0 & 0 & 1/150 \end{pmatrix} \quad (4 \times 4)$$

The following step was to calculate the product matrix below:

$$X^T Y_1 = \begin{pmatrix} 1 & 1 & 1 & 1 & 1 & 1 & 1 & 1 & 1 \\ 8000 & 8000 & 8000 & 8500 & 8500 & 8500 & 9000 & 9000 & 9000 \\ 70 & 75 & 80 & 70 & 75 & 80 & 70 & 75 & 80 \\ 20 & 25 & 30 & 25 & 30 & 20 & 30 & 20 & 25 \end{pmatrix} \times \begin{pmatrix} 0.18 \\ 0.12 \\ 0.16 \\ 0.18 \\ 0.22 \\ 0.3 \\ 0.2 \\ 0.28 \\ 0.18 \end{pmatrix} \quad (4 \times 9) \times (9 \times 1) \rightarrow (4 \times 1)$$

$$= \begin{pmatrix} \frac{91}{50} \\ 15570 \\ \frac{1369}{10} \\ \frac{223}{5} \end{pmatrix}$$

$$\hat{B}_1 = (X^T X)^{-1} X^T Y_1 = \begin{pmatrix} 1619/18 & -17/3000 & -1/2 & -1/6 \\ -17/3000 & 1/1500000 & 0 & 0 \\ -1/2 & 0 & 1/150 & 0 \\ -1/6 & 0 & 0 & 1/150 \end{pmatrix} \times \begin{pmatrix} \frac{91}{50} \\ 15570 \\ \frac{1369}{10} \\ \frac{223}{5} \end{pmatrix} = \begin{pmatrix} -\frac{373}{900} \\ \frac{1}{15000} \\ \frac{1}{375} \\ -\frac{3}{500} \end{pmatrix}$$

(4×4) × (4×1) = (4×1)

$$= \begin{pmatrix} -0.414 \\ 0.000066 \\ 0.00266 \\ -0.006 \end{pmatrix}$$

Therefore, we obtain the coefficients

$$\hat{B}_1 = \begin{pmatrix} b_0 = -0.414 \\ b_1 = 0.000066 \\ b_2 = 0.00266 \\ b_3 = -0.006 \end{pmatrix}$$

Using these coefficients in the multi-linear regression of the equation (2) We obtain the Equation 10 below:

$$\hat{Y}_1 = -0.414 + 0.000066 X_1 + 0.00266 X_2 - 0.006 X_3$$

Same than  $\hat{B}$ , we have used  $\hat{Y}$  rather than  $Y$  as it is an estimated value and not a real value.

Therefore:

$$\text{Deformation } (\hat{Y}_1) = -0.414 + 0.000066 \times \text{Cutting Speed (mm/min)} + 0.00266 \times \text{Pressure (Psi)} - 0.006 \times \text{Intensity (A)} \dots (10)$$

To obtain the multi-linear regression model for the heat affected zones:  $\hat{B}_2 = (X^T X)^{-1} X^T Y_2$

$$Y_2 = \begin{pmatrix} 0.403 \\ 0.383 \\ 0.221 \\ 0.179 \\ 0.154 \\ 0.167 \\ 0.212 \\ 0.195 \\ 0.161 \end{pmatrix} \quad X = \begin{pmatrix} 1 & 8000 & 70 & 20 \\ 1 & 8000 & 75 & 25 \\ 1 & 8000 & 80 & 30 \\ 1 & 8500 & 70 & 25 \\ 1 & 8500 & 75 & 30 \\ 1 & 8500 & 80 & 20 \\ 1 & 9000 & 70 & 30 \\ 1 & 9000 & 75 & 20 \\ 1 & 9000 & 80 & 25 \end{pmatrix} \quad B_2 = \begin{pmatrix} b_0 \\ b_1 \\ b_2 \\ b_3 \end{pmatrix} \quad E = \begin{pmatrix} \varepsilon_1 \\ \varepsilon_2 \\ \varepsilon_3 \\ \varepsilon_4 \\ \varepsilon_5 \\ \varepsilon_6 \\ \varepsilon_7 \\ \varepsilon_8 \\ \varepsilon_9 \end{pmatrix}$$

$(X^T X)^{-1}$  was calculated previously. Therefore:

$$\hat{B}_2 = \begin{pmatrix} 1619/18 & -17/3000 & -1/2 & -1/6 \\ -17/3000 & 1/1500000 & 0 & 0 \\ -1/2 & 0 & 1/150 & 0 \\ -1/6 & 0 & 0 & 1/150 \end{pmatrix} \times \begin{pmatrix} 1 & 1 & 1 & 1 & 1 & 1 & 1 & 1 & 1 \\ 8000 & 8000 & 8000 & 8500 & 8500 & 8500 & 9000 & 9000 & 9000 \\ 70 & 75 & 80 & 70 & 75 & 80 & 70 & 75 & 80 \\ 20 & 25 & 30 & 25 & 30 & 20 & 30 & 20 & 25 \end{pmatrix} \times \begin{pmatrix} 0.403 \\ 0.383 \\ 0.221 \\ 0.179 \\ 0.154 \\ 0.167 \\ 0.212 \\ 0.195 \\ 0.161 \end{pmatrix}$$

$$\hat{B}_2 = \begin{pmatrix} \frac{20117}{9000} \\ -\frac{3000000}{49} \\ \frac{6000}{89} \\ -\frac{15000}{15000} \end{pmatrix} = \begin{pmatrix} 2.235 \\ -0.000146 \\ -0.00817 \\ -0.00593 \end{pmatrix}$$

Replacing the coefficients in the equation (2) we obtain the Equation 11 below:

$$\hat{Y}_2 = 2.33 - 0.000146 X_1 - 0.00817 X_2 - 0.00593 X_3$$

Therefore:

$$HAZ (\hat{Y}_2) = 2.33 - 0.000146 \times \text{Cutting Speed (mm/min)} - 0.00817 \times \text{Pressure (Psi)} - 0.00593 \times \text{Intensity (A)} \dots (11)$$

### 5.2.2 Phase Two – plasma Capability to cut through two layers.

This experimental stage was primarily completed to assess the ability of the plasma to cut with one pass through two separated sheets. A 3D-Structure was created using two sheets of  $500 \times 500 \times 0.7$  mm. The gap was maintained at a desired distance using spacers. After few trials, the spacers were changed using different lengths to increase the gap distance between the two sheets. The spacers were measured for accuracy using a calliper before the assembly. A straight lines of 150 mm long were cut at different settings starting from the edge of the model, after each pass the lower side of the model was checked to verify if the cut was also performed (Figure 35). The successful cuts are shown in the Table 15 below. The full test results can be seen in the [APENDIX-B Table B1](#).

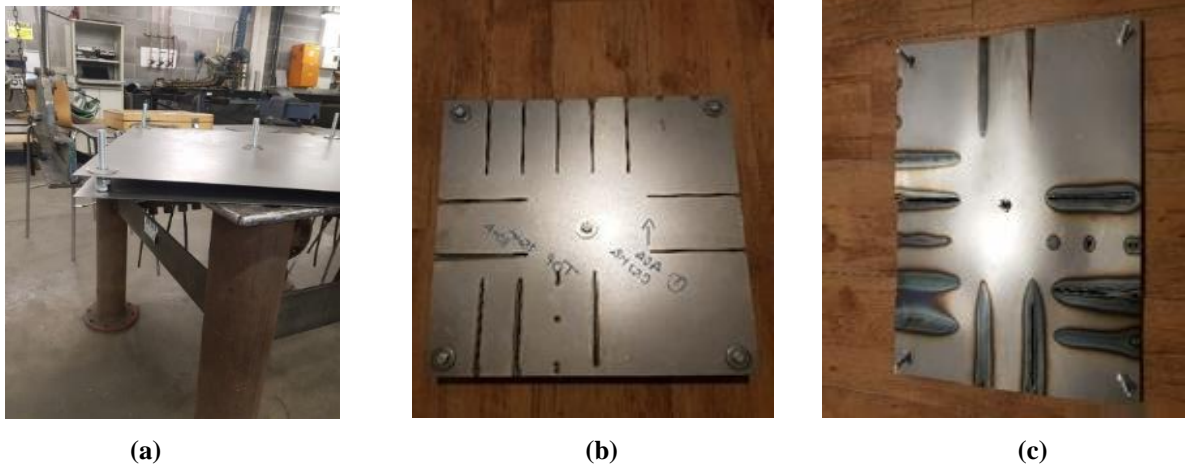


**Figure 38:** First Experiment. (a) part Assembly, (b) Top Cut view of the test model, (c) Bottom Side View

The results confirmed the assumption made and showed that the energy exiting the first sheet can be reused to make an additional cut on neighbouring layer. Hence, cutting two distant layers simultaneously with plasma was possible but this restricted by the gap distance. The 35 mm gap trials did not achieve a full cut on the lower layer.

**Table 15** CNC Plasma Tests 1 results

<b>Gap Distance between the two layers</b>	<b>Pressure (Psi)</b>	<b>Intensity (A)</b>	<b>Cutting Speed (mm/min)</b>
<b>16 mm Gap</b>	90	70	2000
	80	90	2000
<b>25 mm Gap</b>	75	90	2000

### 5.2.3 Phase Three – Starting Reference

The second experiment was made to determine the effective starting parameters necessary to cut two layers at acceptable level of quality. The gap was fixed to 20mm between the two layers as the maximum gap for the test as the 25mm gap or 35 mm did not show a good quality or complete cut. The cut quality at this stage was assessed visually, the settings which resulted to a good quality cut were used as a reference and starting point for the next experiment to optimise the parameters. Straight line cuts of 50mm long were made on the top side of the model using different settings (See Figures 36 and 37). The settings which resulted to a cut in two layers were shown in the Table 16 below. The full tests can be seen in the [APPENDIX-B Table B2](#).

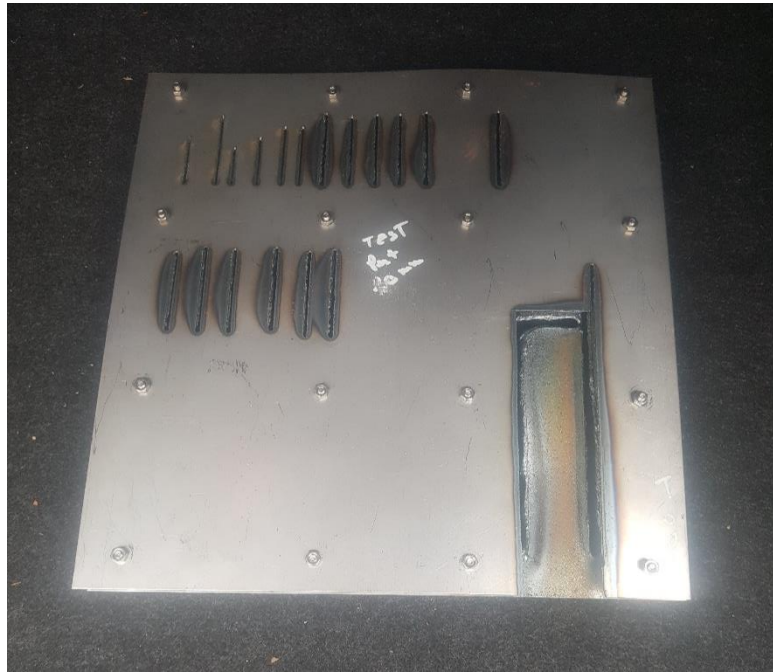


**Figure 39** Second Set of the Tests for Parameters Identification (Top View of the Model)



**Figure 40** Second Set of the Tests for Parameters Identification (Bottom View of the Model)

**Table 16** CNC Cut Test 2 results

Tests	Pressure (Psi)	Intensity (A)	Cutting Speed (mm/min)
<b>Trial Number 7</b>	80	45	500
<b>Trial Number 8</b>	80	45	750
<b>Trial Number 9</b>	80	45	700
<b>Trial Number 12</b>	80	35	500
<b>Trial Number 13</b>	80	33	500
<b>Trial Number 14</b>	80	30	400
<b>Trial Number 16</b>	80	25	300

Trials that showed a cut on both sides of the test model were successively number 7, 8, 9, 12, 13, 14 and 16 but a better-quality cut was obtained using parameters of the trial number 12, pressure 80psi, Intensity 35A and cutting speed 500mm/min. Therefore, these values would be used as a reference setting for the next stage of optimisation using Taguchi parameters design approach.

#### 5.2.4 Phase Four – Optimising the Double sheets cutting

At this stage of the experiment, cutting speed, gas pressure and current were used as the input parameters in addition to a gap distance between the two sheets at three levels 10, 15, 20 mm. Orthogonal arrays using nine trials, four parameters at three levels L9 ( $3^4$ ) was constructed as shown in the Tables 17 and 18 below. Three trials in each model were performed, model one 10 mm, model two 15 mm and model three 20 mm, rectangles of 40×150 mm size were cut. The full result of models and samples collected can be seen on the [APPENDIX-D1](#).

**Table 17** Number of Parameters and levels

Parameters / Levels	L1	L2	L3
<b>Cutting Speed (mm/min)</b>	300	400	500
<b>Air Pressure (Psi)</b>	70	75	80
<b>Current (A)</b>	25	30	35
<b>Gap between the two sheets(mm)</b>	10	15	20

**Table 18** Experimental Layout

<b>Trials</b>	<b>Gap (mm)</b>	<b>Cutting Speed (mm/min)</b>	<b>Intensity (A)</b>	<b>Pressure (Psi)</b>
<b>Trial 1</b>	20	500	35	80
<b>Trial 2</b>	20	400	30	75
<b>Trial 3</b>	20	300	25	70
<b>Trial 4</b>	15	500	30	70
<b>Trial 5</b>	15	400	25	80
<b>Trial 6</b>	15	300	35	75
<b>Trial 7</b>	10	500	25	75
<b>Trial 8</b>	10	400	35	70
<b>Trial 9</b>	10	300	30	80

Sixteen (16) specimens collected from this experiment, Six from each model and three from each side. Samples were analysed for quality, this included kerf analysis, dross, cut edge offset between the top and bottom sheet, hardness, heat affected zones size and sheet deformation.

The model with the 20 mm gap distance resulted only to four samples, three from the top side and only one from the bottom sheet, trial 3 resulted to an uncomplete cut (half profile) on the bottom sheet and the trial 2 performed only a small size of cut. This might be the cause of the accumulation of the heat and pressure of the plasma gas (expansion caused by the air blow) in the gap between the two sheets in addition to slower speed used, this can result to an increase in the gap distance. Therefore, plasma has failed to perform a cut in two sheets simultaneously. In this case, it was not possible to scan the two samples for deformation analysis as the two samples were stack to the model. However, it was possible to assess the half sample obtained on the bottom sheet (trial 3) for other phenomena.

In this work, the requirement was to fit the new customised floor plan on the top of the underbody vehicle (top sheet). There are no requirements for the lower sheet assuming the cut is generated and if the edge is clean and the offset between the two edges is less than 2 mm. Phenomena on the lower sheet were not important, a second processing to clean the edge was unavoidable (based on the data

obtained for dross). Therefore, there is no need to estimate the missing data in the lower sheet, as these would not be used or add any value to this current study.

### 5.2.4.1 Surface Deformation

Samples collected (16 rectangles of 150×40mm, 0.7mm thick) were scanned using a 3D ATOS TripleScan and then inspected with GOM Inspect software using Gaussian best fit virtual plan method. Figure 38 below shows the result obtained from the scan (Trial one bottom sheet). Full scanned parts can be seen in the [APPENDIX-D FIGURES D2](#).

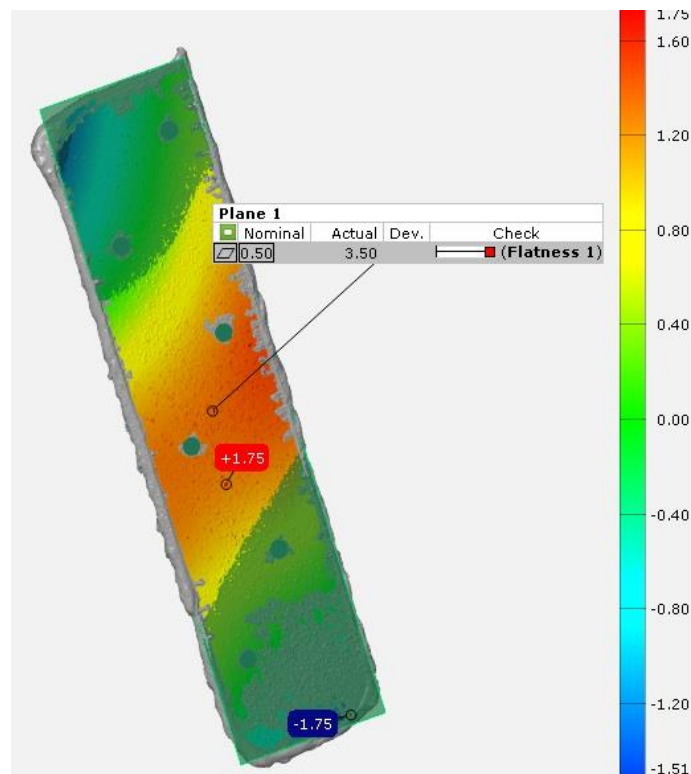


**Figure 41** Part Scanned for a double layered cutting. Trial Number one Lower Sheet Specimen

**Table 19** Surface Deformation

Samples	Surface Deformation (mm)	
	Top Sheet	Bottom Sheet
<b>First Jig Model</b> <b>20mm Air Gap</b>	<b>Trial 1</b>	0.55
	<b>Trial 2</b>	1.15
	<b>Trial 3</b>	0.97
<b>Second Jig Model</b> <b>15mm air Gap</b>	<b>Trial 4</b>	1.03
	<b>Trial 5</b>	0.91
	<b>Trial 6</b>	0.85
<b>Third Jig Model</b> <b>10mm air Gap</b>	<b>Trial 7</b>	1.45
	<b>Trial 8</b>	0.42
	<b>Trial 9</b>	1.12

The results from the Table 19 showed that the deformation phenomenon on the bottom sheets was higher compared to the samples from the top sheets. Minimum value registered for the top sheet was 0.42 obtained from 10 mm model and maximum deformation was 1.45 mm from the same model. The bottom samples exhibited a minimum deformation of 2.03mm in the lowest gap model and a maximum of 3.9mm on 15 mm gap model. Only trials 8 achieved the tolerance required (0.5 mm maximum) on the top sheet.

#### 5.2.4.2 Dross

Dross is the accumulation of unwanted material formed during the cutting process on the top or bottom cut edge [203]. The phenomenon can be caused by a number of factors such as high or low cutting speed, torch standoff, surface condition and worn consumable [204]. Gom Software was used to measure the dross size taking into consideration the highest value measured (see Table 20). The analysis showed that the values on the top samples were varied from 1.3 mm trial 8 (10 mm model gap) to 2.7 mm trial 2 (20 mm model). The bottom samples dross sizes were slightly higher with 1.9 mm as a minimum value trial one and 3.3 mm as a maximum size obtained using trial 3. No trial achieved the tolerance required (1 mm maximum) in either top or bottom sheet. The requirements set at the company for this phenomenon was to perform a second processing to clean the edge if the dross size is higher than 1 mm. Based on the results of the Table 20 below, a second processing to clean the edge was necessary.

**Table 20** Dross Size

Samples	Dross(mm)	
	Top Sheet	Bottom Sheet
First Jig Model 20mm Air Gap	Trial 1	2.3
	Trial 2	2.7
	Trial 3	2.1
Second Jig Model 15mm air Gap	Trial 4	1.6
	Trial 5	2
	Trial 6	2.1
Third Jig Model 10mm air Gap	Trial 7	1.8
	Trial 8	1.3
	Trial 9	2.1

#### 5.2.4.3 Kerf

Kerf can be considered as the void generated on the workpiece during the plasma cutting process. The width of the kerf is affected in general by the incorrect choice of the parameters such as slow cutting speed, high amperage or pressure and also by the orifice of the plasma nozzle. To achieve a correct parts size usually the CNC plasma needs to be adjusted from the software kerf compensation [205]. Gom analysis was used to measure the kerf. The top samples (see Table 21) showed a smaller width size compared to the bottom ones with a minimum of 1.4 mm using parameters of the trial 5

and maximum of 1.9 mm obtained with trial 1. The bottom samples exhibited a maximum width of 4.7 mm using trial number 9 and minimum size was 2.4 mm using trial 5.

**Table 21** Kerf Width

Samples	Kerf(mm)	
	Top Sheet	Bottom Sheet
First Jig Model 20mm Air Gap	Trial 1	1.8
	Trial 2	1.5
	Trial 3	1.6
Second Jig Model 15mm air Gap	Trial 4	1.6
	Trial 5	1.4
	Trial 6	1.7
Third Jig Model 10mm air Gap	Trial 7	1.5
	Trial 8	1.8
	Trial 9	1.9

#### 5.2.4.4 Cut Edge Offset Between the Top and Bottom Sheet

The analysis showed that samples obtained from the bottom of the model were slightly smaller than the ones collected from the top side and were not identical. This meant that there was an offset between the top sheet edges and bottom ones for the same trial. When traditional cutting is used to cut the chassis. The tolerance set at the company for the offset is 2 mm maximum difference between the top and bottom layers cut edge in any side as shown in the Figure 39 below (the full quality requirements set by the company can be seen in Table 3 above in section 4.4.3). To assess the difference, a calliper was used to measure the size of each sample, and then compared the top and bottom specimen of the same trial. The results were given in the Table 22 below.

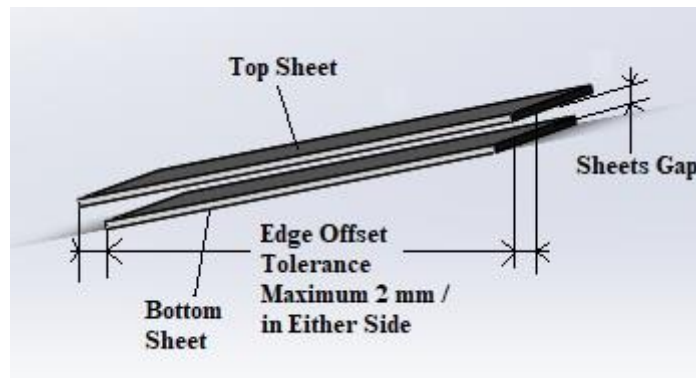


**Figure 42** Offset Between the Top Sheet Cut Edge and the Bottom (Solidworks)

**Table 22** Cut Edge Offset Deviation

Samples		Cut edge offset deviation (mm) Between top and bottom specimens for each side	Total Surface lost of the bottom sample (mm <sup>2</sup> )	% of the total size lost
First Jig Model 20mm Air Gap	Trial 1	1.45	542.59	9%
	Trial 2	/	/	/
	Trial 3	1.25	468.75	7.8%
Second Jig Model 15mm air Gap	Trial 4	1.15	431.71	7.2%
	Trial 5	1.65	616.11	10.27%
	Trial 6	1.35	505.71	8.43%
Third Jig Model 10mm air Gap	Trial 7	1.28	479.85	7.99%
	Trial 8	1.1	413.16	6.89%
	Trial 9	1.3	487.24	8.12%

The widest offset was obtained using parameters of the trial 5 with offset of 1.65mm and surface loss of 616.11mm<sup>2</sup>, the total sample size reduction was 10.27%. The lowest deviation was achieved using parameters of the trial number 8, the area lost was 413.16 mm<sup>2</sup> with a size reduction below 7%. The results showed that plasma can also work within the tolerance (2 mm maximum) set by the company. Furthermore, the size of the sample obtained from the top layers were in all trials falling within the tolerances set  $X^{+/- 1.5 mm}$  (*Width is  $40^{+/- 1.5 mm}$  mm and length is  $150^{+/- 1.5 mm}$  mm*). However, this was not causing any issue as the CNC software possess the ability to compensate and adjust the size of the parts (Kerf Compensation).

#### 5.2.4.5 Heat Affected Zones

The heat affected zones was measured using an optical microscope as shown in the Figure 40 below. The rest of the Figures are given in the [APPENDIX-D FIGURES D3](#). The HAZ analysis results are shown in the Table 23 below. We can see from the results that the heat impacted the lower sheets in overall compared to upper sheets. The model with a smaller gap possessed a lower value in comparison with 15mm gap model or 20mm. The minimum value measured among the top sheets was 0.632 mm using parameters of the trial 7 whereas the maximum size was 1.441 mm with trial 6. The bottom samples exhibited a minimum size of 1.245 mm with trial 9 and a maximum of 3.446 mm trial 5. The values obtained were all above the tolerance set (0.2 mm maximum), if the size is higher than this tolerance value then a second processing is necessary to remove the altered edge

(Company’s requirements for the HAZ). The quality requirements set by AV company is given in a Table 3 (in 4.4.3 section).

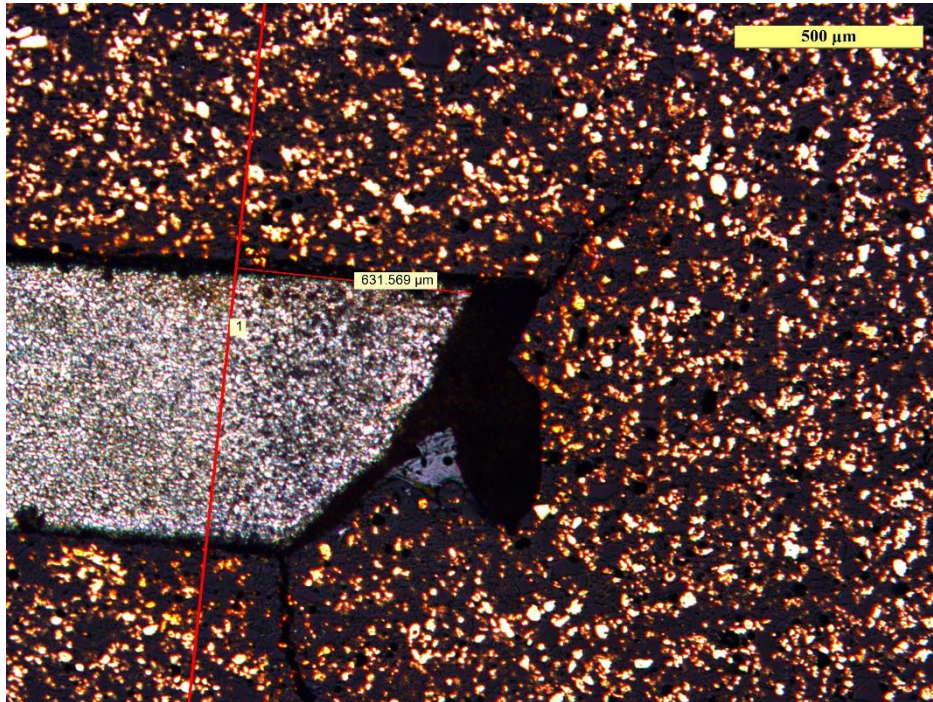


Figure 43 HAZ Width Trial Seven Upper Side

Table 23 HAZ Width

Samples		HAZ (mm)	
		Top Sheet	Bottom Sheet
First Jig Model 20mm Air Gap	Trial 1	0.844	2.36
	Trial 2	1.126	/
	Trial 3	1.222	3.089
Second Jig Model 15mm air Gap	Trial 4	0.947	2.191
	Trial 5	0.714	3.446
	Trial 6	1.441	3.230
Third Jig Model 10mm air Gap	Trial 7	0.632	1.924
	Trial 8	0.834	1.781
	Trial 9	0.682	1.245

#### 5.2.4.6 Hardness

Series of micro hardening tests were performed to find out the maximum hardness change in the material for each trial. The punching started at 0.1 mm from the edge of the cut up to 5 mm using 0.3mm steps, this should cover all the altered area [206]. Struers Durascan 70 model machine Vickers Microhardness HV was used for the tests with 1kg force load applied for 12 seconds. The hardness of the unaffected metal base was measured prior to the test and obtained an average value of HV

123. The maximum hardness values measured, and the hardness proportion increase are shown in the Table 24 below.

**Table 24** Hardness test values and percentage of change

Samples	Hardness (HV)				
	Top Sample		Bottom Sample		
	HV Max	Hardness Change	HV Max	Hardness Change	
First Jig Model 20mm Air Gap	Trial 1	205	66.7%	199	61.79%
	Trial 2	177	43.9%	/	/
	Trial 3	147	19.5%	157	27.6%
Second Jig Model 15mm air Gap	Trial 4	172	39.8%	174	41.6%
	Trial 5	153	24.4%	150	21.9%
	Trial 6	200	62.6%	200	62.6%
Third Jig Model 10mm air Gap	Trial 7	139	13%	151	22.7%
	Trial 8	132	7.3%	183	48.7%
	Trial 9	157	27.6%	146	18.7%

The Table 14 above showed that the material hardness was increased in all specimens and was maximal at the edge of the cut varied from 7.3% to 66.7% for the top samples whereas the bottom exhibited a change starting from 18.7% to a maximum of 80.5% increase. The highest hardness value measured was for the models with a larger gaps 20mm and 15mm trials one and six.

#### 5.2.4.7 Variables Optimisation and Analysis

One of the focuses of this thesis was to investigate on plasma cutting to identify the settings required to achieve an effective cut with only one pass in two sheets separated with an air gap, also to illustrate that phenomenon such as distortion or HAZ can be controlled and reduced to their lowest level on the top sheet (new customised floor pan and chassis assembly).

##### *i. Signal to Noise Ratio*

This section was carried out to find out the effective parameters which can achieve a simultaneous cut in both sheets and at the mean time reduce the surface deformation mainly or the HAZ width on the top layer to their minimum value. Taguchi parameters design was employed to optimise the process, smaller is the better was selected to optimise the settings and reduce the phenomenon [179].

The equation is given as follows [113]:

$$S/N = -10 \log \frac{1}{n} \sum_{i=1}^n Y^2$$

Y is the observed value (response), and n is the number of trials made.

The results obtained are shown in the Tables 25 and 26 below summarised data collected from the tests results.

**Table 25** S/N Ratio for the Top Sheet Deformation

Level Top Sheet Deformation	Gap	cutting speed	Intensity	Pressure
1	1.1078	0.2306	-0.7145	2.5143
2	0.6580	2.3801	-0.8184	-1.0099
3	1.4145	0.5695	4.7131	1.6759
Delta	0.7564	2.1495	5.5315	3.5242
Rank	4	3	1	2

**Table 26** S/N Ratio for the HAZ

Level HAZ Top Sheet	Gap	cutting speed	Intensity	Pressure
1	2.96222	-0.53013	1.72342	0.10275
2	0.07525	1.15732	0.92218	-0.07280
3	-0.43301	1.97727	-0.04115	2.57450
Delta	3.39523	2.50740	1.76457	2.64730
Rank	1	3	4	2

The results above showed that the highest S/N Ratio for top sheet deformation is gap 1.4145 corresponding to level three, cutting speed 2.3801 level two, intensity 4.7131 level three and pressure 2.5143 level one. However, for the heat affected zones the highest S/N registered was for the gap

2.96222 level one, cutting speed 1.97727 level three, intensity 1.72342 level one and pressure 2.57450 level three. This can also be seen clearly from the graphs on the **Figures 41 and 42** below.

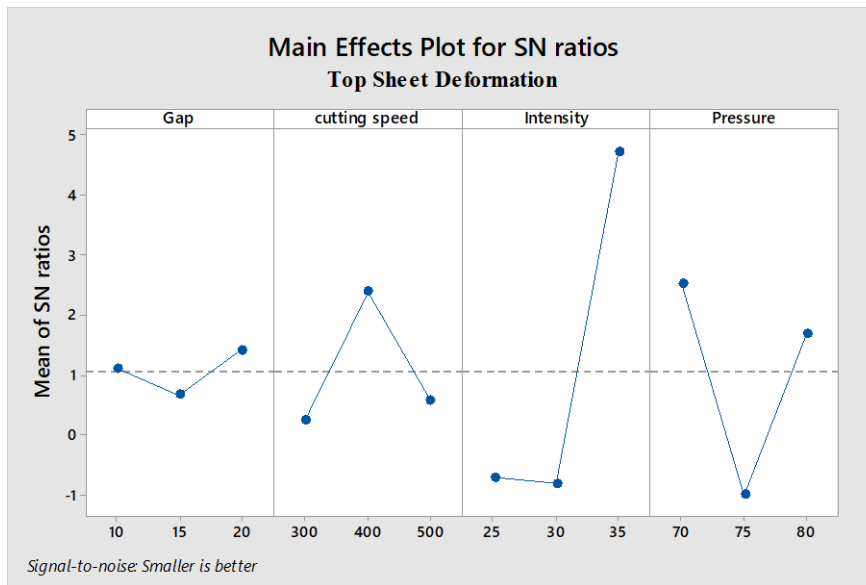


**Figure 44** Main Effect Plot S/N Ratio for the Top Sheet Deformation

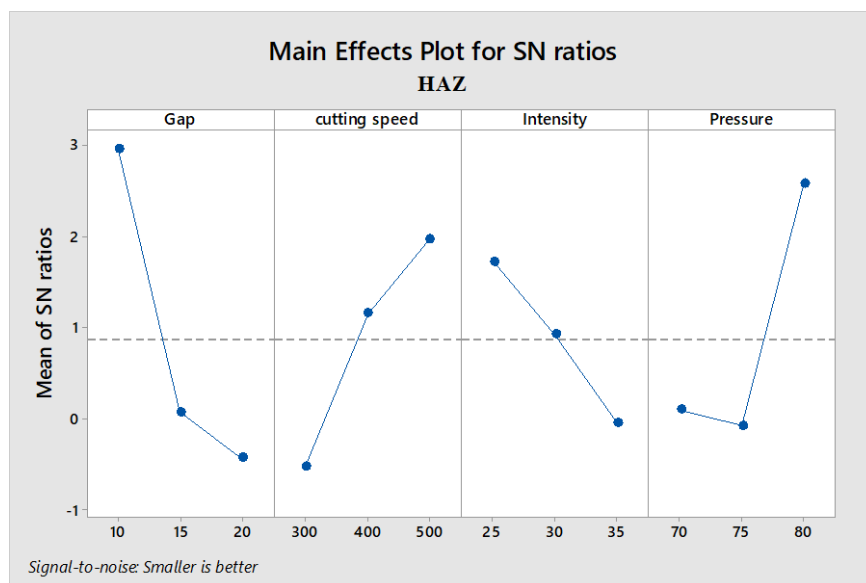


**Figure 45:** Main Effect Plot S/N Ratio for the Top Sheet HAZ.

The S/N Ratio showed that the optimal parameters required to cut a three-dimensional part and achieve less deformation possible on the top sheet are cutting speed level two 400 mm/min , Pressure at level one 70 Psi, Intensity at level three 35 A using a larger gap at level three 20 mm. To minimise the Heat Affected Zones on the top sheet it is necessary to use Cutting speed at level three 500 mm/min, pressure at level three 80 Psi, Intensity at level one 25 A using a smaller gap level one 10mm.

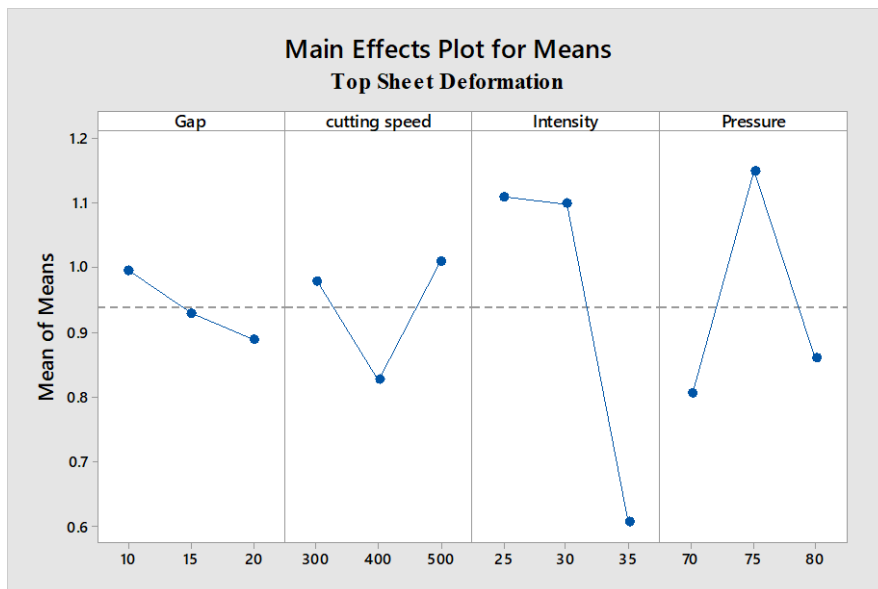
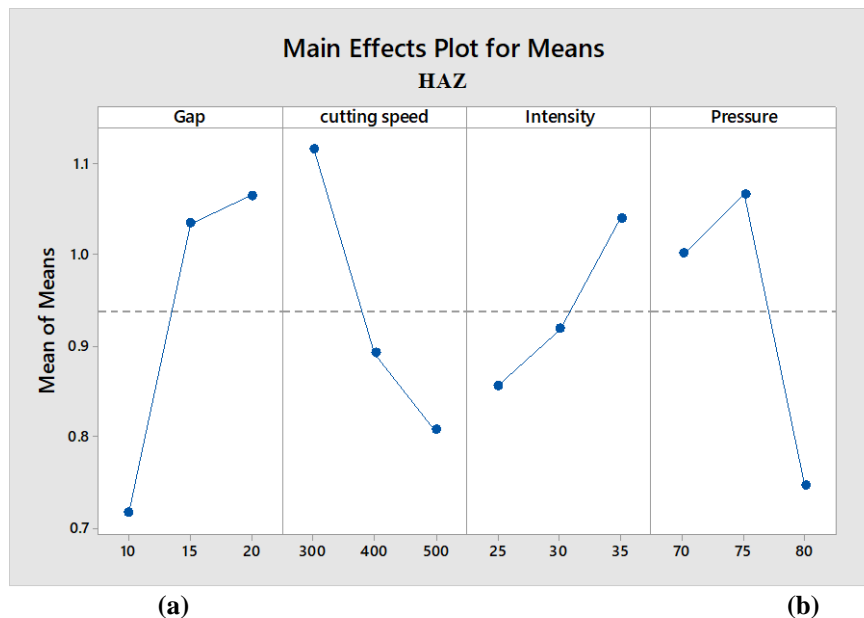


**Figure 46** Main Effect Plot for Means Surface Deformation



(a)

(b)

**Figure 47:** Main Effect Plot for Means HAZ.

The main effect plot above for means in Figures 43 and 44 showed the main factors which reflected on the response. Levels with the higher inclination line to the horizontal and those with the longer amplitude are the most influential [180]. For the top sheet deformation, intensity and pressure were the main effects, cutting speed and gap are less influential. However, it is clear from The Heat Affected Zone Means graph that the gap, cutting speed and pressure are the most influential factors whereas intensity has less of an impact due to small amplitude.

*ii. Analysis of variance (ANOVA)*

ANOVA analysis was performed at 95% level of confidence. The contribution of each parameter is represented in the Table 27 below.

**Table 27** Effects Contribution

Source	Contribution	
	Top Sheet Deformation	HAZ
Intensity	63.93%	8.75%
Pressure	26.36%	28.61%
Gap	2.24%	37.31%
Cutting Speed	7.47%	25.33%

The results above showed that processing simultaneously two sheets, the top layer deformation would mainly be affected by the intensity and then gas pressure, respectively 63.93% and 26.36%. The other factors did not show a considerable impact on the surface flatness. However, gap, pressure and cutting speed were the most influential factors affecting the HAZ with 37.31%, 28.61% and 25.33% respectively, the impact of the intensity was small.

The results obtained showed also that there was statistical evidence that the intensity had significant effect on the top sheet deformation with a P-value of 0.034. However, there was no statistical evidence of the effect significance for any independent parameters on the HAZ as P-values obtained were greater than 0.05, the analysis was done at 95% level of confidence.

*iii. Interaction*

Interaction plot in Figures 45 and 46 below illustrate the effect of the gap distance on the response depending on the level of the second parameter. The deformation on the top sheet can be reduced when cutting two separate layers simultaneously if the largest gap 20 mm is processed using either parameter at settings level three. The 10 mm gap distance associated with pressure 70 Psi also showed a little deformation. However, 15 mm gap did not show a big difference between pressure's settings, but a slight improvement can be seen using 75 Psi. Cutting speed at level two 400mm/min can result to a small deformation if associated with a small gap 10 mm but when 15 mm gap model is used then the speed settings have only a small effect with a slight improvement seen using 300mm/min. The intensity at level three 35A would show less deformation cutting any gap.

The HAZ showed a better result and size reduction when 20 mm gap is used with either parameter at setting level three. The gap distance 15 mm would require using pressure setting 80 Psi to obtain less HAZ whereas 10mm gap a slight improvement can be seen if 75 Psi pressure is used. The cutting

speed at level two 400mm/min is suitable for 15mm gap but for 10 mm gap it is adequate to use level three 500mm/min even though it showed only a small difference. Intensity is more effective if lower setting at level one 25A is used to perform a cut on either 15 or 10mm gaps. Even though the graphs showed an interaction effect. However, there is no statistical evidence that these interactions are significant as the P-values were above 5%.

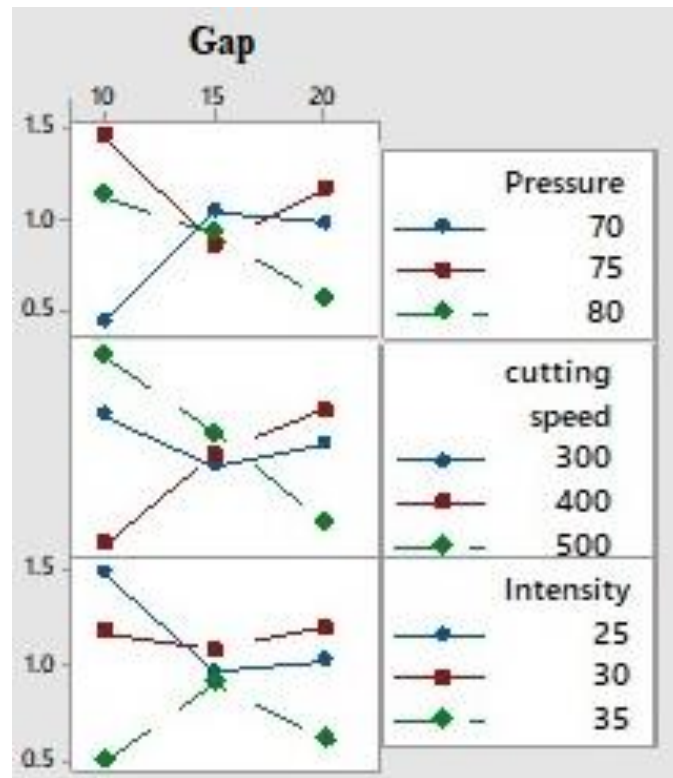


**Figure 48:** Gap Interaction for Top Sheet Deformation

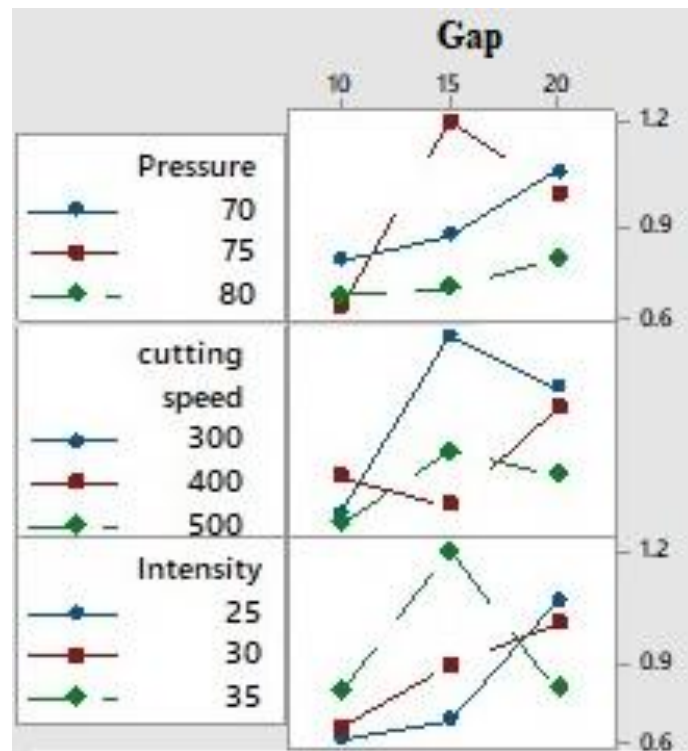
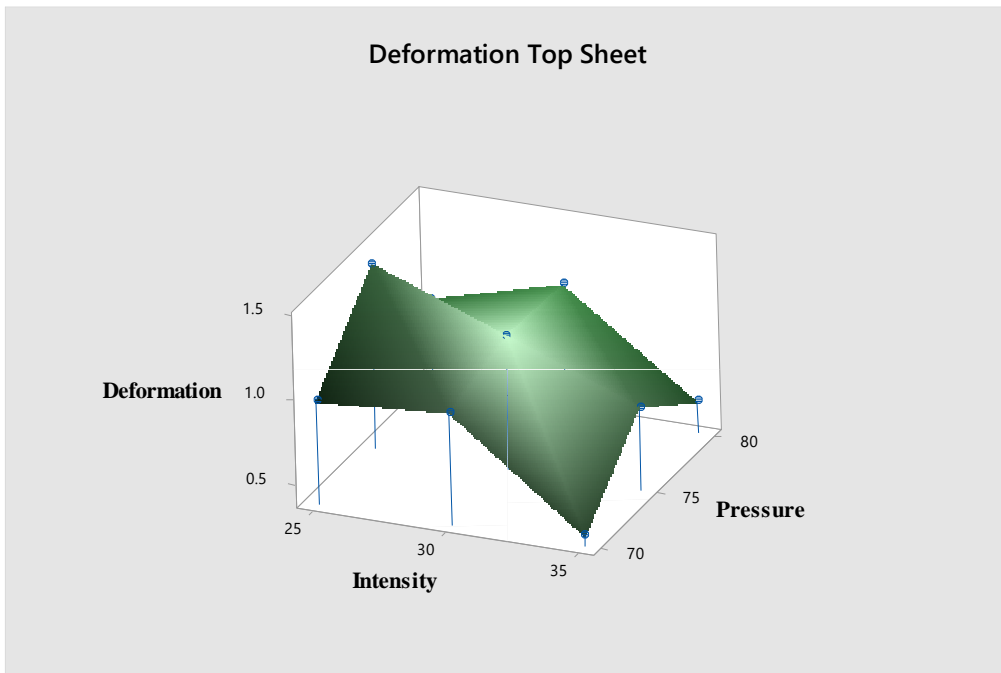


Figure 49 Gap Interaction for Top Sheet HAZ

iv. *Three-Dimensional Surface Plot*

The surface plot in Figures 47 and 48 below shows the response reaction with the two most influential plasma parameters for both phenomenon material deformation and heat affected zones in the top sheet. When cutting two layers simultaneously, the minimum deformation can be obtained when the machine is operating at power level three (Intensity 35A) using the pressure at level one, the highest value of the deformation can be obtained if the power is used at level one associated with pressure gas at level two. The HAZ showed that a lower value can be obtained when using a small gaps (level one primarily) especially when associated with average pressure gaz (level two), increasing the gap would result to an increase of the phenomenon especially when low pressures are used.



**Figure 50** Surface Plot for Top Sheets Surface Deformation

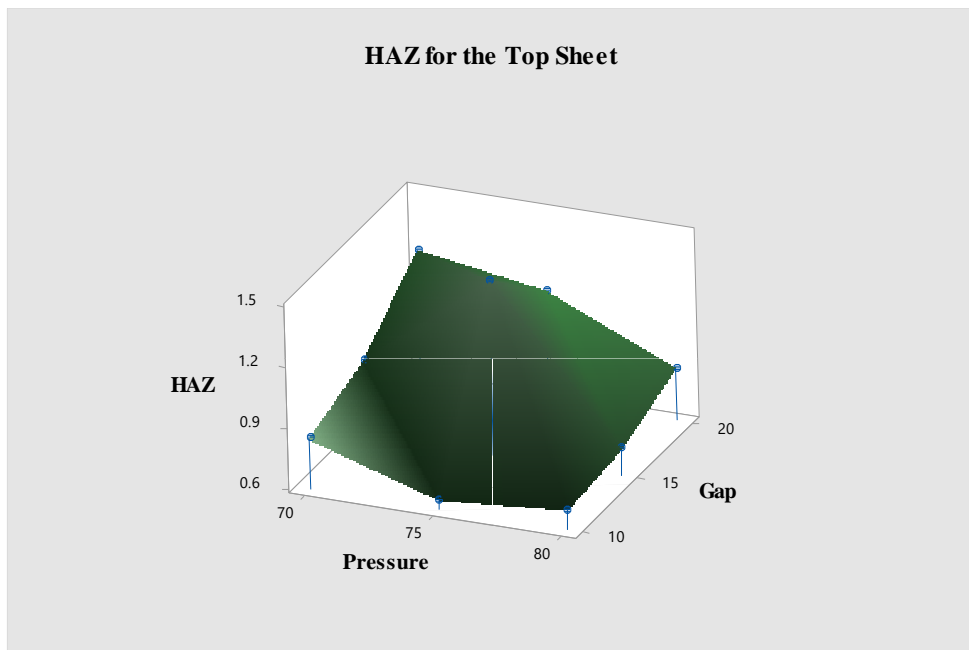


**Figure 51** Surface Plot for Top Sheets HAZ

**v. Double Sheet Modelling**

Regression models were constructed for the two phenomena (deformation and HAZ) to assess the strength relationship between the input parameters and the output variables. The objective of this section was to estimate the response based on what we learnt and observed from the previous experiments.

### v.i Assumptions

The fits in Figures 49 and 50 below shows that for both responses, residuals were spaced and falling randomly around the horizontal zero axis and were not following any pattern, this can give an indication that the errors were unpredictable [184]. The normal plot in Figures 51 and 52 shows that the variation and the distribution of the residuals was similar for each level with no outliers observed. The two assumptions were necessary to conclude that there is a linear relationship between the factors and the response. Therefore, it was possible to build a models for regression and the coefficients can be trusted [207].

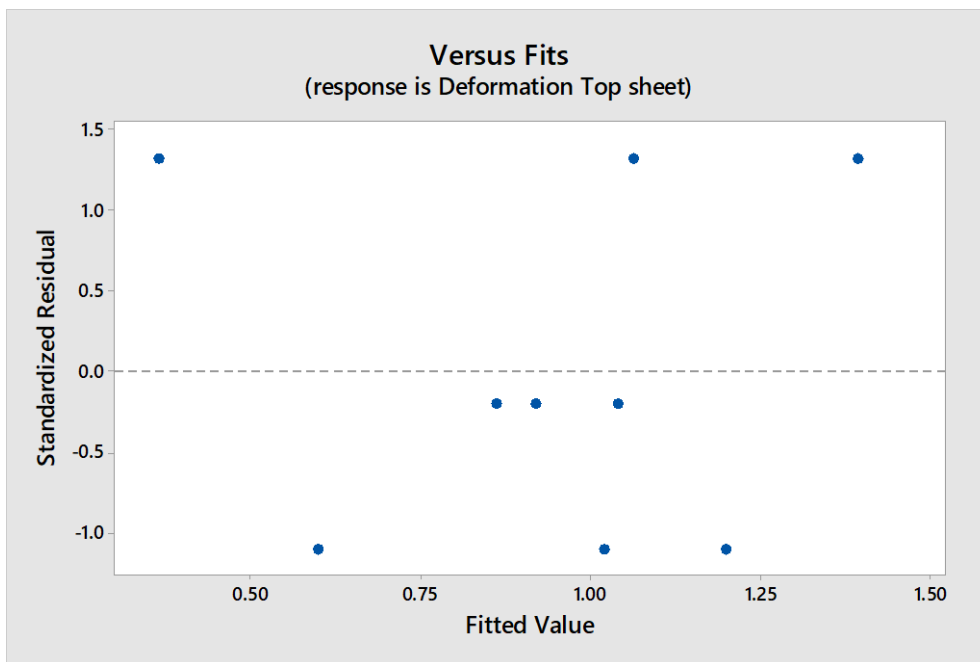
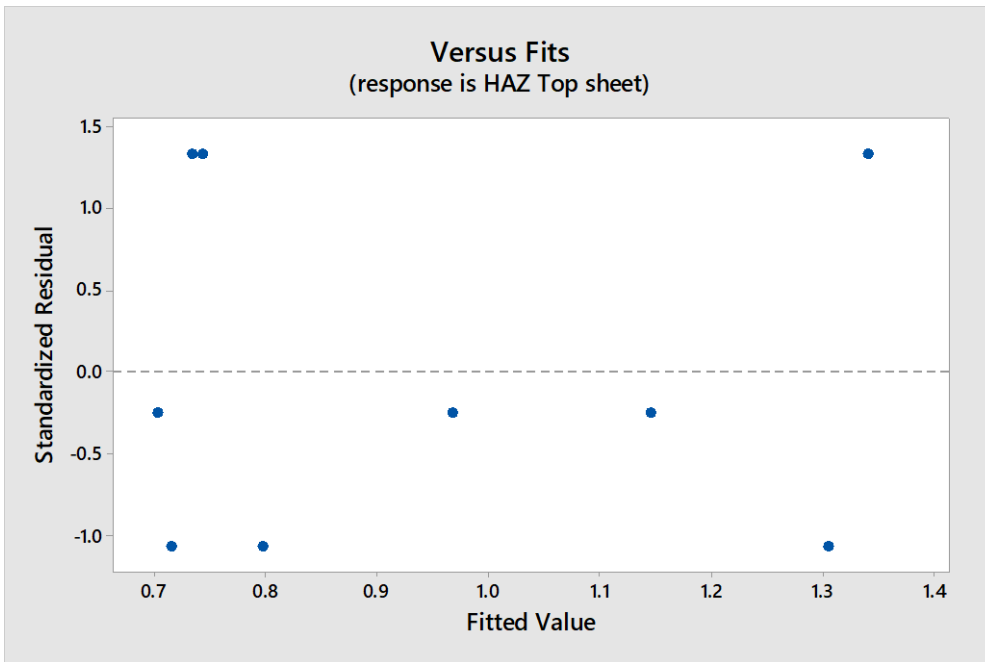
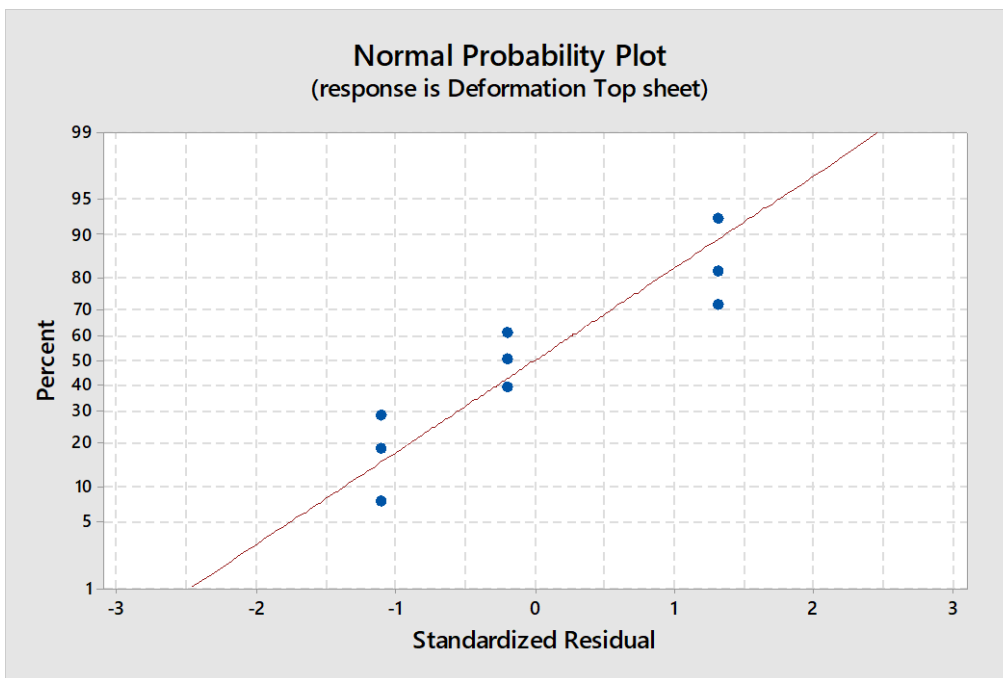


Figure 52 Fits graph Surface Deformation



**Figure 53** Fits graph HAZ



**Figure 54** Residual's graph for top sheet Deformation

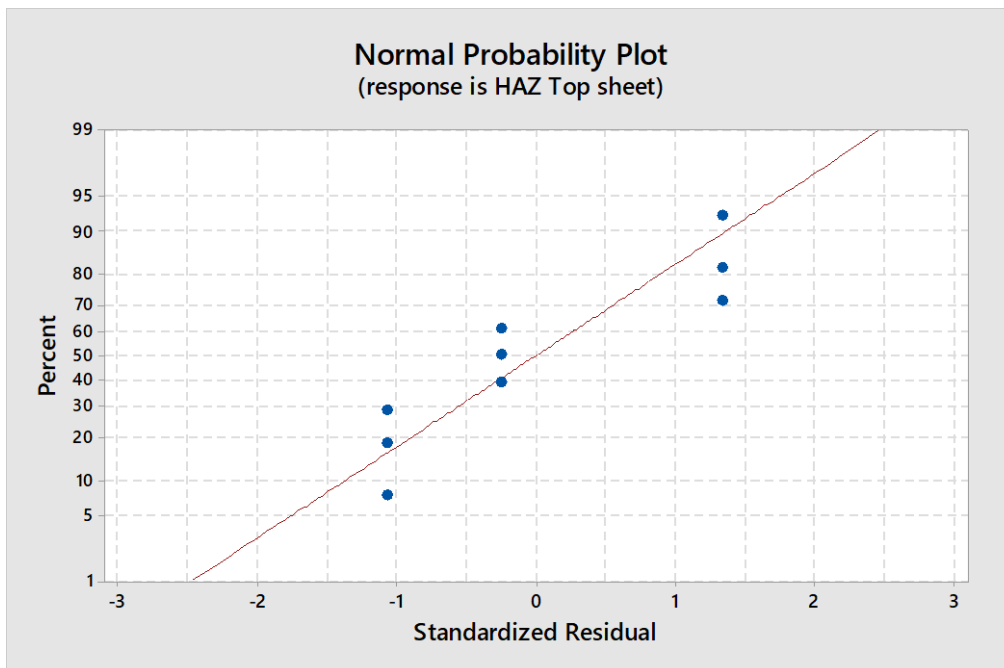


**Figure 55** Residual's graph for top sheet HAZ

Person's correlation analysis showed that there was no multicollineality between the independent variables for both phenomenon as the coefficients obtained were all  $r = 0$ . Furthermore, a good regression model required the residuals to be scattered along the diagonal and close to the theoretical line with small errors. Based on the Figures 53 and 54 below, it is clear that residuals were normally distributed and close to the line. Hence, regression models can be constructed [186].

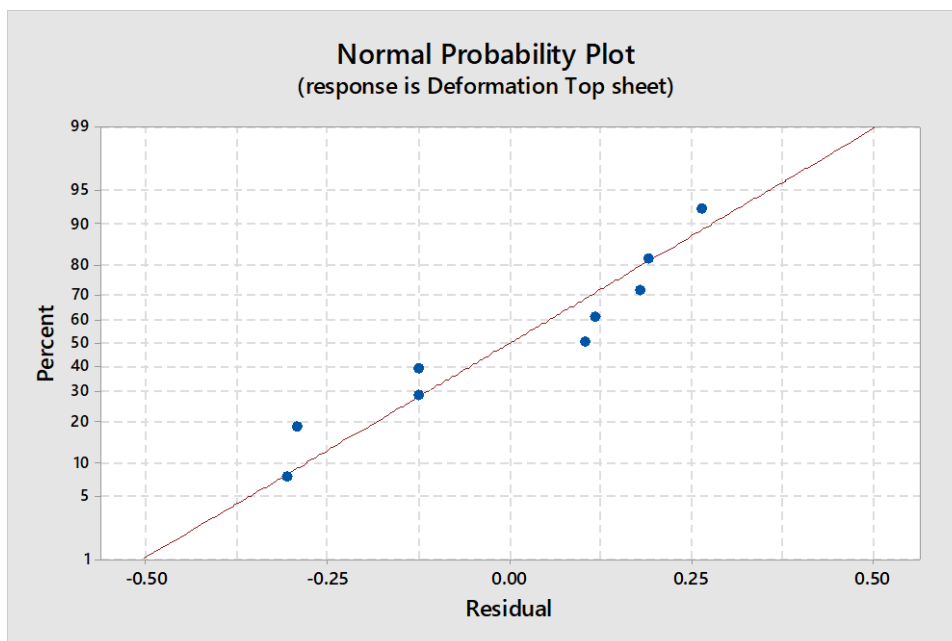


**Figure 56** Probability Plot top sheets Deformation

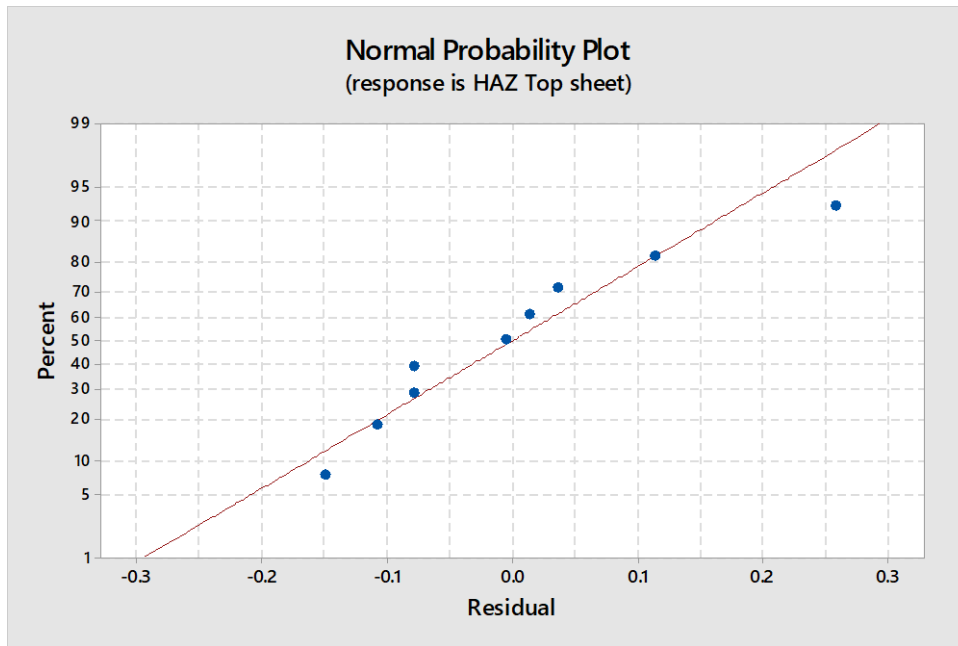


Figure 57 Probability Plot top sheets HAZ

### v.ii Mathematical Modelling

The number of parameters involved in this regression were four parameters Intensity, pressure, gap, cutting speed using one response. From the Equation 1 we the MLR can be written as follows:

$$y = b_0 + b_1x_1 + b_2x_2 + b_3x_3 + b_4x_4 + \epsilon \quad (12)$$

Where respectively  $x_1, x_2, x_3$  and  $x_4$  are intensity, pressure, gap and cutting speed.

We collected nine observations from the experiment ( $n = 9$ ), we can write :

$$\left[ \begin{array}{l} y_1 = b_0 + b_1x_{11} + b_2x_{12} + b_3x_{13} + b_4x_{14} + \epsilon_1 \\ y_2 = b_0 + b_1x_{21} + b_2x_{22} + b_3x_{23} + b_4x_{24} + \epsilon_2 \\ \vdots \\ y_i = b_0 + b_1x_{i1} + b_2x_{i2} + b_3x_{i3} + b_4x_{i4} + \epsilon_i \\ \vdots \\ y_n = b_0 + b_1x_{n1} + b_2x_{n2} + b_3x_{n3} + b_4x_{n4} + \epsilon_n \end{array} \right. \quad (13)$$

From the Equations (13), the generale equation for random observation can be given as:

$$y_i = b_0 + b_1x_{i1} + b_2x_{i2} + b_3x_{i3} + b_4x_{i4} + \epsilon_i \quad (14)$$

From the Equation above (14) we consider the variate of the estimate value  $y_i$  given  $x_i$  ( $x_i = x_{i1}, x_{i2}, x_{i3}, x_{i4}$ ) as :

$$E(y_i/x_i) = b_0 + b_1x_{i1} + b_2x_{i2} + b_3x_{i3} + b_4x_{i4} = \hat{y}_i \quad (15)$$

We replace the Equation 15 in the Equation 14 we obtain:  $y_i = E(y_i/x_i) + \varepsilon_i$

Where  $E(y_i/x_i)$  is the linear regression estimate  $\hat{y}_i$ . [188]

Therefore  $y_i = \hat{y}_i + \varepsilon_i \rightarrow \varepsilon_i = y_i - \hat{y}_i$

$y_i$  is the observed value,  $\hat{y}_i$  is the predicted value and  $\varepsilon_i$  is the residual error.

In the same manner as for modelling for single sheet which was demonstrated already previously in the section (II), we simplify the Equations 13 and we write that in form of matrix and vectors and we obtain:

$$\begin{array}{c}
 \begin{pmatrix} y_1 \\ y_2 \\ \vdots \\ y_i \\ \vdots \\ y_n \end{pmatrix} = \begin{pmatrix} 1 & x_{11} & x_{12} & x_{13} & x_{14} \\ 1 & x_{21} & x_{22} & x_{23} & x_{24} \\ \vdots & \vdots & \vdots & \vdots & \vdots \\ 1 & x_{i1} & x_{i2} & x_{i3} & x_{i4} \\ \vdots & \vdots & \vdots & \vdots & \vdots \\ 1 & x_{n1} & x_{n2} & x_{n3} & x_{n4} \end{pmatrix} \times \begin{pmatrix} b_0 \\ b_1 \\ b_2 \\ b_3 \\ b_4 \end{pmatrix} + \begin{pmatrix} \varepsilon_1 \\ \varepsilon_2 \\ \vdots \\ \varepsilon_i \\ \vdots \\ \varepsilon_n \end{pmatrix} \\
 \text{(n*1) vector dimension} \qquad \qquad \text{(n) * (k+1) matrix dimension} \qquad \qquad \text{(k+1)*1} \qquad \qquad \text{(n*1)}
 \end{array}$$

Where n is the number of observation (in our case n=9) and k is the number of parameters (k=4)

We consider that:

$$\mathbf{Y} = \begin{pmatrix} y_1 \\ y_2 \\ \vdots \\ y_i \\ \vdots \\ y_n \end{pmatrix}; \quad \mathbf{X} = \begin{pmatrix} 1 & x_{11} & x_{12} & x_{13} & x_{14} \\ 1 & x_{21} & x_{22} & x_{23} & x_{24} \\ \vdots & \vdots & \vdots & \vdots & \vdots \\ 1 & x_{i1} & x_{i2} & x_{i3} & x_{i4} \\ \vdots & \vdots & \vdots & \vdots & \vdots \\ 1 & x_{n1} & x_{n2} & x_{n3} & x_{n4} \end{pmatrix}; \quad \mathbf{B} = \begin{pmatrix} b_0 \\ b_1 \\ b_2 \\ b_3 \\ b_4 \end{pmatrix} \quad \text{and} \quad \mathbf{E} = \begin{pmatrix} \varepsilon_1 \\ \varepsilon_2 \\ \vdots \\ \varepsilon_i \\ \vdots \\ \varepsilon_n \end{pmatrix}$$

The overall result can be written then as:  $\mathbf{Y} = \mathbf{X} \times \mathbf{B} + \mathbf{E}$  (16)

The Equation 16 above is the multi-linear regression model (MLR), the objective was to estimate the model parameters of the vector  $\mathbf{B} = (b_0, b_1, b_2, b_3, b_4)^T$  which minimise the errors to its lowest value in order to allow our regression line to be closer to the ideal (theoretical) prediction line as much as possible [193].

The equation of the Sum Squared Errors:

$$\text{SSE} = \sum_{i=0}^n \varepsilon_i^2 = \mathbf{E}^T \times \mathbf{E}$$

Where E is the error vector with (n\*1) dimension and E<sup>T</sup> is its transpose. The demonstration of how the estimate  $\hat{B}$  is obtained is already given in the previous section (II) for single sheet modeling. The Equation can be written as follows:

$$\hat{B} = (X^T X)^{-1} X^T Y \quad (17)$$

The Table 28 below represents the data obtained from the experiemnts performed previously. Using these collected data on the equation constructed above (17) we can estimate  $\hat{B}$ .

**Table 28** Data Parameters and Observations

Trials	Parameters				Observations	
	Intensity (A) X <sub>1</sub>	Pressure (Psi) X <sub>2</sub>	Gap (mm) X <sub>3</sub>	Cutting Speed (mm/min) X <sub>4</sub>	Top Sheet Deformation (mm) Y <sub>1</sub>	Top Sheet HAZ (mm) Y <sub>2</sub>
<b>Trial 1</b>	35	80	20	500	0.55	0.844
<b>Trial 2</b>	30	75	20	400	1.15	1.126
<b>Trial 3</b>	25	70	20	300	0.97	1.222
<b>Trial 4</b>	30	70	15	500	1.03	0.947
<b>Trial 5</b>	25	80	15	400	0.91	0.714
<b>Trial 6</b>	35	75	15	300	0.85	1.441
<b>Trial 7</b>	25	75	10	500	1.45	0.632
<b>Trial 8</b>	35	70	10	400	0.42	0.834
<b>Trial 9</b>	30	80	10	300	1.12	0.682

For numerical applications, we assign values to all variables X<sub>i</sub> and Y<sub>i</sub> in the matrix and vector obtained, starting with top sheet deformation data. We obtain:

$$\begin{matrix}
 Y_1 = \begin{pmatrix} 0.55 \\ 1.15 \\ 0.97 \\ 1.03 \\ 0.91 \\ 0.85 \\ 1.45 \\ 0.42 \\ 1.12 \end{pmatrix} &
 X = \begin{pmatrix} 1 & 35 & 80 & 20 & 500 \\ 1 & 30 & 75 & 20 & 400 \\ 1 & 25 & 70 & 20 & 300 \\ 1 & 30 & 70 & 15 & 500 \\ 1 & 25 & 80 & 15 & 400 \\ 1 & 35 & 75 & 15 & 300 \\ 1 & 25 & 75 & 10 & 500 \\ 1 & 35 & 70 & 10 & 400 \\ 1 & 30 & 80 & 10 & 300 \end{pmatrix} &
 B = \begin{pmatrix} b_0 \\ b_1 \\ b_2 \\ b_3 \\ b_4 \end{pmatrix} &
 E = \begin{pmatrix} \varepsilon_1 \\ \varepsilon_2 \\ \varepsilon_3 \\ \varepsilon_4 \\ \varepsilon_5 \\ \varepsilon_6 \\ \varepsilon_7 \\ \varepsilon_8 \\ \varepsilon_9 \end{pmatrix}
 \end{matrix}$$

(9×1)
(9×5)
(5×1)
(9×1)

We use the equation (17) to estimate the coefficients of vector  $\hat{B}$ :

$$\hat{B} = (X^T X)^{-1} X^T Y_1$$

We calculate first  $X^T X = \begin{pmatrix} 1 & 1 & 1 & 1 & 1 & 1 & 1 & 1 & 1 \\ 35 & 30 & 25 & 30 & 25 & 35 & 25 & 35 & 30 \\ 80 & 75 & 70 & 70 & 80 & 75 & 75 & 70 & 80 \\ 20 & 20 & 20 & 15 & 15 & 15 & 10 & 10 & 10 \\ 500 & 400 & 300 & 500 & 400 & 300 & 500 & 400 & 300 \end{pmatrix} \times \begin{pmatrix} 1 & 35 & 80 & 20 & 500 \\ 1 & 30 & 75 & 20 & 400 \\ 1 & 25 & 70 & 20 & 300 \\ 1 & 30 & 70 & 15 & 500 \\ 1 & 25 & 80 & 15 & 400 \\ 1 & 35 & 75 & 15 & 300 \\ 1 & 25 & 75 & 10 & 500 \\ 1 & 35 & 70 & 10 & 400 \\ 1 & 30 & 80 & 10 & 300 \end{pmatrix}$

(5×9) × (9×5)

$$X^T X = \begin{pmatrix} 9 & 270 & 675 & 135 & 3600 \\ 270 & 8250 & 20250 & 4050 & 108000 \\ 675 & 20250 & 50775 & 10125 & 270000 \\ 135 & 4050 & 10125 & 2175 & 54000 \\ 3600 & 108000 & 270000 & 54000 & 1500000 \end{pmatrix}$$

(5×5)

The inverse of a square matrix (5×5) can be calculated using the following formula below [201].

$$(X^T X)^{-1} = \frac{\text{Adjoint matrix of } (X^T X)}{\text{Determinant matrix of } (X^T X)} = \frac{\text{adj } (X^T X)}{|X^T X|}$$

The matrix inverse exists only if it meets the condition of the determinant  $|X^T X| \neq 0$  [201]. Using matrices calculator, we obtained the result  $|X^T X| = 1822500000000$  which is  $\neq 0$  therefore we can compute the matrix inverse.

The demonstration of how the inverse matrix is obtained is already given in the previous section for single sheet modelling section (II).

The matrix inverse of  $(X^T X)^{-1}$  can be written:

$$(X^T X)^{-1} = \begin{pmatrix} 430/9 & -1/5 & -1/2 & -1/10 & -1/150 \\ -1/5 & 1/150 & 0 & 0 & 0 \\ -1/2 & 0 & 1/150 & 0 & 0 \\ -1/10 & 0 & 0 & 1/150 & 0 \\ -1/150 & 0 & 0 & 0 & 1/60000 \end{pmatrix}$$

(5×5)

The following step was calculating the product below:

$$X^T Y_1 = \begin{pmatrix} 1 & 1 & 1 & 1 & 1 & 1 & 1 & 1 & 1 \\ 35 & 30 & 25 & 30 & 25 & 35 & 25 & 35 & 30 \\ 80 & 75 & 70 & 70 & 80 & 75 & 75 & 70 & 80 \\ 20 & 20 & 20 & 15 & 15 & 15 & 10 & 10 & 10 \\ 500 & 400 & 300 & 500 & 400 & 300 & 500 & 400 & 300 \end{pmatrix} \times \begin{pmatrix} 0.55 \\ 1.15 \\ 0.97 \\ 1.03 \\ 0.91 \\ 0.85 \\ 1.45 \\ 0.42 \\ 1.12 \end{pmatrix} = \begin{pmatrix} \frac{169}{20} \\ 4919 \\ \frac{20}{12691} \\ \frac{20}{2503} \\ \frac{20}{3389} \end{pmatrix}$$

(5×9) × (9×1) → (5×1)

$$\hat{B}_1 = (X^T X)^{-1} X^T Y_1 = \begin{pmatrix} 430/9 & -1/5 & -1/2 & -1/10 & -1/150 \\ -1/5 & 1/150 & 0 & 0 & 0 \\ -1/2 & 0 & 1/150 & 0 & 0 \\ -1/10 & 0 & 0 & 1/150 & 0 \\ -1/150 & 0 & 0 & 0 & 1/60000 \end{pmatrix} \times \begin{pmatrix} 169 \\ 20 \\ 4919 \\ 20 \\ 12691 \\ 20 \\ 2503 \\ 20 \\ 3389 \end{pmatrix} = \begin{pmatrix} 967 \\ 450 \\ -151 \\ 3000 \\ 2 \\ 375 \\ 4 \\ -375 \\ 3 \\ 20000 \end{pmatrix} = \begin{pmatrix} 2.15 \\ -0.0503 \\ 0.0053 \\ -0.0107 \\ 0.00015 \end{pmatrix}$$

(5×5) × (5×1) = (5×1)

Therefore, we obtain the coefficients  $\hat{B}_1 = \begin{pmatrix} b_0 = 2.15 \\ b_1 = -0.0503 \\ b_2 = 0.0053 \\ b_3 = -0.0107 \\ b_4 = 0.00015 \end{pmatrix}$

Using these coefficients in the multi-linear regression (Equation 15) we can obtain:

$$\hat{Y}_1 = 2.15 - 0.0503 X_1 + 0.0053 X_2 - 0.0107 X_3 + 0.00015 X_4$$

Replacing the variables, the mathematical equation that estimates the deformation on the top sheet and at the same time can perform a cut in two parallel thin sheets separated with an air gap distance is given as:

$$\text{Deformation Top Sheet (mm)} = 2.15 - 0.0503 \times \text{Intensity (A)} + 0.0053 \times \text{Pressure (Psi)} - 0.0107 \times \text{Gap (mm)} + 0.00015 \times \text{Cutting Speed (mm/min)} \quad (18)$$

Similarly, we can build the regression equation for the Heat Affected zones (HAZ) using the same approach.

$$X^T X = \begin{pmatrix} 1 & 1 & 1 & 1 & 1 & 1 & 1 & 1 & 1 \\ 35 & 30 & 25 & 30 & 25 & 35 & 25 & 35 & 30 \\ 80 & 75 & 70 & 70 & 80 & 75 & 75 & 70 & 80 \\ 20 & 20 & 20 & 15 & 15 & 15 & 10 & 10 & 10 \\ 500 & 400 & 300 & 500 & 400 & 300 & 500 & 400 & 300 \end{pmatrix} \times \begin{pmatrix} 1 & 35 & 80 & 20 & 500 \\ 1 & 30 & 75 & 20 & 400 \\ 1 & 25 & 70 & 20 & 300 \\ 1 & 30 & 70 & 15 & 500 \\ 1 & 25 & 80 & 15 & 400 \\ 1 & 35 & 75 & 15 & 300 \\ 1 & 25 & 75 & 10 & 500 \\ 1 & 35 & 70 & 10 & 400 \\ 1 & 30 & 80 & 10 & 300 \end{pmatrix}$$

$$X^T X = \begin{pmatrix} 9 & 270 & 675 & 135 & 3600 \\ 270 & 8250 & 20250 & 4050 & 108000 \\ 675 & 20250 & 50775 & 10125 & 270000 \\ 135 & 4050 & 10125 & 2175 & 54000 \\ 3600 & 108000 & 270000 & 54000 & 1500000 \end{pmatrix}$$

(5×5)

The inverse of the matrix  $(X^T X)$  was calculated previously.

$$(X^T X)^{-1} = \begin{pmatrix} 430/9 & -1/5 & -1/2 & -1/10 & -1/150 \\ -1/5 & 1/150 & 0 & 0 & 0 \\ -1/2 & 0 & 1/150 & 0 & 0 \\ -1/10 & 0 & 0 & 1/150 & 0 \\ -1/150 & 0 & 0 & 0 & 1/60000 \end{pmatrix} \quad (5 \times 5)$$

The matrix product will be then:

$$X^T Y_2 = \begin{pmatrix} 1 & 1 & 1 & 1 & 1 & 1 & 1 & 1 & 1 \\ 35 & 30 & 25 & 30 & 25 & 35 & 25 & 35 & 30 \\ 80 & 75 & 70 & 70 & 80 & 75 & 75 & 70 & 80 \\ 20 & 20 & 20 & 15 & 15 & 15 & 10 & 10 & 10 \\ 500 & 400 & 300 & 500 & 400 & 300 & 500 & 400 & 300 \end{pmatrix} \times \begin{pmatrix} 0.844 \\ 1.126 \\ 1.222 \\ 0.947 \\ 0.714 \\ 1.441 \\ 0.632 \\ 0.834 \\ 0.682 \end{pmatrix} = \begin{pmatrix} 4221 \\ 500 \\ 51203 \\ 200 \\ 125867 \\ 200 \\ 2637 \\ 20 \\ 16423 \\ 5 \end{pmatrix}$$

(5×9) × (9×1) → (5×1)

$$\hat{B}_2 = (X^T X)^{-1} X^T Y_2 = \begin{pmatrix} 430/9 & -1/5 & -1/2 & -1/10 & -1/150 \\ -1/5 & 1/150 & 0 & 0 & 0 \\ -1/2 & 0 & 1/150 & 0 & 0 \\ -1/10 & 0 & 0 & 1/150 & 0 \\ -1/150 & 0 & 0 & 0 & 1/60000 \end{pmatrix} \times \begin{pmatrix} 4221 \\ 500 \\ 51203 \\ 200 \\ 125867 \\ 200 \\ 2637 \\ 20 \\ 16423 \\ 5 \end{pmatrix} = \begin{pmatrix} 14323 \\ 6000 \\ 551 \\ 30000 \\ 763 \\ 30000 \\ 87 \\ 2500 \\ 461 \\ 300000 \end{pmatrix} = \begin{pmatrix} b_0 = 2.39 \\ b_1 = 0.0184 \\ b_2 = -0.0254 \\ b_3 = 0.0348 \\ b_4 = -0.001537 \end{pmatrix}$$

Therefore, we obtain the coefficients  $\hat{B}_2 = \begin{pmatrix} b_0 = 2.39 \\ b_1 = 0.0184 \\ b_2 = -0.0254 \\ b_3 = 0.0348 \\ b_4 = -0.001537 \end{pmatrix}$

Using the Equation 15 we obtain:

$$\hat{Y}_2 = 2.39 + 0.0184 X_1 - 0.0254 X_2 + 0.0348 X_3 - 0.001537 X_4$$

Replacing the names of the variables in the equation above, we obtain the mathematical formula which estimates the heat affected zones on the top sheet and at the same time can perform a cut in two parallel thin sheets separated with an air gap distance is:

$$\text{HAZ Top Sheet (mm)} = 2.39 + 0.0184 \times \text{Intensity (A)} - 0.0254 \times \text{Pressure (Psi)} + 0.0348 \times \text{Gap (mm)} - 0.001537 \times \text{Cutting Speed (mm/min)} \quad (19)$$

### v.iii R-Squared

In order to find out if regression models can estimate the response at an acceptable level, it is recommended to verify the R-Squared predictor, known as the coefficient of determination that can assess the quality of the model, the value can indicate the strength of the relationship between the factors and the response [181]. R<sup>2</sup> can give an indication of the percentage of variability in response

Y that can be explained by the variability of the parameters used. The rest of the proportion (1-R<sup>2</sup>) remain unexplained (unknown) due to the errors, meaning that the rest of the proportion (1-R<sup>2</sup>) does not represent the inadequacy of the model. An important point to emphasise was the high or low value of R<sup>2</sup> generally can give an indication of the model strength but it has been proven that R<sup>2</sup> can be misleading in some cases, meaning that we could get a poor R<sup>2</sup> for a good model and vice versa [208]. In certain cases, a low R-Squared can also meet the requirement of the model built, it does not mean necessarily that the model is poor. The convenient way was to use the prediction interval to satisfy the requirements [209].

The equation is given below:

$$R^2 = \frac{SST - SSE}{SST}$$

$$SSE = \sum_{i=1}^n (Y_i - \hat{Y}_i)^2$$

$$SST = \sum_{i=1}^n (Y_i - \bar{Y})^2$$

$$R^2 = \frac{\sum_{i=1}^n (Y_i - \bar{Y})^2 - \sum_{i=1}^n (Y_i - \hat{Y}_i)^2}{\sum_{i=1}^n (Y_i - \bar{Y})^2}$$

$$R^2 = 1 - \frac{\sum_{i=1}^n (Y_i - \hat{Y}_i)^2}{\sum_{i=1}^n (Y_i - \bar{Y})^2} \quad (10)$$

$\bar{Y}$  : Average residuals value.

$\hat{Y}_i$  : Predicted value.

$Y_i$  : Observed value.

n: Number of observed values.

SSE: Sum squared errors.

SST: Sum squared total error.

To compute R<sup>2</sup>, we use the formula (18) and (19) to estimate the  $\hat{Y}_{1, 2}$  and the prediction intervals were taken from Minitab at 95% confidence. For the numerical applications we use the data from the Table 29 below.

$$\hat{Y}_1 = \text{Top sheet Deformation (mm)} = 2.15 - 0.0503 \times \text{Intensity (A)} + 0.0053 \times \text{Pressure (Psi)} \\ - 0.0107 \times \text{Gap (mm)} + 0.00015 \times \text{Cutting Speed (mm/min)}$$

$$\hat{Y}_2 = \text{Top sheet HAZ (mm)} = 2.39 + 0.0184 \times \text{Intensity (A)} - 0.0254 \times \text{Pressure (Psi)} + 0.0348 \times \text{Gap} \\ (\text{mm}) - 0.001537 \times \text{Cutting Speed (mm/min)}$$

**Table 29:** Estimation values

Trials	Parameters				Observed Values		Estimated Values	
	Intensity (A) X <sub>1</sub>	Pressure (Psi) X <sub>2</sub>	Gap (mm) X <sub>3</sub>	Cutting Speed (mm/min) X <sub>4</sub>	Top Sheet Deformation (mm) Y <sub>1</sub>	Top Sheet HAZ (mm) Y <sub>2</sub>	$\hat{Y}_1(\text{mm}) /$ Prediction Interval	$\hat{Y}_2(\text{mm}) /$ Prediction Interval
Trial 1	35	80	20	500	0.55	0.844	0.67 Y <sub>1</sub> ≤1.8	0.92 0.26≤Y <sub>2</sub> ≤1.58
Trial 2	30	75	20	400	1.15	1.126	0.88 Y <sub>1</sub> ≤1.845	1.112 0.55≤Y <sub>2</sub> ≤1.67
Trial 3	25	70	20	300	0.97	1.222	1.09 Y <sub>1</sub> ≤2.22	1.3 0.64≤Y <sub>2</sub> ≤1.96
Trial 4	30	70	15	500	1.03	0.947	0.93 Y <sub>1</sub> ≤1.94	0.911 0.31≤Y <sub>2</sub> ≤1.5
Trial 5	25	80	15	400	0.91	0.714	1.21 0.19≤Y <sub>1</sub> ≤2.23	0.719 0.12≤Y <sub>2</sub> ≤1.31
Trial 6	35	75	15	300	0.85	1.441	0.67 Y <sub>1</sub> ≤1.69	1.1835 0.58≤Y <sub>2</sub> ≤1.77
Trial 7	25	75	10	500	1.45	0.632	1.26 0.18≤Y <sub>1</sub> ≤2.33	0.52 Y <sub>2</sub> ≤1.14
Trial 8	35	70	10	400	0.42	0.834	0.71 Y <sub>1</sub> ≤1.79	0.98 0.35≤Y <sub>2</sub> ≤1.61
Trial 9	30	80	10	300	1.12	0.682	1.004 Y <sub>1</sub> ≤2.08	0.79 0.16≤Y <sub>2</sub> ≤1.41

The second step is to compute the mean  $\bar{Y}$  for both responses Y<sub>1</sub> and Y<sub>2</sub> as follows:

$$\bar{Y}_1 = \frac{\sum_{i=1}^n Y_{1i}}{n} = \frac{0.55+1.15+0.97+1.03+0.91+0.85+1.45+0.42+1.12}{9} = 0.939$$

$$\bar{Y}_2 = \frac{\sum_{i=1}^n Y_{2i}}{n} = \frac{0.844+1.126+1.222+0.947+0.714+1.441+0.632+0.834+0.682}{9} = 0.938$$

Compute R<sup>2</sup> for the top sheet deformation:

$$R_1^2 = 1 - \frac{\sum_{i=1}^n (Y_{1i} - \hat{Y}_{1i})^2}{\sum_{i=1}^n (Y_{1i} - \bar{Y}_1)^2} = 1 - \frac{(0.55-0.67)^2+(1.15-0.88)^2+(0.97-1.09)^2+(1.03-0.93)^2+(0.91-1.21)^2}{(0.55-0.939)^2+(1.15-0.939)^2+(0.97-0.939)^2+(1.03-0.939)^2+(0.91-0.939)^2} \\ + \frac{(0.85-0.67)^2+(1.45-1.26)^2+(0.42-0.71)^2+(1.12-1.004)^2}{(0.85-0.939)^2+(1.45-0.939)^2+(0.42-0.939)^2+(1.12-0.939)^2} = 0.53$$

We can assume that 53% of variability of the response (Top Sheet Deformation) can be explained by the variability of the plasma parameters.

Compute R-squared for the Top Sheet Heat Affected Zones:

$$R_2^2 = 1 - \frac{\sum_{i=1}^n (Y_{2i} - \hat{Y}_{2i})^2}{\sum_{i=1}^n (Y_{2i} - \bar{Y}_2)^2} = 1 - \frac{(0.844-0.92)^2+(1.26-1.112)^2+(1.222-1.3)^2+(0.947-0.911)^2+(0.714-0.719)^2}{(0.844-0.938)^2+(1.26-0.938)^2+(1.222-0.938)^2+(0.947-0.938)^2+(0.714-0.938)^2} \\ + \frac{(1.441-1.1835)^2+(0.632-0.52)^2+(0.834-0.98)^2+(0.682-0.79)^2}{(1.441-0.938)^2+(0.632-0.938)^2+(0.834-0.938)^2+(0.682-0.938)^2} = 0.78$$

The result R-squared showed that 78% of variability of the response (Top Sheet HAZ) can be explained by the variability of the plasma parameters at 95% confidence.

### 5.3 Confirmation Tests

Additional tests were required to verify the level of improvement achieved in quality using the optimal parameters, also to assess the effectiveness of the mathematical models constructed and their level of prediction. The parameters of the plasma machining were selected randomly, then the results were compared against the calculated values of the mathematical model. All the specimens collected from validation tests were processed and assessed in the same manner than the samples analysed previously. The full test validation Figures obtained for the deformation and HAZ can be found in the [APPENDIX-E](#).

#### 5.3.1 Single Sheet

- For optimal parameters, the values measured are given in the Table 30 below.

**Table 30** Optimal parameters tests

	Cutting Speed (mm/min)	Pressure (Psi)	Intensity (A)	Measured (mm)
<b>Deformation</b>	8000	70	25	0.09
<b>HAZ</b>	8500	80	30	0.148

The optimal parameters showed a slight improvement for both responses. The heat affected zones alteration was reduced from 0.154 mm to 0.148 mm whereas the deformation was reduced from 0.12 mm to 0.09 mm.

- For regression model validation we obtained the results shown below in Table 31.

**Table 31** Predicted Tests Analysis

Trials	Cutting Speed (mm/min)	Pressure (Psi)	Intensity (A)	Deformation (mm)			HAZ (mm)		
				Measured	Predicted	Prediction Interval	Measured	Predicted	Prediction Interval
<b>Test 1</b>	9000	80	30	0.27	0.219	0.05-0.38	0.0942	0.087	≤0.32
<b>Test 2</b>	9000	70	20	0.30	0.25	0.09-0.42	0.215	0.23	≤0.46
<b>Test 3</b>	8000	75	20	0.23	0.199	0.04-0.35	0.327	0.333	0.12-0.55
<b>Test4</b>	8500	70	20	0.28	0.219	0.06-0.37	0.291	0.301	0.08-0.52
<b>Test 5</b>	8000	70	25	0.09	0.15	≤0.31	0.169	0.32	0.13-0.56
<b>Test 6</b>	8500	80	30	0.20	0.185	0.029-0.34	0.148	0.16	≤0.38

Table 31 above showed that all the estimated values calculated were close to the measured results obtained from tests validation and none of the values were falling outside the predicted interval. This

indicated the model constructed fit adequately and can be trusted. Therefore, there is a strong relationship between the input variables and the output, also this model can be trusted.

### 5.3.2 Double Sheets

The results obtained for the optimum parameters verification are shown in the Table 32 below.

**Table 32** Optimal parameters tests

	Gap (mm)	Cutting Speed (mm/min)	Pressure (Psi)	Intensity (A)	Measured (mm)
<b>Deformation</b>	20	400	70	35	0.41
<b>HAZ</b>	10	500	80	25	0.38

Second set of tests to validate the regression equation are shown in the Table 33 below.

**Table 33** Predicted Tests Analysis

	Gap (mm)	Cutting Speed (mm/min)	Pressure (Psi)	Intensity (A)	Deformation (mm)			HAZ (mm)		
					Measured	Predicted	Prediction Interval	Measured	Predicted	Prediction Interval
<b>Test 1</b>	20	500	70	25	0.64	1.125	≤2.258	1.1	0.993	0.33-1.65
<b>Test 2</b>	20	300	80	35	0.68	0.645	≤1.778	1.3	1.23	0.57-1.89
<b>Test 3</b>	15	500	70	25	1.11	1.178	≤2.25	0.85	0.819	0.19-1.44
<b>Test4</b>	10	300	80	35	1.19	0.752	≤1.88	0.9	0.882	0.22-1.54
<b>Test 5</b>	20	400	70	35	0.41	0.607	≤1.68	0.8	1.33	0.7-1.96
<b>Test 6</b>	10	500	80	25	1.06	1.28	0.15-2.42	0.38	0.391	≤1.05

The validation tests result showed a better quality using optimal parameters for both responses. Only small reduction obtained for the top sheet deformation compared to the results measured in previous experiments whereas the HAZ result obtained from the validation displayed a lower HAZ width and a decrease in size to just below 50% using the optimal parameters. The values measured in the validation tests were all close to the calculated values by the equations and none of them fell outside the predicted interval.

### 5.4 Summary

An experimental investigation was performed to assess the possibility to re-use the heat energy exiting the kerf during the plasma cutting, and also to find the optimal cutting process necessary to reduce the phenomena to their minimum level during a simultaneous cutting of two separate thin sheets. The investigation research was performed in four progressive stages. The hypothesis was tested experimentally and was proven true. Data was collected and analysed, a regression models were constructed for the surface deformation and the heat affected zones to assess the strength relationship between the input parameters and the response, this was performed for both single sheet and double sheets cutting. The main findings of this chapter are as follows:

- The Experiments were performed in four stages, single sheets analysis tests, plasma cutting two sheets capability tests, parameters identification tests and double sheets cutting optimisation.
- DOE based Taguchi parameters design was used, and optimal parameters were identified for both phenomena surface deformation and heat affected zones.
- Both optimal parameters showed in improvement in quality (a reduction in surface deformation and heat affected zones).
- ANOVA was used to identify the most influential parameters for surface deformation and HAZ.
- The assumptions for the regression analysis were checked and two models for deformation and HAZ were built for each process (single sheet and double sheets cutting).
- The mathematical models were validated, and the predicted values were falling within the predicted interval.

## **Chapter 6**

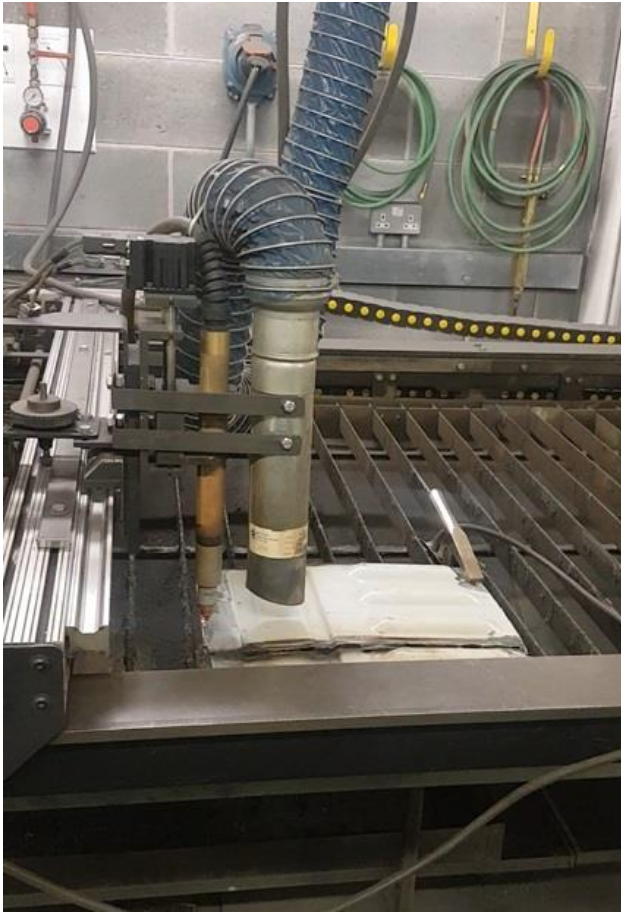
## **Practical Implementation**

### **6.1 Introduction**

This section is performed to show how the findings of this research can be implemented on a real world. For the tests a scrapped vehicle chassis rear floor segment was used (OEM part with no modifications made and the paint was not removed). We used the same machine for controlling the parameters and the feed rate. A propre method of cutting and path was generated for each vehicle brand, this will help to process the chassis in an efficient way and reduce the tool travelling time between top and underneath the underbody vehicle.

### **6.2 Rear Floor Chassis Cutting**

The tests were made on scrapped chassis part (Allied Vehicles Partner Car) as shown in the Figure 50 below. The material contained sealant underneath some sheet's zones. The results showed that the cutting process was reflected dramatically by the sealant as excess fume and fire was generated. Therefore, a quick removal of the sealant using a sand belt tool was required (only on the plasma pathway).



(a)



(b)

**Figure 58** Peugeot Partner Chassis Cutting (a) Torch Position Before Percing (b) Plasma Torch During the Cutting Process

The tests showed that leaving the sealant material underneath the chassis might result to a deterioration of the quality cut. However, after removing the sealant from the plasma path the quality resulted to a better finish, matching but not identical to the ones obtained from the experiments performed on clean sheets. Even though, the quality was good, but the test showed that the paint also has a slight effect on the cut. See Figure 51 below.

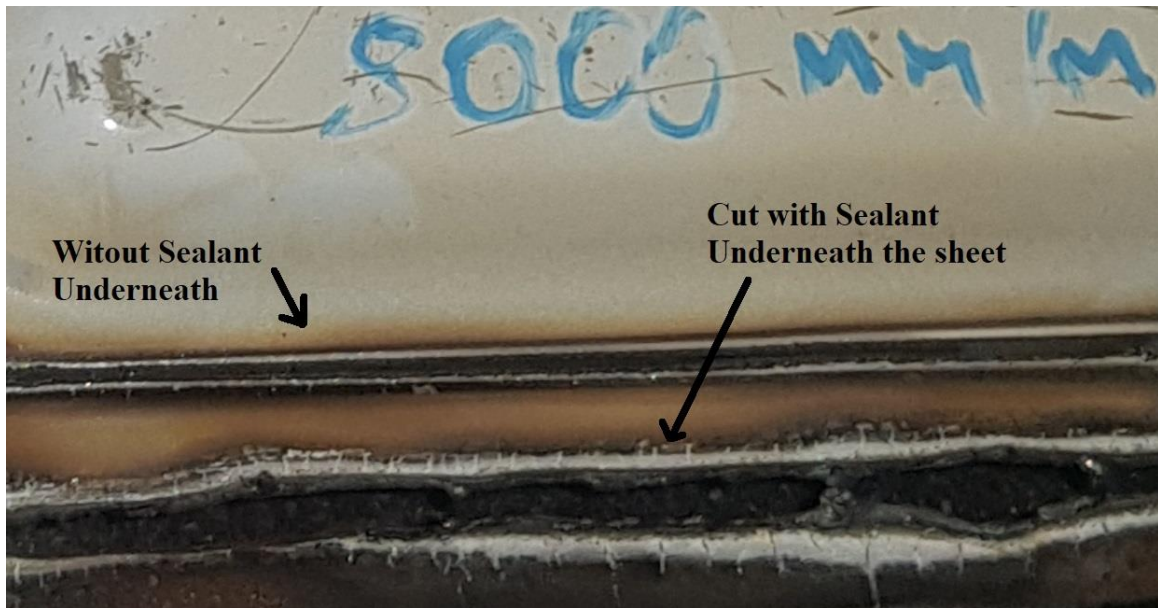


**Figure 59** Different Cuts with or without Sealant Underneath the Sheet

The Figure 52 below can illustrate the difference when the plasma torch travels through a material containing sealant underneath the sheets and the zone without a sealant. The mid zone (with no sealant) of the cut showed a better quality compared to the outer zones of the cut edge.



**Figure 60** Cut Edge Quality (Sealant underneath the material)

On the Figure 53 below, after removing the sealant from the plasma pathway using a sand belt, the quality result was increased dramatically with no second processing required.



**Figure 61** Quality Obtained after Sealant Removed using Sand Belt.

To perform the entire cut out on the vehicle floor effectively, it was necessary to follow some steps and also a bespoke automated machinery or a robotic arm was required to control the speed, path, movement of the tool in 3-dimensional space and the other parameters.

### **6.3 Plasma Cutting Process Automation**

Robotic arm was found to be a better option to automate the process due to their popularity and wide spread in the automotive industry for tasks such as cutting, trimming or welding [210]. Even though CNC can provide a better accuracy (0.005 mm compared to 0.1 ~ 1 mm) and repeatability (0.002 mm compared to 0.03 ~ 0.3 mm). However, CNC is very limited when a nonlinear cutting is involved or a complex trajectory e.g. three-dimensional structure cutting [211]. Six axis robotic arm is taking the lead as they can be operated with a simple programmes and can work at full time [212].

In this study, the required reach to perform the task is approximately 3 m long, this can allow the sectioning on AV chassis floor for all vehicle brands, and also to discard the scrapped parts. The largest vans floor measured was approximately 2500 mm long and 850 mm wide. The plasma arm robot usually (depending on the companies requirements) needs to possess a good isolation from high

frequencies current, isolation shield from dust, dross and sparks, integrated with torch height control (voltage sensing height control mounted on the torch with constant feedback), a vision system was required to recognise the parts/vehicle models in less than 0.1 second [213], this offered a fast and a better flexibility than sensing prob, magnetic gripper, tool changer mounted at the end of the arm robot this will allow to switch between the gripper and the torch at the end of each the task as required. Tool holder was also required, this needs to be integrated as part of the robot path cycle when switching from gripper and torch, fume extractor to reduce smoke, a safety cage [214]. Fire detector and control system must be implemented.

One of the well-known and most implemented robotic arm in the automotive industry is Fanuc [215]. The selected model (according to the company's needs) to perform the floor chassis cut is Fanuc R-2000IB 125L R-30IA 6 axis, the reach was just above 3 m, this will cover all the vehicles brands, the loads was 125kg. The model is well known also for plasma cutting (this was suggested by the robotic company). The cost of the arm robot was approximatively £13000 for a used arm only without any accessories. The approximative amount for the implementation of the robotic arm including the required automated systems and safety was quoted to 110000k (Global Robots Quote).

Some of the potential issues that can faced when implementing the plasma cutter robotic arm and all the equipment required can be summarised as follows:

- Implementation space, the zone required for the installation of the arm can be an issue at the shopfloor as this was estimated to four time the normal space compared to manual processing.
- Ethic problems, even though a smoke extractor is required. However, a percentage of pollution and air contamination is expected.
- Culture issue even though this technique showed an effective cost saving and time reduction, however there is still some resistance and fear of change at the company.
- Lack of an adequate skills, this includes the installation process to British standards and regulation, in addition also to operating skills.
- Initial cost of investment
- Operators' redundancy
- Risk assessment
- Maintenance issue.
- Factory layout change issues.

## 6.4 Cutting Procedures:

The process of the cutting required the tool to follow a defined path, the Figures 54 and 55 below illustrate one of the vehicles that Allied Vehicles use to convert and perform a cut out (ford van short base). The vehicle needs to be uplifted to approximately 1m50 high to offer enough room to the robotic arm to access the underneath car. The robotic arm can use a vision system to identify the vehicle and pathway required for the cut in a fast manner. The double layers cutting with a gap up to 20 mm would be cut simultaneously with one pass from the upper side of the chassis floor. However, beyond this gap distance, the tool required to cut the sheets separately processing one layer at time.

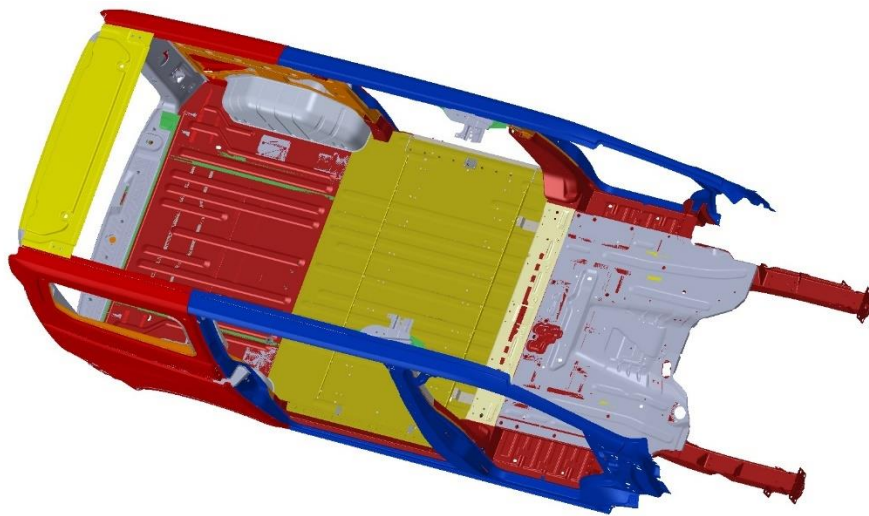


Figure 62 Vehicle Chassis (Allied Vehicles)

Once the arm is positioned and set, the adequate way to section the floor efficiently was to move the plasma torch robotic arm to the edge rear vehicle at position two as shown in the Figure 55 below.

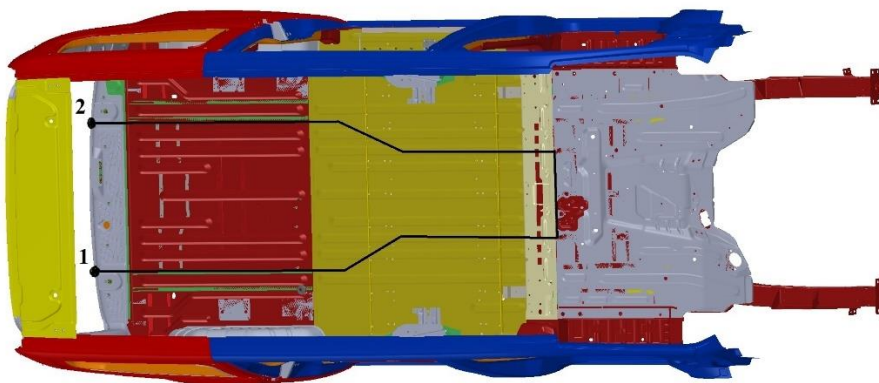
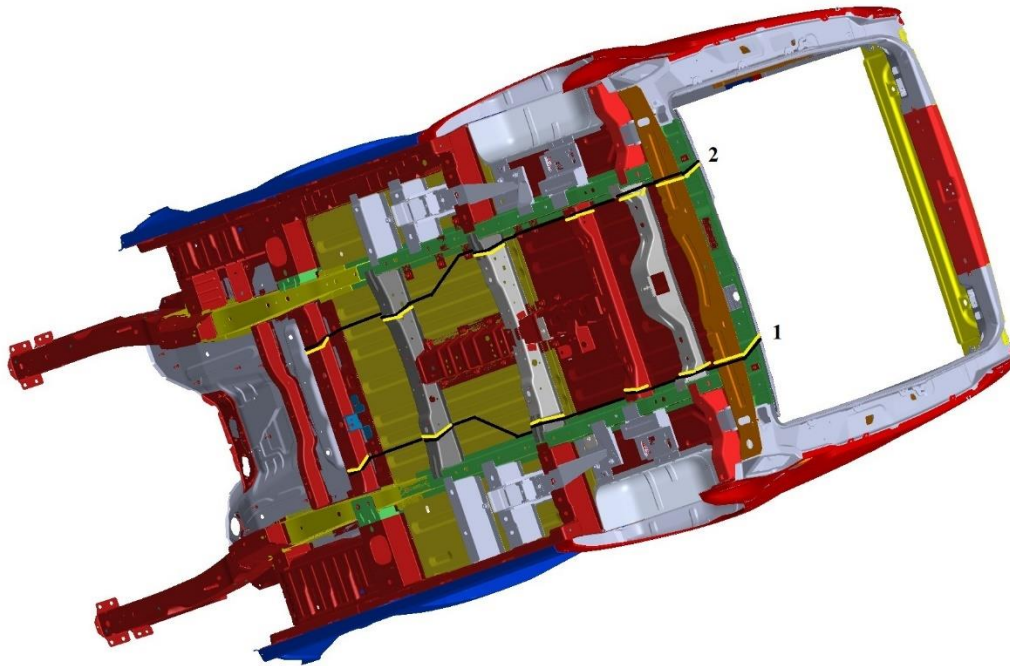


Figure 63 Cutting Profile.

The torch needs to move underneath the underbody first performing cuts around the rails one at a time at clockwise direction as shown in the Figure 56 below with yellow lines. Once the torch reaches the position number one then the arm can continuously finish the cut following anti-clockwise direction until the position number two again. This would allow to keep the better-quality cut to the outer side of the cut out, even though there was no noticeable change of the quality as the sheets were very thin.



**Figure 64** Underneath the Vehicle Cut Profile

The estimation of the processing time for this typical vehicle model can be calculated. We consider a speed of 8000 mm/ min for single sheet and 400 mm/ min for a double sheet cut.

Cut-out length 1900 mm, width 800 mm, rails 300 mm periphery, rail width 150 mm and rear box section 500 mm periphery.

The total periphery size of the profile path on the top side vehicle  $(1900-150 \times 2) \times 2 = 3200$  mm on the top side (need to be cut at 8000 mm/min). The rails under the car which would be cut at 8000 mm/min have a total length  $(500 + 300 \times 3) \times 2 = 2800$  mm, in addition to travelling distance between the rails underneath the chassis when the Robot at rest  $(1900-3 \times 300-500) \times 2 + 800 = 1800$  mm. The cut-out width at the front possesses double layered sheets of 800 mm long and two rails with gap around 20mm and 150 mm wide therefore the total length would be  $(800 + 150 \times 4) = 1400$  mm, this would be cut at 400 mm/min speed. A summary is given in the Table 34 below.

The total periphery covered at 8000 mm/min was 7800 mm. The total periphery covered using 400 mm/min was 1400 mm. The estimation of the cutting time is approximately 5 minutes, this is a reduction of 40 minutes compared to mechanical cutting methods.

**Table 34** Feed Rate and Trajectory of the Robotic Arm

	Quantitative Values	
	Single Sheet	Double Sheet
Feed Rate (mm/min)	8000	400
Total Profile Length (mm)	6000	1400
Total Traveling Distance of the Robot at Rest (mm)	1800	0

## 6.5 Summary

The tests on a real chassis showed an effective cutting using plasma technique. The main findings of this chapter are as follows:

- Coated material did not reflect considerably on the quality compared to clean sheets used in previous tests.
- A good electric contact between the work piece and the plasma is required or alternatively a special torch design might be used.
- Sealant on the chassis reflected on the quality cut.
- It was necessary to remove the material which is located under the chassis on the plasma pathway in order to obtain a good quality cut.
- To speed up the cutting process it is recommended to program the arm robot to perform the tasks at a specific way.
- Plasma technology can reduce the processing time to approximately 5 minutes as an estimation compared to traditional method used at the company. The processing time using manual cutting was approximately 45 mins as an average (measured using stopwatch).
- This new cutting technique can guarantee a constant processing time. In the other hand, the operators failed to keep a constant timing for processing the same vehicle brand.

Plasma arc cutting is an efficient technique for metal cutting. However, until today it was not known if this method can cut two layers with air gap simultaneously. This would help the industry to understand better this technology and their capabilities, also to show the best approach to process these structures e.g., Rails, box sections or double-layered zones without the need to cut in two sides.

The aim of this work was to investigate on the possibility of plasma to cut two separate thin sheets with an air gap distance simultaneously and assess the impact of the heat on thin materials, in addition of the optimisation of the cutting process and the analysis of the relationship strength between the input parameters and the quality obtained. The objectives were to assess the effectiveness of plasma to cut thin sheets under one millimetre, build a 3D structures for the tests, perform the experiments using a DOE method, optimise the process of cutting using the Taguchi parameters design approach at minimum trials, assess the quality obtained (surface deformation and HAZ mainly), identify the most influential parameters using ANOVA, construct mathematical models that represent the design and lastly test the findings in a real chassis.

The research questions addressed in this study lay mainly on assessing the possibility to re-use the excess heat energy exiting the kerf to perform an additional cut. In other words, cutting simultaneously two sheets (separated with an air gap). In addition, to identify the optimal parameters required to process double sheets (to reduce the resulted phenomena to their lower level) and analysing the effect of the heat generated during the cut on thin material. Identifying the maximum deviation between the top and bottom edge of the cut was also one of the key research questions as the offset could cause a problem if the tolerances are not respected. Lastly, assess the relationship strength between the input and output factors. Therefore, to test the hypothesis and assess the cause and effect, quantitative experimental method was adopted in this research and DOE was selected as an effective way to reduce the costing and time of the process. Taguchi parameters design was found to be the adequate approach for this thesis to perform the experiments at a minimum trial whilst preserving the accuracy compared to other techniques. The limitation of this research lays in the number of tests performed to optimize the parameters (performed at minimum trials L9). This might result to the analysis to fail detecting the significance of the other parameters effect and interactions.

The tests were divided into four different stages. The first phase was made to evaluate if plasma was able to perform a cut on thin materials 0.6 mm without altering the surface, and also assess the effect

of the heat on the flatness and the edge of the cut. The following tests were performed to assess the plasma capability to cut simultaneously two layers with an air gap and identify the maximum gap that can be cut simultaneously. The third phase of the tests were made mainly to identify the suitable cutting settings required for an effective process for a fixed gap 20 mm. The last stage of the experiment was made to assess the possibility to optimise the process and reduce the defects.

The hypothesis was tested and proven true and the experiments showed that plasma technique can perform a cut in two separate layers simultaneously. Hence, the reuse of the plasma heat power after exiting the first sheet was possible, contrary to what was assumed previously that only waterjet among the non-traditional techniques possessed the ability to process two layers simultaneously [84].

The experiments revealed that processing two layers was subject to the gap distance between the sheets. The power of the plasma was limited as the tests were performed using low current plasma technology, a more advanced plasmas might achieve a higher cutting gap. Tests were performed by incrementing the gap of the two layers, the highest distance which resulted to a full cut in two layers simultaneously was 25 mm, but this lacked quality. Tests at 35 mm gap did not achieve a complete cut on the bottom side.

Cutting single thin sheets DC01 grade material at 0.6 mm thick using a plasma resulted to good quality without altering the surface. This contradicted previous research claim assuming that plasma was not suitable for this range of thicknesses [157]. Tests showed that plasma cutter can result to a deformation as low as 0.12 mm, the maximum value obtained in all samples observed was 0.3 mm, even though the defects were measured. However, this was not visible. Trials number 5, 6 and 8 were outside the tolerance required (0.2 mm maximum). The parameters that affected mostly deformation were intensity followed by cutting speed successively 51.71% and 42.47%, both effects were statistically significant. The 3D surface plot showed that in order to achieve an effective cut and keep the deformation at their lowest level it is recommended to avoid using high or low intensity associated with fast cutting speed, this meant that if a moderate or elevated feed rate is used and if either low or high power is employed then this would result to a higher degree of surface deformation. Therefore, it was important to use the adequate settings. Taguchi parameters design methods showed that an optimal cutting parameter can be identified and reduce the defect to their lowest levels, it was found that the best parameters that can result to an optimal cut were cutting speed 8000 mm/min, pressure 70 Psi and 25A. The optimal settings were tested and resulted to a small improvement of 0.09 mm deformation, which is 0.03 mm less than the lowest value measured.

The heat affected zones values measured for 0.6 mm single sheet were varied from 0.154 to 0.403 mm, the quality obtained was acceptable, the maximum size measured was less than half millimetre. The parameter which affected mostly the sheets was cutting speed with more than 70%. The results showed that the effect was statistically significant. The other parameters did not exhibit a big impact. The surface plot suggested that in order to reduce the heat affected zones it was necessary to avoid using low speed especially when associated with weak pressure, this might expose the material to longer period of heat. Optimal input variables were obtained using Taguchi parameters design method at cutting speed 8500 mm/min, pressure 80 Psi and intensity 30A. The settings showed an improvement on the quality result, the heat affected zones size was reduced from 0.154 to 0.148 mm. Tolerance set to 0.2 mm maximum, there is no second processing required. The dross and kerf size were very small and not noticeable.

The interaction graphs for single sheet cut illustrated a dependency (both deformation and HAZ). Therefore, the effect of one parameter on the response might depend on the level of another parameter. However, there was no statistical evidence showing that these interactions were significant. This might be the cause of the limited tests performed in this research (9 trials).

The tests showed that cutting simultaneously two separated sheets, the effect of the heat on the lower sheets was higher compared to the top sheets, excluding the hardness which did not exhibit a big difference between the top and bottom layers. This might be the result of the heat energy flow was focused at the top and diverged after exiting the kerf causing the edge of the top sheets to evaporate and the bottom layers to melt. The dross size on the top sheets were from 1.3 mm increasing to 2.7 mm whereas the bottom sheets showed a minimum of 1.9 mm, all the dross measured were beyond the tolerance required (1 mm maximum), this meant that a second processing might be required. The kerf was almost steady for the top sheets less than 2 mm with slight variation, the bottom kerf showed a higher value to almost 5mm. The part size accuracy set was +/- 1.5 mm, all the samples measured on the top sheets were accurate in size and none of them were outside the tolerance.

Simultaneous cutting can result to a noticeable reduction in size on the bottom samples compared to the top side. The phenomenon of edge offset might be the cause of the plasma flame shape was not uniform after exiting the first sheet as explained in the section above. The bottom layers edge of the cut required to be within the tolerance of 2 mm maximum compared to the top edge. Large offset might result to engineering problems such as fitting issues or poor sealing of the new customised floor pan (this might result to water penetration and corrosion issues). The tests showed that cutting with plasma can result to a material loss of 10.27 % compared to the original part with 1.65 mm

deviation between the upper and lower edges, this was registered for the 15mm gap test model 5<sup>th</sup> trial.

The deformation registered for the top sheets was varied from 0.42 mm to 1.45 mm whereas the bottom showed a maximum deformation of 3.9 mm. The wider gaps showed less deformation value compared to small gap on the top sheet, this might be due to the wider space between the two sheets which offered more room for aeration and heat dissipation. There was a missing data in the analysis for the bottom layers trial 2 and 3, for the 20 mm gap model. The trials did not result to a full cut, this might be the result of the gap between the two sheets expanded due to accumulation of the heat, gas pressure and due to lower cutting speed used. The missing values were not estimated as these would not be used in the analysis (there is no requirements for optimising the lower sheets).

Taguchi parameters design method was used for optimisation process, it was found that the best parameters resulted to a lower deformation were cutting speed 400 mm/min, pressure 70 Psi and 35A intensity using a larger gap 20mm. Analysis of variance showed that the top sheets were mainly affected by the intensity at 63.93%, the effect was statistically significant followed by the pressure at 26.36% with no evidence of the effect significance, this might be due to limited tests used in the design L9. Three-Dimensional surface plot showed that cutting simultaneously two sheets, low power and low pressure would result to a high deformation. Therefore, it was recommended to employ a high intensity with low gas pressure. The results showed a very small improvement in deformation using optimal parameters from 0.42 mm to 0.41 mm. However, the tolerance for the deformation on the top sheet was met (0.5 mm maximum).

Heat affected zones measured varied from 0.632 to 1.441 mm on the top sheet, the values were higher on the wider gap, the lower samples were varied from 1.245 to 3.446 mm. Taguchi parameters design approach showed that cutting speed 500 mm/min, pressure 80 Psi, intensity 25 A and 10 mm gap were the best options to achieve a minimum heat affected zones. The parameters that influenced the response were gap at 37.31%, pressure 28.61% and cutting speed 25.33%. However, there was no evidence statistically that these effects were significant. The surface plot showed that a large gap between two sheets would result to a high defect when a low pressure was used, it was recommended in this case to attribute a high pressure for a better result. However, to achieve the lowest heat affected zones possible then a small gap distance was recommended using average pressure. Validation showed an improvement and a reduction in size from 0.632 to 0.38mm. However, second processing might be required to reduce the size of the altered material, the tolerance was not met (0.2 mm maximum).

The interaction plot for both phenomena showed an interference between the variables when processing a double layered. Therefore, the effect of one input variable on the response was also depending on the level of another input variable. The interactions showed that deformation on the top sheet can be reduced when cutting two separate layers simultaneously if the largest gap 20 mm is processed using either parameter at settings level three. The 10 mm gap distance associated with pressure 70 Psi also showed a little deformation. However, 15 mm gap did not show a big difference between pressure's settings, but a slight improvement can be seen using 75 Psi. Cutting speed at level two 400mm/min can result to a small deformation if associated with a small gap 10 mm but when 15 mm gap model is used then the speed settings have only a small effect with a slight improvement seen using 300mm/min. The intensity at level three 35A would show less deformation cutting any gap.

The HAZ showed a better result and size reduction when 20 mm gap is used with either parameter at setting level three. The gap distance 15 mm would require using pressure setting 80 Psi to obtain less HAZ whereas 10mm gap a slight improvement can be seen if 75 Psi pressure is used. The cutting speed at level two 400mm/min is suitable for 15mm gap but for 10 mm gap it is adequate to use level three 500mm/min even though it showed only a small difference. Intensity is more effective if lower setting at level one 25A is used to perform a cut on either 15 or 10 mm gaps. Even though the results showed an interaction effect between variables. However, there is no statistical evidence that the effects of the interactions were significant as the P-values obtained were above 5%. The limitation of the tests performed (at minimum trials) might be the reason of the design failing to detect the level of significance for the parameter's interactions.

To assess the strength of the relationship between the input variables effects and the response, two mathematical models (multi-linear regression) were built for both deformation and heat affected zones affecting the upper layer. The analysis was made for the DC01 steel grade material for single sheet 0.6mm with three variables and for a double sheets cutting also (0.7 mm thick material) with four variables. Coefficient of determination which assessed the quality of the model was computed and resulted to an acceptable values for all models. The method used to build the equations was least square errors approach. The equations were tested, and the results showed a close values between the estimated and the measured ones, none of the measured values were outside the interval of prediction. This was a good indication that the relationship between the input variables and the quality result

was strong, and the models can represent the experimental design. Even though, the equations were tested and provided a good results. However, the interval of the predictions was slightly wide.

A final test was performed on a real chassis to demonstrate the suitability and practicability of the findings of this study. The test results on a chassis showed that it was necessary to remove any sealing (if applicable, depends on the vehicle's brand and zones) which was located under the sheets as this might result to a degradation of quality cut, risk of fire and excessive smoke generation. The removal of the sealing was required only on the plasma pathway. This confirmed also the claim of some articles which emphasised the necessity for verifying and knowing the parts which are processed before proceeding to any type of cutting in order to avoid fire generation[6]. The results showed a considerable deference in quality before and after removing the sealant material. The paint did not show a big impact and reduction in quality (only in low scale and not noticeable) apart a black tint accumulated at the cut edge caused by the fume, this matched the claim of previous article [10]. A good electric connection between work piece and the electrode was necessary especially at the start for the first spark (piercing) or alternatively other plasma model can be used [8], these were referred to non-direct arc transfer plasma cutting [216]. The estimation for processing the underbody vehicle chassis floor was estimated to approximatively 5 mins. Even though the tests showed an effective cutting. However, the technique used to assess the practicability was a CNC plasma, this was tested only in homogenous flat and for linear cutting.

The literature review showed that practically the same cutting method was employed to process the chassis (mechanical tools) in most companies that converted cars to wheelchair accessible vehicles[6]. Tests demonstrated that plasma cutting can be a good and fast alternative solution. The technique showed a better ability compared to circular saw e.g., profiling or cutting sharp corners where mechanical tool clearly showed limitations processing the chassis effectively as illustrated before. Tests showed that plasma can process and cut parts at higher speed rate, meaning that the cycle time for processing the full chassis cut out can be reduced to approximately five minutes, this is a reduction of 40 minutes. Furthermore, plasma technique can be mechanised. Hence, the operating cost can be eliminated. The quality cut obtained from cutting simultaneously two sheets was subject to company's requirements, this meant it can be acceptable for some companies and rejected in others. Certainly, a better quality can be achieved by processing one layer at time. However, extra costs might be required for a better automation. In addition to supplementary tasks involved. To sum up, Plasma cutter can be shaped and structured to satisfy the company's needs. However, this required first to understand properly the challenges and what we trying to achieve, also the nature of material

and the structure of the parts, then we can customise, readjust, and build the cutting tool needed to meet the industry demands.

This alternative technique for cutting the chassis floor was acknowledged by the company (Allied Vehicles). The feedback was to process one sheet at a time in order to avoid a second processing. However, this required automation reinforcement to remove the scrapped sheets using magnetic grippers in order for a robotic arm to access the second layer. The installation of the technique is still under review due to some implementation issues faced such as budget, area where to implement, factory layout change issues and fear of change. In addition to the pandemic delays.

## 7.1 Conclusion

To sum up, Plasma cutting was investigated for the suitability of cutting two layers simultaneously. The aim of the research was to identify whether the heat energy exiting the kerf possesses enough power to cut through an additional layer and the effect of the heat on thin material. The experiments were performed in four progressive stages. DOE based Taguchi parameters design method was selected as the adequate technique to optimise the parameters and reduce the deformation and heat affected zones to their lowest level. Analysis of variance was found to be an effective approach to analyse the data for this research. Mathematical models were constructed to assess the strength relationship between the input and response variables. The key results are as follows:

- Plasma technique can process thin materials without altering the surface, this was tested on DC01 steel material 0.6 mm thick, a good quality cut was obtained.
- Both responses measured in single sheet were small and did not exhibit a visible defect, deformation  $\leq 0.3\text{mm}$  and HAZ  $\leq 0.4\text{mm}$ , dross was very small and not visible. Therefore, a second processing to remove the altered areas was not necessary for single sheet.
- The optimal parameters for deformation to process one sheet were found to be cutting speed 8000mm/min, pressure 70Psi and Intensity 25A whereas HAZ are 8500mm/min, 80psi and 30A.
- The most influential parameters were cutting speed and Intensity for deformation whereas for the heat affected zones was mainly cutting speed.
- Both optimal parameters showed an improvement in quality, a reduction in HAZ from 0.154 to 0.148mm and sheet deformation from 0.12 to 0.09mm.

- Cutting simultaneously two parallel sheets spaced with an air gap was possible, the energy leaving the kerf possess enough heat energy to cut through a second layer, but the ability was restricted by the gap distance.
- The responses measured in double sheets showed a higher impact on the bottom sheets compared to the top side in overall.
- The quality cut analysis showed that a second processing to remove the heat affected zones and dross was recommended when cutting two layers simultaneously. However, this remain depending on the company's requirements.
- The size of the HAZ was 1.45mm maximum on the top sheet and 3.45mm as a maximum on the bottom.
- The cut exhibited an increase of material hardness up 66.7% at the edge and dross size was up to 2.7mm on the upper layer whereas the bottom was up to 3.3mm.
- The edge of the cut on the top sheets showed an offset compared to the bottom edge, this meant that lower samples were smaller than the upper specimens.
- The kerf measured was wider on the bottom side of the jig almost 5 mm for the 10 mm gap model (obtained with the 9th trial).
- The optimal parameters found for cutting two sheets simultaneously and reduce the deformation on the top side were cutting speed level two 400mm/min, Pressure at level one 70Psi, Intensity at level three 35A and Gap at level three 20mm, whereas the optimal parameters to minimise the Heat Affected Zones size were Cutting speed at level three 500mm/min, pressure at level three 80Psi and Intensity at level one 25A and gap at level one 10mm. Both optimal parameters showed an improvement in cut quality, almost 50% decrease in HAZ size and very small improvement of deformation.
- The most influential parameters for the top sheet deformation were the intensity and then pressure whereas the one affecting the HAZ was mainly the gap and then pressure followed by cutting speed.
- Regression models were constructed for both single sheet and double layered cutting to assess the relationship strength, this was made for the deformation phenomenon and HAZ.
- The measured values from the validation tests were all close to the data calculated using the regression equations and were all falling within the range of the predicted interval.
- Both regression models for the double layered sheets cutting showed a good fit value and R-squared respectively for top sheet deformation and HAZ of 0.53% and 0.78%.

- Tests were made on a vehicle chassis and after removing the sealant under the sheets along the cut profile it showed an effective cutting. The paint had a very small effect on the quality.
- Using an adequate automated system in addition to a good method of cutting would result to an effective cut in a short time, an estimation of an approximatively 40 min can be achieved compared to manual cutting.

## **7.2 Limitation and Future Work**

The limitations and the work that can be done and added to widen this research are summarised as follows:

### **7.2.1 Limitation**

- This research was done with a minimum trial L9 (both single sheets and double sheets cutting), this is due to the large number of samples available and collected for the analysis, time constraints and the cost of the experiments. It is common that the analysis in this case might fails to detect the evidence of significance of some parameters or the interactions when using small size of experimental.
- The interactions effects in this research were not considered in the regression analysis as there was no statistical evidence of the significance of the interactions in the ANOVA results. However, the literature showed that at low trials the detection of the effects might be lost.
- Even though the measurement were repeated and checked multiple times for accuracy and also to minimise the errors. However, due to the scope of this research and time constraints the errors in measurement were not estimated.
- In this study, the number of the tests performed, and the samples collected from the experiments was significant. Assessing all the specimens required a long period of time. Therefore, replicating the experiment to estimate the variability would not be convenient due to time constraints and the high costs involved.
- The regression models constructed were tested and showed a good representation of the experimental design. However, the interval was slightly wide due to the limited number of tests performed.
- The tests were performed using a CNC plasma low current. Therefore, cutting two layers simultaneously with an air gap distance in this study is based on this plasma model there is a high probability that other powerful plasma can achieve a cutting in two layers using wider gaps than the ones resulted in these experiments.

- The tests on a real chassis vehicle were made using CNC technology. However, the literature showed that robotic arm is the adequate technique for a non-linear cutting or non-homogenous surfaces. The tests performed were only on scrapped chassis vehicle part. Therefore, the time required for processing the entire cut out was an estimation.
- The implementation of the technique was acknowledged by the Allied Vehicles company but still under review. Therefore, it is too early to assume that this concept can be implemented in other similar companies.

### **7.2.2 Future Work**

- The research was performed using minimum trials, Repeating the same experiment using a full factorial design in addition to including the interactions in the regression models would result certainly to better and accurate models with a tight interval of predictions.
- The analysis was carried out using a common technology of plasma, the cutting edge technology used these days is the high density plasma (HD) known for its capability to achieve a high quality cut similar to laser technique[114]. Therefore, repeating the same experiments using this state-of-the-art HD Plasma and compare the quality results would be beneficial.
- This work was performed considering four variables, intensity, pressure, cutting speed and the gap distance between two layers, adding the thickness of the material as a fifth variable would result to a better understanding of the simultaneous double sheets cutting process.
- Replicating these experiments to assess the variability in the tests would also be beneficial for this research, in addition of analysing the variability in measurement to estimate the errors.
- There was no work has been done in this area before, therefore one of the aims of this research was to generate the necessary knowledge for a simultaneous cutting of two layers, and then the findings of this work can be used as a reference to build an accurate simulation model and help making decision and predict new values.
- Replicating this experiment using Laser cutting technique and then compare the quality obtained and the processing time to plasma cutter would be beneficial.

## References

- [1] Friars Motor Company, 2020, 'A Brief History of the Wheelchair Mobility Car - Friars Motor Company', Friars Mot. Co. [Online]. Available: <https://www.friarsmotorcompany.co.uk/brief-history-wheelchair-mobility-car/>. [Accessed: 19-Jun-2020].
- [2] Calvin Barnett, 2018, 'The Drivers of the Accessible Wheelchair Vehicle Market Growth.', *Thisis Mag.* [Online]. Available: <https://thisis.co.uk/the-drivers-of-the-accessible-wheelchair-vehicle-market-growth-2/>. [Accessed: 19-Jun-2020].
- [3] Allied Vehicles, 2020, 'Company Background - Allied Vehicles Group', AV [Online]. Available: <https://alliedvehiclesgroup.com/about/company-background/>. [Accessed: 19-Jun-2020].
- [4] Fan, J., and Njuguna, J., 2016, 'An Introduction to Lightweight Composite Materials and Their Use in Transport Structures', *Lightweight Composite Structures in Transport: Design, Manufacturing, Analysis and Performance*, J. Njuguna, ed., Woodhead Publishing, Nieuwegein, Netherlands, pp. 3–34.
- [5] Nikitin, A., Schleuss, L., Ossenbrink, R., and Michailov, V., 2017, 'Corrosion Behavior of Brazed Zinc-Coated Structured Sheet Metal', *Int. J. Corros.*, 2017, p. 8.
- [6] Mehok, K., 2007, 'When Is Sectioning Appropriate for Unibody Vehicles in Your Shop?', *Automot. body repair news*, 46(10), pp. 74–82.
- [7] Ramesh, V. R., 2004, "Advanced Welding Equipment & Controls For Thin Sheet Stainless Steel Fabrication" - *ProQuest*, *Indian Weld. J.*, 37(1), p. 19.
- [8] Balasundaram, H. R. R., and Karthikeyan, N. G. N., 2018, 'Experimental Investigation of Cut Quality Characteristics on SS321 Using Plasma Arc Cutting', *J. Brazilian Soc. Mech. Sci. Eng.*, 40(2), pp. 3-11/60.
- [9] Miroslav Radovanovic, M. M., 2011, 'Modelling the Plasma Arc Cutting Process Using ANN - Nonconventional Technologies Review. No. 4/2011.', *Rev. Tehnol. Neconv.*, 15(4), pp. 43–48.
- [10] Rajnikant C Bidajwala, M. A. T., 2014, 'Parametric Optimization On SS 304L Using Plasma Arc Cutting- A Review', *International J. Innov. Res. Sci. Technol.*, 1(7), p. 147.
- [11] Prateek Kumar Gautam, V. G., 2019, 'Analysis of process parameters of plasma arc cutting using design of experiment', *Int. Res. J. Eng. Technol.*, 6(6), p. 2734.
- [12] Leander Schleuss, Thomas Richter, Ralf Ossenbrink, and Vesselin Michailov, 2015, 'Plasma Cutting of Structured Sheet Metals in Comparison with Laser Beam Cutting', *J. Mater. Sci. Eng. B*, 5(4), p. 143.
- [13] Eltawahni, H. A., and Olabi, A.-G., 2011, 'Optimisation of process parameters of high power co 2 laser cutting for advanced materials', *Dublin City University*.
- [14] Borries Burkhard, 2002, 'The Hydroform Revolution - Laser-Robots', *Int. hydroforming forum* [Online]. Available: [http://www.hydroforming.net/hydro/home/html/modules\\_op\\_modload\\_name\\_News\\_file\\_article\\_sid\\_105\\_mode\\_thread\\_order\\_0\\_thold\\_0.html](http://www.hydroforming.net/hydro/home/html/modules_op_modload_name_News_file_article_sid_105_mode_thread_order_0_thold_0.html). [Accessed: 16-Jul-2020].
- [15] Klimpel, A., Cholewa, W., Bannister, A., Luksa, K., Przystalka, P., Rogala, T., Skupnik, D., Cicero, S., and Martín-Meizoso, A., 2017, 'Experimental Investigations of the Influence of Laser Beam and Plasma Arc Cutting Parameters on Edge Quality of High-Strength Low-Alloy (HSLA) Strips and Plates', *Int. J. Adv. Manuf. Technol.*, 92(1–4), pp. 699–713.
- [16] Nedic, B., Janković, M., Radovanović, M., Lakić, G. G., Nedić, B., and Lakić, G. G., 2013, 'Quality of Plasma Cutting', *13th International Conference on Tribology – Serbiatrib'13*, Serbian Tribology Society, Kragujevac, Serbia, p. 314.
- [17] Morphy, G., "Hydroformed Automotive Components: Manufacturing Cost Considerations," *SAE Technical Paper 2000-01-2672*, 2000, <https://doi.org/10.4271/2000-01-2672>.
- [18] Asiabanpour, B., Vejanla, D. T., Jimenez, J., and Novoa, C., 2009, 'Optimising the Automated Plasma Cutting Process by Design of Experiments', *Int. J. Rapid Manuf.*, 1(1), p. 21.
- [19] Iosub, A., Nagit, G., and Negoescu, F., 2008, 'Plasma Cutting of Composite Materials', *Int. J. Mater. Form.*, 1(SUPPL. 1), pp. 1347–1350.
- [20] Limousine, 2020, 'Stretching A Car Into A Limousine | An Extraordinary Limousine, Inc.', *Limousine*

- [Online]. Available: <https://bigcars.com/blog/stretch-limousine/>. [Accessed: 19-May-2020].
- [21] Applications – Car Body – Body Structures. The Aluminium Automotive Manual.’, Eur. Alum. Assoc.2013. p.2. [Online]. Available: [moz-extension://84d63aad-415f-4278-8a1c-fd94c2c5e134/enhanced-reader.html?openApp&pdf=https%3A%2F%2Fwww.european-aluminium.eu%2Fmedia%2F1543%2F1\\_aam\\_body-structures.pdf](moz-extension://84d63aad-415f-4278-8a1c-fd94c2c5e134/enhanced-reader.html?openApp&pdf=https%3A%2F%2Fwww.european-aluminium.eu%2Fmedia%2F1543%2F1_aam_body-structures.pdf). [Accessed: 24-Aug-2021].
- [22] Venkatesh, D., and Govind, N., 2017, ‘Modelling and Structural Analysis of Automobile Lorry Chassis’, 7(7), pp. 14134–14139.
- [23] Morello L., Rossini L.R., Pia G., Tonoli A. (2011) Body Work. In: The Automotive Body vol 1. Mechanical Engineering Series. Springer, Dordrecht. [https://doi-org.proxy.lib.strath.ac.uk/10.1007/978-94-007-0513-5\\_4](https://doi-org.proxy.lib.strath.ac.uk/10.1007/978-94-007-0513-5_4).
- [24] Lesch, C., Kwiaton, N., and Klose, F. B., 2017, ‘Advanced High Strength Steels (AHSS) for Automotive Applications – Tailored Properties by Smart Microstructural Adjustments’, Steel Res. Int., 88(10).
- [25] Taub, A., Krajewski, P., Luo, A., and Owens, J., 2007, ‘The Evolution of Technology for Materials Processing over the Last 50 Years: The Automotive Example’, Jom, 59(February), pp. 58–62.
- [26] Consortium, U., ‘Advanced Vehicle Concepts ULSAB-AVC Body Structure Materials - Materials Selected for the ULSAB-AVC Body Structure - Body Structure Parts List’, Program, 6, pp. 2/3-15.
- [27] WAVCA, 2020, ‘Wheelchair Access Vehicle Convertors Association. WAVCA Members’, [Online]. Available: <https://www.wavca.co.uk/membership.html>. [Accessed: 09-May-2020].
- [28] Ltd, M. O., 2020, ‘Find a Dealer | Cars and WAVs | Motability’, Motability Oper. Ltd, Motability Scheme [Online]. Available: <https://findadealer.motability.co.uk/motability/FindDealer.aspx?t=2>. [Accessed: 05-May-2020].
- [29] Mobility, G., 2020, ‘About Us – Gowrings Mobility’, Gowrings [Online]. Available: <https://www.gowringmobility.co.uk/about-us>. [Accessed: 05-May-2020].
- [30] Scheme, M., 2017, ‘How Is a WAV Covered? - Wheelchair Accessible Vehicles.’, Motability Scheme [Online]. Available: <https://www.youtube.com/watch?v=jZrfW7SiL48>. [Accessed: 05-May-2020].
- [31] Brotherwood, 2011, ‘Brotherwood Company Profile - Brotherwood Wheelchair Accessible Vehicles- YouTube.’ [Online]. Available: [https://www.youtube.com/watch?v=1EehpLdu\\_4M](https://www.youtube.com/watch?v=1EehpLdu_4M). [Accessed: 06-May-2020].
- [32] Brotherwood, 2020, ‘Brotherwood, WAV Conversion Process’, Brotherwood [Online]. Available: <https://www.brotherwood.com/conversion-process/>. [Accessed: 06-May-2020].
- [33] Automotive, S., 2020, ‘About Us | Innovation Through The Years | Sirius Automotive’, Sirius [Online]. Available: <https://siriusautomotive.co.uk/about-us/>. [Accessed: 07-May-2020].
- [34] Automotive, S., 2020, ‘VW Caddy Van Conversions | VW Caddy Rear Seat Conversions’, Sirius [Online]. Available: <https://siriusautomotive.co.uk/vw-caddy-van-conversions-oem-seats-and-parts/>. [Accessed: 07-May-2020].
- [35] Automotive, S., 2016, ‘Sirius Automotive Ltd. Wheelchair Accessible Vehicles - YouTube’ [Online]. Available: [https://www.youtube.com/watch?v=p\\_xUGGY-ZUk&feature=youtu.be](https://www.youtube.com/watch?v=p_xUGGY-ZUk&feature=youtu.be). [Accessed: 07-May-2020].
- [36] BSV, 2016, ‘Bristol Street Versa | Wheelchair Accessible Vehicles | How They’re Made - YouTube’, Bristol Str. Versa [Online]. Available: [https://www.youtube.com/watch?time\\_continue=149&v=uFVnNFOtUIE&feature=emb\\_title](https://www.youtube.com/watch?time_continue=149&v=uFVnNFOtUIE&feature=emb_title). [Accessed: 07-May-2020].
- [37] Versa, B. S., 2020, ‘High Quality Conversions | Wheelchair Accessible Vehicles | Bristol Street Versa’, BSV Mobil. [Online]. Available: <https://www.bristolstreetversa.com/our-conversions/>. [Accessed: 07-May-2020].
- [38] Group, L. R., 2020, ‘Wheelchair Accessible Vehicles, Lewis Reed Group, Design and Development.’, Lewis Reed [Online]. Available: <https://www.lewisreedgroup.co.uk/wheelchair-accessible-vehicle-design-and-development/#1485184489721-585c37a3-fedc>. [Accessed: 08-May-2020].
- [39] Group, L. R., 2020, ‘Wheelchair Accessible Vehicles | The Lewis Reed Story’, Lewis reed [Online]. Available: <https://www.lewisreedgroup.co.uk/wheelchair-accessible-vehicle-the-lewis-reed-story/>. [Accessed: 08-May-2020].
- [40] Group, T. M. C., 2020, ‘About TBC Motability | TBC Conversions’, TBC [Online]. Available: <https://www.tbconversions.com/mobility/about-us/>. [Accessed: 08-May-2020].

- [41] Conversions, T. and B., 2017, 'TBC Conversions Northern Ireland | UK - YouTube', Donnelly Gr. NI. [Available]: [https://www.youtube.com/watch?v=F-DhopJn\\_do](https://www.youtube.com/watch?v=F-DhopJn_do). [Accessed: 08-May-2020].
- [42] Press release news, Stunkellen, S., 2019, 'We Are BraunAbility | BraunAbility Europe', Press release news [Online]. Available: <https://www.braunability.eu/en/information/news/press/2019/we-are-braunability/>. [Accessed: 10-May-2020].
- [43] BraunAbility, 2020, 'Handicap Vans, SUVs, Wheelchair Lifts | BraunAbility', BraunAbility [Online]. Available: <https://www.braunability.com/us/en/mobility-products/wheelchair-accessible-vehicles.html>. [Accessed: 10-May-2020].
- [44] Ford, 2016, 'BraunAbility MXV - a Ford Explorer Conversion - Is World's First Wheelchair-Accessible SUV | Ford Media Center', Ford Media Center, Chicago [Online]. Available: <https://media.ford.com/content/fordmedia/fna/us/en/news/2016/02/09/braunability-mxv-is-worlds-first-wheelchair-accessible-SUV.html>. [Accessed: 10-May-2020].
- [45] Braun Ability, 2015, 'Inside BraunAbility - YouTube', Wheel. Access. Veh. [Online]. Available: [https://www.youtube.com/watch?time\\_continue=47&v=OGpmSN\\_aSEA&feature=emb\\_title](https://www.youtube.com/watch?time_continue=47&v=OGpmSN_aSEA&feature=emb_title). [Accessed: 10-May-2020].
- [46] How it's made, and BraunAbility, 2017, 'How It's Made - BraunAbility Wheelchair Accessible Vehicles - YouTube' [Online]. Available: [https://www.youtube.com/watch?v=FW\\_0KmURoEA](https://www.youtube.com/watch?v=FW_0KmURoEA). [Accessed: 10-May-2020].
- [47] Study, B. C., 2019, 'Designing Freedom of Movement. Signicast. A Form Technologies Company.', Braun Abil., p. 2 [Online]. Available: [https://www.signicast.com/knowledge-center/case-studies/~media/project/signacast/Signicast\\_Braunability\\_Freedom\\_of\\_Movement.pdf](https://www.signicast.com/knowledge-center/case-studies/~media/project/signacast/Signicast_Braunability_Freedom_of_Movement.pdf). [Accessed: 15-Feb-2020].
- [48] BraunAbility, 2020, 'What Is a Conversion Van? | Handicap Van Conversion | BraunAbility', BraunAbility [Online]. Available: <https://www.braunability.com/us/en/resources/conversion-van.html>. [Accessed: 10-May-2020].
- [49] BraunAbility, 2009, 'BraunAbility - This Is Your Rampvan! Part 1 - YouTube', BraunAbility [Online]. Available: <https://www.youtube.com/watch?v=gmPLnCiMklc>. [Accessed: 10-May-2020].
- [50] VMI, 2020, 'About Vantage Mobility International (VMI)', VMI [Online]. Available: <https://www.vantagemobility.com/about-vmi/>. [Accessed: 10-May-2020].
- [51] How it's build, and Vantage Mobility International, 2012, 'How It's Built - VMI Wheelchair Van - YouTube' [Online]. Available: [https://www.youtube.com/watch?v=gRhUVi0\\_0-k](https://www.youtube.com/watch?v=gRhUVi0_0-k). [Accessed: 10-May-2020].
- [52] Kent Swart, 2009, 'Plasma Cutting and How It Works', Fabr. [Online]. Available: <https://www.thefabricator.com/thefabricator/article/shopmanagement/plasma-cutting-and-how-it-works>. [Accessed: 18-Jun-2020].
- [53] VMI, 2020, 'How It's Built: Handicap Van Conversions | Wheelchair Van Conversions', VMI [Online]. Available: <https://www.vantagemobility.com/how-a-van-is-built/>. [Accessed: 10-May-2020].
- [54] Rollx Vans, 2020, 'Wheelchair Van Conversion Manufacturer | The Rollx Vans Story', Roll. vans [Online]. Available: <https://www.rollxvans.com/about-us/our-story-2/>. [Accessed: 11-May-2020].
- [55] Rollx Vans, 2012, 'Rollx Vans Intro -Wheelchair Accessible Vehicles. YouTube.', Roll. Vans [Online]. Available: <https://www.youtube.com/watch?v=l6RQiGQuM6M>. [Accessed: 11-May-2020].
- [56] Rollx Vans, 2014, 'The Rollx Vans Wheelchair Accessible Van Production Process - YouTube' [Online]. Available: <https://www.youtube.com/watch?v=Fpoz5ijhia8>. [Accessed: 11-May-2020].
- [57] Rollx Vans, 2020, 'Conversion Process | Handicap + Wheelchair Van Sales | Rollx Vans', Roll. Vans [Online]. Available: <https://www.rollxvans.com/convert-your-vehicle/the-process/>. [Accessed: 11-May-2020].
- [58] Ben Coxworth, 2011, 'MV-1 van Is Designed Specifically for Wheelchair Users', New Atlas [Online]. Available: <https://newatlas.com/mv1-van-for-wheelchair-users/19921/>. [Accessed: 13-May-2020].
- [59] MV-1, 2014, 'MV-1 The Only Purpose-Built American Made Mobility Vehicle - YouTube'.
- [60] RUSTY BLACKWELL, 2016, 'Mobility Ventures MV-1 ', Car Driv. [Online]. Available: <https://www.caranddriver.com/reviews/a15098391/2016-mobility-ventures-mv-1-first-drive-review/>. [Accessed: 13-May-2020].
- [61] Savaria, 2015, 'About Savaria Corporation - Wheelchair Accessible Vehicles- YouTube.' [Online]. Available: <https://www.youtube.com/watch?v=BDr6xn1GFv8>. [Accessed: 13-May-2020].

- [62] Savaria, 2020, 'How to Choose the Right Vehicle for van Conversion | Savaria', Savaria [Online]. Available: <https://www.wheelchairvans.ca/van-conversion/>. [Accessed: 13-May-2020].
- [63] Savaria, 2014, 'How Wheelchair Vans Are Made - YouTube' [Online]. Available: <https://www.youtube.com/watch?v=D8Od9mne6Gw>. [Accessed: 13-May-2020].
- [64] BrandL Mobility Finance, 2020, 'ATC Wheelchair Accessible Trucks | Brandl Mobility Finance', Brand. Mobil. Financ. [Online]. Available: <https://www.brandlmobility.com/all-terrain-conversions>. [Accessed: 14-May-2020].
- [65] All-Terrain Conversions, 2020, 'ATC | Wheelchair Accessible Trucks & SUVs', ATC [Online]. Available: <https://www.atconversions.com/>. [Accessed: 14-May-2020].
- [66] ATC, 2020, 'ATC Inventory', ATC [Online]. Available: <https://www.atconversions.com/listings/?location=atc>. [Accessed: 14-May-2020].
- [67] ATC, 2019, 'How One Company Makes Accessible Vehicles For People Who Use Wheelchairs - YouTube' [Online]. Available: [https://www.youtube.com/watch?time\\_continue=124&v=f2cx83xL3QU&feature=emb\\_title](https://www.youtube.com/watch?time_continue=124&v=f2cx83xL3QU&feature=emb_title). [Accessed: 14-May-2020].
- [68] Limousine, 2018, 'How Limos Are Made - YouTube' [Online]. Available: [https://www.youtube.com/watch?v=\\_IokLRog3kk](https://www.youtube.com/watch?v=_IokLRog3kk). [Accessed: 19-May-2020].
- [69] Limousines, W., and Vehicles, S., 2013, 'A Stretch in Time Pt2', JAGUAR Enthus., pp. 20–26. Northhaption. UK.
- [70] James E. Daffy, and Robert Scharff, 2003, Auto Body Repair Technology - James E. Duffy, Robert Scharff - Google Books, Ringgold Inc, Portland, USA.
- [71] Andrew Livesey, A. R., 2019, The Repair of Vehicle Bodies, Routledge, Taylor and Francis Group, Abingdon, Oxon.
- [72] Eastwood, 2020, 'Why Eastwood', Eastwood [Online]. Available: <https://www.eastwood.com/about-us>. [Accessed: 18-May-2020].
- [73] Kevin Tetz, 2014, 'Removing Rusty Floor Pans (Hands On Cars E.03) | Eastwood Blog', Eastwood [Online]. Available: <https://garage.eastwood.com/tech-articles/how-to-remove-replace-floor-pans/>. [Accessed: 18-May-2020].
- [74] I-CAR, 2020, 'I-CAR - About Us', I-CAR [Online]. Available: <https://info.i-car.com/about-us>. [Accessed: 19-May-2020].
- [75] I-CAR, 2017, 'Structural Sectioning Procedures: General Motors', I-CAR Repairability Tech. Support [Online]. Available: <https://rts.i-car.com/collision-repair-news/structural-sectioning-procedures-general-motors.html>. [Accessed: 19-May-2020].
- [76] John Huetter, 2017, 'I-CAR: Follow OEM on Sectioning or Don't Do It - and Don't Ever Clip - Repairer Driven News', RDN Repair. Driven News [Online]. Available: <https://www.repairerdrivennews.com/2017/08/16/i-car-follow-oem-on-sectioning-or-dont-do-it-and-dont-ever-clip/>. [Accessed: 19-May-2020].
- [77] I-CAR, 2013, 'I-CAR Replacement (SPS10) and Sectioning (SPS11) of Steel Unitized Structures - YouTube' [Online]. Available: <https://www.youtube.com/watch?v=2XA82Ij5bLk>. [Accessed: 19-May-2020].
- [78] Szataniak, P., Novy, F., and Ulewicz, R., 2014, 'HSLA Steels - Comparison of Cutting Techniques', Metal 2014 - 23rd International Conference on Metallurgy and Materials, Conference Proceedings, W. S.A., ed., MeTal, Brno, Czech Republic, pp. 778–783.
- [79] Mert, T., 2012, 'Water jet cutting technology and its comparison with other cutting methods in some aspects', Acad. J. Sci., 1(3), p. 275.
- [80] Andrés, D., García, T., Cicero, S., Lacalle, R., Álvarez, J. A., Martín-Meizoso, A., Aldazabal, J., Bannister, A., and Klimpel, A., 2016, 'Characterization of Heat Affected Zones Produced by Thermal Cutting Processes by Means of Small Punch Tests', Mater. Charact., 119, p. 55.
- [81] Nemchinsky V. (2017) Heat Transfer in Plasma Arc Cutting. In: Kulacki F. (eds) Handbook of Thermal Science and Engineering. Springer, Cham. [https://doi.org/10.1007/978-3-319-32003-8\\_28-1](https://doi.org/10.1007/978-3-319-32003-8_28-1).
- [82] Romina Ronquillo, 2019, 'Understanding Plasma Arc Cutting', Thomas, Thomas Ind. Updat. [Online]. Available: <https://www.thomasnet.com/articles/custom-manufacturing-fabricating/understanding-plasma-arc-cutting/>. [Accessed: 11-Nov-2019].
- [83] Kechagias, J., Petousis, M., Vidakis, N., and Mastorakis, N., 2017, 'Plasma Arc Cutting Dimensional Accuracy Optimization Employing the Parameter Design Approach', ITM Web Conf., 9(03004), p. 1.

- [84] Krajcarz, D., 2014, 'Comparison Metal Water Jet Cutting with Laser and Plasma Cutting', *Procedia Engineering*, 24th DAAAM International Symposium on Intelligent Manufacturing and Automation, Elsevier, Science Direct, Kielce, Poland, p. 840.
- [85] ESAB, 'The Basics of Plasma Cutting', ESAB Knowl. Cent. [Online]. Available: <https://www.esabna.com/us/en/education/blog/the-basics-of-plasma-cutting.cfm>. [Accessed: 03-Sep-2019].
- [86] S R Rajpurohit, P. . D. M. P., 2012, 'Striation Mechanism in Laser Cutting – the Review ', *Int. J. Eng. Res. Appl.*, 2(2), pp. 457–461.
- [87] Grepl, M., Pagáč, M., and Petru, J., 2012, 'Laser Cutting of Materials of Various Thicknesses', *Acta Polytech.*, 52(4), p. 62.
- [88] The welding Institute, 2020, 'Laser Cutting - Cutting Processes - TWI', *Weld. Inst.* [Online]. Available: <https://www.twi-global.com/technical-knowledge/job-knowledge/cutting-processes-laser-cutting-052>. [Accessed: 28-Oct-2020].
- [89] ESAB, 'How Does Laser Cutting Work?', ESAB Knowl. Cent. [Online]. Available: <https://www.esabna.com/us/en/education/blog/how-does-laser-cutting-work.cfm>. [Accessed: 12-Aug-2021].
- [90] Brožek, M., 2017, 'Steel Cutting Using Abrasive Water Jet', 16th International Scientific Conference Engineering for Rural Development, Engineering for Rural Development, Prague, p. 1.
- [91] Abrasive, I., 2018, 'Abrasive water-jet cutting', *IDC Technol.*, pp. 15–17.
- [92] ESAB, 'How Does Waterjet Cutting Work?', ESAB Knowl. Cent. [Online]. Available: <https://www.esabna.com/us/en/education/blog/how-does-waterjet-cutting-work.cfm>. [Accessed: 12-Aug-2021].
- [93] Andreas W. Momber and R. Kovacevic. 1998. *Water Jet Cutting ' Principles of Abrasive Water Jet Machining' 1<sup>st</sup> Edition*. Springer-Verlag London. p 5-18, DOI: 10.1007/978-1-4471-1572-4.
- [94] James Harris, and Milan Brandt, 2004, 'Cutting Thick Steel Plate - Industrial Laser Solutions', *Ind. Laser Solut. Manuf.* [Available]: <https://www.industrial-lasers.com/cutting/article/16490449/cutting-thick-steel-plate>. [Accessed: 2021-03-10].
- [95] Jim Colt, H. I., 2014, 'Determining the Best Process for Metal Cutting: Plasma, Oxy-Fuel, Laser or Abrasive Waterjet?', *Millenn. Steel India*, pp. 135–139. [Available]: [http://millennium-steel.com/wp-content/uploads/2014/11/pp135-139\\_msi14.pdf](http://millennium-steel.com/wp-content/uploads/2014/11/pp135-139_msi14.pdf). [Accessed: 2021-03-10]
- [96] Steffen Donath, 2019, 'Water Jet Cutting - Function, Methods and Application Examples', *ETMM* [Online]. Available: <https://www.etmm-online.com/water-jet-cutting--function-methods-and-application-examples-a-834966/>. [Accessed: 10-Mar-2021].
- [97] ESAB, 'ESAB Knowledge Centre, What Is the Best Value – Plasma, Laser, or Waterjet?', ESAB [Online]. Available: <https://www.esab.co.uk/gb/en/education/blog/what-is-the-best-value-plasma-laser-or-waterjet.cfm>. [Accessed: 10-Mar-2021].
- [98] ESAB welding and cutting products, 'Knowledge Center, What Is Cutting Kerf?', ESAB [Online]. Available: <https://www.esabna.com/us/en/education/blog/what-is-cutting-kerf.cfm>. [Accessed: 10-Mar-2021].
- [99] Health and Safety Executive HSE, 1997, 'Plasma Cutting: Control of Fume, Gases and Noise', HSE [Online]. Available: [https://www.hse.gov.uk/foi/internalops/ocs/600-699/oc668\\_22.htm](https://www.hse.gov.uk/foi/internalops/ocs/600-699/oc668_22.htm). [Accessed: 10-Mar-2021].
- [100] Rich Greene, 2008, 'Laser Safety in the Industrial Workplace', *Fabr.* [Online]. Available: <https://www.thefabricator.com/thefabricator/article/lasercutting/laser-safety-in-the-industrial-workplace>. [Accessed: 10-Mar-2021].
- [101] Kmec, J., 2013, 'safe working conditions for the water jet', *acta tech. corviniensis –Bulletin Eng.* Vol 6. Issue 2. pp. 113–116. Hunedoara, Romania.
- [102] Peržel, V., Hloch, S., Tozan, H., Yagimli, M., and Hreha, P., 2011, 'Comparative Analysis of Abrasive Waterjet (AWJ) Technology with Selected Unconventional Manufacturing Processes', *Int. J. Phys. Sci.*, 6(24), pp. 5587–5593.
- [103] Radu, C., Herghelegiu, E., and Schnakovszky, C., 2015, 'Comparative Study on the Effects of Three Unconventional Cutting Technologies on Cut Surface Quality', *Indian J. Eng. Mater. Sci.*, 22(2), pp. 127–132.
- [104] Sobih, M., Crouse, P. L., and Li, L., 'Laser Cutting of Variable Thickness Materials – Understanding the Problem-Paper 408', 25 Th International Congress on Applications of Lasers and Electro-Optics ICALEO06, *Journal of Laser Applications*, Scottsdale, AZ, USA, pp. 1–7.
- [105] Jim Colt, 2011, 'National Robotic Arc Welding Conference and Exhibition', *Robotic Applications*,

Recent Technology Enhancements That Allow for Easier Robotic Integration, AWS, FMA., Hypertherm, Muskego, USA, p. 17.

- [106] Kirkpatrick, I. (1999), "Profile cutting options", *Aircraft Engineering and Aerospace Technology*, Vol. 71 No. 5. <https://doi.org/10.1108/aeat.1999.1277leaf.002>. pp. 55–63.
- [107] Iosub, A., Nagit, G., and Negoescu, F., 2008, 'Plasma Cutting of Composite Materials', *Int. J. Mater. Form.*, pp. 1347–1350 DOI: 10.1007/s12289-008-0113-1.
- [108] Lazarevic, D. A., 2014, 'Experimental Research of the Plasma Arc Cutting Process', *Orig. Sci. Pap. iipp*, 124(304), p. 291.
- [109] Çelik, Y. H., 2013, 'Investigating the Effects of Cutting Parameters on Materials Cut in CNC Plasma', *Mater. Manuf. Process.*, 28(10), p. 1055.
- [110] Aldazabal, J., Martín-Meizoso, A., Klimpel, A., Bannister, A., and Cicero, S., 2018, 'Mechanical and Microstructural Features of Plasma Cut Edges in a 15 Mm Thick S460M Steel Plate', *Met. MDPI*, 8(6), p. 447.
- [111] Rana, K., Kaushik, P., and Chaudhary, S., 2013, 'Optimization of Plasma Arc Cutting by Applying Taguchi Method', *Int. J. Enhanc. Res. Sci. Technol. Eng.*, 2(7), pp. 106–110.
- [112] Ilii, S. M., and Coteață, M., 2009, 'Plasma Arc Cutting Cost', *Int. J. Mater. Form.*, 2(SUPPL. 1), pp. 689–692.
- [113] Pawar, S. S., and Inamdar, K. H., 2017, 'Analysis of Heat Affected Zone in Plasma Arc Cutting of SS 316l Plates', *ijirset*, 6(5), p. 8165.
- [114] Rakhimyanov, K., Rakhimyanov, A., and Heifetz, M., 2015, 'High-Precision Plasma Cutting of the Steel - Aluminum "Bimetallic Composition"', *Appl. Mech. Mater.*, 788, p. 41.
- [115] Wang, J., Hoang, T., Floyd, E. L., and Regens, J. L., 2017, 'Characterization of Particulate Fume and Oxides Emission from Stainless Steel Plasma Cutting', *Ann. Work Expo. Heal.*, 61(3), pp. 311–320.
- [116] P Mariya Felix, K. R. and S. R., 2017, 'An Investigation and Prediction of Flatness and Surface Roughness during Plasma Cutting Operation on SS410 Material', *Int. J. Emerg. Technol. Eng. Res.*, 5(6), p. 160.
- [117] Dattu, B. G., Abhang, L. B., Makasare, P. A., & Kharad, B. N. (2019). Optimization on operating parameters of CNC plasma machine by experimentation. *I-Manager's Journal on Instrumentation & Control Engineering*, 7(1), 26-32. doi:<http://dx.doi.org/10.26634/jic.7.1.15952>.
- [118] Kavka, T., Tossen, S., Maslani, A., Konrad, M., Pauser, H., and Stehrer, T., 2014, 'Experimental Investigation of Energy Balance in Plasma Arc Cutting Process', *J. Phys. Conf. Ser.*, 511(1), p. 6.
- [119] Kavka, T., Mašláni, A., Hrabovský, M., Křenek, P., Stehrer, T., and Pauser, H., 2013, 'Experimental Study of the Effect of Gas Nature on Plasma Arc Cutting of Mild Steel', *J. Phys. D. Appl. Phys.*, 46(22), pp. 1–13.
- [120] Kechagias, J., Stavropoulos, P., Maropoulos, S., Salonitis, K., Air, H., Academy, F., Base, D. A., and Design, I., 2014, 'On the Multi – Parameter Optimization of CNC Plasma-Arc Cutting Process Quality Indicators Using Taguchi Design of Experiments', *Recent Adv. Electr. Eng.*, 2(December), pp. 128–133.
- [121] Abdunnasser, B., and Bhuvanesh, R., 2016, 'Plasma Arc Cutting Optimization Parameters for Aluminum Alloy with Two Thickness by Using Taguchi Method', *The 2nd International Conference on Functional Materials and Metallurgy (ICoFM 2016)*, AIP Conference Proceedings, Perlis, Malaysia, pp. 1–6.
- [122] Bhuvanesh, R., Norizaman, M. H., and Manan, M. S. A., 2012, 'Surface Roughness and MRR Effect on Manual Plasma Arc Cutting Machining', *Int. J. Ind. Manuf. Eng.*, 6, pp. 503–506.
- [123] Rana, K., Kaushik, P., and Chaudhary, S., 2013, 'Optimization of Plasma Arc Cutting by Applying Taguchi Method', *Int. J. Enhanc. Res. Sci. Technol. Eng.*, 2(7).
- [124] Chen, J. C., Li, Y., and Cox, R. A., 2009, 'Taguchi-Based Six Sigma Approach to Optimize Plasma Cutting Process : An Industrial Case Study', *Int. J. Adv. Manuf. Technol.* Springer, p. 763.
- [125] Salonitis, K., and Vatousianos, S., 2012, 'Experimental Investigation of the Plasma Arc Cutting Process', *Procedia CIRP*.
- [126] Freton, P., Gonzalez, J. J., Gleizes, A., Peyret, F. C., Caillibotte, G., and Delzenne, M., 2002, 'Numerical and Experimental Study of a Plasma Cutting Torch', *J. Phys. D. Appl. Phys.*, 35, p. 115.

- [127] Çelik, Y. H., 2013, 'Investigating the Effects of Cutting Parameters on Materials Cut in CNC Plasma', *Mater. Manuf. Process.*, 28(10), pp. 1053–1060.
- [128] Chamarthi, S., Reddy, N. S., Elipey, M. K., and Reddy, D. V. R., 2013, 'Investigation Analysis of Plasma Arc Cutting Parameters on the Unevenness Surface of Hardox-400 Material', *Procedia Eng.*, 64, p. 855.
- [129] Gariboldi, E., and Previtali, B., 2005, 'High Tolerance Plasma Arc Cutting of Commercially Pure Titanium', *J. Mater. Process. Technol.*, 160(1), pp. 77–89.
- [130] Nedic, B., and Lakic, G. G., 2013, 'Quality of Plasma Cutting', 13th International Conference on Tribology, Serbian Tribology Society., Serbiatrib'13, Kragujevac, Serbia., p. 315.
- [131] Deb, D., Dey, R., and Balas, V., 2019, *Engineering Research Methodology. A Practical Insight for Researchers*, Springer, Gateway East, Singapore.
- [132] Che, M., Marcu, M. V., and Iordache, E., 2020, 'Testing the Capability of Low-Cost Tools and Artificial Intelligence Techniques to Automatically Detect Operations Done by a Small-Sized Manually Driven Bandsaw', *For. MDPI*, 11(7), p. 10.
- [133] Jiao, Y., Pei, Z. J., Lei, S., and Lee, E. S., 2003, 'Fuzzy Adaptive Networks in the Modeling and Forecasting of Manufacturing Processes', *Inst. Ind. Syst. Eng. (IISE), IIE Annu. Conf. Proceedings; Norcross*.
- [134] Bowden, G. D., Pichler, B. J., and Maurer, A., 2019, 'A Design of Experiments ( DoE ) Approach Accelerates the Optimization of Copper-Mediated F-Fluorination Reactions of Arylstannanes', *Sci. Reports, Nat. Res.*, (May), pp. 1–10.
- [135] Ujah, C. O., Popoola, A. P. I., Popoola, O. M., and Aigbodion, V. S., 2019, 'Optimisation of Spark Plasma Sintering Parameters of Al-CNTs-Nb Nano-Composite Using Taguchi Design of Experiment', *Int. J. Adv. Manuf. Technol.*, p. 1569.
- [136] Jiju Antony, 2003, *Design of Experiments for Engineers and Scientists*, Butterworth-Heinemann Elsevier, Oxford.
- [137] Mishra, A., and Gangele, A., 2012, 'Application of Taguchi Method in Optimization of Tool Flank Wear Width in Turning Operation of AISI 1045 Steel', *Ind. Eng. Lett.*, 2(8), p. 11.
- [138] John, R. D. and P., 2018, 'Application of Taguchi-Based Design of Experiments for Industrial Chemical Processes', *Statistical Approaches With Emphasis on Design of Experiments Applied to Chemical Processes*, V. Silva, ed., Intech Open Science, London, pp. 138–150.
- [139] Astakhov, V. P., 2012, *Statistical and Computational Techniques in Manufacturing, Design of Experiment Methods in Manufacturing: Basics and Practical Applications.*, Springer, Aveiro, Portugal.
- [140] Astakhov, V. P., 2016, *Design of Experiments in Production Engineering, Management and Industrial Engineering*, Springer International, Aveiro, Portugal.
- [141] Mohd Sazali Md Said, Jaharah A. Ghani, Mohd Shahir Kassim, Siti Haryani Tomadi, C. H., 2013, 'Comparison between Taguchi Method and Response Surface Methodology (RSM) In Optimizing Machining Condition', 1st International Conference on Robust Quality Engineering (ICRQE 2013), P.D.Z.M. Prof. Dr. Bo Bergman, Prof. Dr. Masayoshi Koike, ed., International Conference on Robust Quality Engineering Editorial, Kuala Lumpur, Malaysia, pp. 60–64.
- [142] Sylajakumari, P. A., and Ramakrishnasamy, R., 2018, 'Taguchi Grey Relational Analysis for Multi-Response', *Materials (Basel)*, 1743(11), p. 4 of 17.
- [143] Muhamedagic, K., Begic-Hajdarevic, D., Ahmet, C., and Mehmedovic, M., 2017, 'Multi-Response Optimization of Plasma Cutting Parameters Using Grey Relational Analysis', 28th daaam international symposium on intelligent manufacturing and automation. *annals of daaam and proceedings.*, DAAAM International, Vienna, Austria, p. 1079.
- [144] Chiang, Y., and Hsieh, H., 2009, 'Applying Grey Relational Analysis and Fuzzy Neural Network to Improve The Yield of Thin-Film Sputtering Process in Color Filter Manufacturing', *Proceedings of the 13th IFAC Symposium on Information Control Problems in Manufacturing*, IFAC, Moscow Russia, p. 408.
- [145] Venkatesan, S., Mohan, P., Ranjith Kumar, T., and Artralarasan, E., 2019, 'Experimental Investigation and Optimisation of Treatment Parameters in Plasma Arc Cutting of D3 Tool Steel by Response Surface Modification', *ICRTCCNT, International Conference on Recent Trends in Computing, Communication and Networking Technologies*, TamilNadu, India., p. 3.
- [146] Smith, R. E., 2010, *Prefab Architecture: A Guide to Modular Design and Construction.*, John Wiley & Sons Inc, Hoboken, N.J. USA.
- [147] Durakovic, B., 2018, 'Design of Experiments Application , Concepts , Examples : State of the Art',

- Period. Eng. Nat. Sci., 5(3), pp. 424–425.
- [148] Ali, Z., and Bhaskar, S. B., 2016, 'Basic Statistical Tools in Research and Data Analysis', *Indian J. Anaesth.*, 60(9), pp. 662–669 [Online]. Available: <https://www.ncbi.nlm.nih.gov/pmc/articles/PMC5037948/>. [Accessed: 01-Jun-2020].
- [149] Paul Boughton, and Michelle Paret, 2014, 'The Analysis of Data, Minitab | Engineer Live', *Eng. Live* [Online]. Available: <https://www.engineerlive.com/content/analysis-data>. [Accessed: 01-Jun-2020].
- [150] Sinharay, S., 2010, 'An Overview of Statistics in Education', *International Encyclopedia of Education*, Elsevier, New Jerzy USA, p. 6.
- [151] Abe, J. O., Popoola, O. M., Popoola, A. P. I., Ajenifuja, E., and Adebisi, D. I., 2019, 'Application of Taguchi Design Method for Optimization of Spark Plasma Sintering Process Parameters for Ti-6Al-4V/ h -BN Binary Composite', *Eng. Res. Express*, 1(2), p. 12.
- [152] jim frost, 'Understand Precision in Predictive Analytics to Avoid Costly Mistakes - Statistics By Jim', *Stat. By Jim Mak. Stat. intuitive* [Online]. Available: <https://statisticsbyjim.com/regression/prediction-precision-applied-regression/>. [Accessed: 02-Sep-2019].
- [153] Phulli, R., Arora, P., and Neema, P. K., 2019, 'Application of Student's t-Test, Analysis of Variance, and Covariance', *Ann. Card. Anaesthesia. Wolters Kluwer - Medknow.*, 22(4), pp. 378–380.
- [154] Leica Microsystems, 2011, *Leica DM8000 M & DM12000 M*, Wetzlar Germany.
- [155] Claudia Angelini, 2019, 'Regression Analysis - an Overview | ScienceDirect Topics', *Encycl. Bioinforma. Comput. Biol. Sci. Direct*, 1, pp. 722--730.
- [156] D.J. Bartholomew, 2010, 'Regression Analysis - Analysis and Interpretation of Multivariate Data', *Int. Encycl. Educ.*, 3.
- [157] Tsiolikas, A., Kechagias, J., Salonitis, K., and Mastorakis, N., 2016, 'Optimization of Cut Surface Quality during CNC Plasma Arc Cutting Process', *Int. J. Syst. Appl. Eng. Dev.*, 10, p. 305.
- [158] Hypertherm, 2013, *Hypertherm, Powermax 1250, Plasma Arc Cutting System, Operator Manual*.
- [159] Max, H., Jared, R., Don, A., and Kathleen, L., 2001, 'Negotiation Reproduced with Permission of the Copyright Owner . Further Reproduction Prohibited without Permission .', *Weld. Des. Fabr. Incl. Weld. Eng.*, 74(2), p. 3.
- [160] Hypertherm, 2004, 'Hypertherm, Powermax1250 G3 SERIES, The Performance Standard for Air Plasma Cutting Technology', *Hypertherm*, pp. 2–3.
- [162] ESAB, 2019, 'Plasma Cutting - Recommended Gases', *ESAB Knowl. center-education* [Online]. Available: <https://www.esab.ca/ca/en/education/blog/plasma-cutting-recommended-gases.cfm>. [Accessed: 26-Nov-2019].
- [163] Hypertherm, 2015, 'Gas Selection Guide for Plasma Cutting Aluminum, Stainless Steel, Mild Steel', *Tips Tech. Guid. to plasma gas Sel.* [Online]. Available: <https://www.hypertherm.com/learn/articles/guide-to-plasma-gas-selection/>. [Accessed: 26-Nov-2019].
- [164] Thyssenkrupp, 2018, *Deep-Drawing Steels DD, DC Und DX: Product Information*.
- [165] Strathclyde University, *Advanced Forming Rsearch Centre, Equipment Directory, Brochure 2016*. [Online]. Available: [https://www.strath.ac.uk/media/1newwebsite/centres/advancedformingresearchcentre/AFRC\\_equipment\\_brochure.pdf](https://www.strath.ac.uk/media/1newwebsite/centres/advancedformingresearchcentre/AFRC_equipment_brochure.pdf). [Accessed: 05-Jun-2020].
- [166] GOM., 2018, 'Atos 3D Scanner, Capture 3D, Gom.', *GOM* [Online]. Available: <https://www.capture3d.com/3d-metrology-solutions/3d-scanners/atos-compact-scan>. [Accessed: 23-Aug-2019].
- [167] Capture 3D, 2020, 'GOM ATOS Triple Scan | Capture 3D', *Gom* [Online]. Available: <https://www.capture3d.com/3d-metrology-solutions/3d-scanners/atos-triple-scan>. [Accessed: 04-Jun-2020].
- [168] Kim, C., Lee, T. I., Kim, M. S., and Kim, T. S., 2015, 'Warpage Analysis of Electroplated Cu Films on Fiber-Reinforced Polymer Packaging Substrates', *Polymers (Basel).*, 7(6), p. 989.
- [169] 2014, 'The Metallurgy and Weldability of a Carbon Steel'.
- [170] moodlemech, learn easy, 2014, 'Properties and Grain Structure', *BBC 1973 Eng. Cr. Stud.*
- [171] The Welding Institute, 'Austenite Martensite Bainite Pearlite and Ferrite Structures - TWI', *twi* [Online]. Available: <https://www.twi-global.com/technical-knowledge/faqs/faq-what-are-the-microstructural-constituents-austenite-martensite-bainite-pearlite-and-ferrite>. [Accessed: 25-Aug-2019].
- [172] Sloderbach, Z., and Pajak, J., 2015, 'Determination of Ranges of Components of Heat Affected Zone

- Including Changes of Structure', *Arch. Metall. Mater.*, 60(4), p. 2608.
- [173] The Welding Institute, 'What Is the Heat Affected Zone (HAZ)? - TWI', TWI [Online]. Available: <https://www.twi-global.com/technical-knowledge/faqs/what-is-the-heat-affected-zone>. [Accessed: 23-Aug-2019].
- [174] Struers, Ensuring Certainty, DuraScan G5 Manual 11.2016A / 62140122 Printed in Denmark 2017, Automatic Micro/Macro hardness tester, DuraScan 50/70/80 G5. Page 5. [Online]. Available: <https://sem-technologies.com/wp-content/uploads/2017/04/DuraScan-G5.pdf>. [Accessed: 05-Jun-2020].
- [175] Stephanie Glen, 2016, 'Measurement Error (Observational Error)', *Stat. Elem. Stat. rest us* [Online]. Available: <https://www.statisticshowto.com/measurement-error/>. [Accessed: 19-Aug-2021].
- [176] ArcelorMittal, 2018, 'Extract from the Automotive Product Catalogue - High Formability Steels for Drawing Drawing Steels - Application', *Automot. Worldw.*, p. 105.
- [177] Vasile, R., Racz, S. G., and Bologa, O., 2017, 'Experimental and Numerical Investigations of the Steel Sheets Formability with Hydroforming', *MATEC Web Conf.*, 94, p. 2.
- [178] HUAFEI, 2020, 'Analysis Of Cutting Effect And Processing Size Error Of CNC Cutting Machine "Cnc Plasma Cutter Guide"', HUAFEI [Online]. Available: <https://thebestcnc.com/analysis-of-cutting-effect-and-processing-size-error-of-cnc-cutting-machine/>. [Accessed: 20-Aug-2021].
- [179] V.N. Gaitonde, S.R. Karnik, J. P. D., 2015, 'Multiple Performance Optimization in Drilling Using Taguchi Method with Utility and Modified Utility Concepts', *Sci. Direct, Mater. Form. Mach.*, p. 104.
- [180] Kumar Das, M., Kumar, K., Kr Barman, T., and Sahoo, P., 2014, 'Optimization of Process Parameters in Plasma Arc Cutting of EN 31 Steel Based on MRR and Multiple Roughness Characteristics Using Grey Relational Analysis', *Procedia Mater. Sci.*, 5, p. 1556.
- [181] Adam Hayes, 2019, 'R-Squared Definition', Investopedia [Online]. Available: <https://www.investopedia.com/terms/r/r-squared.asp>. [Accessed: 02-Dec-2019].
- [182] Christensen, R., 2017, 'Comment on "The Target Parameter of Adjusted R-Squared in Fixed-Design Experiments" by Bar-Gera (2017)', *Am. Stat.*, 71(4), pp. 373–375.
- [183] Dhanalakshmi, S., and Rameshbabu, T., 2020, 'Multi-Aspects Optimization of Process Parameters in CNC Turning of Lm 25 Alloy Using the Taguchi-Grey Approach', *Metals (Basel)*, 10(4), p. 11.
- [184] Jim Frost, 'Check Your Residual Plots to Ensure Trustworthy Regression Results! - Statistics By Jim', *Stat. By Jim Mak. Stat. intuitive* [Online]. Available: <https://statisticsbyjim.com/regression/check-residual-plots-regression-analysis/>. [Accessed: 02-Sep-2019].
- [185] Allen, M. P., 1997, 'The Problem of Multicollinearity', *Understanding Regression Analysis*, Springer, Boston USA, pp. 176–180.
- [186] Minitab blog editor, 2013, 'Regression Analysis: How Do I Interpret R-Squared and Assess the Goodness-of-Fit?', Minitab blog [Online]. Available: <https://blog.minitab.com/blog/adventures-in-statistics-2/regression-analysis-how-do-i-interpret-r-squared-and-assess-the-goodness-of-fit>. [Accessed: 31-Aug-2019].
- [187] Bremer, M., 2012, 'Multiple Linear Regression', *mezeylab, lab members, Math 261 A*, (1), p. 18,21,22,23 [Online]. Available: [http://mezeylab.cb.bscb.cornell.edu/labmembers/documents/supplement 5 - multiple regression.pdf](http://mezeylab.cb.bscb.cornell.edu/labmembers/documents/supplement%205%20-%20multiple%20regression.pdf).
- [188] Molugaram, K., and Rao, G. S., 2017, 'Correlation and Regression', *Statistical Techniques for Transportation Engineering*, Chapter 6. Elsevier, Butterworth-Heinemann. p. 323. <https://doi.org/10.1016/B978-0-12-811555-8.00006-4>.
- [189] Kubovský, I., Krišťák, L., Suja, J., Gajtanska, M., Igaz, R., Ružiak, I., and Réh, R., 2020, 'Optimization of Parameters for the Cutting of Wood-Based Materials by a Co2 Laser', *Appl. Sci.*, 10(22), pp. 6–16.
- [190] Williams, M. N., Alberto, C., and Grajales, G., 2013, 'Practical Assessment, Research, and Evaluation Article 11. Assumptions of Multiple Regression: Correcting Two Misconceptions', *Sch. Work. Umass Educ.*, 18(1), p. 8.
- [191] Marco Peixeiro, 2018, 'Linear Regression — Understanding the Theory - Towards Data Science', *M, Mediu. Data Sci.* [Online]. Available: <https://towardsdatascience.com/linear-regression-understanding-the-theory-7e53ac2831b5>. [Accessed: 11-Dec-2019].
- [192] Molugaram, K., Rao, G. S., Molugaram, K., and Rao, G. S., 2017, 'Curve Fitting', *Stat. Tech. Transp. Eng.*, p. 282.
- [193] Marco Peixeiro, 2017, 'Linear Regression — Understanding the Theory', *Stat. Tech. Transp. Eng.*, p.

- 281 [Online]. Available: <https://linkinghub.elsevier.com/retrieve/pii/B9780128115558000052>. [Accessed: 11-Dec-2019].
- [194] Hội Đình, 2018, '2 Multireg - Econometrics - English as a Germanic Language - StuDocu- Lecture 2- Regression Analysis', Univ. Antwerpen, p. 1 [Online]. Available: <https://www.studocu.com/en/document/universiteit-antwerpen/english-as-a-germanic-language/lecture-notes/2-multireg-econometrics/1676368/view>. [Accessed: 15-Dec-2019].
- [195] Keller, F., 2010, 'Computational Foundations of Cognitive Science - Lecture 1: Algebraic Properties of Matrices; Transpose; Inner and Outer Product', Sch. Informatics Univ. Edinburgh, pp. 1–21 [Online]. Available: [http://www.inf.ed.ac.uk/teaching/courses/cfcs1/lectures/cfcs\\_110.pdf](http://www.inf.ed.ac.uk/teaching/courses/cfcs1/lectures/cfcs_110.pdf).
- [196] Education, T., 1392, 'MATH 304 Linear Algebra Lecture 6: Transpose of a Matrix. Determinants.', Math TAMU Educ., p. 3 [Online]. Available: <https://www.math.tamu.edu/~yvorobet/MATH304-2010A/Lect1-06web.pdf>.
- [197] Beck, N., 2001, 'OLS in Matrix Form', Lect. Notes, 1(2), p. 2. Staford. UK. [available]: [https://web.stanford.edu/~mrosenfe/soc\\_meth\\_proj3/matrix\\_OLS\\_NYU\\_notes.pdf](https://web.stanford.edu/~mrosenfe/soc_meth_proj3/matrix_OLS_NYU_notes.pdf). [Accessed: 07-05-2019].
- [198] Petersen, K. B., and Version:, M. S. P., 2012, 'The Matrix Cookbook', Mathematics, University of Waterloo, Waterloo Canada, p. 6 and 10.
- [199] Cottrell, A., 2019, 'Regression Basics in Matrix Terms', Economics, 215(2), pp. 1–3. [Available]: <https://users.wfu.edu/~cottrell/ecn215/ols.pdf>. [Accessed: 07-05-2019].
- [200] Barnes, R. J., 2006, 'Matrix Differential', Springs J., p. 9. Minnesota, USA. [Available]: <https://atmos.washington.edu/~dennis/MatrixCalculus.pdf>.
- [201] Pearson education ltd, 2000, 'The Inverse of a Matrix', Pearson Educ. math center, Eng. maths, first aid kit, p. 5.5.1 [Online]. Available: [http://www.mathcentre.ac.uk/resources/Engineering maths first aid kit/latexsource and diagrams/5\\_5.pdf](http://www.mathcentre.ac.uk/resources/Engineering%20maths%20first%20aid%20kit/latexsource%20and%20diagrams/5_5.pdf). [Accessed: 22-Dec-2019].
- [202] Kindred, P., 2012, 'Matrices , Transposes and Inverses, Math 40, Introduction to Linear Algebra, Lecture 7.', Spring, p. 4 [Online]. Available: <https://www.math.hmc.edu/~dk/math40/math40-lect07.pdf>. [Accessed: 26-Dec-2019].
- [203] Jim Colt, 2015, 'The Welder, Cutting and Weld Prep, Troubleshooting CNC Plasma Cutting, Part II', Fabr. [Online]. Available: <https://www.thefabricator.com/thewelder/article/cuttingweldprep/troubleshooting-cnc-plasma-cutting-part-ii>. [Accessed: 14-Oct-2019].
- [204] American Torch Tip, 2017, 'How To Reduce Dross and Slag During Plasma Cutting', ATTC [Online]. Available: <https://www.americantorchtip.com/blog/reduce-dross-and-slag-buildup>. [Accessed: 14-Oct-2019].
- [205] Hypertherm, 2019, 'Troubleshooting Plasma Cutting System Cut Quality Problems - Cut Angularity', Hypertherm Shap. Possibility [Online]. Available: <https://www.hypertherm.com/customer-support/getting-the-most-from-your-products/cut-quality/cut-angularity/?region=EMEA>. [Accessed: 15-Oct-2019].
- [206] Open University, 2018, 'Plasma Arc Cutting', OpenLearn [Online]. Available: <https://www.open.edu/openlearn/science-maths-technology/engineering-technology/manupedia/plasma-arc-cutting>. [Accessed: 11-Nov-2019].
- [207] Minitab, 2019, 'Residual Plots for Fit Regression Model', Minitab [Online]. Available: <https://support.minitab.com/en-us/minitab/18/help-and-how-to/modeling-statistics/regression/how-to/fit-regression-model/interpret-the-results/all-statistics-and-graphs/residual-plots/>. [Accessed: 05-Nov-2019].
- [208] Lewis-Beck, M., Bryman, A., and Futing Liao, T., 2012, 'R-Squared', SAGE Encycl. Soc. Sci. Res. Methods, p. 1189. [Accessible]: <http://pages.stat.wisc.edu/~mchung/papers/R2.pdf>.
- [209] Frost, J., 2014, 'How High Does R-Squared Need to Be? - Statistics By Jim', Mak. statistics intuitive [Online]. Available: <https://statisticsbyjim.com/regression/how-high-r-squared/>. [Accessed: 07-Jan-2020].
- [210] Bogue, R., 2011, 'Cutting Robots: A Review of Technologies and Applications', Ind. Robot An Int. J., 38(2), pp. 113–118.
- [211] Pérez, R., Gutiérrez, S. C., and Zotovic, R., 2018, 'A Study on Robot Arm Machining: Advance and Future Challenges', Ann. DAAAM Proc. Int. DAAAM Symp., 29(1), pp. 931–940.
- [212] Defaux, M., 2004, 'Welding and Cutting: Robots Take the Lead in 3D', Ind. Rob., 31(1), p. 41.
- [213] Sam Daley, 2020, 'Six Automotive Robotics Companies To Keep In Mind', Built In [Online]. Available: <https://builtin.com/robotics/automotive-cars-manufacturing-assembly>. [Accessed: 09-Dec-

- 2020].
- [214] Ken Trumbull, 2006, 'Plasma Cutting with a Robot', Fabr. [Online]. Available: <https://www.thefabricator.com/thefabricator/article/cuttingweldprep/plasma-cutting-with-a-robot>. [Accessed: 22-Jun-2020].
- [215] Sam Francis, 2018, '30 Industrial Robot Manufacturers to Watch', Robot. Autom. [Online]. Available: <https://roboticsandautomationnews.com/2018/01/03/30-industrial-robot-manufacturers-to-watch-in-2018/15542/>. [Accessed: 09-Dec-2020].
- [216] Kogelschatz, U., 2004, 'Atmospheric-Pressure Plasma Technology', Plasma Phys. Control. Fusion, 46(B), p. B65.

# APPENDIX

## APPENDIX-A Stages and Line Layout

The stages required for converting the vehicles including the parts added and removed in each stage.

**Table A1 Vehicle Conversion Process**

	Work Performed	Cycle Time(mn)	Queuing Time(mn), prior admission
Preparation \ Cut	Remove rear Bumper, carpet, plastic panels, protect front seats, put the bracing frame, mark the cutting profile, and then cut and put the cross member	255	10
Cables Wiring	Wiring implementations	35	55
Brakes	Implementation of new brake pipes and bleed brakes	58	45
Loom/ Battery	ABS wire loom, Fuel Sender Unit Wires loom, Electro Reel Wire Loom, Pin Switch wire, clips, connectors, wire protector	45	40
Pan Fit	Front Pan, D Loop spreader plate, Ramp Module, Brackets	40	40
Suspension	Suspension damper Mount, suspension bracket, shock absorber, spring, Electro reel bolt	50	15
Fuel Tank	Charcoal Filter (Petrol Car: Foam Tape, Connectors, Fuel line cable, Rubber hose), Fuel Tank, Wire Hoses, wire protector, ADblue Tank (For Diesel Car), FAP tank (For Diesel Car), FAP Bleeder	50	25
Exhaust	Exhaust pipe, Bracket, Rubber mount, Heat Shield refit.	50	15
Winch Loom	Winch control, Wiring Kit	45	105
Side Bumper	Gloss Black Paint, Bumper end caps, Small Brackets, Large Brackets	20	5
Winch\Sensors	Earth Wire, Winch, Q-straint, Electro reel harness and Mount, Mushrooms Bolts, Red Rubber, Cups cover, Bracket seat mount, Brand Sticker Parking Sensors (additional operator)	40	10
Carpet/Winch Cover	customised carpet, Double sided tape, Plastics pan covers, reel box trim, black caps	40	20
Seats/Belts	Q-straint upper brackets, Q-straint belt kit, D-loop, Cap, seat belts, Seats	40	5
Mid-Bumper Fit	Customised Mid-Bumper, Brackets, side covers, plastic caps.	50	20
QC	Visual Control, fuel fill	30	30
PDI	Final check and vehicle memory computer reprogramming	60	20
Test Drive	Take the car for a test road	20	20
<b>Total Time</b>		928	480

## APPENDIX-B Double Layered Cutting and Trials Results

The table below B1 shows different setting for the trials performed to assess the capability of the chosen plasma technique to cut simultaneously two layers, the settings were recorded.

**Table B1 Settings Used to cut two layers simultaneously.**

Distance Between the two Sheets	Tests	Pressure (Psi)	Intensity I (A)	Cutting Speed (mm/min)	Cut performed	
					Top Layer	Bottom layer
16 mm	<b>Trial Number 1</b>	82	40	2000	yes	None
	<b>Trial Number 2</b>	82	50	2000	yes	None
	<b>Trial Number 3</b>	82	80	2000	yes	None
	<b>Trial Number 4</b>	90	60	2000	yes	None
	<b>Trial Number 5</b>	90	70	2000	yes	Yes
35 mm	<b>Trial Number 6</b>	70	90	2000	yes	None
	<b>Trial Number 7</b>	75	90	2000	yes	None
	<b>Trial Number 8</b>	80	90	2000	yes	None
25 mm	<b>Trial Number 9</b>	80	90	2000	yes	Yes
	<b>Trial Number</b>	70	90	2000	yes	None
	<b>10</b>					
	<b>Trial Number</b>	75	90	2000	yes	Yes
<b>11</b>						

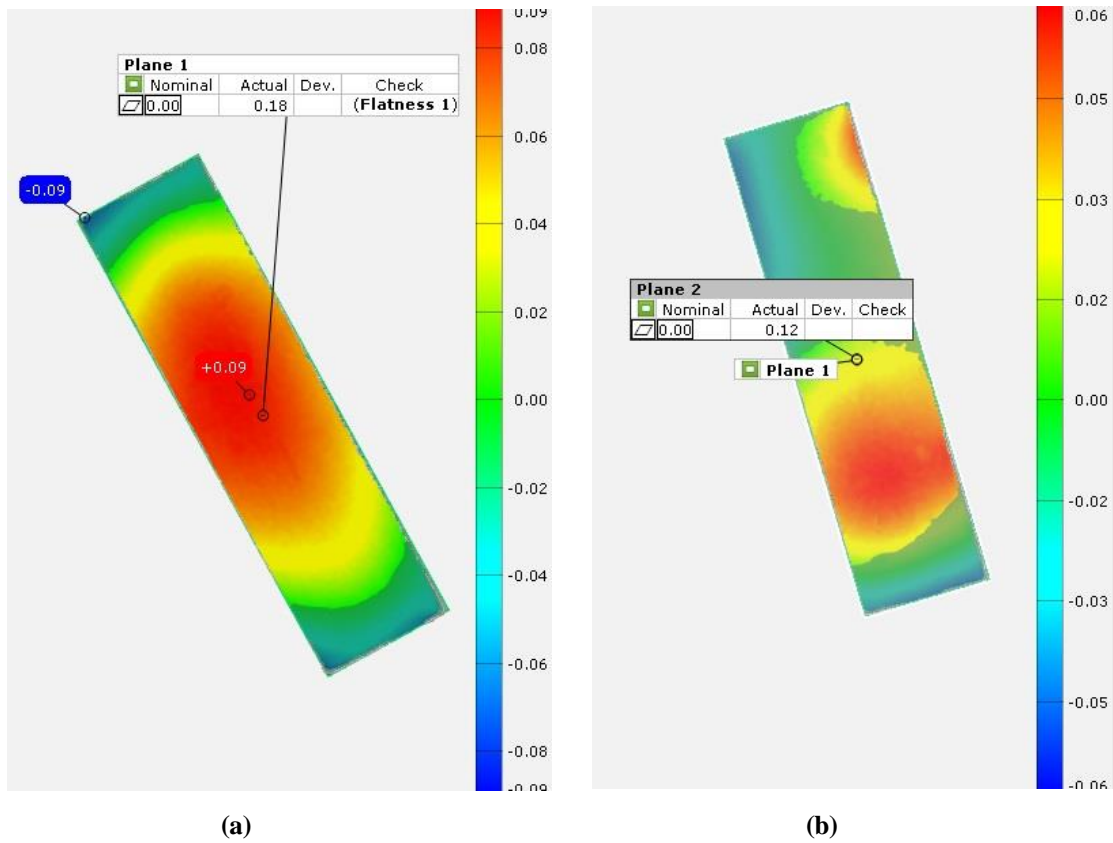
The Table below B2 shows the trials made to determine the settings suitable to use as a cutting reference for the optimisation Taguchi experiment, settings of each trial were recorded as follows.

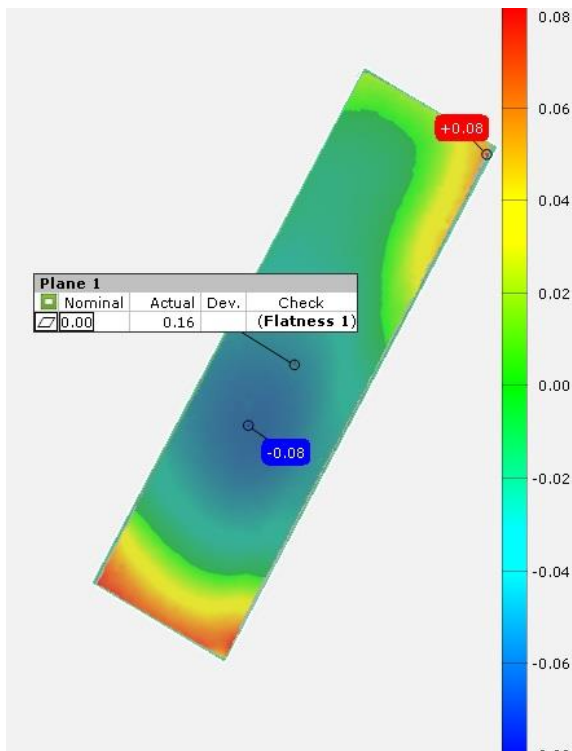
**Table B2 Settings Recorded for the Trials Performed Cut Two Layers Simultaneously at a Fixed Gap**

<b>TESTS</b>	<i>Pressure</i> <i>(Psi)</i>	<i>Intensity</i> <i>I(A)</i>	<i>Cutting Speed</i> <i>(mm/min)</i>	<i>Cut performed</i>	
				<i>Top Sheet</i>	<i>Bottom Sheet</i>
<b>TRIAL NUMBER 1</b>	80	45	8000	Yes	None
<b>TRIAL NUMBER 2</b>	80	45	6000	Yes	None
<b>TRIAL NUMBER 3</b>	80	45	5000	Yes	None
<b>TRIAL NUMBER 4</b>	80	45	4000	Yes	None
<b>TRIAL NUMBER 5</b>	80	45	2000	Yes	None
<b>TRIAL NUMBER 6</b>	80	45	1000	Yes	None
<b>TRIAL NUMBER 7</b>	80	45	500	Yes	Yes
<b>TRIAL NUMBER 8</b>	80	45	750	Yes	yes
<b>TRIAL NUMBER 9</b>	80	45	700	Yes	yes
<b>TRIAL NUMBER 10</b>	80	45	600	Yes	None
<b>TRIAL NUMBER 11</b>	80	30	500	Yes	None
<b>TRIAL NUMBER 12</b>	80	35	500	Yes	Yes
<b>TRIAL NUMBER 13</b>	80	33	500	Yes	Yes
<b>TRIAL NUMBER 14</b>	80	30	400	Yes	Yes
<b>TRIAL NUMBER 15</b>	80	20	300	Yes	None
<b>TRIAL NUMBER 16</b>	80	25	300	Yes	Yes

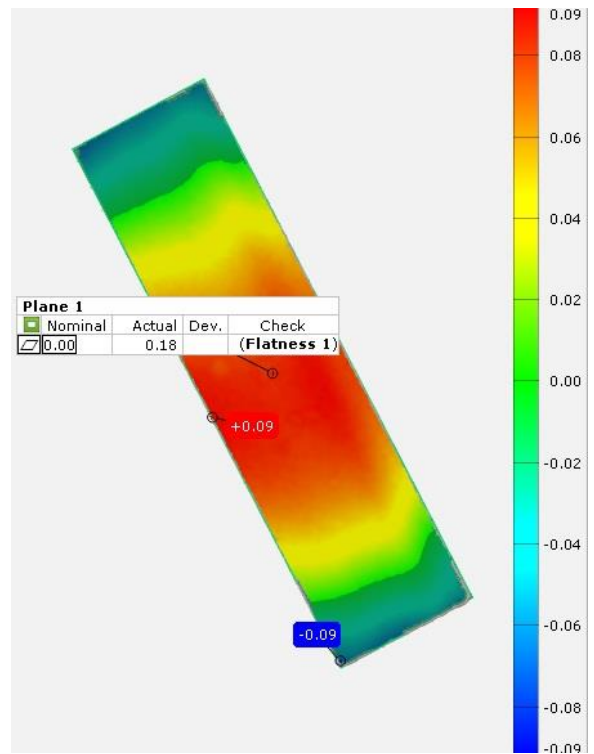
## APPENDIX-C Single Sheets Parts Scanned and Material Microstructure

figures C1 below (a to i) represent the trials performed to assess the deformation for a single sheet 0.6 mm using a Taguchi method to optimise the cutting process. The figures are in alphabetic order for trial one to nine successively.

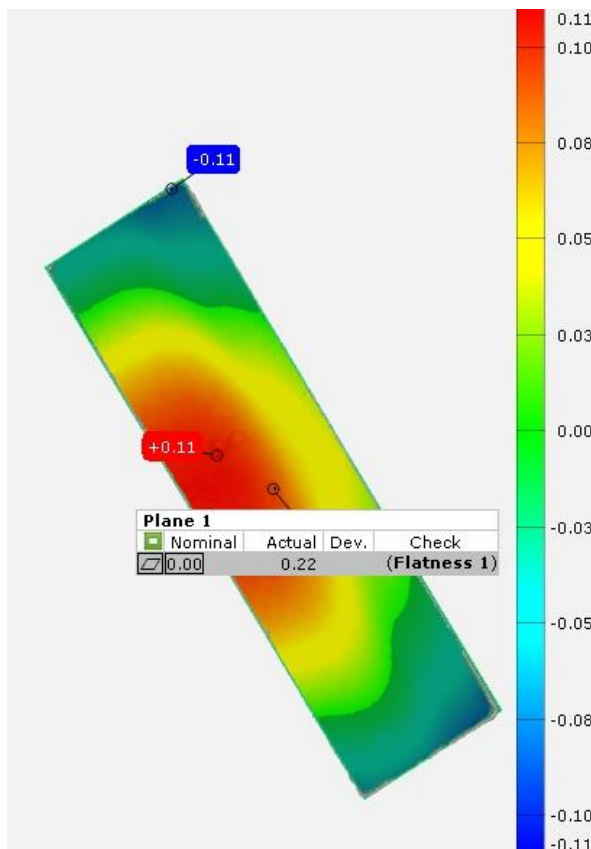




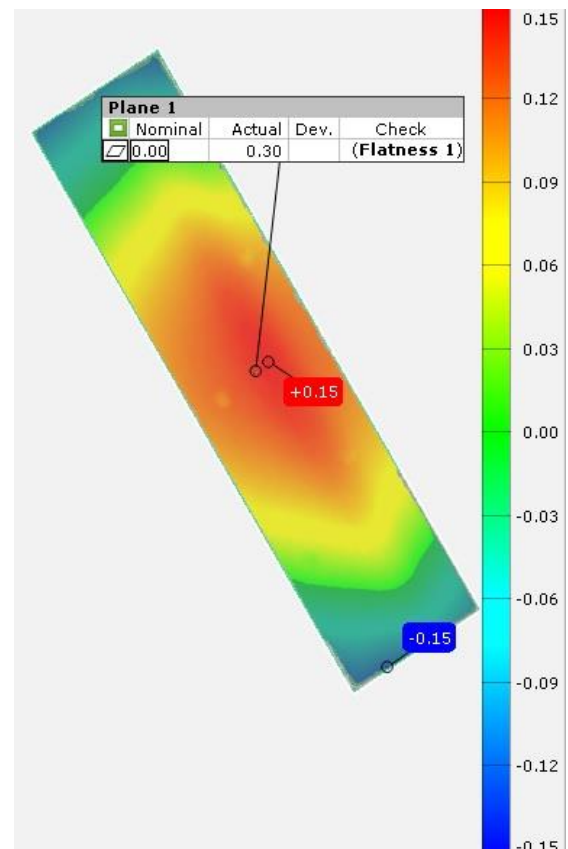
(c)



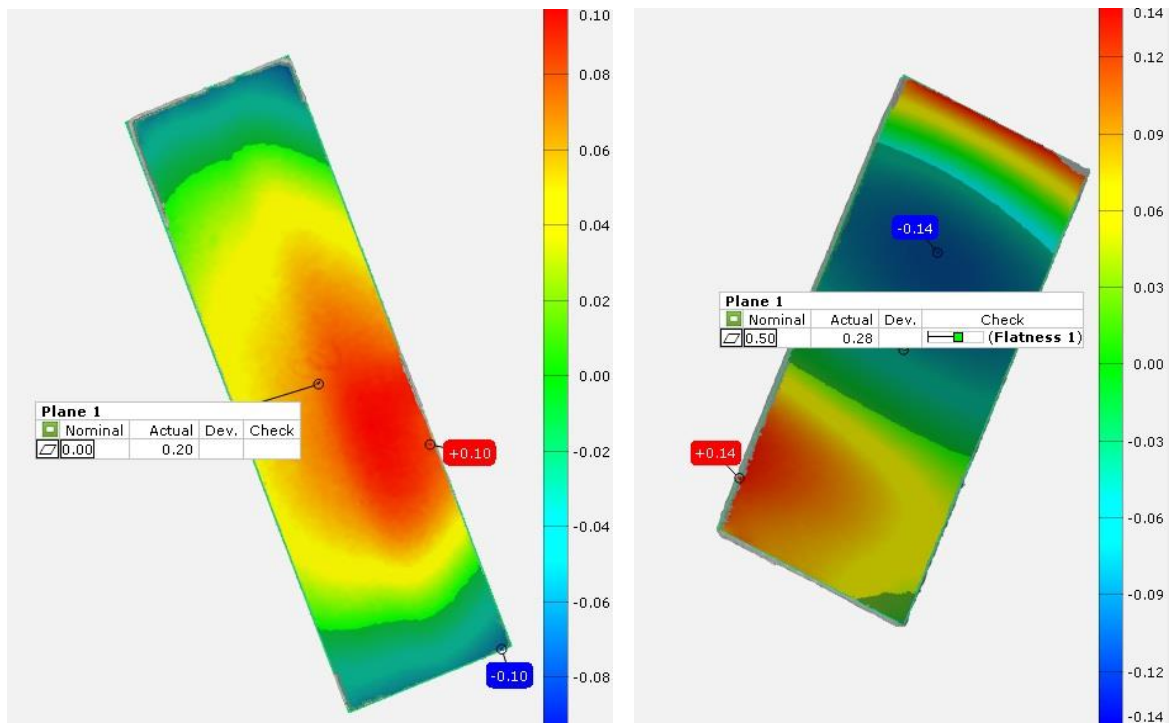
(d)



(e)

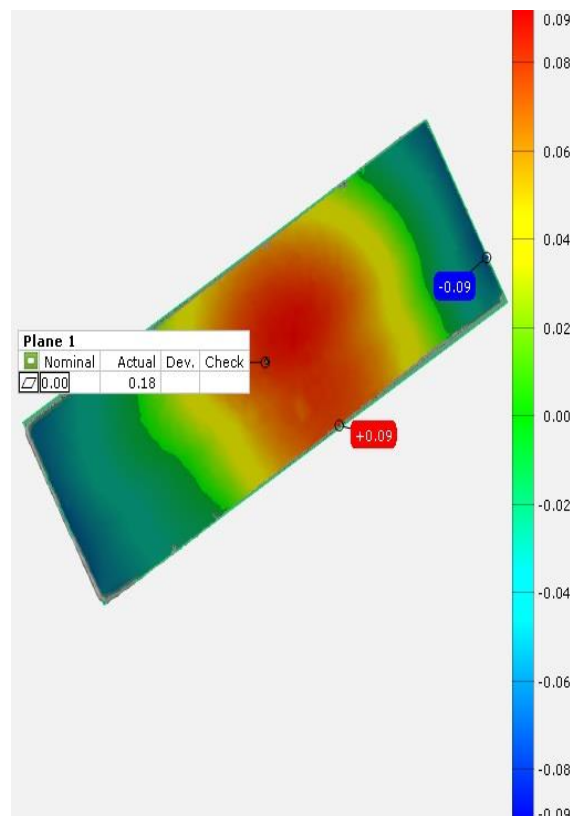


(f)



(g)

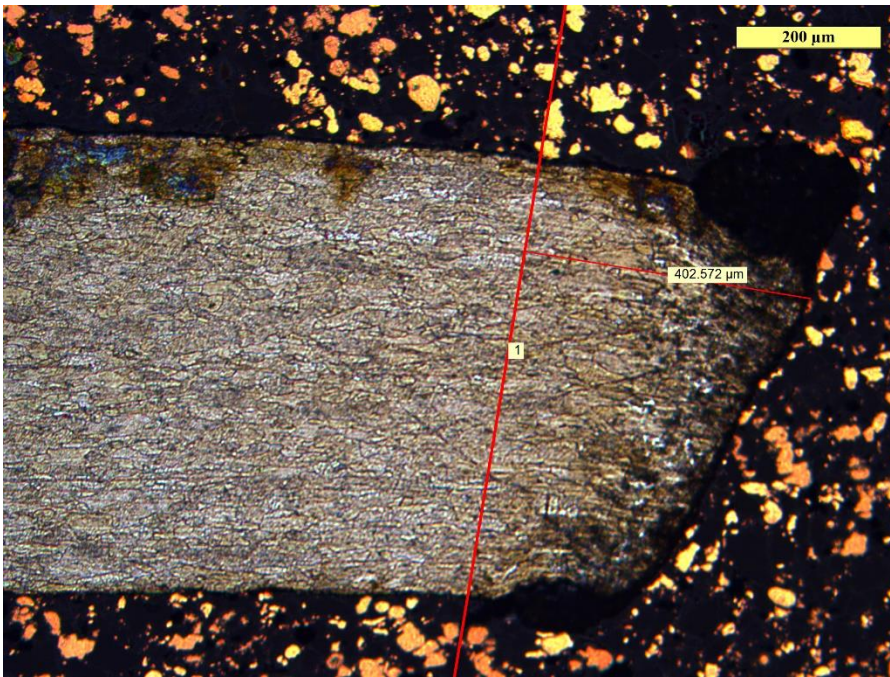
(h)



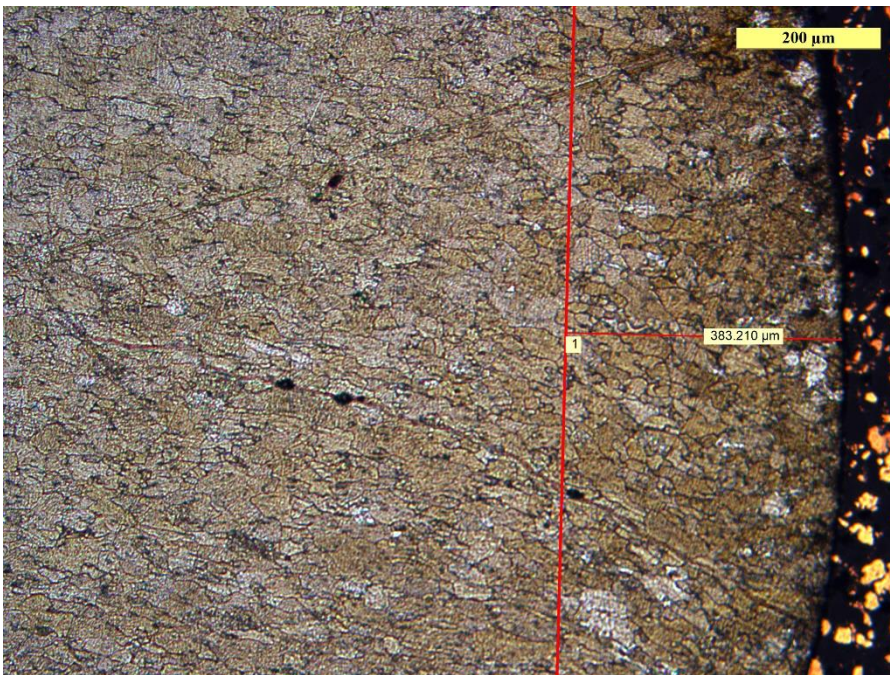
(i)

**Figure C1 Parts Scanned for Deformation Single Sheets 0.6 mm, respectively (a) to (i) Represent Trial one to Trial Nine**

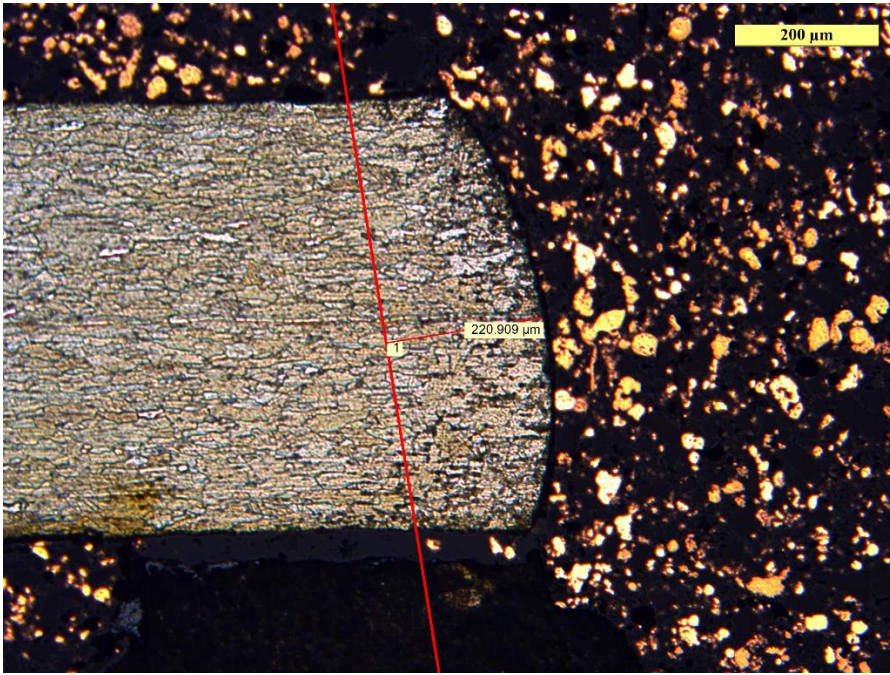
The figures C2 below represent the width of the Heat Affected Zones measured for the single sheets 0.6 mm, the specimens are in order from (a to i) represent samples from trial one to trial nine.



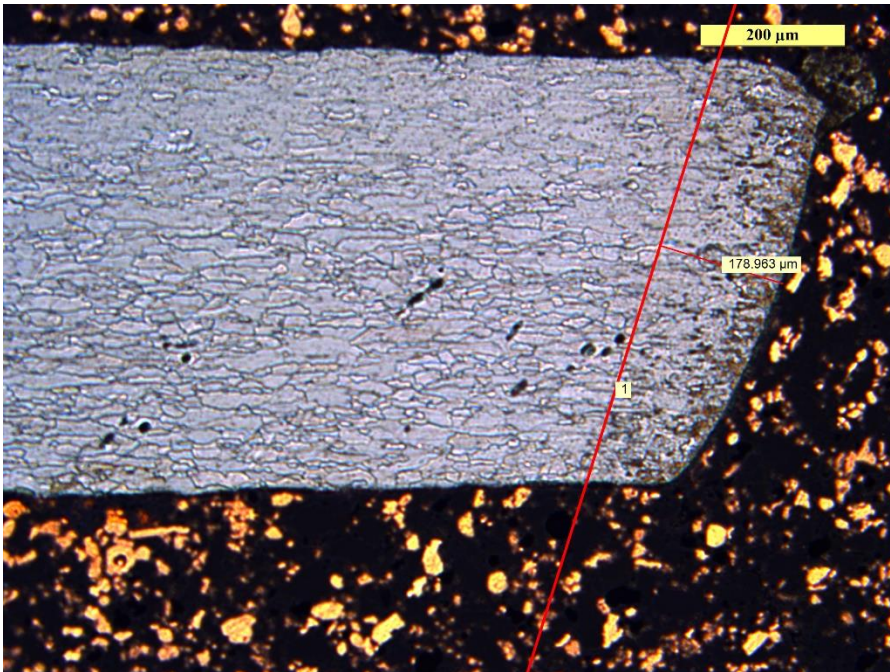
(a)



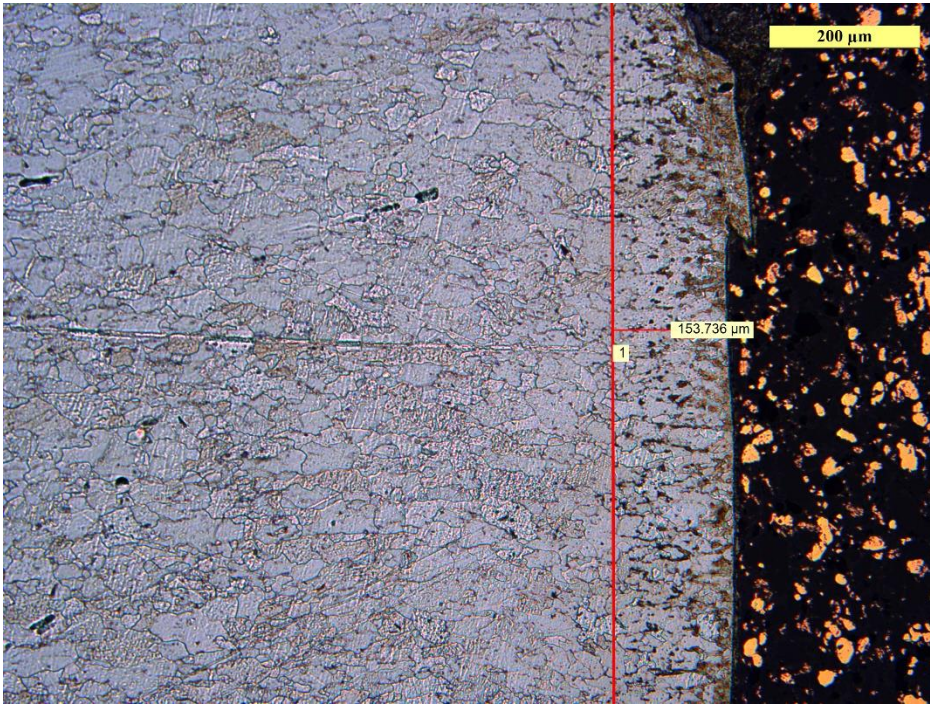
(b)



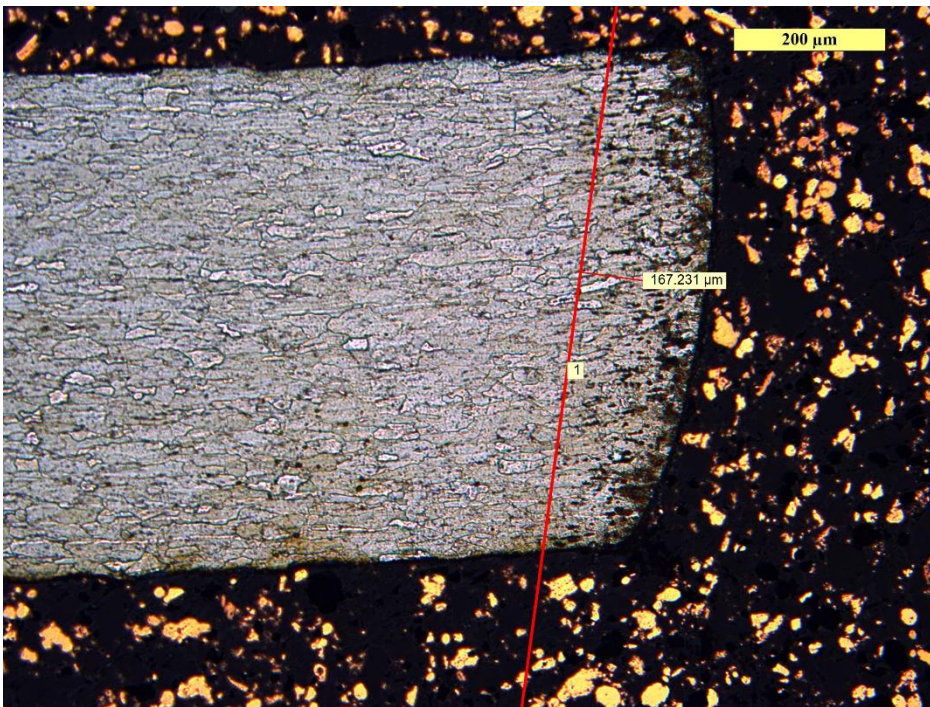
(c)



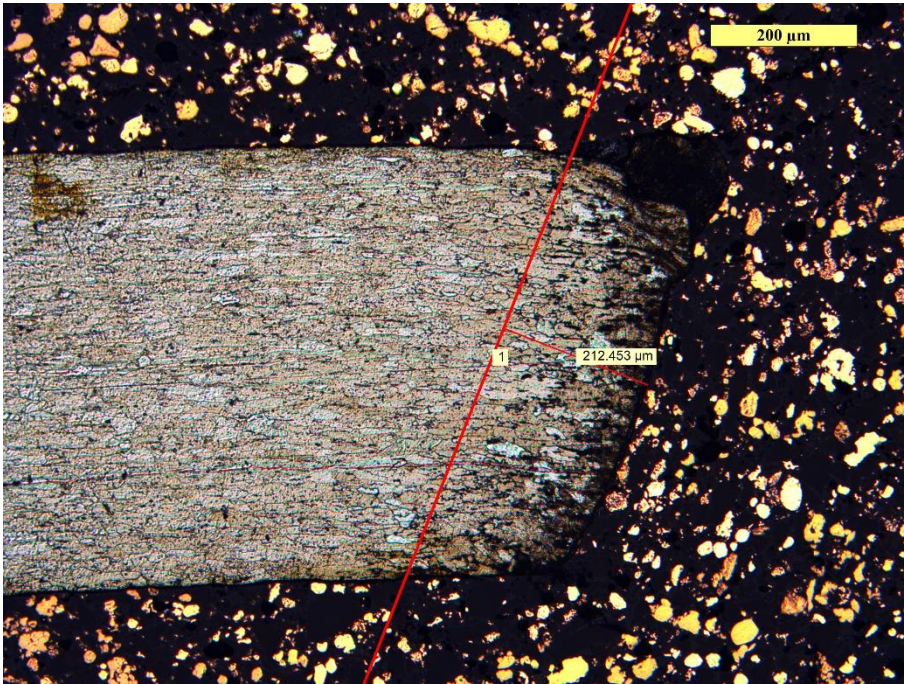
(d)



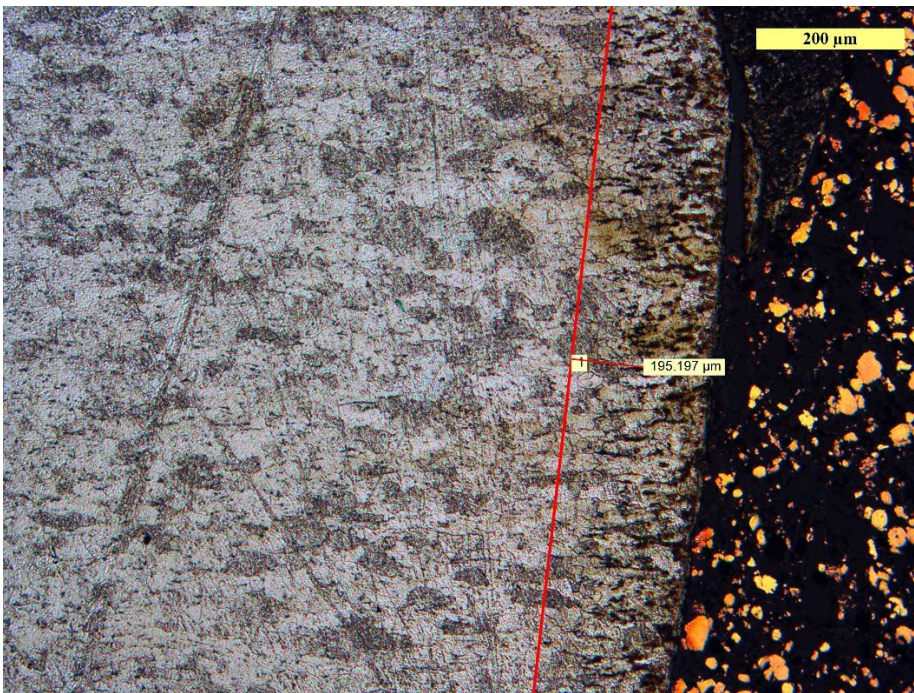
(e)



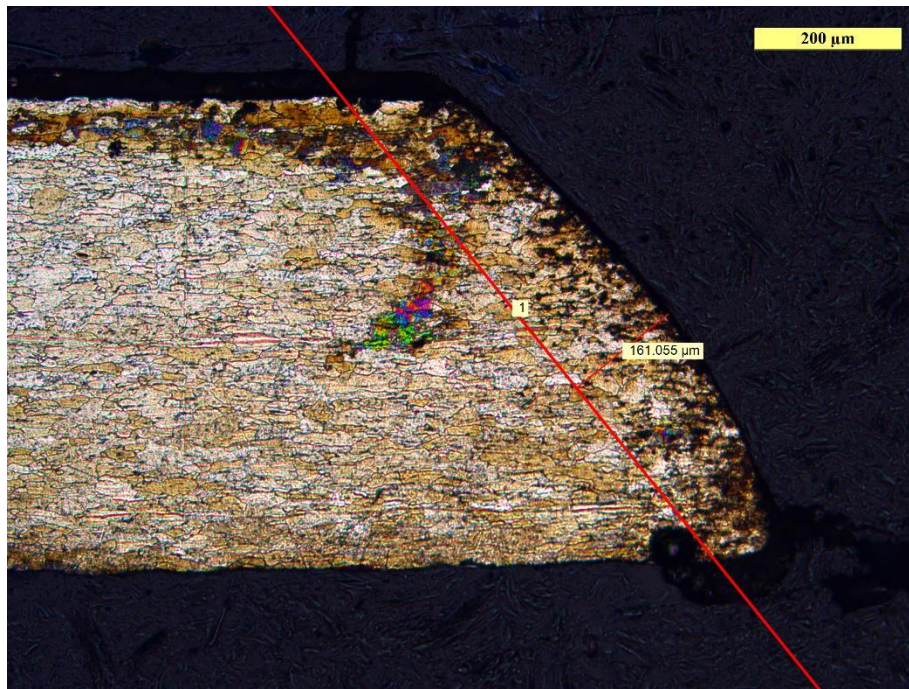
(f)



(g)



(h)



(i)

**Figures C2 Material Microstructure of the Specimens, Heat Affected Zones Width, (a) to (i) Represent Trial One to Nine**

## APPENDIX-D Simultaneous Cutting of Two Parallel Sheets Using Taguchi Method

The figures D1 show the three models at different gap distance after the plasma cutting experiment, the samples collected for each model are also presented. The upper samples are from the top side and the lower ones are from the bottom side of the same model.

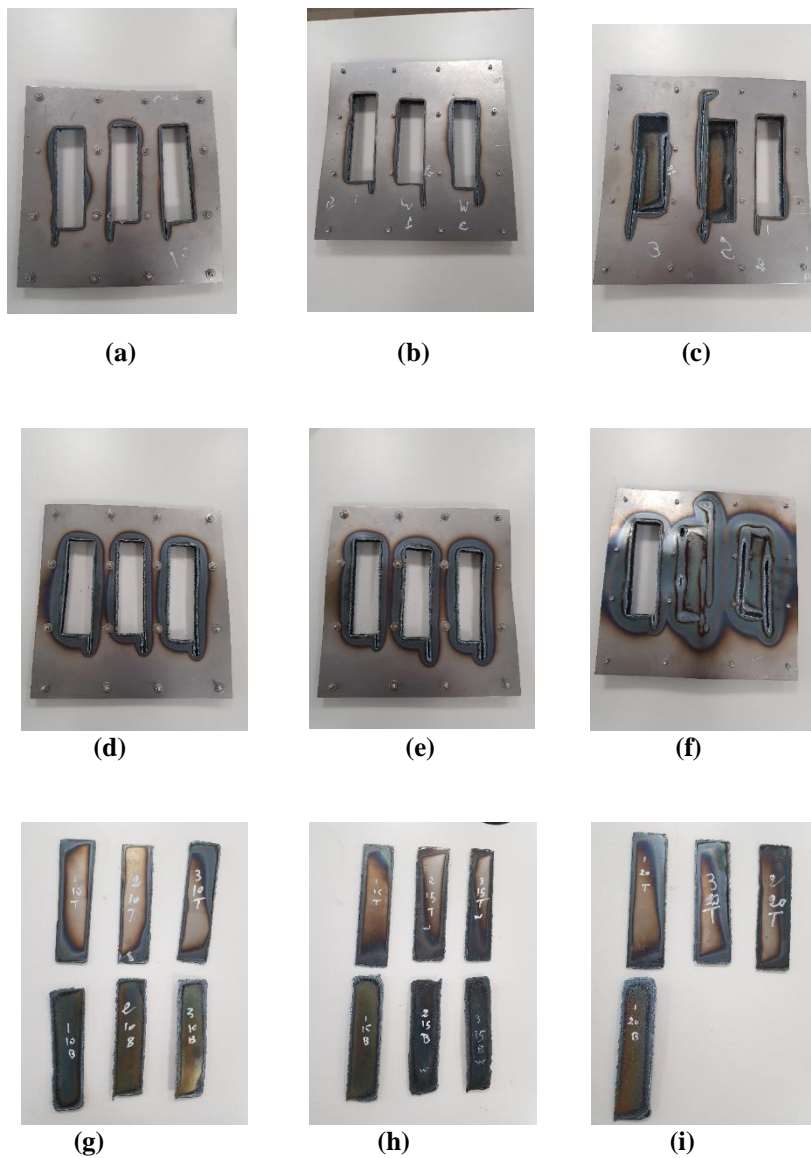
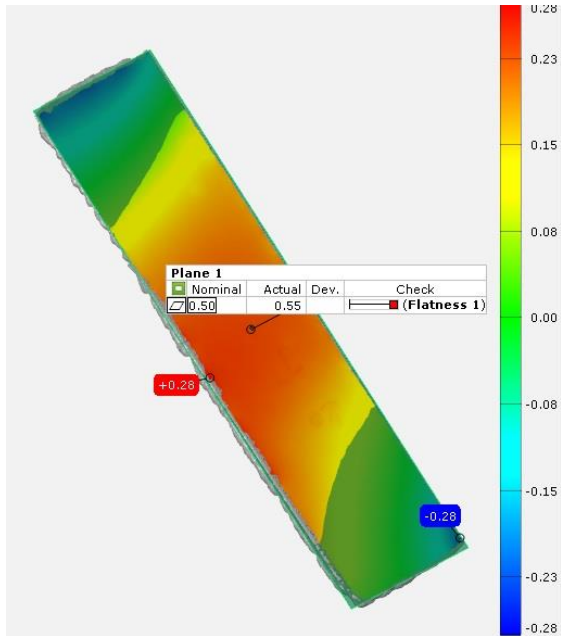
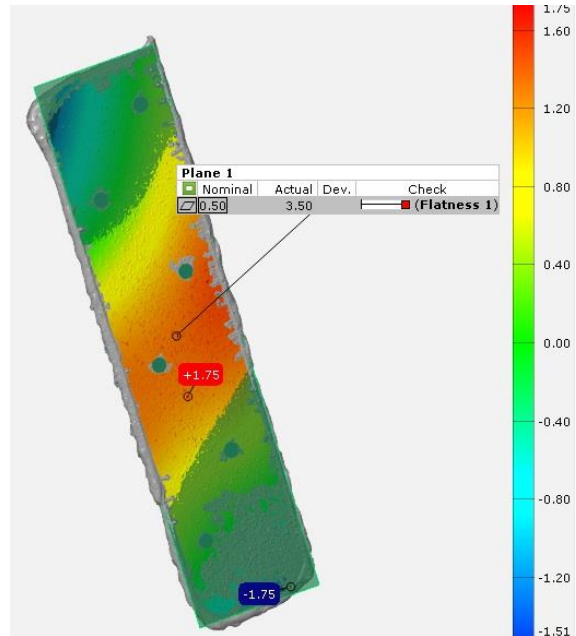


**Figure D1 Tests Result.** figures (a), (b) and (c) are the top view of the experiment models respectively for gap distances 10, 15 and 20mm, (d), (e) and (f) Bottom view of the model for same order gap distances, (g), (h) and (i) samples collected from the model.

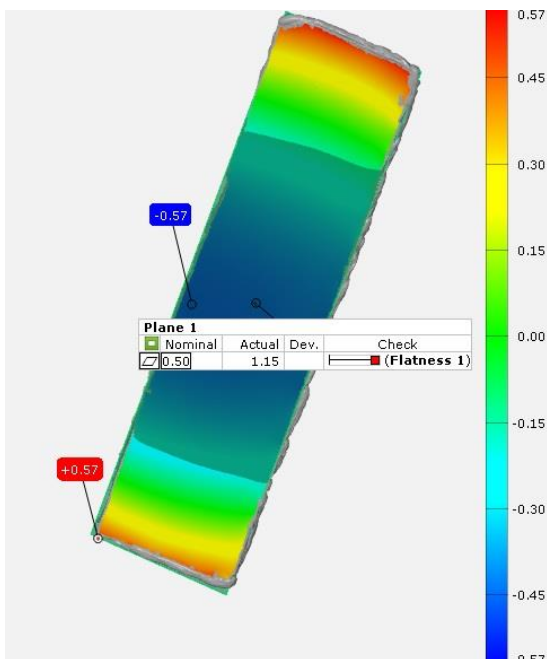
The figures D2 below illustrate the parts collected from a simultaneous two sheets cutting experiment using Taguchi method. The specimens were scanned and assessed for deformation and the results are shown on the figures. Trial number one to trial nine are represented in the figures successively with (a) to (i) for sheets collected from the top side of the models and (a') to (i') for those collected from the bottom side of the model. For instance, (a) and (a') are the top and bottom specimens from the same trial number one.



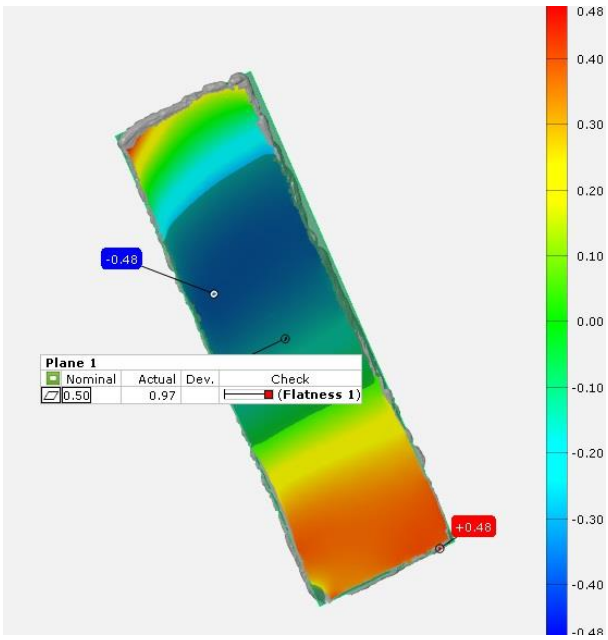
**Trial one (a)**



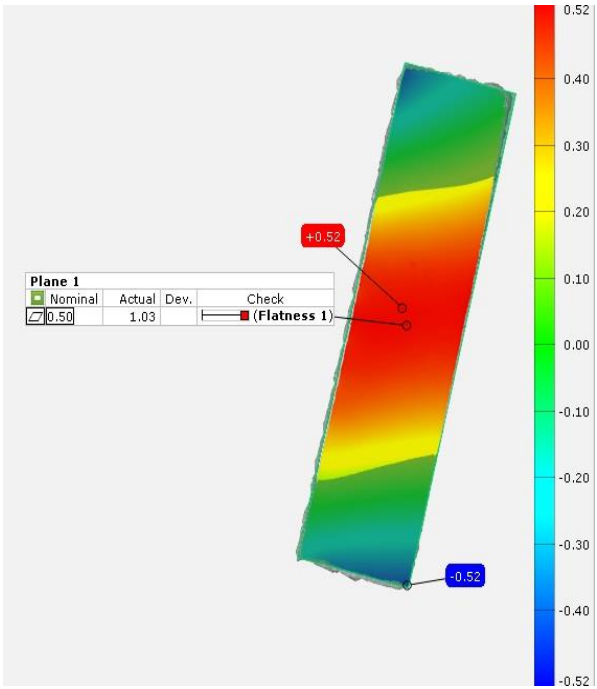
**Trial one (a')**



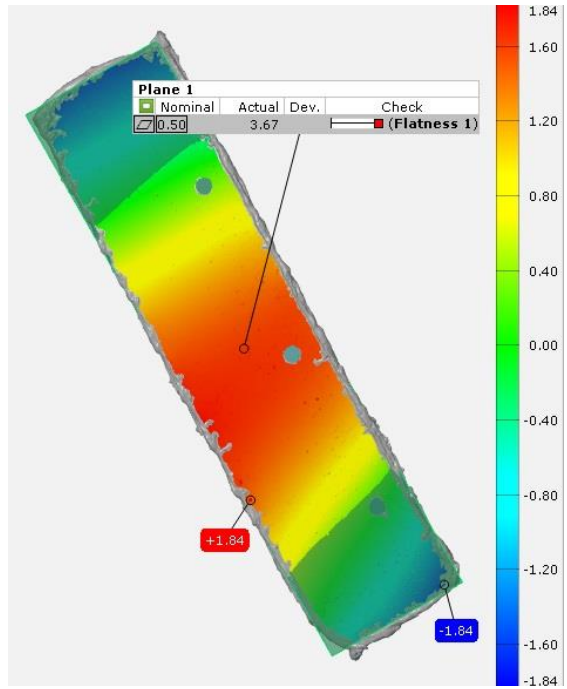
**Trial two (b)**



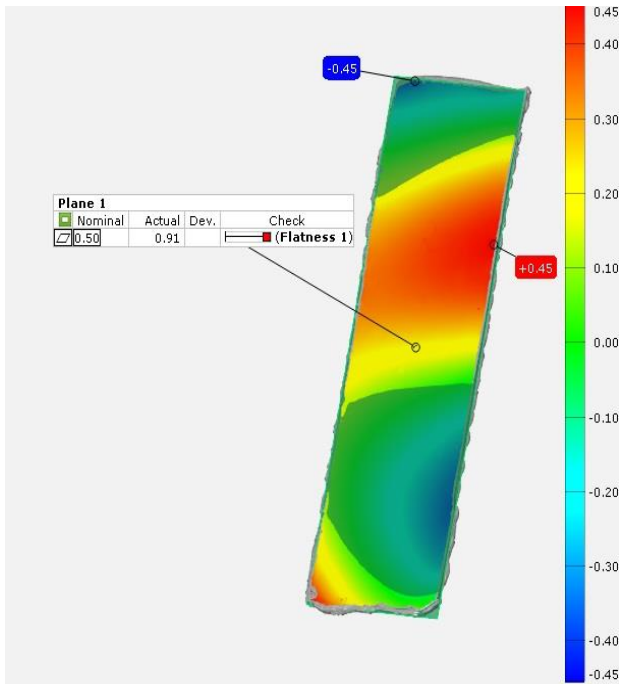
**Trial three (c)**



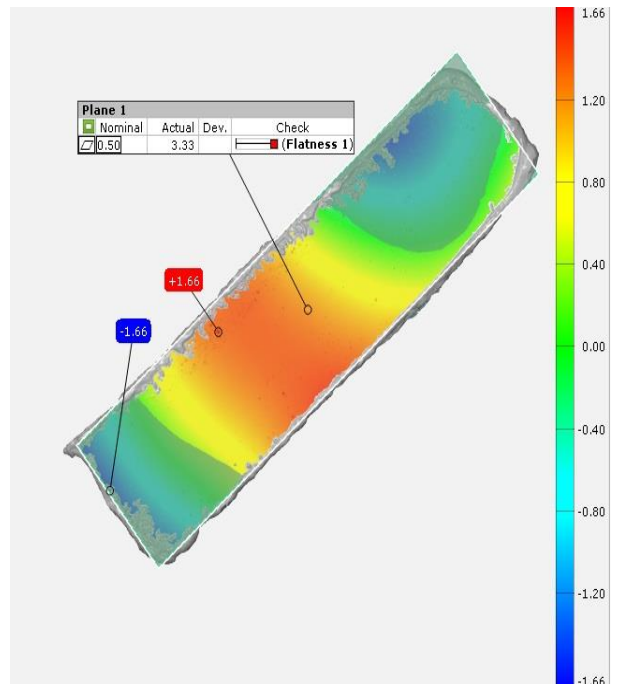
**Trial four (d)**



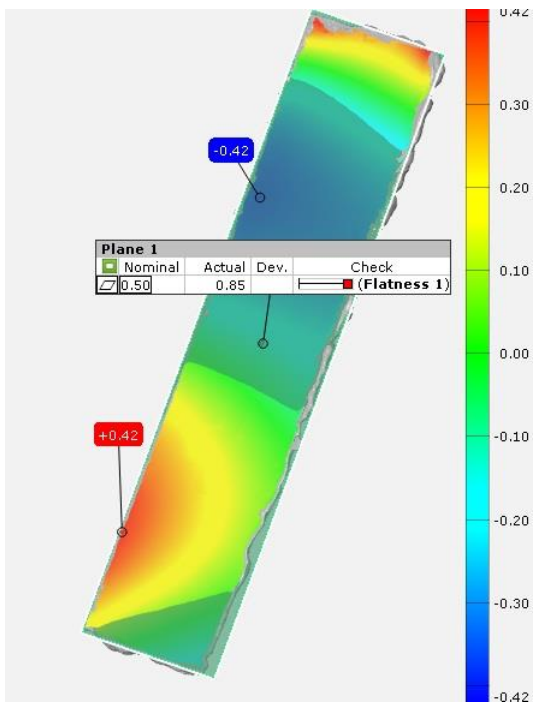
**Trial four (d')**



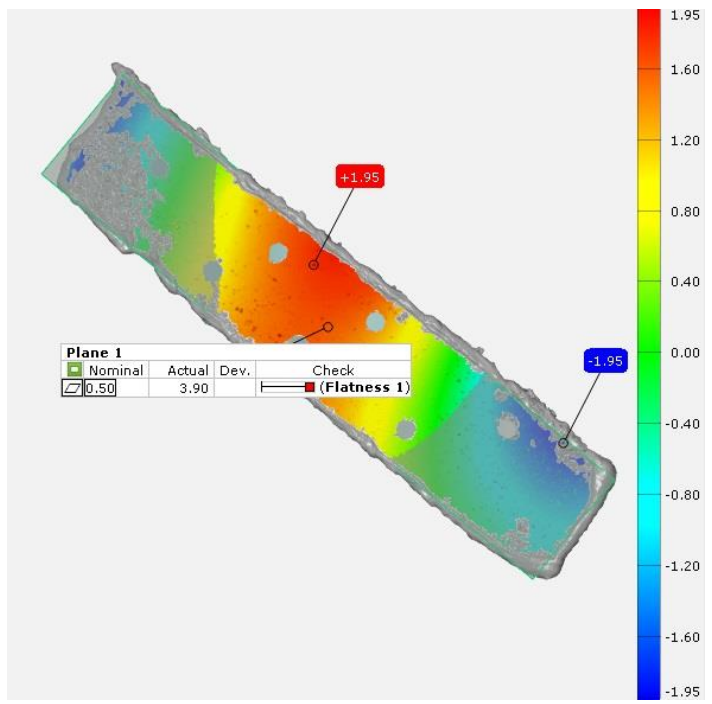
Trial five (e)



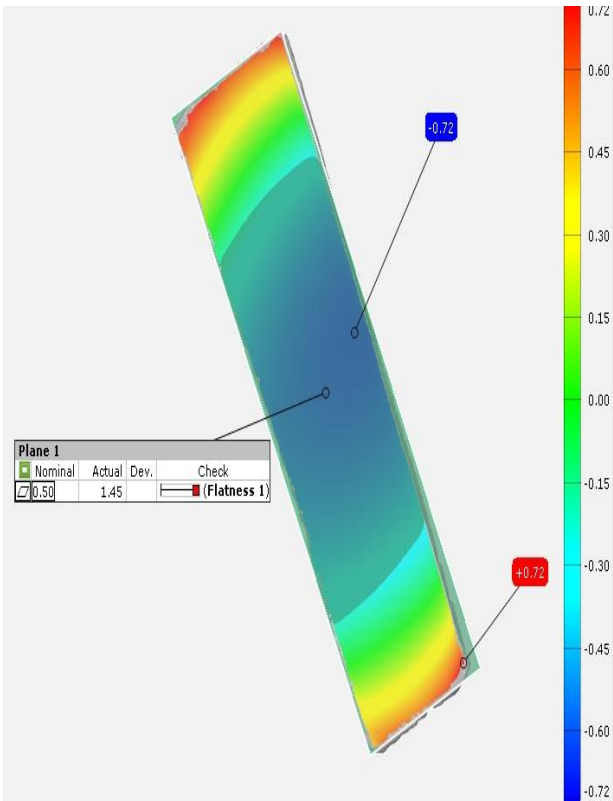
Trial five (e')



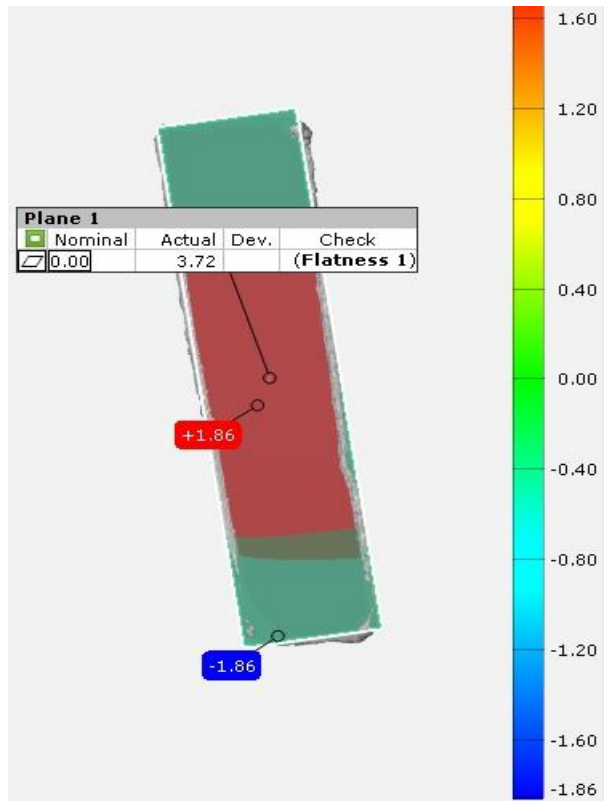
Trial six (f)



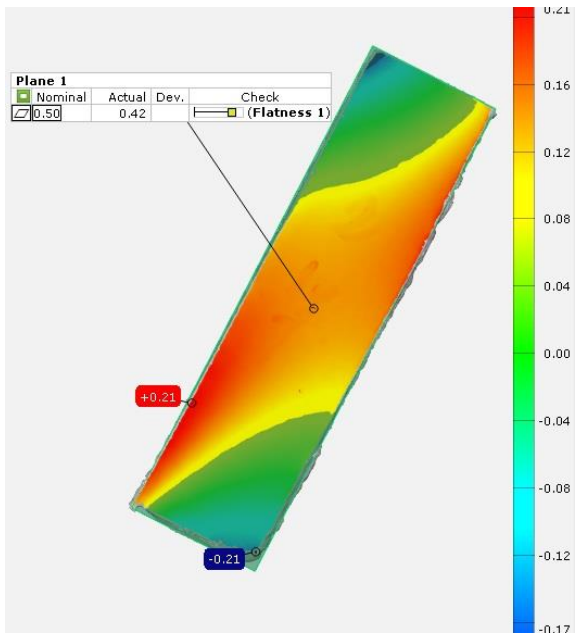
Trial six (f')



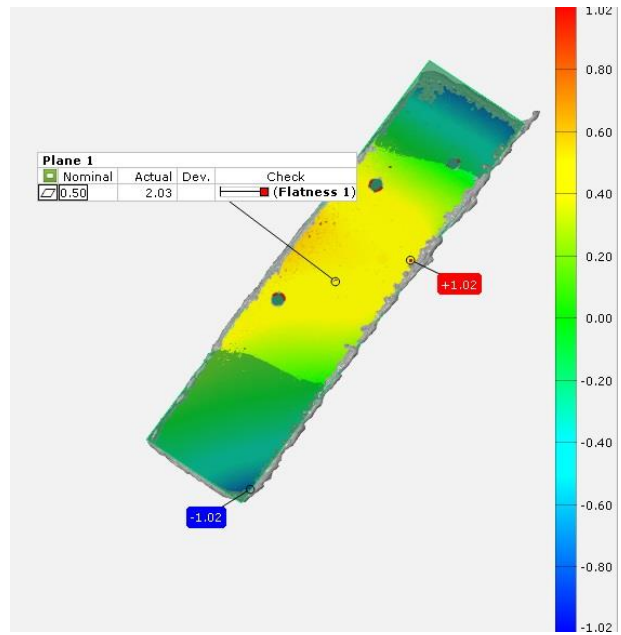
**Trial seven (g)**



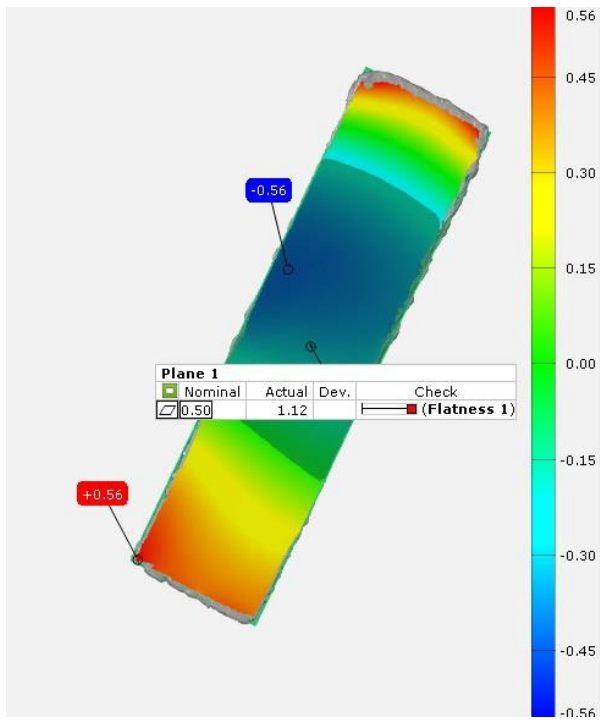
**Trial seven (g')**



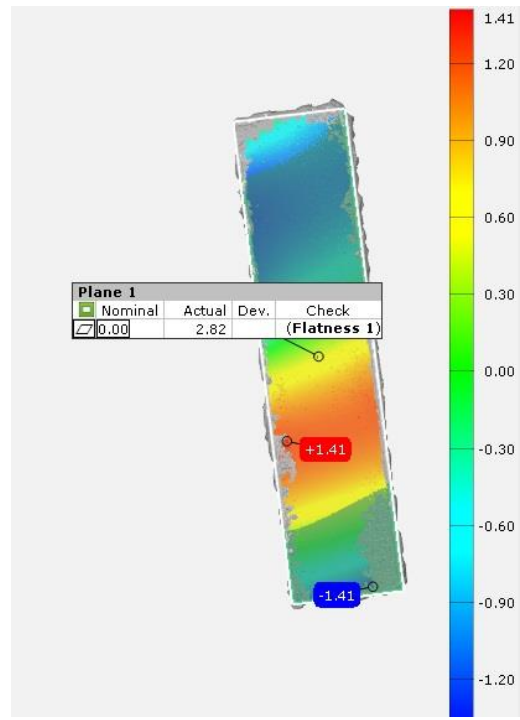
**Trial eight (h)**



**Trial eight (h')**



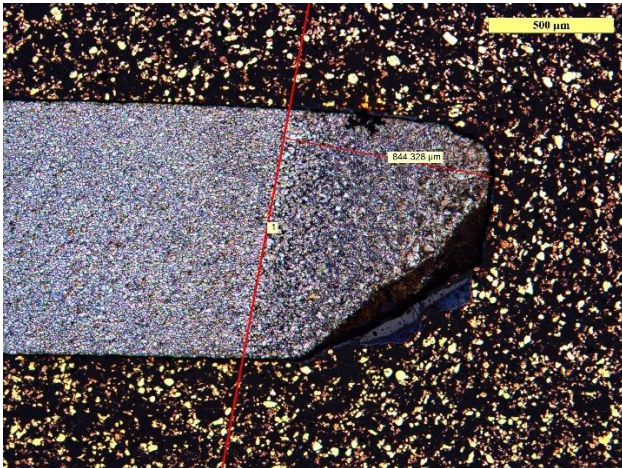
Trial nine (i)



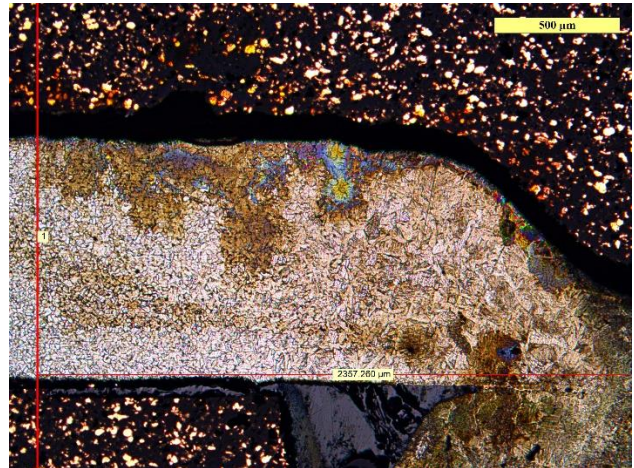
Trial nine (i')

Figures D2 Samples collected from the experiment, maximum deformation measured, (a) to (i) represent trial one to nine, left side figures are taken from the top side of the model and the right side of the figures are the lower sheets collected from the model represented by the sign prime (a') to (i')

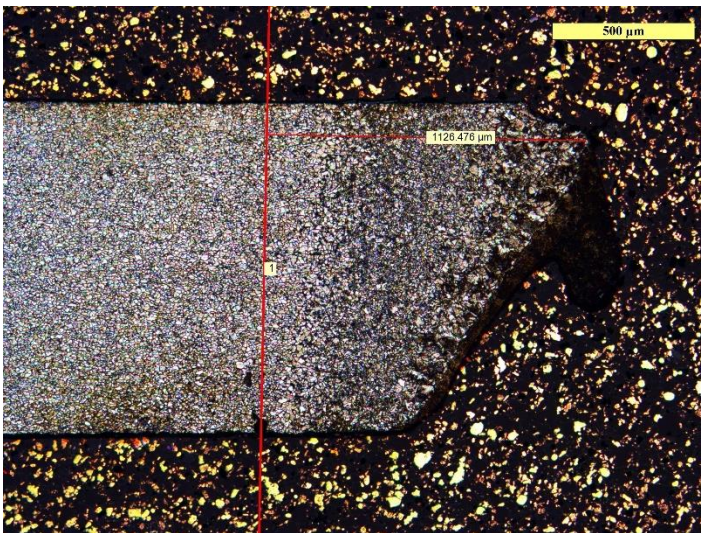
The **figures** D3 below illustrate the width of the heat affected zones measured for the double cutting process. The **figures** (a) to (i) are the samples collected from the top side of the model, (a') to (i') are the samples from the lower sheets of the model



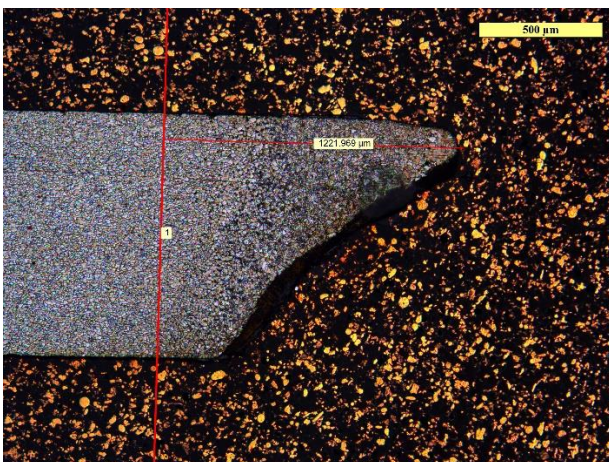
**Trial one (a)**



**Trial one (a')**



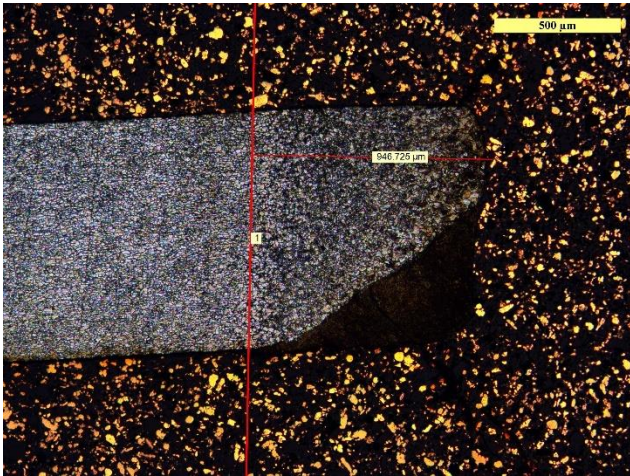
**Trial two (b)**



**Trial three (c)**



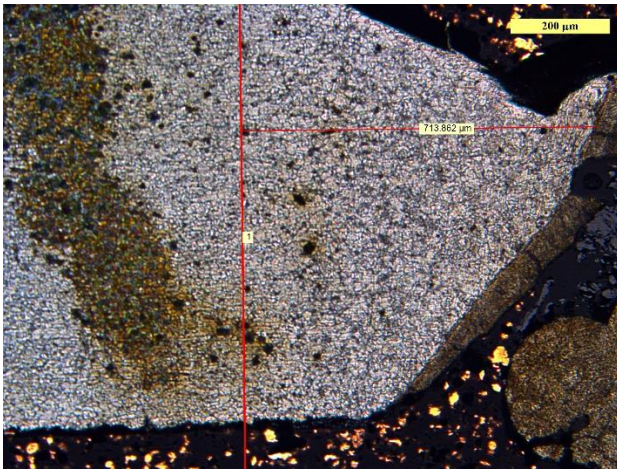
**Trial three (c')**



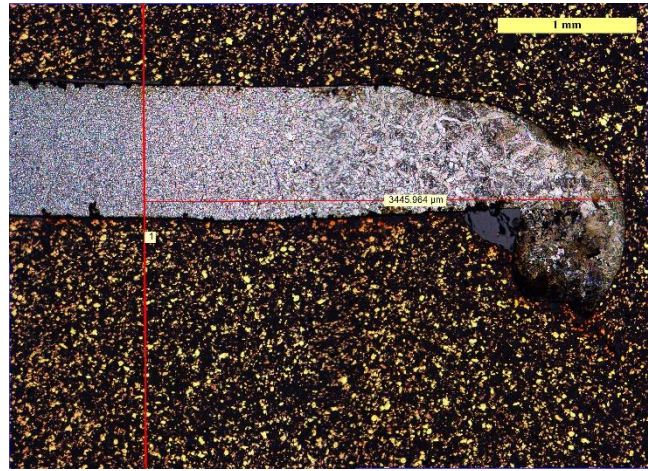
**Trial four (d)**



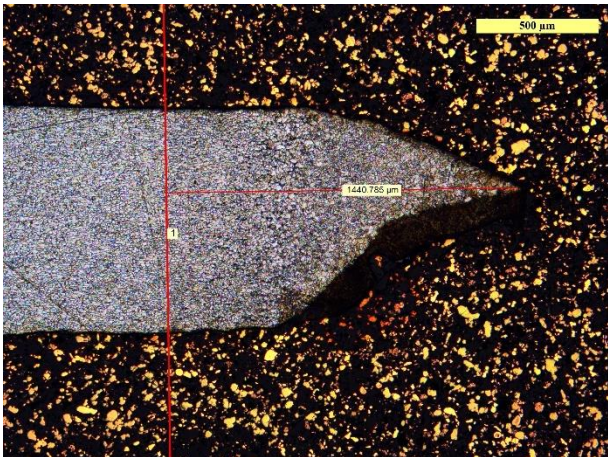
**Trial four (d')**



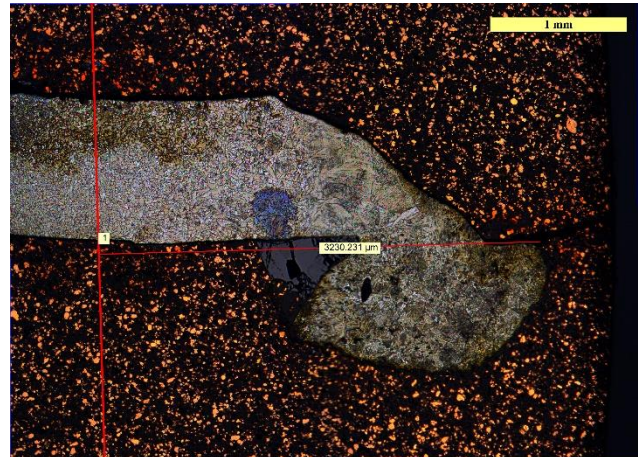
**Trial five (e)**



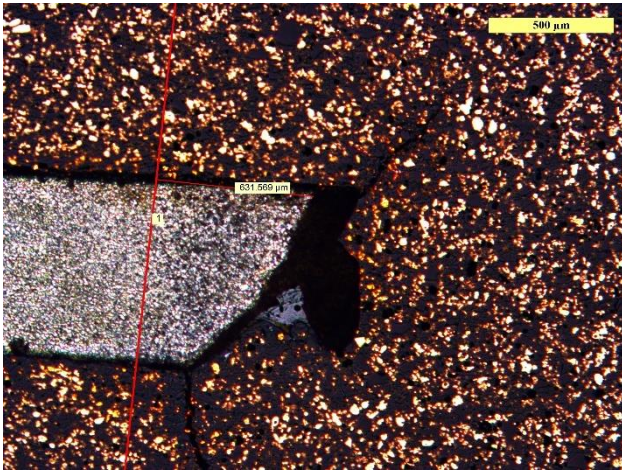
**Trial five (e')**



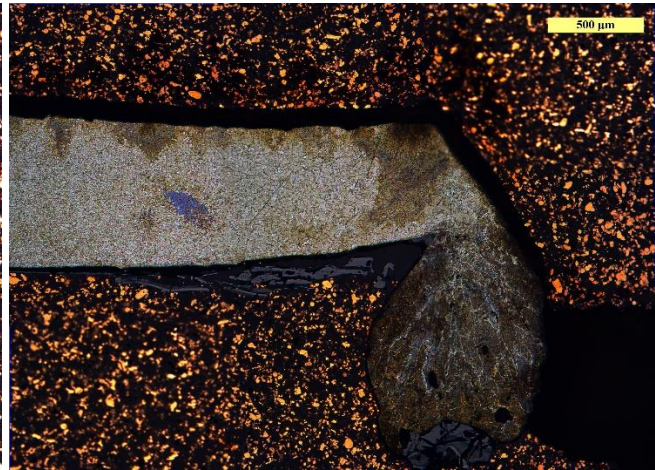
**Trial six (f)**



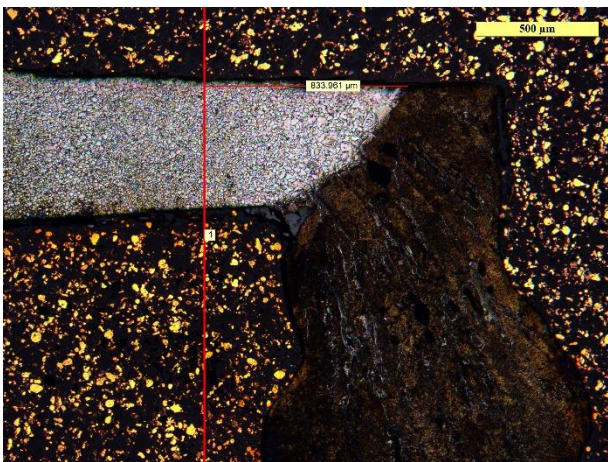
**Trial six (f')**



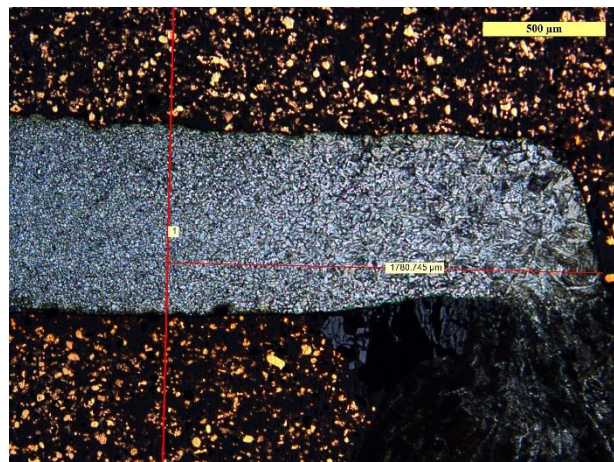
**Trial seven (g)**



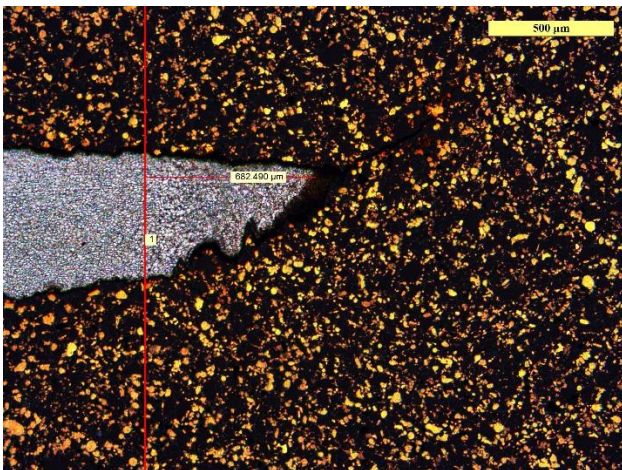
**Trial seven (g')**



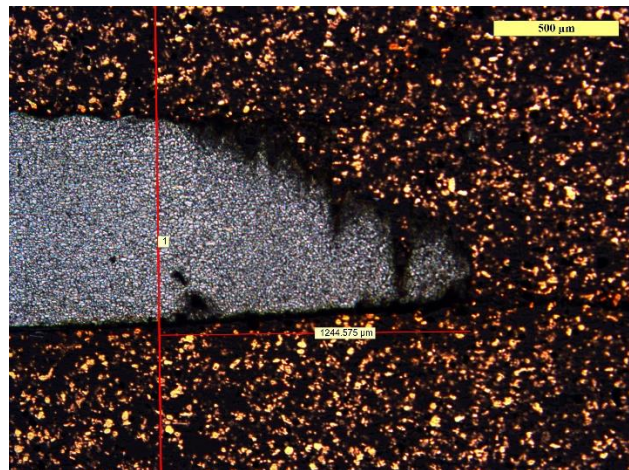
**Trial eight (h)**



**Trial eight (h')**



**Trial nine (i)**

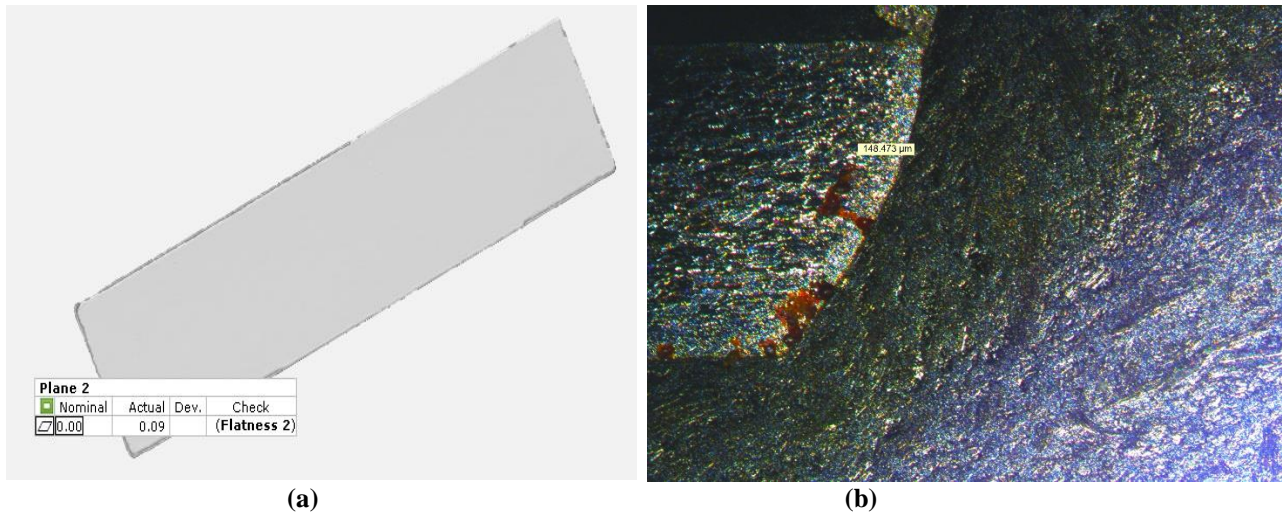


**Trial nine (i')**

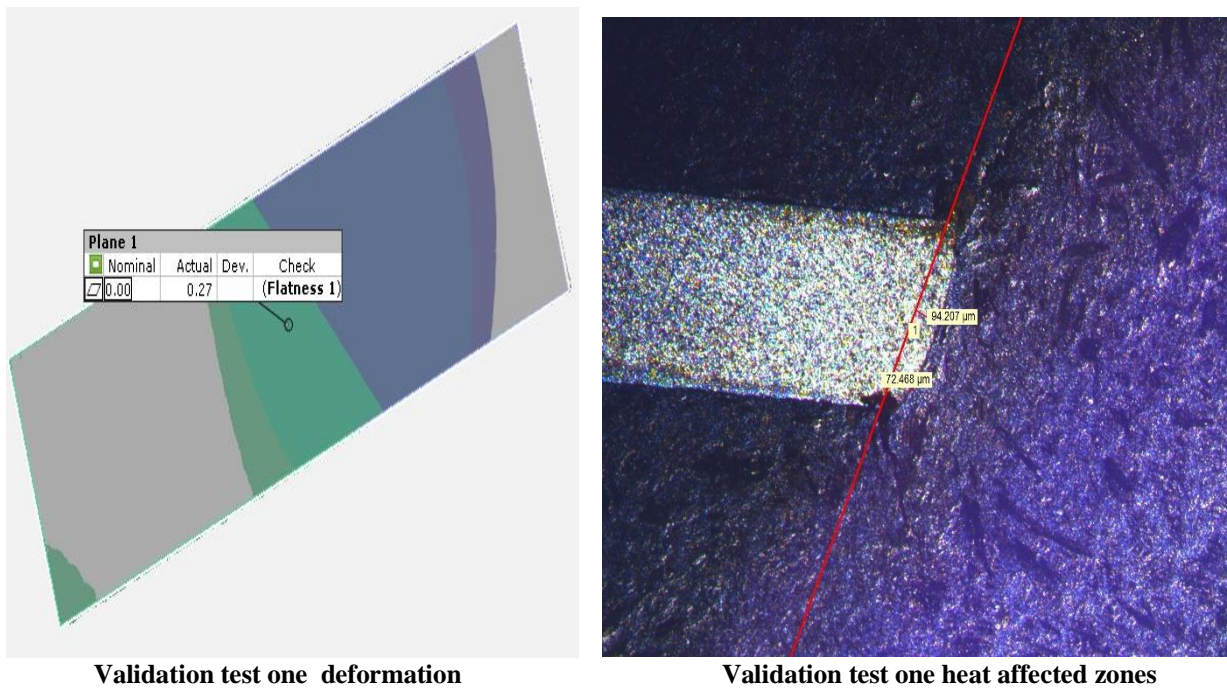
**Figures D3 Microstructure of the material and heat affected zones width, sample from the top layers of the model (a) to (i) and specimens from the bottom layers of the model (a') to (i')**

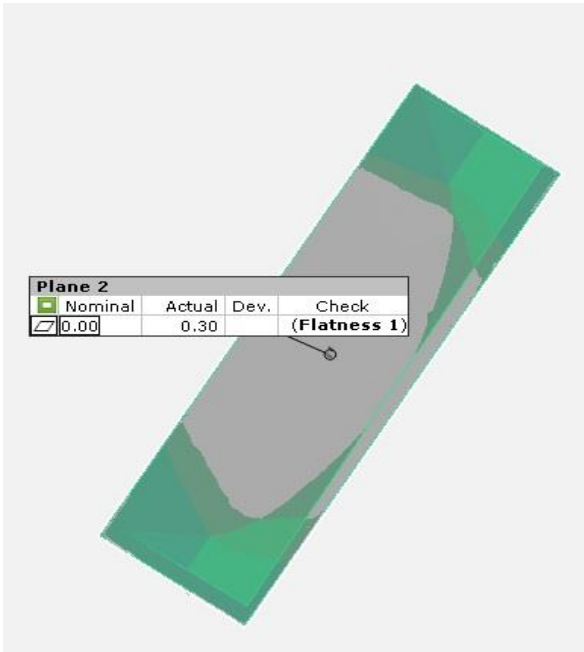
## APPENDIX-E Validation Tests

Figures below E are obtained from the validation tests for deformation and heat affected zones. The first figures E1 was for testing the optimal parameters and assess the level of improvement of a single sheet cutting 0.6 mm thick, the second tests figures E2 were to validate the regression model for a single sheet 0.6 mm thick. The third figures E3 were the optimal parameters for a simultaneous two sheets cutting and level of improvement 0.7 mm material thick, and the figures E4 were to validate the regression made for the double sheets.

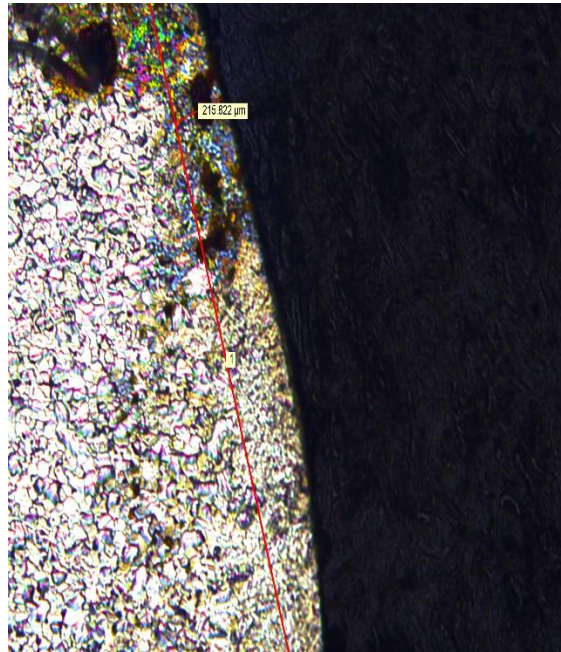


**Figure E1** Optimal parameters tests and level of improvement 0.6 mm. (a) deformation, (b) Heat affected zones.

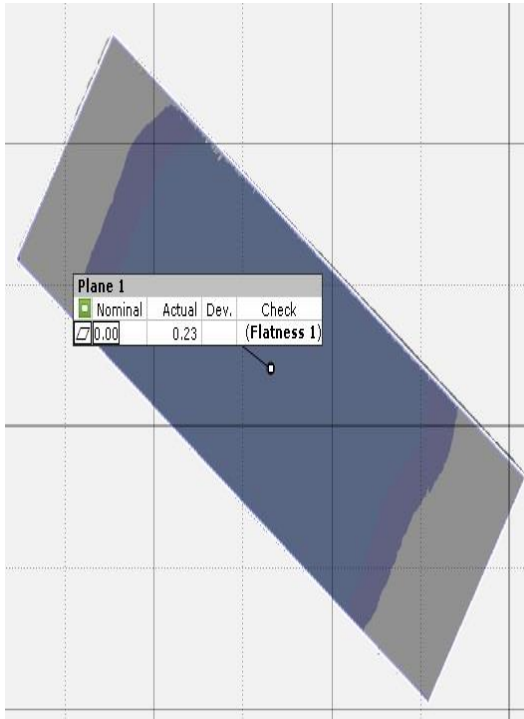




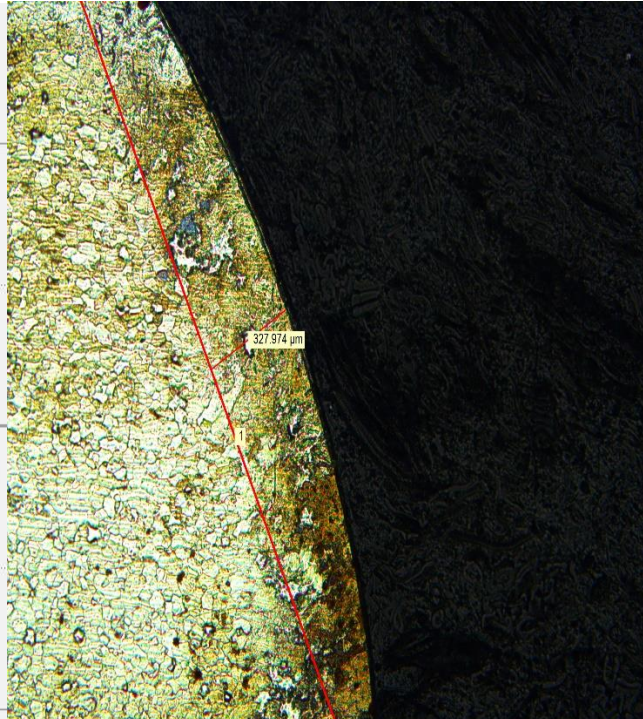
**Validation test Two deformation**



**Validation test two HAZ**



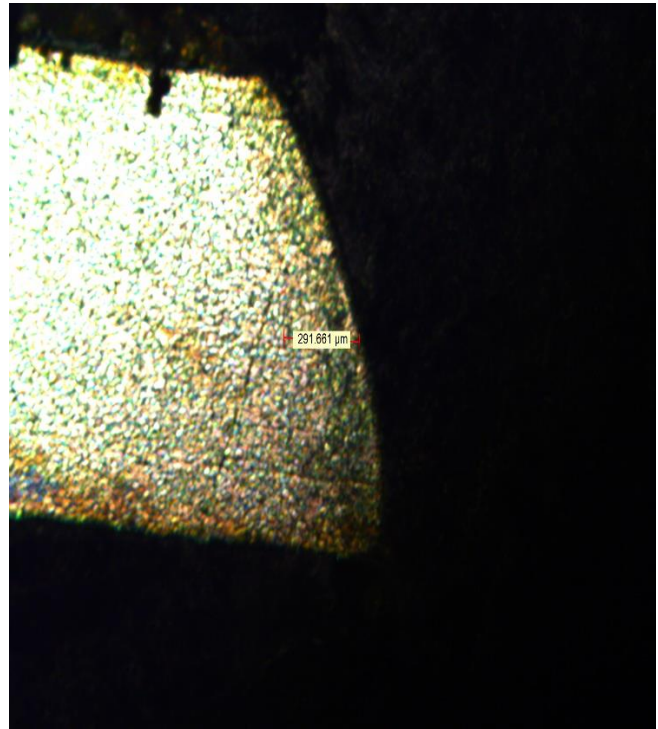
**Validation test three deformation**



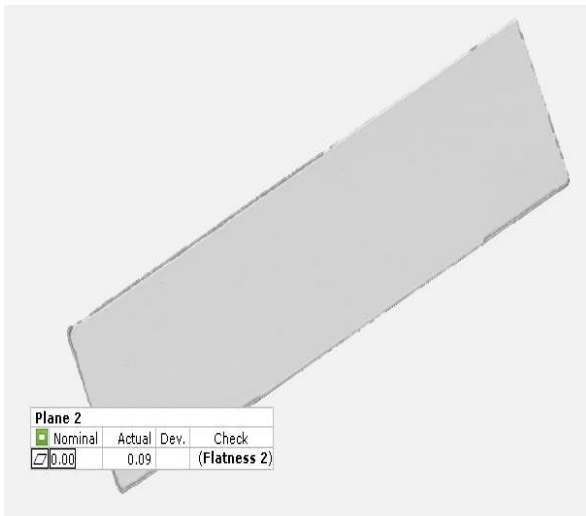
**Validation test three HAZ**



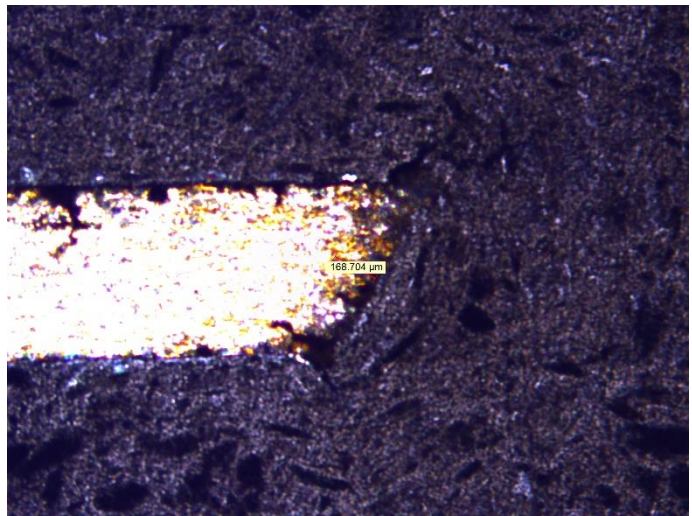
**Validation four deformation**



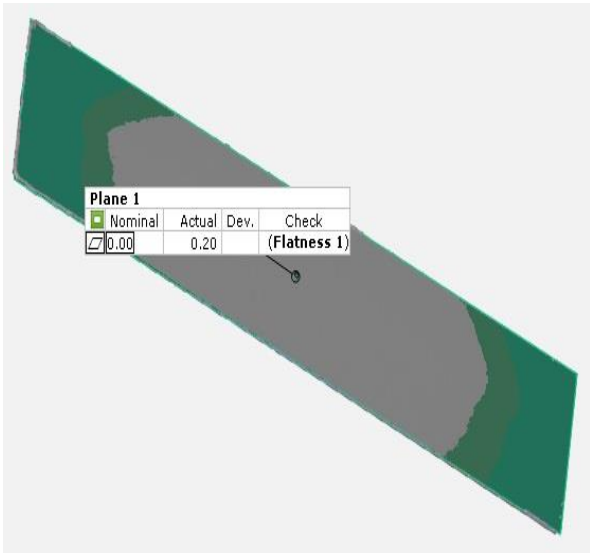
**Validation four HAZ**



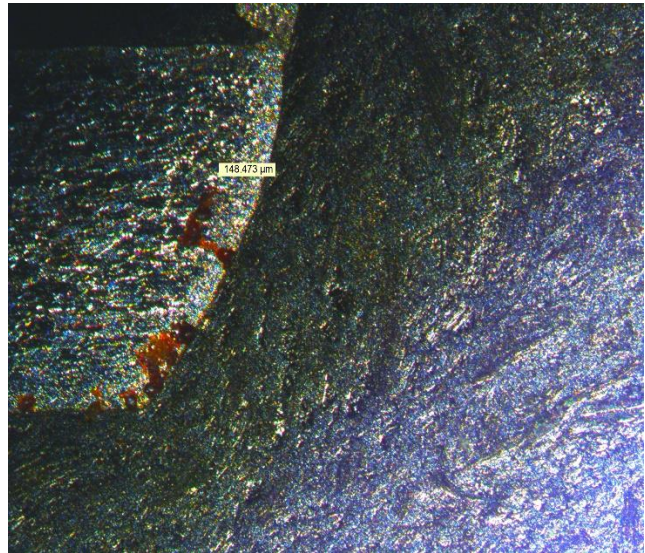
**Validation five deformation (Optimal)**



**Validation five HAZ**



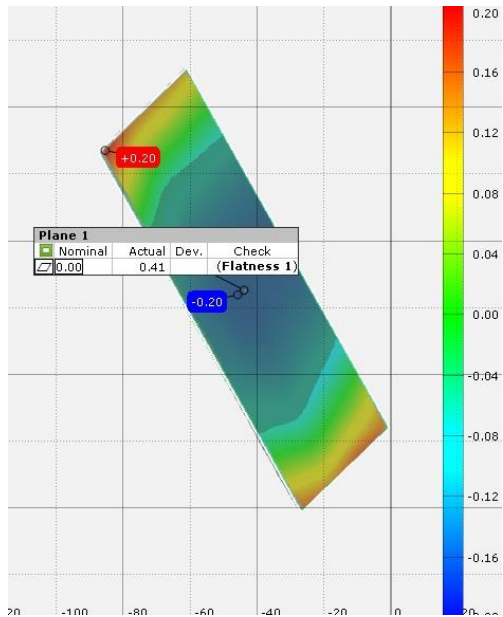
Validation six deformation



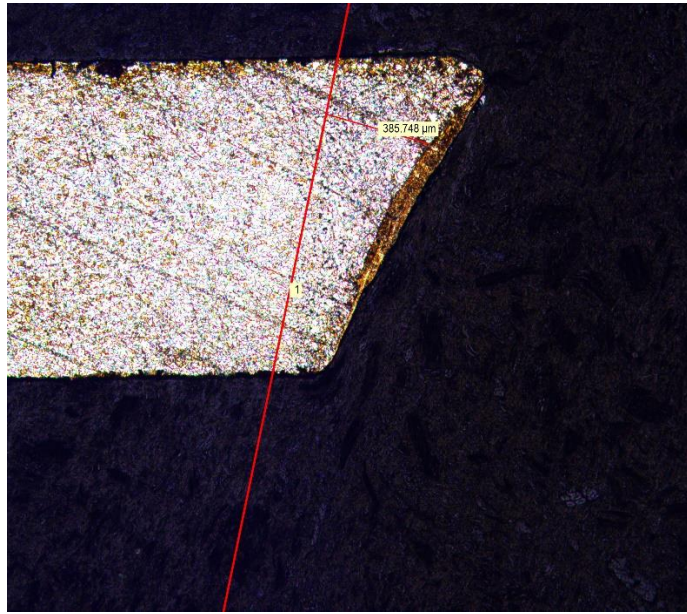
Validation six HAZ (optimal)

**Figures E2 Validation tests for the prediction model deformation sheet 0.6 mm and Heat Affected Zones**

The following figures E3 are the validation for the optimal parameters to reduce the deformation and heat affected zones on the top sheet (simultaneous double cutting using sheets material 0.7 mm thick).



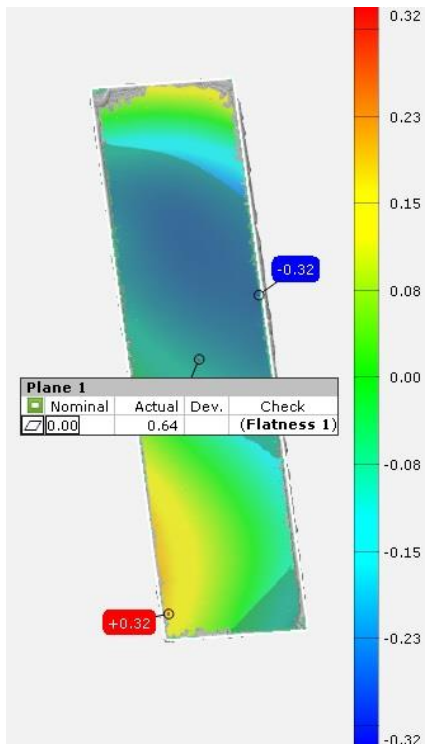
Validation optimal deformation



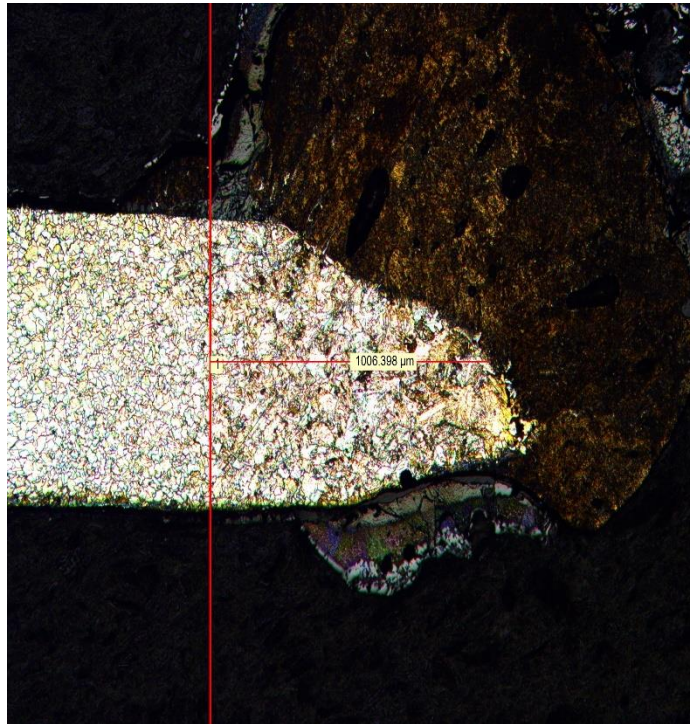
Validation Optimal HAZ

**Figures E3 Optimal parameters validation for double sheets cutting. Maximum deformation of the material and the heat affected zones.**

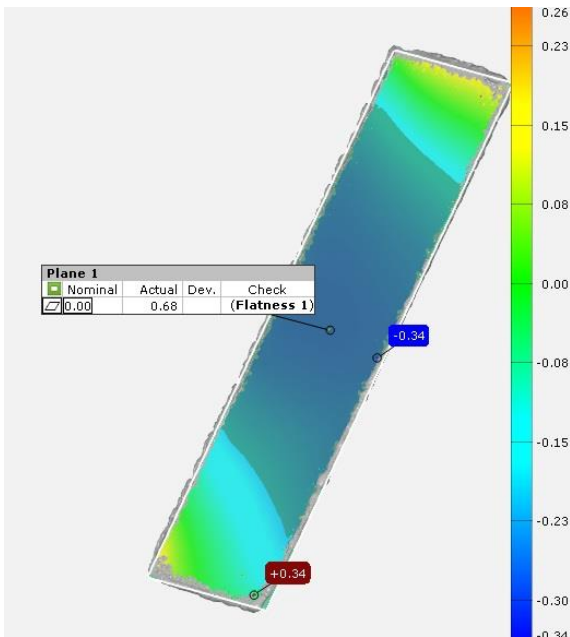
Figures E4 below are for the validation of the regression models for the double sheets, left side are figures of the deformation and the right side are for the heat affected zones



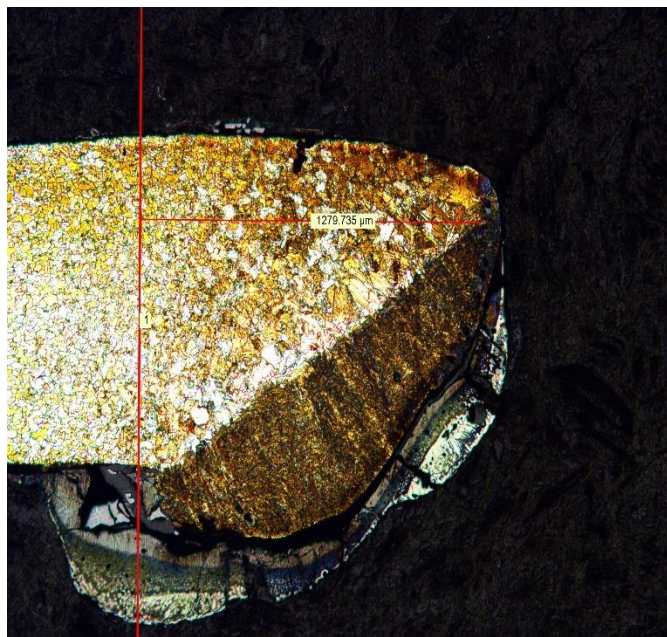
**Trial one for Deformation**



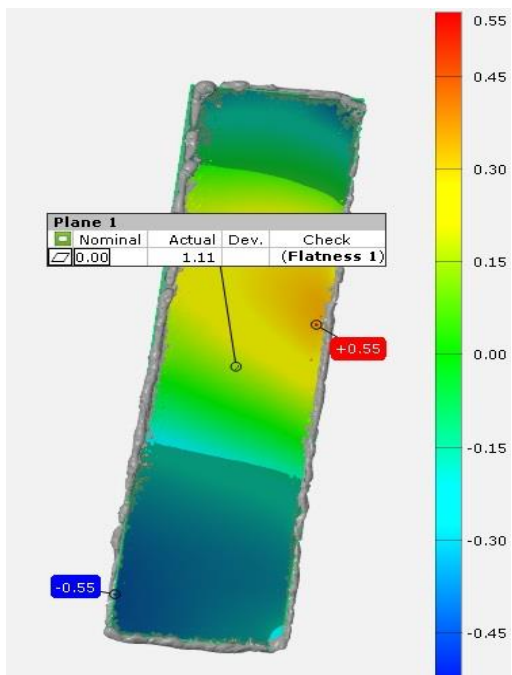
**Trial one validation HAZ**



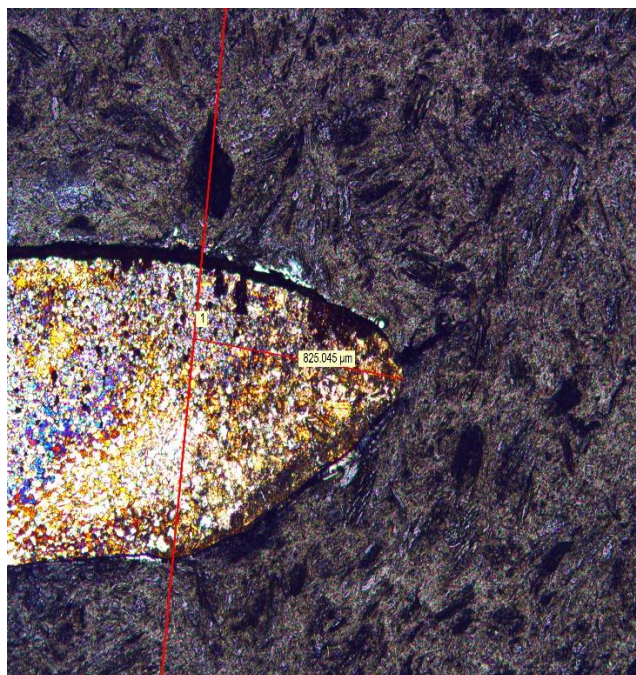
**Trial two deformation**



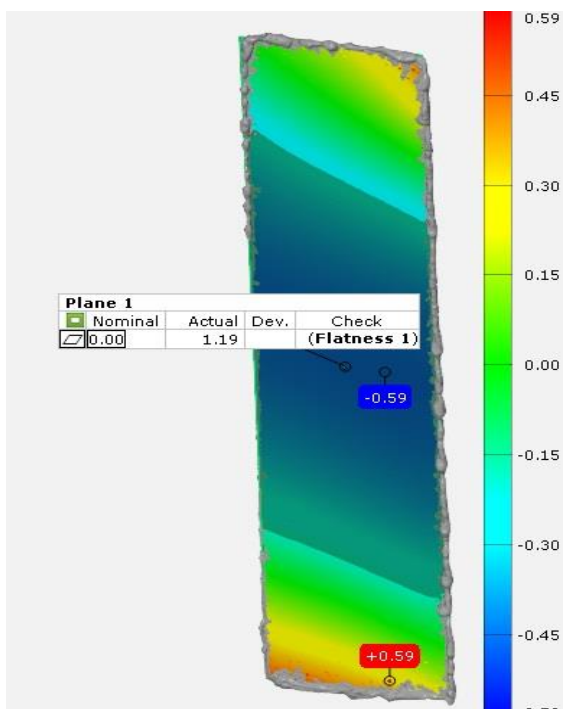
**Trial two HAZ**



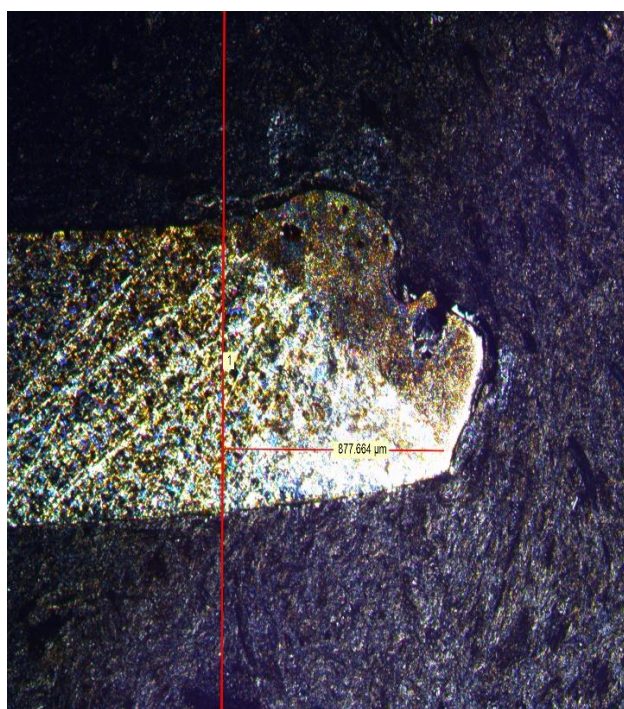
**Trial three deformation**



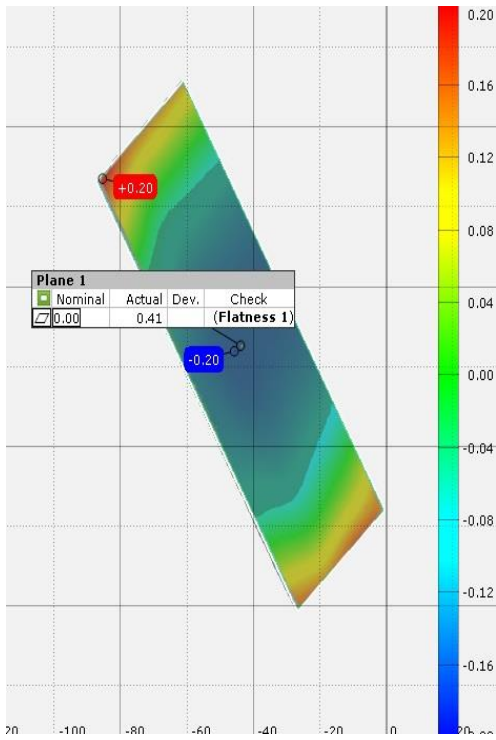
**Trial three HAZ**



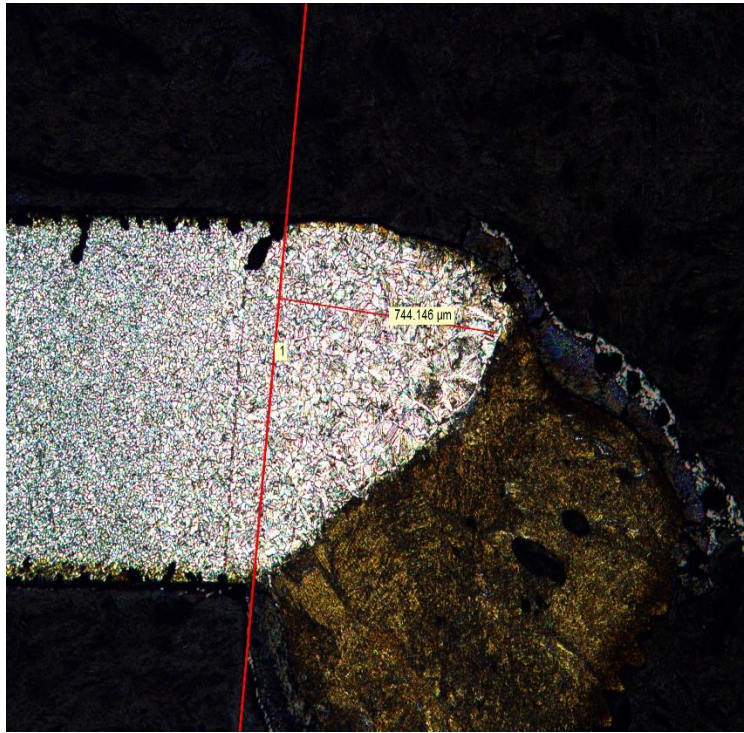
**Trial four deformation**



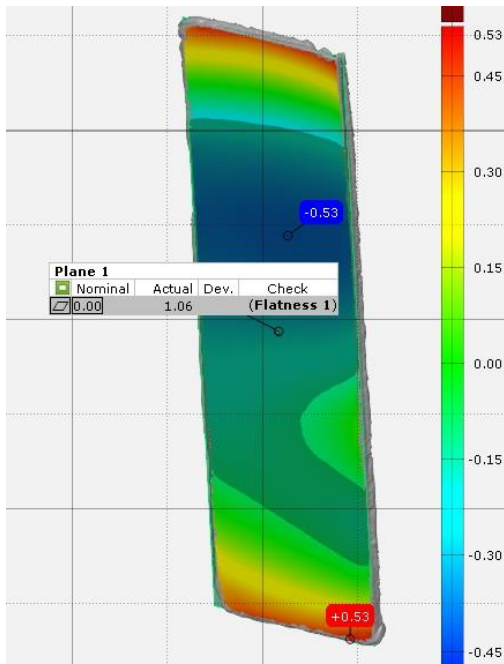
**Trial four HAZ**



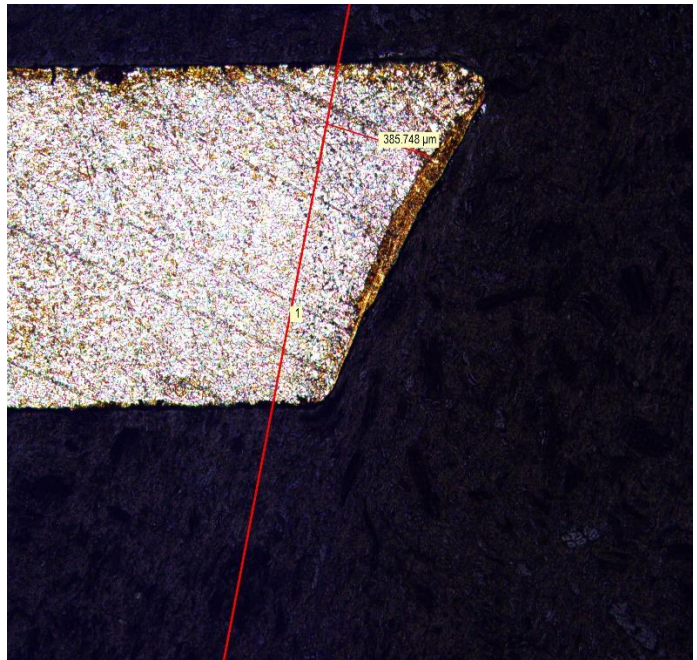
**Trial five deformation**



**Trial five HAZ**



**Trial six deformation**



**Trial six HAZ**

**Figures E4 Validation tests for the deformation and heat affected zones respectively from trial one to six. Two sheets cutting simultaneously.**